THE JOURNAL
OF
CHEMICAL PHYSICS

VOLUME 17, NUMBER 6 JUNE, 1949

The Mechanism of the Photo-Chemical Decomposition of Diethyl Ketone*

LEON M. DORFMAN AND ZACHARY D. SHELDON**
Department of Chemistry, University of Rochester, Rochester, New York
(Received November 26, 1948)

The photo-chemical decomposition of gaseous diethyl ketone in light of 3130A has been investigated at 56°C and 120°C over a wide range of absorbed intensities. The quantum yield of butane was found to increase with increasing intensity, while the quantum yield of total C_2 hydrocarbons was found to decrease with increasing intensity. On the basis of a kinetic analysis of these data, the proposed free radical mechanism for the decomposition of this ketone is adequately substantiated.

Assuming zero activation energy for the recombination of ethyl radicals to form butane, the activation energy for the disproportionation of ethyl radicals has been determined as $E=4.8$ kcal./mole, and that for the reaction of an ethyl radical with a diethyl ketone molecule to form ethane has been found to be $E=4.1$ kcal./mole.

PREVIOUS work[1–4] on the photolysis of diethyl ketone has indicated that the decomposition follows a pattern that would be expected on the basis of a free radical mechanism. In all cases where quantum yields have been reported, the quantum yield of carbon monoxide formation was found to be nearly unity over a wide range of pressures, intensities, and temperatures. Ethane, ethylene, and butane, in addition to carbon monoxide, have been reported among the products of the reaction.

The present investigation has been carried out to obtain data in such a way that a precise kinetic analysis of the mechanism, similar to that reported recently for the photolysis of gaseous acetone[5,6] could be applied. The use of light beams such that the number of quanta absorbed per unit volume per second is as constant as possible throughout the illuminated volume is essential to a proper interpretation of the data. The absorbed intensity has been varied over a somewhat wider range and has been carried to substantially lower values than have normally been employed in the photochemical decomposition of this compound.

EXPERIMENTAL

Three types of mercury arc lamp were used as the source of radiation: a General Electric Company AH-6 high pressure arc was used for high intensity runs; a Hanovia U A30 A2 medium pressure arc and a Hanovia Alpine burner, Type S-100, provided convenient sources of radiation for the medium intensity runs. The filters used to provide monochromatic illumination with 3130A have been described.[7] For the low intensity runs the light intensity was reduced by inserting in the light path additional filters of Corning No. 9863 glass, and in the runs with the lowest absorbed intensity, by interposing a thin Pyrex window. The equations for the calculation of absorbed intensity have been presented in detail.[8,9]

The photo-chemical decomposition of acetone was used as an actinometer, since it has been shown

* This work was supported by Contract N6onr-241, Task I, with the Office of Naval Research, United States Navy.
** Present address: The General Electric Company, Schenectady, New York.
[1] T. G. Pearson, J. Chem. Soc., 1718 (1934).
[2] T. G. Pearson, and R. H. Purcell, J. Chem. Soc., 1151 (1935).
[3] V. R. Ells and W. A. Noyes, Jr., J. Am. Chem. Soc. 61, 2492 (1939).
[4] W. Davis, Jr., J. Am. Chem. Soc. 70, 1868 (1948).
[5] L. M. Dorfman and W. A. Noyes, Jr., J. Chem. Phys. 16, 557 (1948).
[6] W. A. Noyes, Jr., and L. M. Dorfman, J. Chem. Phys. 16, 788 (1948).
[7] R. E. Hunt and W. Davis, Jr., J. Am. Chem. Soc. 69, 1415 (1947).
[8] R. E. Hunt and T. L. Hill, J. Chem. Phys. 15, 111 (1947).
[9] W. Davis, Jr. and W. A. Noyes, Jr., J. Am. Chem. Soc. 69, 2153 (1947).

TABLE I.

Run No.	Temp. °C	Press. mm	(D) molecules/cc $\times 10^{-18}$	Absorbed intensity q/cc/sec. $\times 10^{-10}$	Quantum yield of gaseous products CO	C_2 hydrocarbons	C_4H_{10}	$\frac{\Phi C_2}{\Phi C_4H_{10}}$	$\frac{(D)}{\Phi C_4H_{10} I_a^{\frac{1}{2}}} \times 10^{-12}$
*5	55.9	41.4	1.21	109.7	1.17	0.551	0.624	0.88	1.45
*6	57.3	38.8	1.13	67.9	0.96	0.742	0.587	1.26	1.79
**2	57.1	46.1	1.31	8.64	0.86	1.03	0.343	3.00	7.78
**1	57.0	44.4	1.30	5.96	0.98	—	—	—	—
***9	55.5	43.9	1.29	4.43	0.96	1.31	0.265	4.94	11.95
***7	58.8	51.3	1.49	5.41	0.89	1.13	0.175	6.46	15.32
**3	54.8	43.5	1.28	1.77	1.00	1.27	0.158	8.04	24.2
Mean:	56.6				0.97				

* AH-6 arc.
** U A30 A2 arc.
*** Alpine burner—Type S-100.

by various workers[10,11] that the quantum yield of carbon monoxide in this photolysis is unity at temperatures slightly in excess of 100°C.

The reaction vessel consisted of a cylindrical quartz cell, 200 mm in length and 22 mm in inside diameter. The AH-6 arc provided a slightly divergent beam with an incident cross section of 1.16 cm^2 and an emergent cross section of 2.15 cm^2 and hence an illuminated volume of 33.1 cc. The light beam obtained from the U A30 A2 arc was parallel with a diameter of 15 mm and consequently provided an illuminated volume of 35.4 cc. The beam from the Alpine burner was nearly parallel, with an incident cross section of 1.50 cm^2, an emergent cross section of 1.42 cm^2, and hence an illuminated volume of 29.2 cc. It has been assumed that the absorbed intensity is uniform over the entire path length. The inaccuracy in this assumption is negligible at the low percentage absorption (18 percent to 33 percent) used in all the runs.

Reagent diethyl ketone was purified by distillation in a 35-plate column, the middle third, with a boiling point of 102.4°C constant to 0.1°C, being retained then dried over anhydrous copper sulfate. When originally stored in the system, the ketone was degassed by several bulb-to-bulb distillations, and, subsequently, the small amount used in each run was again degassed at the beginning of the run.

The gaseous products, CO, C_2 hydrocarbons, and C_4H_{10} were separated by means of a Ward apparatus and Toepler pump and analyzed by combustion on a hot platinum wire. These methods have been described by various authors.[9,10] The carbon monoxide could be separated almost, but not quite, completely from the C_2 hydrocarbons by distillation at −195°C. The C_2 content of this fraction was then determined by combustion. The C_2 hydrocarbons were then pumped off at −155°C to −150°C. The butane was removed at −120°C to −115°C. Repeated rewarming and pumping was necessary to obtain a quantitative separation of the butane from the ketone at this temperature. The results of combustion analyses showed that, within experimental error, a complete separation of the butane and C_2 hydrocarbons was effected.

[10] D. S. Herr and W. A. Noyes, Jr., J. Am. Chem. Soc. **62**, 2052 (1940).
[11] J. A. Leermakers, J. Am. Chem. Soc. **56**, 1899 (1934); C. A. Winkler, Trans. Faraday Soc. **31**, 761 (1935).

RESULTS AND DISCUSSION

Runs were carried out at two temperatures, 56°C and 120°C. Table I consists of the runs at 56°C in which the absorbed intensity has been varied over a 62-fold range. Table II contains the runs at 120°C in which the absorbed light intensity has been varied 45-fold.

Because of the instability of the AH-6 arc, the possible error in the determination of quantum yields is somewhat greater for the high intensity runs than for the runs in which the medium pressure arcs have been used. For the four runs with the AH-6 arc, errors in the quantum yields may be as high as 18 percent. For the runs with the medium pressure arcs, the experimental quantum yields may be expected to have an error of 14 percent or less.

The Primary Process

The following facts are pertinent to a decision concerning the nature of the primary process: (a) The existence of ethyl radicals during the decomposition has been demonstrated by Pearson[3]

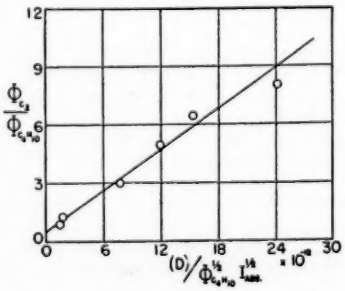

FIG. 1. A plot of Eq. (I) at 56.6°C. The slope is equal to 3.52×10^{-13}, and the intercept is 0.50.

TABLE II.

Run No.	Temp. °C	Press. mm	(D) molecules/cc $\times 10^{-18}$	Absorbed intensity q/cc/sec. $\times 10^{-10}$	Quantum yield of gaseous products: CO	C_2 hydrocarbons	C_4H_{10}	$\frac{\Phi C_2}{\Phi C_4H_{10}}$	$\frac{(D)}{\Phi C_4H_{10} I_a^{\frac{1}{2}}} \times 10^{-12}$
*1A	120.9	40.5	0.992	142	1.21	1.16	0.419	2.77	1.29
*2A	120.5	41.1	1.008	80.0	1.04	1.10	0.263	4.18	2.20
**5A	119.1	45.6	1.122	5.74	1.00	1.58	0.107	14.8	14.30
***6A	120.2	45.5	1.116	5.77	1.04	1.64	0.106	15.5	14.31
***3A	121.1	43.5	1.065	5.39	1.04	1.62	—	—	—
***4A	120.0	42.8	1.051	3.13	1.18	2.00	0.083	24.2	20.62
Mean:	120.3				1.08				

* AH-6 arc.
** U A30 A2 arc.
*** Alpine burner—Type S-100.

and by Pearson and Purcell[4] using mirror techniques. (b) The quantum yield of carbon monoxide is unity within experimental error, and shows no significant trend with variation in pressure, absorbed light intensity, or temperature. That this is clearly the case may be seen from Table III in which are listed the values obtained by Ells and Noyes[3] and by Davis[4] as well as the results of the present investigation. (c) The very weak fluorescence exhibited by diethyl ketone has been shown by Matheson and Zabor[12] to have a maximum at the same wave-length as the fluorescence maximum obtained when propionaldehyde is irradiated. These authors suggested that the similarity in the fluorescence may possibly result from the formation of bipropionyl formed in the decomposition. However, the fluorescent efficiency for diethyl ketone is much less than that of acetone, so that fluorescence certainly accounts for much less than one percent of the total radiant energy absorbed. Furthermore, bipropionyl has never successfully been identified among the products, probably because of the extremely small amount, if it is formed at all. (d) The quantum yield of carbon monoxide at lower wave-lengths (1850–2000A) was found by Ells and Noyes[5] to be nearly unity. In fact, if the deviation of their values from unity is significant, the quantum yield of CO at this lower wave-length is slightly less than unity. If the propionyl radical were to have an appreciable stability, then the reverse of this would be expected, namely, that the CO quantum yield would be slightly higher at the lower wave-length because of the greater amount of excess energy retained by the radical following the primary process.

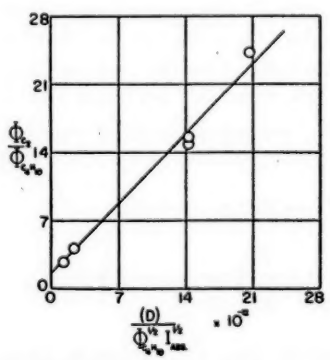

FIG. 2. A plot of Eq. (I) at 120.3°C. The slope is equal to 10.2×10^{-13}, and the intercept is 1.64.

On the basis then, of the apparent instability of the propionyl radical as evidenced by the CO quantum yield of unity, invariant with changes in temperature and other conditions, one is justified in writing, as Davis[4] has done, the following reaction for the primary process:

$$C_2H_5COC_2H_5 + h\nu = 2C_2H_5 + CO \quad \phi I_a, \qquad (1)$$

where the primary quantum yield $\phi \cong 1$.

Secondary Reactions

The known gaseous products which must be accounted for in the mechanism are butane, ethylene, and ethane. Butane may be formed by association of ethyl radicals:

$$C_2H_5 + C_2H_5 = C_4H_{10} \quad k_2(C_2H_5)^2. \qquad (2)$$

Disproportionation of ethyl radicals would produce both ethylene and ethane:

$$C_2H_5 + C_2H_5 = C_2H_4 + C_2H_6 \quad k_3(C_2H_5)^2. \qquad (3)$$

However, in view of the inverse variation of C_2 quantum yield with absorbed intensity change, the rate of formation of C_2 hydrocarbons cannot depend solely on the second power of the ethyl radical concentration, as is the case in reaction (3). Davis[4] has suggested that ethane can arise from the following reaction:

$$C_2H_5 + C_2H_5COC_2H_5 = C_2H_6 + C_2H_4COC_2H_5 \quad k_4(C_2H_5)(D). \qquad (4)$$

This reaction is analogous to that of methane formation in the photolysis of acetone.[5, 6, 13]

[12] M. S. Matheson and J. W. Zabor, J. Chem. Phys. **7**, 536 (1939).

[13] W. Davis, Jr., J. Am. Chem. Soc. **70**, 1867 (1948).

TABLE III. Diethyl ketone at 3130A.

Author	Pressure mm	Temperature °C	Absorbed intensity q/cc/sec. $\times 10^{-10}$	Φ_{CO}
5	10	27	—	0.98
5	10	27	—	0.67
5	21	27	—	0.97
6	22	26	84	1.05
6	34.5	25	140	0.99
5	36	27	—	1.04
6	38.0	26	150	0.97
6	37	27	170	1.05
6	38	27	160	0.93
6	38	27	170	0.93
6	39.6	26.8	14	1.03
6	40	28	190	0.99
6	41	28	220	1.03
	38.8	57.3	67.9	0.96
	41.4	55.9	109.7	1.17
	43.5	54.8	1.77	1.00
	43.9	55.5	4.43	0.96
	44.4	57.0	5.96	0.98
	46.1	57.1	8.64	0.86
	51.3	58.8	5.41	0.89
	40.5	120.9	142	1.21
	41.1	120.5	80.0	1.04
	42.8	120.0	3.13	1.18
	43.5	121.1	5.39	1.04
	45.5	120.2	5.77	1.04
	45.6	119.1	5.74	1.00
6	36.8	136	17	1.05
6	41.0	137.5	19	1.02
			Mean:	1.00

If reactions (2)–(4) represent the sole modes of formation of butane and C_2 hydrocarbons, respectively, the quantum yields of these products will be related by the following equation:

$$\frac{\Phi_{C_2}}{\Phi_{C_4H_{10}}}=\frac{2k_3}{k_2}+\frac{k_4}{k_2^{\frac{1}{2}}}\cdot\frac{(C_2H_5COC_2H_5)}{\Phi_{C_4H_{10}}I_a^{\frac{1}{2}}} \qquad (I)$$

Figure 1 shows a plot of $\Phi_{C_2}/\Phi_{C_4H_{10}}$ against $(D)/\Phi_{C_4H_{10}}I_a^{\frac{1}{2}}$ for the series of runs at 56.6°C. (D) represents the concentration of diethyl ketone. Figure 2 shows the plot of these same expressions for the runs at 120.3°C. The straight lines obtained, with a positive intercept in each case, indicate the validity of reactions (2)–(4). The intercept is equal to $2k_3/k_2$, and the slope gives the value of $k_4/k_2^{\frac{1}{2}}$.

Figure 1 gives $k_3/k_2=0.25$ at 56.6°C, and Fig. 2 gives $k_3/k_2=0.82$ at 120.3°C. Writing $k_3=a_3\exp(-E_3/RT)$ and $k_2=a_2\exp(-E_2/RT)$, these values may be used to calculate $E_3-E_2=4800$ cals. per mole. The uncertainty in this value, because of the possible error in the intercepts of the lines, may be as high as 1.5 kcal./mole. From the two straight lines, one obtains also $k_4/k_2^{\frac{1}{2}}=3.52\times10^{-13}$ at 56.6°C, and $k_4/k_2^{\frac{1}{2}}=10.2\times10^{-13}$ at 120.3°C. In the same manner these two values may be used to calculate $E_4-\frac{1}{2}E_2=4100$ cals. per mole. The $T^{\frac{1}{2}}$ factor in the pre-exponential term has been taken into account in this calculation. Assuming, as LeRoy and Kahn[14] have done, that the activation energy for ethyl recombination, $E_2=0$, one obtains $E_3=4.8$ kcal./mole and $E_4=4.1$ kcal./mole. The value of 4.8 kcal./mole for the disproportionation reaction is somewhat larger than the value of $E_3\geqslant 1.2$ kcal./mole reported by these authors, but is in agreement with the suggestion of Moore and Taylor,[15] that $E_3>4$ kcal./mole.

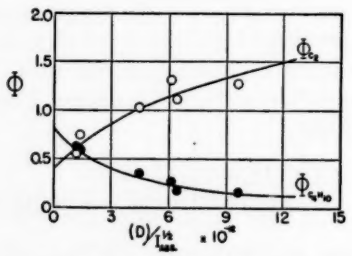

FIG. 3. The quantum yields of butane (●) and of C_2 hydrocarbons (○) as a function of $(D)/I_{abs}^{\frac{1}{2}}$ at 56.6°C. (D) is the concentration of diethyl ketone. The curves are the theoretical ones from Eqs. (IV) and (II).

The $C_2H_4COC_2H_5$ radicals formed in reaction (4) may combine with ethyl radicals to form ethyl butyl ketone:

$$C_2H_5+C_2H_4COC_2H_5=C_4H_9COC_2H_5 \qquad k_5(C_2H_5)(C_2H_4COC_2H_5), \qquad (5)$$

or they may recombine to form the diketone:

$$2C_2H_4COC_2H_5=(C_2H_4COC_2H_5)_2 \qquad k_6(C_2H_4COC_2H_5)^2. \qquad (6)$$

Reactions (5) and (6) are analogous to the reactions of the acetonyl radical in the photolysis of acetone.[5, 6, 13] The decomposition of the $C_2H_4COC_2H_5$ radical to form ethylene and a propionyl radical is ruled out for two reasons. Firstly, an appreciable occurrence of such a reaction would result in CO quantum yields greater than unity, increasing with decreasing intensity and with increasing temperature; this is not the case. And secondly, the inclusion of such a reaction in the mechanism would result in a rate relationship differing from Eq. (I) which would not fit the experimental data.

It is desirable to subject the mechanism, consisting of reactions (1)–(6), to as many tests of validity as possible. In addition to Eq. (I), establishing the validity of reactions (2)–(4), another relationship (from reactions (1)–(6)) would be:

$$\frac{(2-2\Phi_{C_4H_{10}}-\Phi_{C_2})^2}{\left(\Phi_{C_2}+\left(1-\frac{k_3}{k_2}\right)\Phi_{C_4H_{10}}-1\right)\Phi_{C_4H_{10}}}=\frac{k_5^2}{k_2k_6}. \qquad (II)$$

The nature of Eq. (II) is such that good constancy could hardly be expected, since errors in the

[14] D. J. LeRoy and A. Kahn, J. Chem. Phys. **15**, 816 (1947).
[15] W. J. Moore and H. S. Taylor, J. Chem. Phys. **8**, 396 (1940).

individual quantum yields will be magnified considerably in ascertaining the values of k_5^2/k_2k_6. Thus an error of only 10 percent in each individual quantum yield could result in an error of 90 percent in the value of the constant. Particularly in the range where $(2\Phi_{C_4H_{10}}+\Phi_{C_2})$ is not very different from 2, considerable errors may be expected. This equation has been applied to the series of runs at 56.6°C, using $k_3/k_2=0.25$ as obtained from Fig. 1. The resulting values of k_5^2/k_2k_6 are shown in Table IV. The values, although varying considerably, show no significant trend over a 62-fold variation in absorbed intensity, and are of a reasonable order of magnitude, since k_2, k_5, and k_6 are all rate constants for association reactions.

The quantum yield of butane may be determined, for the over-all mechanism, as a function of diethyl ketone concentration and absorbed light intensity. This relationship is shown in Eq. (III):

$$\left(1+\frac{k_3}{k_2}\right)\left\{4\left(1+\frac{k_3}{k_2}\right)-\frac{k_5^2}{k_2k_6}\right\}\Phi_{C_4H_{10}}^2$$

$$+\frac{k_4}{k_2^{\frac{1}{2}}}\left\{4\left(1+\frac{k_3}{k_2}\right)-\frac{k_5^2}{k_2k_6}\right\}\frac{(D)}{I_a^{\frac{1}{2}}}\Phi_{C_4H_{10}}^{\frac{1}{2}}$$

$$-\left\{8\left(1+\frac{k_3}{k_2}\right)-\left(\frac{k_4}{k_2^{\frac{1}{2}}}\right)^2\left[\frac{(D)}{I_a^{\frac{1}{2}}}\right]^2-\frac{k_5^2}{k_2k_6}\right\}\Phi_{C_4H_{10}}$$

$$-4\frac{k_4}{k_2^{\frac{1}{2}}}\frac{(D)}{I_a^{\frac{1}{2}}}\Phi_{C_4H_{10}}^{\frac{1}{2}}+4=0. \quad \text{(III)}$$

Taking the values of the constants obtained in Fig. 1 at 56.6°C, namely, $k_3/k_2=0.25$, $k_4/k_2^{\frac{1}{2}}=3.52\times10^{-13}$, and the value of $k_5^2/k_2k_6=2$ from Table IV, this equation becomes:

$$3.75\Phi_{C_4H_{10}}^2+10.6y\Phi_{C_4H_{10}}^{\frac{1}{2}}+(8.0-12.4y^2)\Phi_{C_4H_{10}}$$
$$-14.1y\Phi_{C_4H_{10}}^{\frac{1}{2}}+4=0, \quad \text{(IV)}$$

TABLE IV.

Run No.	Absorbed intensity q/cc/sec. $\times10^{-10}$	$\frac{k_5^2}{k_2k_6}$
5	109.7	3.4
6	67.9	0.1
2	8.64	0.8
9	4.43	0.2
7	5.41	5.9
3	1.77	2.8
		Mean = 2.2

where $y=(D)/I_a^{\frac{1}{2}}\times10^{-13}$, and (D) is the concentration of diethyl ketone. The theoretical curve for $\Phi_{C_4H_{10}}$ as a function of $(D)/I_a^{\frac{1}{2}}$, as obtained from Eq. (IV) is shown in Fig. 3. The curve is not very sensitive to values of k_5^2/k_2k_6 used in Eq. (III). The experimental values of $\Phi_{C_4H_{10}}$ are plotted, and, as may be seen, good agreement between predicted and experimental values is obtained.

Since the quantum yields of butane and of C_2 hydrocarbons are related by Eq. (II), the theoretical curve for Φ_{C_2} may be calculated from the curve for $\Phi_{C_4H_{10}}$ using this equation. The curve for Φ_{C_2} as a function of $(D)/I_a^{\frac{1}{2}}$ is shown in Fig. 3, and the experimental values plotted. Again, this curve gives the correct trend to the results.

Thus, the proposed mechanism and the rate equations derived therefrom account for the yields of hydrocarbon products within experimental error. The precise determination of I_a, expressed in quanta absorbed per cubic centimeter per second is important, and a sharply diverging or converging light beam will make exact rate calculations impossible.

The authors wish to express their appreciation to Dr. W. Albert Noyes, Jr. for the many fruitful suggestions made during the course of the investigation.

The Metastability of the Lowest Excited Singlet Level of Naphthalene*

M. KASHA** AND R. V. NAUMAN†
Department of Chemistry, University of California, Berkeley, California
(Received September 24, 1948)

The fluorescence lifetime of naphthalene has been determined by direct observation to be on the order of 10^{-6} sec. The comparatively weak absorption band on the long-wave-length side of the ultraviolet spectrum of naphthalene is thereby established as a separate electronic transition to a metastable level, and as the lowest singlet-singlet transition. This weak absorption band and the fluorescence and phosphorescence bands of naphthalene in rigid glass solution at 77°K are presented. The absorption (Prikhotko) and fluorescence (Obreimov and Shabaldas) spectra of single crystals of naphthalene at 20°K are reinterpreted in terms of the above results; in particular, the lowest singlet-singlet band in the crystal is shown to be the 31060 cm^{-1} band. An anomalous crystal absorption band at 29945 cm^{-1} is accounted for in terms of absorption to an excited triplet state. A π-electron energy scheme for naphthalene for the experimentally observed singlet and triplet levels below 50000 cm^{-1} is given.

1. INTRODUCTION

THE theoretical calculation and interpretation of the π-electron energy levels of naphthalene has recently attracted the attention of a number of investigators.[1–6] The two approaches which have been used have led to a discrepancy concerning the nature of the lowest excited singlet level, suggesting alternative interpretations of the absorption spectrum. In the present work we have established the fluorescence lifetime to be on the order of 10^{-6} sec., indicating that the lowest excited singlet level is metastable. The results of the Valence-Bond energy level calculation[2, 5] actually indicate that the lowest singlet-singlet transition should be forbidden on symmetry grounds. On the other hand the Molecular-Orbital method[1, 3, 4, 6] offers conflicting information on this point. However, a suggestion has been made[6] to account for the comparatively low transition probability, in which it is pointed out that the presence of positive and negative terms of the same order of magnitude in the transition moment integral could result in a small value of the transition probability, even though the selection rules for the lowest transition indicate that it should be allowed.[7]

2. METASTABILITY: EXPERIMENTAL RESULTS ON THE FLUORESCENCE OF NAPHTHALENE

The absorption spectrum of naphthalene[8] exhibits fine structure, on the long-wave-length side of its absorption (near 3000A), which is considerably lower in intensity than the strong absorption which it overlaps at shorter wave-lengths. If a low intensity singlet-singlet absorption band lies actually at lower frequencies than any other singlet-singlet band (comparing O—O bands), it should give rise to a relatively long-lived fluorescence. As a test of this, an attempt was made to photograph the *fluorescence* of naphthalene by means of a relatively slow mechanical "phosphoroscope." The result is illustrated in Fig. 1, in which the fluorescence bands of naphthalene (in solid solution in a rigid hydroxylic glass[9] at 77°K) obtained by means of a phosphoroscope (resolving time *ca.* 5×10^{-4} sec.) may be seen (lower part), superimposed on the scattered light of the high-pressure mercury arc (*AH*-6). The identification of the bands is made certain by comparison with the fluorescence spectrum obtained by the static (continuous) illumination method. The apparatus was arranged to illuminate and view the sample from the front face; a detailed description will be given elsewhere. The arrangement used excludes the possibility that scattered *fluorescence* light entered the spectrograph slit during the illuminating phase of the phosphoroscope rotation.

Using a phosphoroscope[10] which gives no scattered exciting light, a clearer result was obtained, although the fluorescence bands were much fainter because of the longer resolving time (10^{-3} sec.) of

* Presented at the meeting of the Pacific Division of the American Association for the Advancement of Science (Pacific Intersectional Group of the American Chemical Society) held at the University of California, Berkeley, June 22, 1948.

** Work done under a contract between the Office of Naval Research and the University of California.

† Present address: Department of Chemistry, Cornell University, Ithaca, New York.

[1] V. L. German, J. Phys. (U.S.S.R.) **8**, 276 (1944).

[2] L. A. Blumenfeld, J. Phys. Chem. (U.S.S.R.) **21**, 529 (1947).

[3] A. S. Davydov, J. Exper. Theor. Phys. (U.S.S.R.) **17**, 1106 (1947).

[4] C. A. Coulson, Proc. Phys. Soc. (London) **60**, 257 (1948).

[5] D. P. Craig, "Energy levels in naphthalene" (University College, London, in press) (presented at the XIth International Congress of Pure and Applied Chemistry, London, July 17th to 24th, 1947). We are greatly indebted to Dr. Craig for the opportunity of reading his manuscript before its publication.

[6] W. T. Simpson, J. Chem. Phys. **16**, 1124 (1948).

[7] *Note added in proof:* "Relined Molecular-Orbital calculations" by Miss J. Jacobs (University of King's College, London) indicates that the $A_{1g}-A_{1g}$ *may be* the lowest singlet-singlet transition, which *would* be in agreement with the results of the Valence-Bond method. We are indebted to Professor C. A. Coulson for the opportunity of reading this manuscript before its publication.

[8] Cf. Fig. 78, p. 375, *International Critical Tables*, McGraw-Hill Book Company, Inc., New York (1929), Vol. 5.

[9] EPA: absolute ethyl alcohol, 2; isopentane, 5; ethyl ether, 5; in parts by volume. Frozen in a liquid nitrogen bath. Cf. G. N. Lewis and D. Lipkin, J. Am. Chem. Soc. **64**, 2801 (1942).

[10] G. N. Lewis and M. Kasha, J. Am. Chem. Soc. **66**, 2100 (1944).

this rotor. By contrast, a brilliantly fluorescent substance such as anthracene (see last lines of this section) failed to give any bands with either phosphoroscope.

From spectrogram tracings of simultaneous fluorescence and phosphorescence emission, and of the same emissions obtained by means of a phosphoroscope, it is estimated that a 60000-fold diminution of the intensity ratio of fluorescence/phosphorescence takes place during the 5×10^{-4} sec. resolution time of the rotating disk. Since the phosphorescence intensity may be considered constant during this time,[11] the fluorescence lifetime calculated from the exponential decay law is $\tau_F=3.3\times10^{-5}$ sec.

The integrated absorption permits an independent calculation of the fluorescence lifetime. The validity and accuracy of such a calculation, aside from intrinsic errors, depends on the knowledge of the emitting level and on the separability of the low-intensity absorption from the strong absorption band which it overlaps. In view of the above demonstration of the relatively long lifetime of the fluorescence, we are justified in making the arbitrary separation shown in Fig. 2. From the graphical integration of the area between the fine structure and the dotted line, $\int\epsilon d\bar{\nu}=350{,}000$. From the equation.[12, 13]

$$\tau=\frac{3.47\times10^{8}}{\bar{\nu}_A^{2}n^{2}}\cdot\frac{g_u}{g_l}\cdot\frac{1}{\int\epsilon d\bar{\nu}}$$

setting $\bar{\nu}_A=31250$ cm^{-1}, $g_u/g_l=1$ (and neglecting[14] n^2) it is calculated that $\tau_F=1.02\times10^{-6}$ sec. This is in good agreement with the value of $\tau_F=1.06\times10^{-6}$ sec. calculated by West,[15] though without the fundamental justification presented above.

The two different approximate calculations agree sufficiently well to justify the correlation of the fluorescence of naphthalene with the low intensity absorption band shown in Fig. 2.

The fluorescence lifetimes of several complex molecules (mainly dyes) have been measured directly[16] and found to be in the range 10^{-8} to 10^{-10} sec. It has been assumed usually that this is true of the fluorescence lifetimes of most of the complex molecules. The present example of a fluorescence lifetime in the range 10^{-5} to 10^{-6} is an exception, and must lead to a considerable diminution of the quantum yield of fluorescence in fluid solutions of this substance, by external "concentration quenching." A study[17] of the latter phenomenon indicates that "long-lived fluorescences" are to be expected also in several other common polynuclear aromatic hydrocarbons (e.g. phenanthrene, chrysene; not anthracene, fluorene).

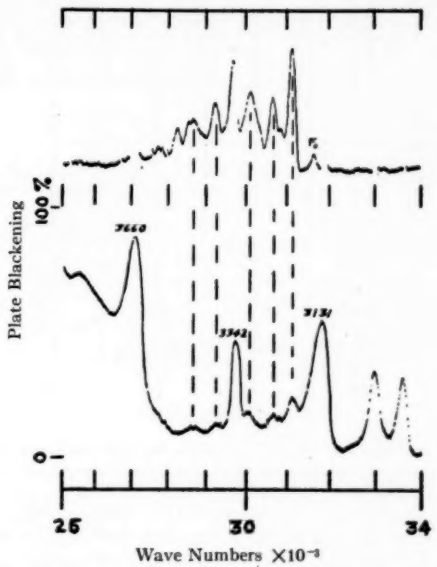

FIG. 1. Comparison of spectrogram tracings of naphthalene fluorescence photographed by mechanical phosphoroscope and by static illumination. *Upper curve*, fluorescence spectrum statically excited by unfiltered light of low pressure quartz mercury arc (E. K. 103F plate, slit 0.10 mm, 5 min.); *lower curve*, fluorescence bands as obtained by phosphoroscope, superposed on scattered continuum of *AH6* high pressure mercury arc (E. K. 103F plate, slit 0.25 mm, 6.5 hours). Front face illumination, and rigid glass solutions at 77°K in both. The breaks in the upper tracing are due to the simultaneously photographed mercury lines, which correspond to the broadened mercury lines marked in the lower tracing.

3. ABSORPTION AND EMISSION SPECTRA OF NAPHTHALENE IN RIGID GLASS SOLUTION AT 77°K

Confirmatory spectroscopic evidence for the correlation of the fluorescence of naphthalene with the low-intensity absorption near 3000A was obtained by a study of the naphthalene spectra at 77°K for rigid glass solutions.

Naphthalene was purified by repeated recrystallization from iso-octane; the criterion of purity was the absence of a spurious phosphorescence occurring just to the high frequency side of the naphthalene phosphorescence (sublimation failed to remove this impurity). The absorption spectrum was obtained by photographing with the ultraviolet continuum of the hydrogen arc. The fluorescence was excited by the light of the low pressure mercury arc, filtered by 5 cm of 500 g/l $NiSO_4\cdot6H_2O$ in water. A Hilger medium quartz spectrograph (dispersion *ca.* 164 cm^{-1}/mm at 33333 cm^{-1}) was used with the slit set at sufficiently small width to resolve the *UV* mercury lines, photographed simultaneously with the fluores-

[11] D. S. McClure, unpublished work, this laboratory. $\tau_P=2.6$ sec. for naphthalene in EPA at 77°K. Manuscript in preparation.

[12] G. N. Lewis, and M. Kasha, J. Am. Chem. Soc. **67**, 994 (1945).

[13] Cf. R. C. Tolman, Phys. Rev. **23**, 693 (1924); F. Perrin, J. de phys. et rad. **7**, 390 (1926).

[14] R. S. Mulliken and C. A. Riecke, The Physical Society (London) **8**, 231 (1941).

[15] W. West, Ann. N. Y. Acad. Sci. **41**, 203 (1941).

[16] E.g., E. Gaviola, Zeits. f. Physik **35**, 748 (1926); *ibid.* **42**, 853, 862 (1927); W. Szymanowski, Zeits. f. Physik **95**, 440, 450, 460 (1935); W. Kirchhoff, Zeits. f. Physik **116**, 115 (1940).

[17] M. Kasha, to be published.

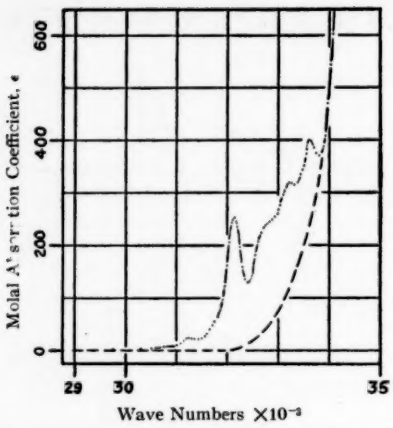

FIG. 2. Integrated area of the absorption curve of naphthalene (in methylcyclohexane at room temperature, Beckman spectrophotometer), corresponding to the singlet-singlet transition to the metastable level. (Cf. *Ultraviolet Spectrograms Issued by the American Petroleum Institute Project 44* at the National Bureau of Standards, Nos. 87, 130, 169.)

cence spectrum. The plates were traced by means of a Zeiss recording microphotometer, using a frequency-scale magnification of 2. The tracings were measured by means of a SIP (Societe Genevoise) microscope comparator, and calibrated from the dispersion curve of the spectrograph.

The important result of these experiments is the near coincidence of the O−O bands of absorption and fluorescence, evident in Fig. 3,[18] with $\bar{\nu}_A = 31737$ cm^{-1} and $\bar{\nu}_F = 31626$ cm^{-1}. (O−O bands.) The phosphorescence spectrum[10] is included for comparison, with $\bar{\nu}_P = 21320$ cm^{-1}.

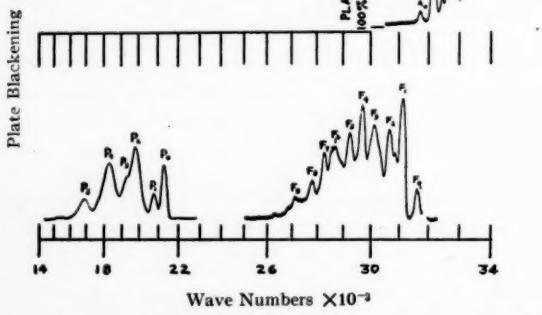

FIG. 3. Absorption and luminescence spectra of naphthalene in rigid glass solution at 77°K. *Absorption bands*, A_0−31737 cm^{-1}, A_1−32104, A_2−32437, A_3−32596, A_4−32810, A_5−33103, A_6−33628, A_7−33559 (±30 cm^{-1}; E. K. 103F plate, slit 0.05 mm, 60 sec.). *Fluorescence bands*, F_0−31626, F_1−31144, F_2−30675, F_3−30148, F_4−29736, F_5−29274, F_6−28752, F_7−28329, F_8−27871, F_9−27211 (±30 cm^{-1}; E. K. 103F plate, slit 0.10 mm, 30 min. (Cf. footnote 18.) *Phosphorescence bands*, from the paper by Lewis and Kasha, spectrum recalibrated, P_0−21316, P_1−20854, P_2−19895, P_3−19412, P_4−18438, P_5−17046 (±60 cm^{-1}; E. K. III-F plate, slit 0.50 mm, 1 hour).

It was found also that the naphthalene fluorescence spectra (rigid glass solutions, 77°K) excited by approximately monochromatic 3000A and 2600A light[19] were indistinguishable from that shown in Fig. 3, despite the fact that different electronic states are excited by these two wave-lengths. This result is a consequence of the phenomenon of internal conversion,[20] by which a unique fluorescence from lowest excited singlet state is effected.

The frequency of the O−O band is found to vary with the nature of the medium in which the molecule is studied. A comparison of data for the frequency of the O−O band of the lowest singlet-singlet transition in naphthalene in various phases is made in Table I. The same pattern is followed by analogous data for phenanthrene, whereas for anthracene the data seem to follow another trend.[20a]

4. RE-INTERPRETATION OF THE ABSORPTION AND FLUORESCENCE SPECTRA OF THE NAPHTHALENE SINGLE CRYSTAL AT 20°K

Prikhotko[21] has studied the absorption spectrum of single crystals of naphthalene at 20°K, using natural and polarized light; she measured a multitude of extremely sharp lines, with varied polarization characteristics. Prikhotko's analysis indicated pure electronic transitions at (I) 33736 cm^{-1}, (II) 31960 cm^{-1}, (III) 31060 cm^{-1}, and an unidentified state (IV) at 29945 cm^{-1}. Without inquiring into the vibrational[22] analysis in any detail, it may be noted that the *fluorescence* spectrum[23] of crystals of naphthalene at 20°K begins with the principle line 31062 cm^{-1} (see below) and consists of a sequence of lines extending to lower frequencies. This line corre-

[18] The break (caused by the 3126 Hg line group) in the fluorescence tracing just to the right of band marked F_0, hides an additional fluorescence band, sharper and fainter than F_0, and at 31946 cm^{-1}. If F_0 at 31626 cm^{-1} is the O−O fluorescence band as assumed (and which seems plausible from the comparison made in Fig. 3), the 31946 cm^{-1} band would correspond to emission from a vibrationally excited level of the excited state, 320 cm^{-1} above the zero-point level; the Boltzman factor for 320 cm^{-1} at 77°K is 0.0025. A number of exceedingly faint fluorescence lines at even higher frequencies is obtained upon prolonged exposure.

[19] Filter combinations *C* and *E*, M. Kasha, J. Opt. Soc. Am. **38**, 929 (1948).

[20] An excellent discussion of this phenomenon has been given by J. Franck and H. Sponer, "A comparison of predissociation and internal conversion in polyatomic molecules," Victor Henri Commemorative Volume (*Contribution á l'Etude de la Structure Moléculaire*), Desoer, Liège, Belgium, 1948, p. 169.

[20a] *Note added in proof:* Dr. G. Nordheim at Duke University (Unpublished results presented at the American Physical Society Meeting, Washington, D. C., April 29, 1949), using a new assignment of the O−O band in the vapor spectrum of naphthalene, has obtained a more reasonable comparison of frequencies for the various states of aggregation. Dr. Nordheim has further pointed out that the low relative intensity of the O−O band in absorption and fluorescence is evidence for a forbidden transition mechanism.

[21] A. Prikhotko, J. Phys. (U.S.S.R.) **8**, 257 (1944).

[22] The tacit assumption was made that vibrational frequencies for the ground state of naphthalene (Raman data) could be applied to the analysis of vibrational combinations for the excited state, determined by the absorption spectrum.

[23] I. V. Obreimov and C. G. Shabaldas, J. Phys. (U.S.S.R.) **7**, 168 (1943). Also given in Prikhotko's paper (reference 21) as Fig. 1.

sponds within experimental error with the first principle absorption line at 31060 cm^{-1} (the faint anomalous 29945 cm^{-1} absorption band is considered in Section 5).

Several faint anomalous fluorescence lines, occurring at higher frequencies than 31062 cm^{-1}, may be interpreted as follows. The coincidence of these fluorescence lines with some of the absorption lines may be considered to be fortuitous. The existence of the former may be accounted for by assuming (a) they represent emissions from a *lattice-oscillation plus an electronic level* $=l+E$, or (b) *the lines are Raman lines representing lattice oscillations* $=R_l$ (the crystal fluorescence spectrum was obtained by exposure to the light of the mercury arc for times up to 17 hours). The anomalous lines (1–7, below) may be accounted for according to the following scheme. The observed lattice oscillation frequencies[21, 23, 24] of the naphthalene crystal are 18, 24, 44, 71, 105, 124 cm^{-1}. Line (1) 31965; assume R_l from 31985 Hg: calc. $1(18)=18$, obs. 20. Line (2) 31960; assume R_l from 31985 Hg: calc. $1(24)=24$, obs. 25. Line (3) 31463; assume $l+E$ (31060): calc. $2(124)+2(71)=390$, obs. 401 (above zero point energy). Line (4) 31239; assume $l+E$: calc. $1(105)+1(71)=176$, obs. 177. Line (5) 31212; assume $l+E$: calc. $1(105)+1(44)=149$, obs. 150. Line (6) 31109; assume $l+E$: calc. $1(44)=44$, obs. 47. Line (7) 31090; assume $l+E$: calc. $1(24)=24$, obs. 28. It is also possible that some of the lines may represent anti-Stokes emission from excited molecular vibrational levels.

Comparing the results presented in Section 3 on the absorption and fluorescence bands of naphthalene in rigid glass solution at 77°K with those obtained[21, 23] for the single crystal at 20°K, it is evident that the observed optical phenomena are virtually identical. In particular, accepting the above interpretation of the anomalous fluorescence lines, it is found that in both condensed systems a unique fluorescence emission from the lowest excited singlet state to the ground state occurs. The only significant difference is that in dilute rigid glass solutions molecular vibrational levels of the upper state may be observed (in addition to the ground state vibrations of the molecule, which of course, dominate the fluorescence spectrum), while in crystals lattice-vibrational levels may also be excited, both giving rise to anti-Stokes fluorescence lines. Although the Boltzman factors are very small at these low temperatures, the photographic technique used permits the recording of very faint lines. When line sources are used to excite the luminescence, Raman scattering may complicate the spectrum as well.

Thus, in the crystal the 31060 cm^{-1} band is the lowest O−O singlet-singlet absorption band. Since many vibrations of each symmetry class must exist in naphthalene, varied polarization characteristics may be expected for various vibrational-electronic bands. This, and the nature of Prikhotko's vibrational analysis[22] throw doubt on the postulate of any separate electronic levels between the 31060 cm^{-1} level and the 33736 cm^{-1} level[24a] (assuming that the latter represents the O−O band of the first *strong* singlet-singlet transition). In particular, evidence for several electronic states in this region is not to be had from the previous interpretation[21, 23] of "resonance fluorescence" from each electronic level. Such an interpretation overlooks the phenomenon of internal conversion (Cf. Section 3), and also fails to account for most of the lower frequency fluorescence lines. It remains to explain the 29945 cm^{-1} band.

TABLE I. Influence of environment on O−O frequency of lowest singlet-singlet transition in naphthalene.

Rigid glass solution,* 77°K	31680†
Vapor, *ca.* 570°K	31322[a, b]
	31320[c]
Methylcyclohexane solution, 298°K	31250**
hexane solution, 298°K	31182[b]
Single crystal, 20°K	31060[d]
Crystal, 298°K	30580[c]

* Cf. reference 9. ** Cf. Fig. 2. † Present work, mean of absorption and fluorescence O−O band.
[a] V. Henri and H. de Laszlo, Proc. Roy. Soc. (London) **A105**, 662 (1924).
[b] H. G. de Laszlo, Zeits. f. physik. Chemie **118**, 369 (1925).
[c] P. K. Seshan, Proc. Indian Acad. Sci. **A3**, 148 (1936).
[d] See reference 21.

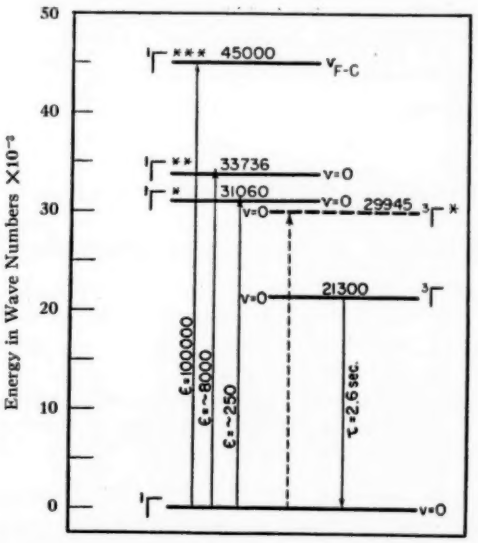

FIG. 4. Energy scheme for the π-electron levels of the naphthalene molecule observed below 50000 cm^{-1} (source of data given in Section 6).

[24] E. Gross and M. Vuks, Nature **135**, 998 (1935); J. de phys. et rad. **7**, 113 (1936).

[24a] *Note added in proof:* However, a recent study by A. S. Davydov [J. Exper. Theor. Phys. (U.S.S.R.), **18**, 210 (1948)] suggests that in a *crystal* a non-degenerate molecular energy level may become degenerate for the crystal as a whole, as a consequence of interaction between molecules having different lattice orientations. The 31960 and 31060 cm^{-1} bands, if true O−O bands, could be the split components of such a level.

5. HYPOTHESIS OF THE 29945 cm^{-1} ABSORPTION BAND AS A $^3\Gamma^* \leftarrow {}^1\Gamma$ TRANSITION

The anomalous 29945 cm^{-1} absorption band of naphthalene is a very faint band, requiring a 1.5 mm path of crystal for its detection;[21] it is accompanied by a sequence of observed but immeasurable faint lines at higher frequencies. The 31060 cm^{-1} level was shown to be the lowest excited singlet level (Section 4). Therefore, the 29945 cm^{-1} level is either a level of another multiplicity, or it is due to an impurity.

The *lowest triplet* ($^3\Gamma$) level of naphthalene has been found[10] to be at 21320 cm^{-1} (cf. Fig. 3). This assignment has been confirmed by subsequent work.[11,17] If the 29945 cm^{-1} band is due to a triplet level, there are but two alternatives for its explanation: (a) the 29945 cm^{-1} band represents absorption from the ground singlet ($^1\Gamma$) to the first *excited* triplet level ($^3\Gamma^*$). This interpretation would allow the band to appear in a fluid system as well as in a crystalline one. Furthermore, the lowest triplet-triplet difference would be 8640 cm^{-1}, for which there should exist an absorption band ($^3\Gamma^* \leftarrow {}^3\Gamma$) in the near infra-red at this frequency ($\lambda = 11500$A), *while a crystal or a rigid glass* (both at low temperature) *is illuminated with an intense beam of ultraviolet light of wave-length* <3000A, so that a moderate concentration of the naphthalene molecules may be excited to the lowest triplet state.[25]

The other, and less likely explanation is, (b) the 29945 cm^{-1} band already represents the $^3\Gamma^* \leftarrow {}^3\Gamma$ absorption. In this case, the faintness of the band could be attributed to the small concentration of triplet state ($^3\Gamma$) molecules excited by the source used in the study of the 20°K crystal absorption spectrum. Thus, the intensity of the 29945 cm^{-1} absorption band would depend on the intensity of the light source used to obtain the absorption spectrum in the normal absorption region. It should be emphasized that the crystal must be at a low temperature (20°K, or 77°K) to minimize external quenching of the lowest triplet state. This implies that the 29945 cm^{-1} band would selectively vanish from the spectrum of liquid naphthalene or naphthalene in liquid solution, if the second interpretation is correct.

[25] Cf. Section 11, in M. Kasha, Chem. Rev. 41, 401 (1947).

6. THE π-ELECTRON ENERGY LEVELS OF NAPHTHALENE BELOW 50000 CM^{-1}

Figure 4 presents the experimentally observed singlet and triplet π-electron energy levels of naphthalene below 50000 cm^{-1}. The singlet levels 31060 and 33736 cm^{-1} are from the 20°K crystal work of Prikhotko,[21] as discussed in Section 4. The 29945 cm^{-1} level, also given by Prikhotko's measurements, is assigned tentatively according to one of the suggestions made in Section 5. The lowest triplet level is obtained from the phosphorescence spectrum,[10] and the singlet level at 45000 cm^{-1} (Franck-Condon frequency; O−O frequency at about 43000 cm^{-1}) is taken from the absorption spectrum in solution.[8]

The molar absorption coefficients are those obtained for solutions also, and the phosphorescence lifetime is from McClure's work.[11]

Note added in proof: Since the data given in Fig. 4 are for various states of aggregation, which, as seen from Table 1, affect the absolute energy of a transition, the electronic states compared may be considered to be properly represented only to about ± 500 cm^{-1}, unless one takes proper account of the phases involved.

THE JOURNAL OF CHEMICAL PHYSICS VOLUME 17, NUMBER 6 JUNE, 1949

Statistical Mechanics of Adsorption. V. Thermodynamics and Heat of Adsorption*

TERRELL L. HILL
Department of Chemistry, University of Rochester, Rochester, New York
(Received May 17, 1948)

The thermodynamics of an adsorbate on an inert adsorbent is discussed in some detail. Heats of adsorption are given particular attention in an attempt to clarify and extend the available methods in this field. It is found that the true equilibrium $\Delta H = T\Delta S$ of adsorption for *adsorbate molecules* is given by

$$(\partial \ln p/\partial T)_\varphi = -\Delta H/RT^2,$$

where φ is the two-dimensional spreading pressure.

The relation of the work of Rowley and Innes to the present paper is considered.

I. INTRODUCTION

THERE appears to be a certain amount of disagreement among workers in the field of adsorption concerning the application of thermodynamics to adsorption data. The purpose of this paper is to attempt to clarify this situation and, at the same time, to introduce a number of new results.[1-3]

* Presented at an A.A.A.S. Gordon Research Conference, New London, New Hampshire, June 23, 1948.

[1] For a recent discussion of heats of adsorption see S. Brunauer, *The Adsorption of Gases and Vapors* (Princeton University Press, Princeton, 1943), pp. 218–226.

[2] A very detailed treatment of certain aspects of the heat

Statistical models will be used only incidentally here. However, because of the close relationship between thermodynamics and statistical mechanics, it does not seem improper to include this paper in a series which has used statistical methods for the most part.

Perhaps the most important application anticipated of the results obtained here is the following: Up to the present time, an adsorption theory for an adsorbate on an inert adsorbent (e.g., the *BET* theory) could be tested correctly only by comparing theoretical and experimental isotherms. (This means, essentially, comparing theoretical and experimental Gibbs free energies.) The methods of this paper show how to break down both the experimental and theoretical free energies of the *adsorbate* molecules into internal energies, heat contents, and entropies. This will allow a much more intimate experimental test of these adsorption theories. The agreement between theoretical and experimental isotherms is a necessary, but not a sufficient, condition for the correctness of a theory. The theory must also predict correctly the entropy (or the heat content, or the temperature dependence of the isotherm).

II. THERMODYNAMICS OF ADSORPTION

We do not attempt a completely general treatment here. We hope to extend the generality in various obvious directions at a later time. However, the special case considered is the one of by far the greatest interest to most workers in the field at present.

We restrict ourselves to adsorption of a single gas (except for the first few equations) onto a solid or liquid phase. We assume further that the adsorbent is completely inert—that all its thermodynamic properties are the same in the presence as in the absence of adsorbate molecules. This approximation allows one to make more detailed progress (in a limited field) over that permitted by Gibbs' general thermodynamic treatment of surface phases.[4] Certainly adsorbate[4a] molecules will perturb surface adsorbent molecules but this perturbation is probably (the problem has not been studied as far as the writer is aware) a strictly second-order effect in the case of physical adsorption on solids, especially solids with relatively strong intermolecular or interionic forces. However, this approximation may well be inaccurate in the physical adsorption of gases on liquids or in chemisorption. In fact, in chemisorption, except when a very light atom is adsorbed on a very heavy atom (e.g., hydrogen on tungsten), the approximation is presumably quite unjustified. We indicate in Appendix II, as an example, how the adsorption isotherm is affected by adsorbent perturbation in an extremely simple case.

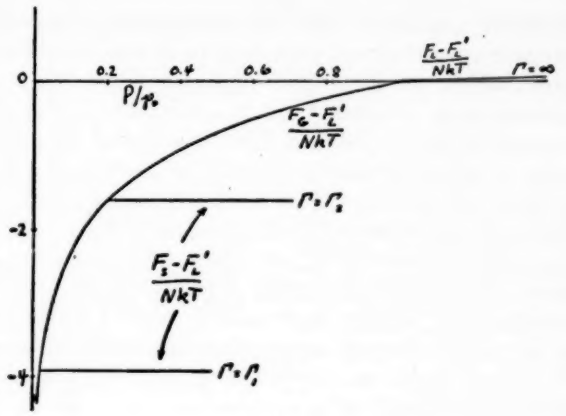

FIG. 1.

Porous adsorbents are not excluded. In fact, so long as the above fundamental assumption is valid (see also below), adsorption or absorption of a gas by any material is included. A polymeric adsorbent that swells is obviously excluded, as is a liquid in which the gas is soluble.

With the above assumption we can discuss the thermodynamic functions of the *adsorbate*[4a] *molecules alone*, as is done, for example, by Fowler and Guggenheim[5] for unimolecular adsorption. This is in contrast with thermodynamic discussions of the type given by W. D. Harkins and co-workers, in which the solid is explicitly included, following Gibbs.

We assume further that the surface area and structure of the adsorbent are independent of temperature and pressure.

We now proceed to a discussion of the adsorbate,[4a] using standard thermodynamic methods.[6] Suppose we have an adsorbed phase (considered by itself and in general not in equilibrium with gas) of internal energy E_s, entropy S_s, on a surface of area $\mathfrak{A}$, and containing N_{si} molecules of type i. To be as general as possible, we must think of E_s, for example, as depending not only on S_s, $\mathfrak{A}$, and the N_{si}, but also on the volume of the adsorbate V_s (Eq. (1)). For many purposes it will be desirable to substitute the pressure P for V_s as an inde-

of adsorption is given by E. Huckel, *Adsorption and Kapillarkondensation* (Akademische Verlagsgesellschaft, Leipzig, 1928).

[3] The related work of H. H. Rowley and W. B. Innes is discussed in Section VI.

[4] E. A. Guggenheim, *Modern Thermodynamics* (Methuen and Company, Ltd., London, 1933), Chapter 12.

[4a] We use the term "adsorbate" to refer specifically to adsorbed molecules and do *not* include gas molecules in equilibrium with adsorbed molecules.

[5] R. H. Fowler and E. A. Guggenheim, *Statistical Thermodynamics* (Cambridge University Press, London, 1939), Chapter 10. The energy of interaction between the adsorbate molecules and the adsorbent is assigned to the adsorbate. The adsorbent merely furnishes an external potential field for the adsorbate.

[6] See, for example, reference 4, Chapter I; or reference 5, pp. 55–62 and especially Eq. (1012, 16).

pendent variable. Now the properties of an adsorbate consisting of only one or a few layers will presumably be even less dependent on P as an independent variable than is a liquid (see the discussion of Fig. 1 below). (In most cases it is difficult, if not impossible, to think of an *experimental* method of varying P as an independent variable without otherwise perturbing the adsorbate.) However, the properties of an adsorbate consisting of *many* layers will certainly depend on P. As the number of layers approaches infinity, the dependence on P approaches that of the liquid state. We shall want to show the transition from adsorbate to liquid in a number of cases, so we include the extra independent variable P in many equations. One can think of the pressure P as being defined by an equation such as Eq. (3), if one likes.

Note added November 12, 1948: We shall discuss the fundamental point of view from which the present paper is developed, including the significance of the pressure P introduced above, in more detail in a subsequent paper (IX) devoted primarily to the thermodynamics of adsorption on a perturbed adsorbent (e.g., in chemisorption). For perturbations that do not involve changes in area or volume of the adsorbent, it turns out that the equations of the present paper still apply provided somewhat more general definitions of the thermodynamic functions are adopted. Also, reference will be made to an important paper by Guggenheim [Trans. Faraday Soc. **36**, 397 (1940)] which recasts the general treatment of Gibbs into a form that is more satisfactory from a physical point of view.

Note added in proof: In fact, we have recently found that it is easy to extend formally the thermodynamic methods of this paper to *any* kind of adsorbent or absorbent (including swelling, solution, etc.). This is accomplished by avoiding the concept of "area."

In considering the internal energy E_s of the adsorbate, the natural[6] choice of independent variables is S_s, V_s, $\mathfrak{A}$, and the N_{si}. Let φ be the usual two-dimensional (spreading) pressure and μ_{si} be the chemical potential of the ith component in the adsorbate. Then

$$dE_s = TdS_s - PdV_s - \varphi d\mathfrak{A} + \sum_i \mu_{si} dN_{si}. \quad (1)$$

Also

$$dE_s = (\partial E_s/\partial S_s)_{V_s,\mathfrak{A},N_{si}} dS_s + (\partial E_s/\partial V_s)_{S_s,\mathfrak{A},N_{si}} dV_s + (\partial E_s/\partial \mathfrak{A})_{S_s,V_s,N_{si}} d\mathfrak{A} + \sum_i (\partial E_s/\partial N_{si})_{S_s,V_s,\mathfrak{A},N_{sj}} dN_{si} \quad (2)$$

Comparing Eqs. (1) and (2) we have

$$(\partial E_s/\partial N_{si})_{S_s,V_s,\mathfrak{A},N_{sj}} = \mu_{si},$$

$$(\partial E_s/\partial V_s)_{S_s,\mathfrak{A},N_{si}} = -P, \text{ etc.} \quad (3)$$

We define the Helmholtz free energy in the usual way: $A_s = E_s - TS_s$. Then

$$dA_s = dE_s - TdS_s - S_s dT = -PdV_s - \varphi d\mathfrak{A} - S_s dT + \sum_i \mu_{si} dN_{si}. \quad (4)$$

This gives

$$(\partial A_s/\partial N_{si})_{V_s,\mathfrak{A},T,N_{sj}} = \mu_{si},$$

$$(\partial A_s/\partial \mathfrak{A})_{V_s,T,N_{si}} = -\varphi, \text{ etc.} \quad (5)$$

We define the Gibbs free energy by

$$F_s = \sum_i \mu_{si} N_{si}. \quad (6)$$

Then, by integrating Eq. (1) or Eq. (4), keeping intensive properties constant, we find $F_s = A_s + PV_s + \varphi\mathfrak{A}$. Using this result and Eq. (4), we obtain

$$dF_s = -S_s dT + V_s dP + \mathfrak{A} d\varphi + \sum_i \mu_{si} dN_{si} \quad (7)$$

and

$$(\partial F_s/\partial N_{si})_{T,P,\varphi,N_{sj}} = \mu_{si},$$

$$(\partial F_s/\partial P)_{T,\varphi,N_{si}} = V_s, \text{ etc.} \quad (8)$$

We define H_s by the equation $F_s = H_s - TS_s$. From this definition it follows that $H_s = E_s + PV_s + \varphi\mathfrak{A}$, and

$$dH_s = TdS_s + V_s dP + \mathfrak{A} d\varphi + \sum_i \mu_{si} dN_{si}. \quad (9)$$

As is well known, $\varphi = \gamma_0 - \gamma$, where γ_0 is the surface tension of the clean surface and γ is the

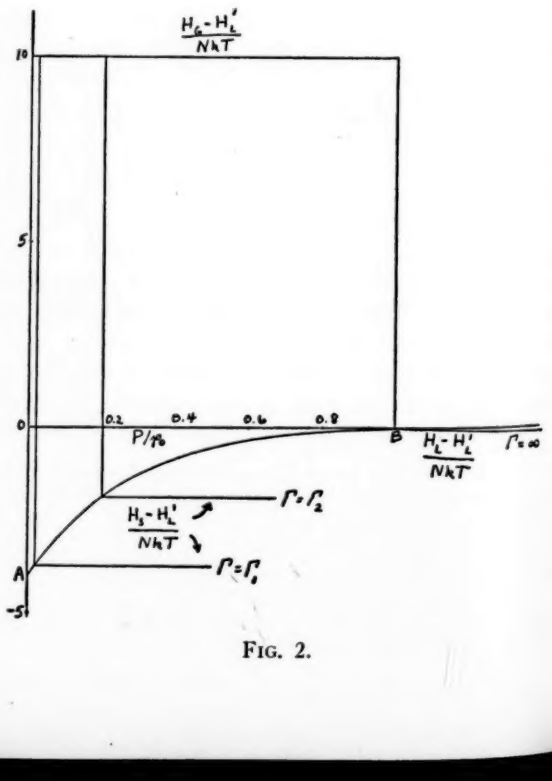

FIG. 2.

surface tension of the surface with adsorbate.[7a] It is not necessary to know the absolute area $\mathfrak{A}$ in order to carry out thermodynamic calculations of interest; it suffices that $\mathfrak{A}$ is proportional to the mass of adsorbent. Indeed, for some porous adsorbents (or absorbents) there is no unique definition of $\mathfrak{A}$, but $\varphi\mathfrak{A}$ is always uniquely defined.

The term PV_s in the above equations is in general of negligible importance. $\varphi\mathfrak{A}$ plays here the role analogous to PV in ordinary three-dimensional thermodynamics.

From

$$dF_s=\sum_i \mu_{si}dN_{si}+\sum_i N_{si}d\mu_{si}$$

and Eq. (7), we have

$$\sum_i N_{si}d\mu_{si}=-S_sdT+V_sdP+\mathfrak{A}d\varphi, \qquad (10)$$

$$d\varphi=\sum_i \Gamma_i d\mu_{si}-(V_sdP/\mathfrak{A}), \quad (T \text{ constant}) \qquad (11)$$

where $\Gamma=N_s/\mathfrak{A}$. From this point on in the present paper we consider only a one-component adsorbate. Now suppose we have a gas phase in equilibrium with the adsorbate. Then[7b] (we write p for the equilibrium or vapor pressure—this use of p and P seems desirable but it is not a completely satisfactory notation),

$$d\mu_s=d\mu_G=(\partial\mu_G/\partial p)_T dp=v_G dp \quad (T \text{ constant}), \qquad (12)$$

where

$$v_G=V_G/N_G. \quad \text{Also,} \quad v_s=V_s/N_s.$$

Then

$$d\varphi=\Gamma(v_G-v_s)dp \quad (T \text{ constant}). \qquad (13)$$

This derivation is equivalent to putting $dT=0$ in Eq. (83). For a perfect gas this becomes

$$d\varphi=\Gamma[(kT/p)-v_s]dp \quad (T \text{ constant}). \qquad (14)$$

If we ignore the usually negligible quantity v_s, we have

$$d\varphi=\Gamma kTd\ln p \quad (T \text{ constant}). \qquad (15)$$

This is the well-known "Gibbs equation" which can be used in integral form, as pointed out by Bangham, to calculate φ from the adsorption isotherm $\Gamma=\Gamma(p)$. It should be remembered, though, that Eq. (14) involves two approximations, as the above derivation shows. Equation (12), on the other hand, is exact.[8a]

If the gas dissociates on adsorption, we can simply ignore this from a *thermodynamic* point of view. The *gas species* is taken as the fundamental component.

For convenience, the following discussion applies specifically to a non-porous adsorbent and to a temperature below the critical temperature but above the triple point of the gas being adsorbed. (Let us call this "case A" for future reference.) The chemical potentials μ_G and μ_L for the gas and liquid phases are functions of P and T only. At equilibrium between the two phases, $\mu_G(p,T)=\mu_L(p,T)$. This equation gives the equilibrium (vapor) pressure $p=p(T)$. In the P,T plane, only at points on the curve $p=p(T)$ can liquid and gas phases be in equilibrium. When there is equilibrium between gas and adsorbate, $\mu_G(p,T)=\mu_s(\Gamma,p,T)$, where $\Gamma=N_s/\mathfrak{A}$. For small Γ the dependence of μ_s on P is negligible. As Γ approaches infinity, the dependence of μ_s on Γ becomes negligible (liquid). In any case this equality gives the equilibrium pressure $p=p(\Gamma,T)$. Thus a Γ can usually be found such that equilibrium can exist for an *arbitrary* point in the P,T plane.

Figures 1, 2, and 3 (see Eqs. (93)) are designed to illustrate qualitatively for a *hypothetical* case the relationships between F, H, and S for gas, liquid, and adsorbate.[4a] Curves for actual theoretical and experimental systems will be published later. Figure 1 gives $(F_G-F_L')/NkT$, $(F_L-F_L')/NkT$ and $(F_s-F_L')/NkT$ plotted against P/po (po is the vapor pressure of the liquid at T) at constant

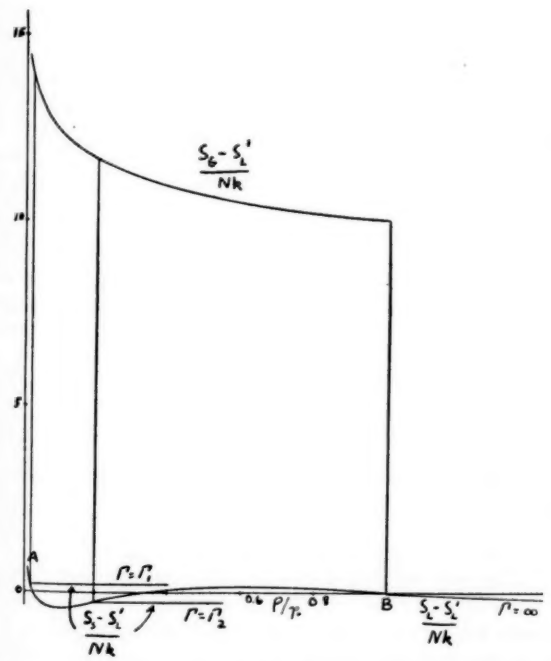

FIG. 3.

[7a] The symbol π is used by Harkins and co-workers where we use φ. We are following the notation of Fowler and Guggenheim. The mathematical constant π occurs in statistical mechanical equations and π is also used for osmotic pressure, so we prefer φ to π for the spreading pressure. Harkins' σ is $1/\Gamma=\mathfrak{A}/N_s$ in our notation.

[7b] The discussion in Fowler and Guggenheim (reference 5) on pp. 60–61 and 65 is sufficiently general to show that $\mu_G=\mu_s$ is the condition for equilibrium here, as usual. It therefore follows that $H_G-H_s=T(S_G-S_s)$ at equilibrium.

[8a] By "exact" used in this sense we shall mean that the equation has been deduced without introducing approximations in addition to those discussed prior to Eq. (1).

temperature. F_L' refers to a reference state which is chosen, for convenience, as the liquid state at $P=po$. For the adsorbate a different curve is needed for each value of Γ (e.g., Γ_1 and Γ_2). The liquid curve corresponds to $\Gamma=\infty$. Equilibrium between gas and adsorbate, for a given Γ, exists where the gas and adsorbate free energy (chemical potential) curves intersect. The equilibrium gas pressure can then be read off as a function of Γ. The dependence of F_L (and also H_L and S_L) on P at constant temperature is rather slight ($\Gamma=\infty$). The extent of this dependence should decrease with Γ so that the hypothetical curves for small Γ are virtually parallel to the pressure axis.

Figure 2 gives $(H_S-H_L')/NkT$, etc., and Fig. 3 gives the entropy. There are, of course, equal discontinuities in H and TS on adsorption, since $\Delta F=0$. ΔH, and therefore $T\Delta S$, depends on the value of Γ. The curves AB in Figs. 2 and 3 connect the various equilibrium values of H_s and S_s for different Γ's. As $P\to 0$, $\Delta H\to$finite and $S_G\to+\infty$. It therefore follows that $S_s\to+\infty$.

III. INTEGRAL, DIFFERENTIAL, ISOTHERMAL, AND RELATED HEATS OF ADSORPTION. HEAT CAPACITY

We shall use small capital letters to represent molecular thermodynamic functions (e.g., $H_s=H_s/N_s$). Suppose we have a system consisting of a closed container immersed in a large isolated constant temperature bath (at temperature T). The adsorbent (see below) and the walls of the container are considered part of the bath. The bath has an initial internal energy E_b. The container is divided into two parts connected by a stopcock. Initially, one part contains N molecules of a perfect gas and the other part contains an evacuated adsorbent of area $\mathfrak{A}$. The stopcock is opened and equilibrium is eventually established. Initially, the total energy of the complete isolated system is E_b+NE_G. E_G is a function of temperature only. Let E_b' be the internal energy of the bath in the final equilibrium state and suppose N_s molecules have been adsorbed. Then the total final energy of the system is $E_b'+(N-N_s)E_G+N_sE_s$. E_s is nominally a function of $\Gamma=N_s/\mathfrak{A}$, T, and P. But, since this is an equilibrium state, $P=p=p(\Gamma,T)$. Hence $E_s=E_s(\Gamma,T)$. The system is isolated so

$$E_b+NE_G=E_b'+(N-N_s)E_G+N_sE_s. \tag{16}$$

The integral heat of adsorption $Q(N_s,\mathfrak{A},T)$ is defined as the heat absorbed by the bath in the above process:

$$Q=E_b'-E_b=N_s(E_G-E_s). \tag{17}$$

The differential heat of adsorption q_d is defined as

$$q_d=(\partial Q/\partial N_s)_{\mathfrak{A},T}.$$

Hence

$$q_d=E_G-E_s-N_s(\partial E_s/\partial N_s)_{\mathfrak{A},T}. \tag{18}$$

These expressions for Q and q_d are, of course, well known.

We now consider the isothermal heat of adsorption. Suppose we have a container immersed in a bath as before. There is (perfect) gas in equilibrium with adsorbate in the container. Let V be the volume of the container less the volume of the adsorbent. Then $N=N_G+N_s$ and $V=V_G+V_s$. A frictionless piston forms one wall of the container. The piston is moved infinitely slowly (T constant) so that V changes by dV and a new equilibrium state is reached. Let E be the total initial internal energy of the system (bath plus container):

$$E=E_b+(N-N_s)E_G+N_sE_s. \tag{19}$$

Then, as a result of the change dV,

$$dE=-pdV=dE_b-E_GdN_s+N_sdE_s+E_sdN_s. \tag{20}$$

The quantities dV, dN_s, and dE_s are not independent. We have

$$p(V-N_sv_s)=(N-N_s)kT, \tag{21}$$

where $v_s=V_s/N_s$. Let us ignore the trivial change in v_s in the process; then

$$pdV-pv_sdN_s+(V-V_s)dp=-kTdN_s. \tag{22}$$

We now make use of the (equilibrium) adsorption isotherm in the form $N_s=\mathfrak{A}\Gamma(p,T)$. This gives, for $\mathfrak{A}$ and T constant as in the present discussion,

$$dN_s=\mathfrak{A}(\partial\Gamma/\partial p)_Tdp. \tag{23}$$

Combining Eqs. (22) and (23), we get

$$-pdV=\left[\frac{V-V_s}{\mathfrak{A}(\partial\Gamma/\partial p)_T}-pv_s+kT\right]dN_s. \tag{24}$$

We now substitute Eq. (24) and

$$dE_s=(\partial E_s/\partial N_s)_{\mathfrak{A},T}dN_s \tag{25}$$

into Eq. (20), obtaining finally, on dividing through by dN_s,

$$q_{ih}=(\partial E_b/\partial N_s)_{\mathfrak{A},T}=E_G+kT-(E_s+pv_s) -N_s(\partial E_s/\partial N_s)_{\mathfrak{A},T}+[(V-V_s)/\mathfrak{A}(\partial\Gamma/\partial p)_T], \tag{26}$$

where q_{ih} is the isothermal heat of adsorption. For all practical purposes Eq. (26) may be written (dropping pv_s and V_s)

$$q_{ih}=H_G-E_s-N_s(\partial E_s/\partial N_s)_{\mathfrak{A},T} +[V/\mathfrak{A}(\partial\Gamma/\partial p)_T]. \tag{27}$$

Then

$$q_d+kT+[V/\mathfrak{A}(\partial\Gamma/\partial p)_T]=q_{ih}. \tag{28}$$

The significance of the important term involving $(\partial\Gamma/\partial p)_T$ can perhaps best be seen from (Eqs.

(23) and (24))

$$dN_s = -pdV/[kT+(V/\mathfrak{A}(\partial\Gamma/\partial p)_T)] \quad (29)$$

and

$$dp = -pdV/[V+\mathfrak{A}kT(\partial\Gamma/\partial p)_T]. \quad (30)$$

Consider (case A) two special cases. (i) If no gas molecules are adsorbed or desorbed when the piston is moved, $(\partial\Gamma/\partial p)_T=0$, $dN_s=0$, and $dp=-pdV/V$ (i.e., $pV=$constant). Also, $dE_b=-pdV$ (Eq. (20)). (ii) If $\Gamma=\infty$ (adsorbate=liquid), $(\partial\Gamma/\partial p)_T=\infty$, $dN_s=-pdV/kT$, $dp=0$, and (Eq. (26)) $q_{th}=H_G-H_L'$. The adsorption case is intermediate between these two extremes. The term involving $(\partial\Gamma/\partial p)_T$ is clearly the crucial term in tracing the transition from case (i), through the intermediate adsorption case, to case (ii). This term has, so far as the writer is aware, always been omitted from Eq. (28). The error has arisen because $-dV$ has been taken as the volume of gas adsorbed. Actually, the volume adsorbed is, from Eq. (29),

$$kTdN_s/p = -dV/[1+[V/\mathfrak{A}kT(\partial\Gamma/\partial p)_T]]. \quad (31)$$

This volume is equal to $-dV$ only for the liquid case.

Calorimetric Heat of Adsorption

The meaning of calorimetric heats as usually measured is obscure[1]—each case depends on the apparatus and procedure. One way of avoiding this in principle is to use the schematic apparatus described above relating to the integral and differential heats of adsorption. That is, let the perfect gas reservoir, the adsorption bulb, and the connection between these two containers all be in the calorimeter and at the same temperature. The calorimetric heat will then give just the integral and differential heats discussed above. This is, unfortunately, rather impractical from an experimental point of view. An alternative arrangement would be to have the perfect gas reservoir and the connection not in the calorimeter but in a separate thermostat at the same temperature as the calorimeter. However, this is not satisfactory for the same reason that calorimetric heats as currently measured are not satisfactory—one does not know how much of the heat evolved after the stopcock is opened goes to the calorimeter and how much to the separate thermostat (unless this thermostat is a second calorimeter).

What would seem to be a better way of measuring calorimetric heats is the following: A container is inside the calorimeter. The container is divided into two parts connected by a stopcock. Initially, one part contains the adsorbent, N_s molecules of adsorbate[4a] and $N-N_s$ molecules of a perfect gas (occupying a volume $V_G=V_1$) in equilibrium with the adsorbate, while the other part of the container (of volume V_2) is evacuated. Preferably $V_1 \gg V_2$. The stopcock is now opened, and a new equilibrium state is reached with $N_s'<N_s$ and $V_G'=V_1+V_2-\Delta V_s>V_1$. Let us suppose first that V_2 is a differential volume dV. Then (Eq. (19)) is initially,

$$E=E_b+(N-N_s)E_G+N_sE_s \quad (32)$$

and, as a result of the change dV,

$$dE=0=dE_b-E_GdN_s + N_s(\partial E_s/\partial N_s)_{\mathfrak{A},T}dN_s+E_sdN_s. \quad (33)$$

Thus the heat absorbed by the calorimeter is

$$dE_b=q_ddN_s. \quad (34)$$

Then

$$(\partial E_b/\partial N_s)_{\mathfrak{A},T}=q_d. \quad (35)$$

For a finite change

$$\int_{E_b}^{E_b'} dE_b=\int_{N_s}^{N_s'} q_ddN_s=\int_{N_s}^{N_s'}(\partial Q/\partial N_s)_{\mathfrak{A},T}dN_s \quad (36)$$

or

$$E_b'-E_b=Q(N_s')-Q(N_s) = N_s'[E_G-E_s(N_s')]-N_s[E_G-E_s(N_s)], \quad (37)$$

where Q is the integral heat of adsorption already discussed.

Entropy Changes. Reversible and Irreversible Processes

In any of the above processes let q_b be the heat absorbed by the bath, let q_m be the heat absorbed by the N molecules and let ΔS_m be the entropy change in the N molecules. Then $q_m=-q_b$, $\Delta S_m=q_m/T$ for a reversible process, and $\Delta S_m>q_m/T$ for a natural (irreversible) process. For a reversible process q_b therefore gives ΔS_m immediately.

We may first note that the process leading to Eqs. (26) and (28) is reversible while the process giving Eq. (35) is natural (taking $dV>0$, $dN_s<0$). The two processes have the same initial and final states and therefore the same ΔS_m. This requires then that $q_m(\text{rev.})>q_m(\text{nat.})$ or $q_{th}(-dN_s)>q_d(-dN_s)$, or $q_{th}>q_d$, which is verified by Eq. (28), as kT and $V/\mathfrak{A}(\partial\Gamma/\partial p)_T$ are always positive. ΔS_m here is equal to $-q_{th}dN_s/T$.

We consider next the integral heat of adsorption from this standpoint. For the process leading to Eq. (17), $q_m(\text{nat.})=-Q=N_s(E_s-E_G)$. If this process (Eq. (17)) were carried out reversibly, using suitable pistons, we would have

$$q_m(\text{rev.})=T\Delta S_m=T\{[N_sS_s + (N-N_s)S_G(p)]-NS_G(P_1)\}, \quad (38)$$

where P_1 is the initial gas pressure and p is the final equilibrium gas pressure ($P_1>p$). Now $q_m(\text{rev.})>q_m(\text{nat.})$, and hence we have the inequality

$$\Delta S_m=N_s[S_s-S_G(p)]+Nk\ln(P_1/p) > [N_s(E_s-E_G)/T]. \quad (39)$$

But (neglecting V_s),

$$T[S_s - S_G(p)] = H_s - H_G = E_s + (\varphi\mathfrak{A}/N_s) - E_G - kT,$$

so Eq. (39) can be written

$$NkT \ln(P_1/p) > N_s kT - \varphi\mathfrak{A}. \quad (40a)$$

The special case which corresponds to P_1 having its minimum possible value is

$$NkT \ln[N/(N-N_s)] > N_s kT - \varphi\mathfrak{A}. \quad (40b)$$

It should be emphasized that, as shown above, the differential and integral heats of adsorption, q_d and Q, *cannot* be used to give *directly* (q/T), the entropy change in the processes for which they are defined, because these processes are not reversible.

There are a number of other conceivable reversible processes for all of which $T\Delta S_m = -q_b = q_m$. However, with one exception which we shall discuss below, the initial and final states are such that ΔS_m is of little interest.

$N_s(S_s - S_G)$[8b] is the entropy change when N_s gas molecules at pressure P form an adsorbate on an area $\mathfrak{A}$ with vapor (equilibrium) pressure $p = P$. The following reversible process gives this entropy change directly. In contrast to much of the above discussion, we do not assume a perfect gas and the volume of the adsorbate is not ignored. We use the same arrangement (and notation) as for q_{th} (Eq. (19)), but there is an additional (surface) piston which allows an increase in the area of adsorbent. We start with gas in equilibrium with adsorbate. Using the original piston, we change V by dV and at the same time change $\mathfrak{A}$ by $d\mathfrak{A}$ with the surface piston so that p, φ, and T all stay constant while a new equilibrium state is reached (that is, N_s has changed by dN_s). *All* intensive properties of gas and adsorbate therefore stay constant, including $N_s/\mathfrak{A}$, $N_G/V_G = (N-N_s)/(V-V_s)$, N_s/V_s, E_s, and E_G. The surface piston moves reversibly against an external surface pressure φ. The volume of adsorbate alters reversibly by dV_s against the interior gas pressure p (but does no external work). Instead of Eq. (20) we have, therefore,

$$dE = -pdV - \varphi d\mathfrak{A} = dE_b - E_G dN_s + E_s dN_s. \quad (41)$$

Because of the constancy of $N_s/\mathfrak{A}$, N_s/V_s, and N_G/V_G,

$$d\mathfrak{A} = \mathfrak{A}dN_s/N_s \quad \text{and}$$
$$dV = [(V_s/N_s) - (V_G/N_G)]dN_s. \quad (42)$$

Equation (41) becomes, for the heat absorbed by the bath,

$$dE_b = [(E_G + (pV_G/N_G)) - (E_s + (pV_s/N_s) + (\varphi\mathfrak{A}/N_s))]dN_s \quad (43)$$

or

$$(\partial E_b/\partial N_s)_{p,\varphi,T} = H_G - H_s = T(S_G - S_s) = (\Delta E_b/\Delta N_s)_{p,\varphi,T}. \quad (44)$$

In this process, which yields $H_G - H_s$ and $S_G - S_s$ directly, *there is thus no distinction between the finite (integral) quotient and the differential quotient* (Eq. (44)) owing to the fact that intensive properties are kept constant. Therefore, if we start with $N_s = 0$,

$$\Delta S_m = -q_b/T = (S_s - S_G)N_s. \quad (45)$$

It will be noted that ΔS_m in Eqs. (39) and (45) differ by a term $Nk \ln(P_1/p)$ as expected.

Differential Quantities**

The above discussion suggests a brief digression, the purpose of which is to emphasize the status of the extensive thermodynamic functions being used. This seems desirable in view of comments of several readers of the manuscript. Let us choose the entropy as a typical extensive quantity.

First, we recall that by assuming the adsorbent to be completely inert, we can treat the *adsorbate* as a pseudo one component system. In this special case at least, it is therefore possible and hence very desirable (from a molecular-statistical mechanical point of view) to employ the entropy of the *adsorbate molecules alone* rather than the total entropy of the system adsorbate-adsorbent and the related partial molar total entropy (applying solution thermodynamics in the standard way to adsorbate-adsorbent as a two component system). The relations between the equations of this paper and analogous equations using "solution thermodynamics" will be discussed at a later time (see below, also).

In our notation S_s is the entropy of the N_s adsorbate molecules. The molecular entropy $S_s = S_s/N_s$ is clearly the mean entropy per molecule. (For convenience in statistical applications we refer here to a single molecule rather than to one mole—there is of course no essential distinction.) A number of differential entropies, $\partial S_s/\partial N_s$, can be defined depending on what properties are held constant. In general, a given differential entropy will not be the same as the molecular entropy, but will be of roughly the same order of magnitude. There is, however, one particular differential entropy of special interest; it is that differential entropy for which the intensive properties of the system are held constant (one component system). The most convenient choice of (independent) intensive properties is φ and T (also P if one wants to be completely general, as in Section II). But for a one component system this special differential entropy is obviously equal to the molecular entropy:

$$(\partial S_s/\partial N_s)_{\varphi,P,T} = S_s/N_s = S_s.$$

[8b] It is to be understood from this point on that S_s, S_G, H_s, H_G, etc., in $S_s - S_G$, $H_s - H_G$, etc., refer to equilibrium states without writing $S_G = S_G(p,T)$, $S_s = S_s(N_s/\mathfrak{A},T)$, etc.

** This section was added in proof.

The analogous equation for a gas is

$$(\partial S_G/\partial N_G)_{P,T}=S_G/N_G=S_G.$$

At equilibrium between gas and adsorbate, the chemical potentials μ_s and μ_G are equal. It therefore follows (Eq. (8)) that $H_s-H_G=T(S_s-S_G)$ at equilibrium.[7b]

The above expression for S_s is to be contrasted with the usual partial molecular (molar) *total* entropy (of adsorbate *plus* adsorbent)

$$\bar{S}_s = (\partial S/\partial N_s)_{P,T,\mathfrak{A}},$$

taking the number of adsorbent molecules as proportional to the area. In this notation, ordinary solution thermodynamics gives

$$q_{st}=H_G-\bar{H}_s=T(S_G-\bar{S}_s).$$

The quantity S_s-S_G (or H_s-H_G, E_s-E_G, etc.) may be referred to as the *equilibrium* entropy (heat, energy, etc.) of adsorption and is analogous to the usual entropy of fusion of a solid, entropy of vaporization of a liquid, etc. (i.e., in all these cases the same equilibrium point is maintained during the process—intensive properties are held constant, as in Eq. (44)).

Heat Capacity and Entropy

We assume a perfect gas and neglect the volume of the adsorbate throughout this section. We have a closed container in which are adsorbent and adsorbate in equilibrium with gas. As usual, the container is immersed in a bath (calorimeter), the container walls and adsorbent being considered part of the bath. The temperature of the entire system is now changed by dT to a new equilibrium state, as a consequence of the absorption of an amount of heat q from an external source. We have

$$E=E_b+N_sE_s+(N-N_s)E_G \tag{46}$$

and

$$dE=q=dE_b+N_sdE_s+E_sdN_s+N_GdE_G-E_GdN_s \tag{47}$$
$$=(dE_b/dT)dT+N_s[(\partial E_s/\partial T)_{N_s,\mathfrak{A}}dT + (\partial E_s/\partial N_s)_{T,\mathfrak{A}}dN_s]+E_sdN_s$$
$$+N_G(\partial E_G/\partial T)_{V_G}dT-E_GdN_s \tag{48}$$
$$=C_bdT+C_{VG}dT+C_\Gamma dT-q_ddN_s, \tag{49}$$

where C_b is the heat capacity of the bath, C_{VG} is the heat capacity at constant volume of N_G gas molecules, and C_Γ is the heat capacity at constant Γ of N_s adsorbate molecules. Hence

$$C_\Gamma=(q/dT)-C_b-C_{VG}+q_d(dN_s/dT). \tag{50}$$

The heat capacity of the adsorbate is thus obtained by correcting q/dT for the heat capacity of bath and gas, and for the heat of adsorption of dN_s molecules. Equation (50), as derived from Eq. (47), shows that q_d is the correct heat of adsorption to use.

We now find the dependence of dN_s on dT, for use in Eq. (50). Let $N_s=N_s(p,T)$ represent the equilibrium adsorption data. Then

$$dN_s=\left(\frac{\partial N_s}{\partial p}\right)_{T,\mathfrak{A}}dp+\left(\frac{\partial N_s}{\partial T}\right)_{p,\mathfrak{A}}dT. \tag{51}$$

Further, from $pV=(N-N_s)kT$,

$$Vdp=N_Gkd T-kTdN_s. \tag{52}$$

Eliminating dp from Eqs. (51) and (52) we find

$$\frac{dN_s}{dT}=\left[\frac{p}{T}\left(\frac{\partial N_s}{\partial p}\right)_{T,\mathfrak{A}}+\left(\frac{\partial N_s}{\partial T}\right)_{p,\mathfrak{A}}\right]\Big/ \left[1+\frac{kT}{V}\left(\frac{\partial N_s}{\partial p}\right)_{T,\mathfrak{A}}\right]. \tag{53a}$$

Experimental isotherms and isobars are thus needed to use Eq. (53a) in Eq. (50).

We make a slight digression here, using some results of Section IV. We have from Eq. (66),

$$\left(\frac{\partial p}{\partial T}\right)_\Gamma=-\frac{(\partial\Gamma/\partial T)_p}{(\partial\Gamma/\partial p)_T}=\frac{pq_{st}}{kT^2},$$

or

$$\left(\frac{\partial\Gamma}{\partial T}\right)_p=-\frac{pq_{st}}{kT^2}\left(\frac{\partial\Gamma}{\partial p}\right)_T,$$

where q_{st} is the isosteric heat of adsorption. Now always $(\partial\Gamma/\partial p)_T\geq 0$ so $(\partial\Gamma/\partial T)_p<0$ only if $q_{st}>0$. This ($q_{st}>0$) is the most common situation (a high temperature isotherm falls below a low temperature isotherm for the same system).

The numerator in Eq. (53a) can then be written

$$\frac{p}{T}\left(\frac{\partial N_s}{\partial p}\right)_{T,\mathfrak{A}}-\frac{pq_{st}}{kT^2}\left(\frac{\partial N_s}{\partial p}\right)_{T,\mathfrak{A}}=-q_d\frac{p}{kT^2}\left(\frac{\partial N_s}{\partial p}\right)_{T,\mathfrak{A}},$$

using Eq. (74). Therefore

$$\frac{dN_s}{dT}=\frac{-q_d(p/kT^2)(\partial N_s/\partial p)_{T,\mathfrak{A}}}{1+(kT/V)(\partial N_s/\partial p)_{T,\mathfrak{A}}}. \tag{53b}$$

The term $q_d(dN_s/dT)$ in Eq. (50) is therefore never positive (this result is expected intuitively). Equation (53b) is more practical to use in Eq. (50) than Eq. (53a) because adsorption isobars are not needed. $dN_s/dT<0$ only if $q_d>0$, which is usually the case.

Finally, we wish to obtain the change in entropy of the adsorbate, dS_s, in terms of C_Γ. For the adsorbate ($\mathfrak{A}$ constant)

$$dE_s=TdS_s+\mu_sdN_s=(\partial E_s/\partial N_s)_{T,\mathfrak{A}}dN_s + (\partial E_s/\partial T)_{N_s,\mathfrak{A}}dT. \tag{54}$$

Now

$$(\partial E_s/\partial N_s)_{T,\mathfrak{A}}=E_s+N_s(\partial E_s/\partial N_s)_{T,\mathfrak{A}}. \tag{55}$$

so Eq. (54) can be written, using $\mu_s=\mu_G$ and Eqs. (18) and (55),

$$dS_s=[1/T][C_\Gamma dT+(E_G-\mu_G-q_d)dN_s] \quad (56a)$$

$$=[1/T][C_\Gamma dT+(TS_G-kT-q_d)dN_s], \quad (56b)$$

where dN_s is given by Eqs. (53). The entropy change would be $C_\Gamma dT/T$ if N_s were constant (see below); the extra term corrects for dN_s. On integrating (N and $\mathfrak{A}$ constant) Eq. (56) from T_1 to T_2, we get $S_s(N_{s2},T_2)-S_s(N_{s1},T_1)$, where N_{s1} and N_{s2} are the equilibrium values of N_s at T_1 and T_2. This applies to the simplest experimental procedure.

On the other hand, if measurements are made in such a way (by altering N or V_G) that the equilibrium N_s is the *same* at each temperature between T_1 and T_2, say $N_s=N_s'$, and if $C_\Gamma(N_s')$ is computed from Eq. (50) at each temperature, then

$$S_s(N_s',T_2)-S_s(N_s',T_1)$$

$$=\int_{T_1}^{T_2}[C_\Gamma(N_s',T)dT/T] \quad (N_s' \text{ constant}). \quad (57)$$

The entropy of an adsorbate can thus be calculated from heat capacity data using Eq. (56) or (57) if we can (i) extrapolate from $T=0$ to $T=T_1$ to find $S_s(N_s,T_1)-S_s(N_s,0)$, and (ii) obtain the zero point entropy $S_s(N_s,0)$. Unfortunately, both (i) and (ii) appear to be difficult. Alternatively, the zero-point entropy might be calculated from (a) an extrapolation as above and (b) S_s from isotherm data (see Section IV) or isotherm data combined with heat capacity measurements. If available, zero-point entropy can give information about surface heterogeneity.[9]

IV. EQUATIONS OF THE CLAUSIUS-CLAPEYRON TYPE

The Isosteric Heat of Adsorption

When equilibrium exists between gas and adsorbate we have $\mu_G(p,T)=\mu_s(\Gamma,p,T)$. Suppose now conditions are changed infinitesimally to a new equilibrium state. Then $d\mu_G=d\mu_s$ and hence

$$(\partial\mu_G/\partial p)_T dp+(\partial\mu_G/\partial T)_p dT=(\partial\mu_s/\partial\Gamma)_{p,T}d\Gamma$$
$$+(\partial\mu_s/\partial p)_{\Gamma,T}dp+(\partial\mu_s/\partial T)_{\Gamma,p}dT. \quad (58)$$

Let us consider the special case $\Gamma=$ constant, $d\Gamma=0$. Then

$$(\partial p/\partial T)_\Gamma=\frac{(\partial\mu_s/\partial T)_{\Gamma,p}-(\partial\mu_G/\partial T)_p}{(\partial\mu_G/\partial p)_T-(\partial\mu_s/\partial p)_{\Gamma,T}}. \quad (59)$$

Now

$$(\partial\mu_G/\partial T)_P=[\mu_G-H_G]/T \text{ and } (\partial\mu_G/\partial P)_T=v_G. \quad (60)$$

Also, considering $\mu_s=\mu_s(\varphi,P,T)$ in which $\varphi=\varphi(\Gamma,P,T)$, we have

$$(\partial\mu_s/\partial T)_{\Gamma,P}=(\partial\mu_s/\partial T)_{P,\varphi}+(\partial\mu_s/\partial\varphi)_{T,P}(\partial\varphi/\partial T)_{\Gamma,P} \quad (61)$$

and

$$(\partial\mu_s/\partial P)_{\Gamma,T}=(\partial\mu_s/\partial P)_{T,\varphi}+(\partial\mu_s/\partial\varphi)_{T,P}(\partial\varphi/\partial P)_{\Gamma,T}. \quad (62)$$

Using Eqs. (8) these become

$$(\partial\mu_s/\partial T)_{\Gamma,P}=[[\mu_s-H_s]/T]+[1/\Gamma](\partial\varphi/\partial T)_{\Gamma,P}, \quad (63)$$

$$(\partial\mu_s/\partial P)_{\Gamma,T}=v_s+[1/\Gamma](\partial\varphi/\partial P)_{\Gamma,T}. \quad (64)$$

We now substitute Eqs. (60), (63), and (64) into Eq. (59):

$$\left(\frac{\partial\ln p}{\partial T}\right)_\Gamma=\frac{H_G-H_s+[T/\Gamma](\partial\varphi/\partial T)_{\Gamma,p}}{pT[v_G-v_s-[1/\Gamma](\partial\varphi/\partial p)_{\Gamma,T}]}$$

$$=\frac{q_{st}}{pT(v_G-v_s)}, \quad (65)$$

where q_{st} is the isosteric heat of adsorption (*defined* by the first and third members of this equation, by analogy with Eq. (84)). This equation is exact. Ignoring pressure effects, dropping the term in v_s, and assuming a perfect gas, we have

$$\left(\frac{\partial\ln p}{\partial T}\right)_\Gamma=\frac{H_G-H_s+[T/\Gamma](\partial\varphi/\partial T)_\Gamma}{kT^2}=\frac{q_{st}}{kT^2}. \quad (66)$$

We digress briefly to give an alternative derivation of Eq. (65). From the *equilibrium* $\varphi=\varphi(p,T)$ in which we consider $p=p(\Gamma,T)$, we find

$$(\partial\varphi/\partial T)_\Gamma=(\partial\varphi/\partial T)_p+(\partial\varphi/\partial p)_T(\partial p/\partial T)_\Gamma.$$

On solving for $(\partial p/\partial T)_\Gamma$ and using Eq. (12) and, in anticipation, Eqs. (90a) and (84), we obtain the exact equation

$$\left(\frac{\partial\ln p}{\partial T}\right)_\Gamma=\frac{H_G-H_s+[T/\Gamma](\partial\varphi/\partial T)_\Gamma}{pT(v_G-v_s)}$$

$$=\frac{q_{st}}{pT(v_G-v_s)}. \quad (65a)$$

The relation between Eq. (65) and Eq. (65a) can be verified as follows. In general, $\varphi=\varphi(\Gamma,P,T)$, but when there is equilibrium between gas and adsorbate, $P=p=p(\Gamma,T)$. We then have

$$(\partial\varphi/\partial T)_\Gamma=(\partial\varphi/\partial T)_{\Gamma,p}+(\partial\varphi/\partial p)_{\Gamma,T}(\partial p/\partial T)_\Gamma.$$

One should, perhaps, use different symbols for equilibrium (e.g., $\varphi(\Gamma,T)$) and general (e.g., $\varphi(\Gamma,P,T)$) thermodynamic functions to avoid confusion. But in the present notation the meaning is always clear from the number of independent variables.

[9] See Paper VI of this series, to be published.

We now wish to relate q_{st} to q_d. We have $E_s = A_s + TS_s$ and, ignoring pressure effects,[10]

$$(\partial E_s/\partial N_s)_{\mathfrak{A},T} = (\partial A_s/\partial N_s)_{\mathfrak{A},T} + T(\partial S_s/\partial N_s)_{\mathfrak{A},T}. \quad (67)$$

Next we note that (Eqs. (5))

$$(\partial A_s/\partial N_s)_{\mathfrak{A},T} = \mu_s = (\partial N_s A_s/\partial N_s)_{\mathfrak{A},T} = N_s(\partial A_s/\partial N_s)_{\mathfrak{A},T} + A_s, \quad (67a)$$

so that

$$(\partial A_s/\partial N_s)_{\mathfrak{A},T} = [\mu_s - A_s]/N_s = [Pv_s/N_s] + [\varphi/\Gamma N_s]. \quad (68)$$

Furthermore, considering $S_s = S_s(\Gamma,T)$ in which $\Gamma = N_s/\mathfrak{A}$, we find

$$(\partial S_s/\partial \mathfrak{A})_{N_s,T} = -[\Gamma/\mathfrak{A}](\partial S_s/\partial \Gamma)_T.$$

Also,

$$(\partial S_s/\partial N_s)_{\mathfrak{A},T} = [1/\mathfrak{A}](\partial S_s/\partial \Gamma)_T.$$

Hence

$$(\partial S_s/\partial N_s)_{\mathfrak{A},T} = -[1/\Gamma](\partial S_s/\partial \mathfrak{A})_{N_s,T}. \quad (69)$$

But, from Eqs. (5),

$$(\partial S_s/\partial \mathfrak{A})_{N_s,T} = -[1/N_s](\partial^2 A_s/\partial \mathfrak{A}\partial T)_{N_s} = [1/N_s](\partial \varphi/\partial T)_\Gamma. \quad (70)$$

Finally, we substitute Eqs. (68), (69), and (70) into Eq. (67):

$$N_s(\partial E_s/\partial N_s)_{\mathfrak{A},T} = Pv_s + [\varphi/\Gamma] - [T/\Gamma](\partial \varphi/\partial T)_\Gamma. \quad (71)$$

We thus find, using Eqs. (18), (66), and (71),

$$q_d + kT = H_G - E_s - N_s(\partial E_s/\partial N_s)_{\mathfrak{A},T} = H_G - H_s + [T/\Gamma](\partial \varphi/\partial T)_\Gamma \quad (72)$$

$$= q_{st}. \quad (73)$$

Hence we have the result

$$(\partial \ln p/\partial T)_\Gamma = [q_d + kT]/kT^2 = q_{st}/kT^2. \quad (74)$$

There are two limiting or special cases worthy of mention: (i) If $\varphi(\Gamma,T)$ happens to be of the special form $\varphi = Tf(\Gamma)$, we see from Eq. (72) that

$$H_G - E_s = q_{st} = q_d + kT \quad (75)$$

or

$$E_G - E_s = q_d.$$

Langmuir adsorption with the number of sites B independent of T is an example (see Eqs. (115), (117), and (119)). (ii) As $\Gamma \to \infty$ (case A), $q_d \to E_G - E_L'$ and $q_{ih} \to q_{st} \to H_G - H_L'$. Also, in $H_s = E_s + Pv_s + (\varphi/\Gamma)$, the term $\varphi/\Gamma \to 0$ as $\Gamma \to \infty$. In the adsorbate (Γ finite) the term Pv_s is usually negligible, as mentioned before.

The above discussion, leading to Eq. (74), provides an independent thermodynamic proof of a relation which was generally accepted as correct until Wilkins[11] suggested an alternative equation. (Wilkins claimed that Γ in Eq. (74) should be replaced by $\Gamma' = N_s/B$—see below.)

We might state at this point that all of the important general thermodynamic results in Section IV have been verified with three different statistical models as special cases: (a) A monatomic perfect gas adsorbed in a localized monolayer according to a Langmuir model, but with the number of sites B in the area $\mathfrak{A}$ a function of temperature; (b) a monatomic perfect gas adsorbed as a mobile monolayer which follows a two-dimensional van der Waals equation,

$$(\varphi + (a'N_s^2/\mathfrak{A}^2))(\mathfrak{A} - N_s b') = N_s kT, \quad (76)$$

as equation of state, but with $a' = 0$ and b' a function of temperature; and (c) the *BET* model.[12] The first two of these models present the "difficulty" first pointed out by McBain[1, 11] and supposedly resolved by Wilkins.[11] The fact that the thermodynamic results of this section have thus been checked by completely independent calculation of the various thermodynamic functions from statistical partition functions in these three special cases is sufficient to convince the present writer that Wilkins is in error.[13] McBain's difficulty does not actually exist in principle. In principle one can take two temperatures infinitesimally close to each other. It arises in practice only because a finite ΔT must be used. One way of avoiding the difficulty in practice is to represent the experimental adsorption data $\Gamma = \Gamma(p,T)$ by an empirical expression valid in the region of interest. One can then evaluate $(\partial \ln p/\partial T)_\Gamma$ by analytical differentiation.

The first two statistical models mentioned above are discussed in more detail in Appendix I. The *BET* model is discussed elsewhere.[14]

Suppose instead of keeping Γ constant as in Eq. (65) we keep some function $\chi = \chi(\Gamma,T)$ constant (i.e., we have so far considered the special case $\chi = \Gamma$). Then

$$(\partial \ln p/\partial T)_\chi = (\partial \ln p/\partial T)_\Gamma + (\partial \ln p/\partial \Gamma)_T(\partial \Gamma/\partial T)_\chi \quad (77)$$

$$= [q_{st}/kT^2] + (\partial \ln p/\partial \Gamma)_T(\partial \Gamma/\partial T)_\chi. \quad (78)$$

[10] E_s is an equilibrium function in Eqs. (18) and (67). That is, $E_s = E_s(\Gamma,T)[= E_s(\Gamma,p(\Gamma,T),T)]$. The approximation starts with Eq. (67a), since, rigorously, $\mu_s = (\partial A_s/\partial N_s)_{\mathfrak{A},T,V_s}$. An exact treatment of the adsorbate gives, in place of Eq. (72),

$$q_d + kT = H_G - H_s + [T/\Gamma](\partial \varphi/\partial T)_{\Gamma,v_s} + [p - T(\partial p/\partial T)_{\Gamma,v_s}][\Gamma(\partial v_s/\partial \Gamma)_T + v_s],$$

in which we can put (compare Eq. (65))

$$(\partial \varphi/\partial T)_{\Gamma,v_s} = (\partial \varphi/\partial T)_{\Gamma,p} + (\partial \varphi/\partial p)_{\Gamma,T}(\partial p/\partial T)_{\Gamma,v_s}.$$

[11] F. J. Wilkins, Proc. Roy. Soc. **A164**, 496 (1938).

[12] Terrell L. Hill, J. Chem. Phys. **14**, 263 (1946).

[13] It seems to the writer that there is a rather fundamental reason for expecting intuitively that it would be incorrect to replace Γ in Eq. (74) by $\Gamma' = N_s/B$: p, T, Γ, q_d, and q_{st} are thermodynamic quantities whereas Γ' is essentially a statistical mechanical quantity. One does not expect the two types of quantities to be mixed in an equation such as Eq. (74).

[14] Paper VII of this series, J. Chem. Phys., to be published.

One, of course, obtains the same result keeping any function $f(\chi)$ constant. In general, the maximum number of molecules B in the first layer can be written as $B(T)=\alpha(T)\mathfrak{A}$. Wilkins examined the special case $\chi=N_s/B=\Gamma'$ so that $\Gamma=\alpha(T)\Gamma'$. Then

$$(\partial\Gamma/\partial T)_{\Gamma'}=\Gamma'[d\alpha/dT]$$

and

$$(\partial \ln p/\partial T)_{\Gamma'}=[q_d+kT/kT^2]+(\partial \ln p/\partial\Gamma)_T\Gamma'[d\alpha/dT], \quad (79)$$

in disagreement with Wilkins, who omitted the second term on the right. According to Eq. (79), the choice $\chi=\Gamma'$ does not lead to a particularly simple result (see, however, Appendix I).

It is clear from Eq. (77) that an infinite number of heats of adsorption can be defined by equations of the Clausius-Clapeyron type. For each choice χ, a different heat of adsorption is obtained. This is due to the fact that the quantity $d \ln p/dT$ is incompletely defined for the equilibrium between a non-homogeneous phase (adsorbate) and a gas, unless some $\chi(\Gamma,T)$ is specified as being held constant.

Part of the deviation of Eq. (53b) is of interest in connection with the isosteric heat of adsorption.

The Equilibrium ΔH, ΔS, and ΔE of Adsorption

The dispute over the correct way of obtaining q_{st} should not lead one to overlook the fact that actually this quantity is not really of great interest in the present case (inert adsorbent) because of the term $N_s(\partial E_s/\partial N_s)_{\mathfrak{A},T}$ in Eq. (18), which is difficult to interpret. (In fact, $q_{st}=H_G-\bar{H}_s$, as mentioned above.)

The quantities of most interest are E_G-E_s and H_G-H_s, especially the latter because $H_G-H_s=T(S_G-S_s)$. From Eq. (72)

$$H_G-H_s=q_{st}-[T/\Gamma](\partial\varphi/\partial T)_\Gamma, \quad (80)$$

$$E_G-E_s=q_{st}-[T/\Gamma](\partial\varphi/\partial T)_\Gamma+[\varphi/\Gamma]-kT. \quad (81)$$

φ can be found from the Gibbs equation (Eq. (14)),

$$\varphi=kT\int_0^p \Gamma(p,T)d \ln p \quad (T \text{ constant}). \quad (82)$$

However, an alternative and more direct way of obtaining H_G-H_s and E_G-E_s exists. Let us choose $\chi=\varphi$. Instead of Eq. (58) we write

$$(\partial\mu_G/\partial p)_T dp+(\partial\mu_G/\partial T)_p dT=(\partial\mu_s/\partial\varphi)_{p,T}d\varphi+(\partial\mu_s/\partial p)_{\varphi,T}dp+(\partial\mu_s/\partial T)_{\varphi,p}dT. \quad (83)$$

Then from Eqs. (8) and (60) we obtain the exact equation

$$(\partial \ln p/\partial T)_\varphi=[H_G-H_s]/pT(v_G-v_s), \quad (84)$$

or approximately,

$$(\partial \ln p/\partial T)_\varphi=[H_G-H_s]/kT^2. \quad (85)$$

An alternative form for $T_{\text{triple point}}<T<T_c$ is $(x=p/p_0)$

$$(\partial \ln x/\partial T)_\varphi=[H_L'-H_s]/kT^2, \quad (86)$$

assuming the vapor (p_0) is a perfect gas. Now choose $\chi=\varphi/T$. We replace $d\varphi$ in Eq. (83) by $Td(\varphi/T)+[\varphi/T]dT$. Then

$$(\partial \ln p/\partial T)_{\varphi/T}=[H_G-H_s+[\varphi/\Gamma]]/pT(v_G-v_s) \quad (87)$$

or, approximately,

$$E_G-E_s=kT^2(\partial \ln p/\partial T)_{\varphi/T}-kT. \quad (88)$$

This can also be written

$$(\partial \ln x/\partial T)_{\varphi/T}=[H_L'-E_s]/kT^2=[E_L'-E_s]/kT^2. \quad (89)$$

Two equations which are useful, if an analytical expression is available for the equilibrium $\varphi(p,T)$, are

$$(\partial p/\partial T)_\varphi=-(\partial\varphi/\partial T)_p/(\partial\varphi/\partial p)_T \quad (90a)$$

$$(\partial p/\partial T)_{\varphi/T}=[[\varphi/T]-(\partial\varphi/\partial T)_p]/(\partial\varphi/\partial p)_T. \quad (90b)$$

These follow from $d\varphi=0$ and $d(\varphi/T)=0$, respectively.

Finally, we might recall that, for a perfect gas, E_G-E_s is also given immediately by Q/N_s (Eq. (17)). Also

$$E_G-E_s=1/N_s\int_0^{N_s}(q_{st}-kT)dN_s$$

$$=-kT+[1/N_s]\int_0^{N_s}q_{st}dN_s \quad (T \text{ constant}). \quad (91)$$

Calculations from Experimental Data

We shall present some actual calculations in detail elsewhere. We mention here a number of general points which should be helpful to those interested in applying the equations.

(i) Equation (85) is convenient for practical use. One has to calculate $\varphi(p)$ from Eq. (82) along two isotherms (T_1 and T_2). All the necessary information is then available. One plots the two curves (T_1 and T_2) of φ *versus* p, and $p_1(\varphi)$ and $p_2(\varphi)$ are read off for some particular φ. An approximation to the quantity H_G-H_s for this value of φ is then given by

$$\ln p_2-\ln p_1=[(H_G-H_s)/k][(1/T_1)-(1/T_2)]. \quad (92)$$

These values of φ and H_G-H_s may be associated (somewhat arbitrarily) with the average quantities $1/\bar{T}=\frac{1}{2}[(1/T_1)+(1/T_2)]$ and $\ln\bar{p}=\frac{1}{2}(\ln p_1+\ln p_2)$.[15]

[15] Perhaps the most consistent way to find the corresponding value of Γ is the following. Plot Γ *versus* p for T_1 and T_2, and read off $p_1'(\Gamma)$ and $p_2'(\Gamma)$, respectively, for some particular Γ. This value of Γ at $\bar{T}$ is associated with $\ln\bar{p}'=\frac{1}{2}(\ln p_1'+\ln p_2')$. This procedure is necessary in any case to calculate q_{st} as in Eq. (92). A smooth plot is made of Γ *versus* $\bar{p}'$ and the value of Γ corresponding to $\bar{p}'=\bar{p}$ (above) may then be found.

Similar procedures can be used in connection with Eqs. (86), (88), and (89).

(ii) The practical difficulty pointed out by McBain is eliminated by the use of Eqs. (85), (86), (88), and (89) (see Eq. (115), for example).

(iii) The following are useful equations for plotting from experimental data curves of the type shown in Figs. 1–3, assuming the gas phase is a perfect gas:

$$\begin{aligned} H_G - H_L' &= \text{constant} = \Lambda \\ &= \text{heat of vaporization per molecule}, \\ E_G - E_L' &= \text{constant} = \Lambda - kT, \\ T(S_G - S_L') &= \Lambda - kT \ln x, \\ F_s - F_L' &= F_G - F_L' = kT \ln x, \\ H_s - H_L' &= \Lambda - (H_G - H_s), \\ E_s - E_L' &= \Lambda - kT - (E_G - E_s), \\ T(S_s - S_L') &= (H_s - H_L') - kT \ln x. \end{aligned} \tag{93}$$

(iv) In order to use equations such as Eq. (85) or Eq. (88) it is *not* necessary to know the absolute value of φ. This means essentially that the surface area does not have to be known. We can write

$$\varphi = KkT \int_0^p v\, d \ln p, \tag{94}$$

where $\Gamma = Kv$ and v is, say, the volume of gas adsorbed (in cc, for a perfect gas at N.T.P.) per gram of adsorbent (or v could be the number of grams of gas adsorbed per gram of adsorbent, etc.). K is simply a proportionality constant defined by Eq. (94). K depends only on the surface area, and is inversely proportional to it. K must be given the same value at different temperatures. (One of our fundamental assumptions in Section II was that the surface area is independent of temperature.) Further, $K = 1/b'v_m$, where v_m is the value of v necessary to cover the surface with one layer of molecules and b' is the area per molecule under these conditions. v_m and b' are separately somewhat temperature dependent.[16] The conclusion is that φ/K and φ/Kk can be used in place of φ to calculate thermodynamic functions, since K and Kk are independent of T.

(v) If there is a first-order phase change in the adsorbate, this presents no difficulty in the calculation of φ provided that the system passes through only stable equilibrium states (no metastable states—see Section V). In the plot of Γ/p *versus* p (preparatory to integrating Eq. (82)), there is a discontinuity (a sudden increase) in Γ/p at a certain $p = p'$. The integration is carried out formally as usual, leading[9] to a φ with no discontinuity at p' but with a discontinuity in $(\partial\varphi/\partial p)_T$ at p' (see also Fig. 5).

(vi) $H_G - H_s$ may be calculated from Eq. (85), and also from Eqs. (66) and (88). These latter equations therefore provide checks on the more direct Eq. (85). Now suppose such checks are actually obtained in a numerical case for some particular value of p, $p = p'$. The question is, does this assure us that the value of $\varphi(p')$ used is correct? This is an important question because the accurate calculation of φ from experimental data requires considerable care.

Suppose $H_G - H_s$ at $p = p'$ from Eqs. (85) and (88) agree. We can then eliminate $H_G - H_s$ from Eqs. (85) and (88) and obtain an equality which holds at p'. From this equality and Eqs. (90a) and (90b), we deduce easily Eq. (14). Similarly, from Eqs. (85) and (66) one can deduce[17] Eq. (14) by a somewhat more lengthy argument. This shows that a check at p' (or two checks—one check is sufficient, the second is redundant as far as φ is concerned) on Eq. (85) by either Eq. (88) or Eq. (66) implies that $d\varphi$ is correct at p' but does *not* prove that φ is correct at p'. If a check is obtained from $p = p'$ to $p = p''$, this implies that the contribution to (the integral) φ between p' and p'' has been computed correctly but says nothing about $0 \leqslant p < p'$. If, at $p = p'$, $d\varphi$ is correct but φ is incorrect, $H_G - H_s$ (even though it has been "checked") will, in general, be incorrect.

Thus, suppose an error is made in evaluating the integral for φ at low pressures ($0 \leqslant p < p'$), but no error is made in the range $p' < p < p''$. Let Φ be the apparent and φ the true spreading pressure. In general, the error made may be different at different temperatures. Then

$$\Phi(p,T) = \varphi(p,T) + a(T) \quad p' < p < p'', \tag{95}$$

where $a(T)$ is the error in Φ. Clearly,

$$(\partial\Phi/\partial p)_T = (\partial\varphi/\partial p)_T, \quad p' < p < p'', \tag{96}$$

so that $d\Phi$ is correct ($d\Phi = d\varphi$) in this range, as assumed, even though Φ is not. However, from Eq. (90a),

$$(\partial p/\partial T)_\Phi = (\partial p/\partial T)_\varphi - [[da/dT]/(\partial\varphi/\partial p)_T] \cdot p' < p < p''. \tag{97a}$$

This shows that an incorrect $H_G - H_s$ will be obtained from Φ unless $da/dT = 0$. That is, in a numerical calculation if the *same* error in φ is made at T_1 and T_2 for $p < p'$, then $H_G - H_s$ is correct if "checked" at $p = p'$.

Also, one finds that

$$(\partial p/\partial T)_{\Phi/T} = (\partial p/\partial T)_{\varphi/T} - [T[d(a/T)/dT]/(\partial\varphi/\partial p)_T], \tag{97b}$$

[16] This is one reason why it is preferable to plot the thermodynamic functions against x in figures analogous to Figs. 1–3 rather than against $\theta = v/v_m$. Better reasons are that v_m is never known extremely accurately, that x gives (case A) a finite abscissa while θ gives an infinite one, and that v_m need not be calculated (*BET* plot) at all if x is used.

[17] Equation (14) is obtained in both cases by a purely mathematical argument. No thermodynamics is used.

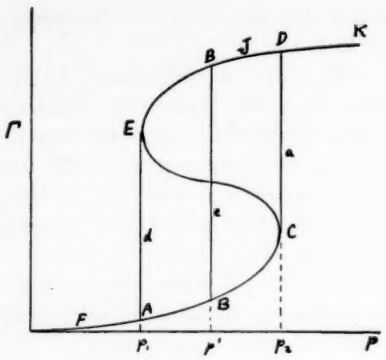

FIG. 4.

so that an incorrect E_G-E_s will be obtained from Eq. (88) using Φ unless $d(a/T)/dT=0$. Clearly, if Φ is incorrect ($a\neq 0$), at least one of E_G-E_s and H_G-H_s must be incorrect and, in general, both will be. On the other hand, q_{st} (Eq. (66)) is independent of any error in Φ. This implies that the errors in H_G-H_s and in $[T/\Gamma](\partial\Phi/\partial T)_\Gamma$ always cancel. In Eqs. (96), (97a), and (97b), $(\partial\varphi/\partial p)_T=kT\Gamma/p$, from Eq. (14).

We have been discussing the practical equations, Eqs. (85), (66), (88), and (14). Precisely the same argument applies to the corresponding exact equations, Eqs. (84), (65), (87), and (12), respectively.

V. FIRST-ORDER PHASE CHANGES AND HYSTERESIS IN THE ADSORBATE

There are important first-order phase changes in the adsorbate to be considered, especially (a) the phenomenon of the condensation of a dilute monolayer into a condensed two-dimensional phase[17a, 18] and (b) capillary condensation.[18] In case (b) one does not observe a really sharp phase change because of the pore size distribution. This condensation is thus quasi-continuous. But the fact that phase changes are really involved is what leads here to the possibility of hysteresis.[18]

We consider first a simple first-order phase change, as, for example, in (a) above. Consider the state of equilibrium between two surface phases 1 and 2 and the gas phase. We have

$$\mu_G(p,T)=\mu_1(p,T,\varphi)=\mu_2(p,T,\varphi). \tag{98}$$

We now imagine an infinitesimal change to a new equilibrium state: $d\mu_G=d\mu_1=d\mu_2$, or

$$(\partial\mu_G/\partial p)_T+(\partial\mu_G/\partial T)_p dT=(\partial\mu_1/\partial\varphi)_{p,T}d\varphi+(\partial\mu_1/\partial p)_{\varphi,T}dp+(\partial\mu_1/\partial T)_{\varphi,p}dT \tag{99}$$

$$=(\partial\mu_2/\partial\varphi)_{p,T}d\varphi+(\partial\mu_2/\partial p)_{\varphi,T}dp+(\partial\mu_2/\partial T)_{\varphi,p}dT. \tag{100}$$

Equation (58) provides one constraint on $d\Gamma$, dp, and dT: two of these variations are independent (and hence one has to specify some $\chi(\Gamma,T)=$ constant to define $\partial p/\partial T$). There is now an additional phase involved so that Eqs. (99) and (100) provide two constraints on $d\varphi$, dp, and dT. Therefore, only one variation, say dT, is independent and dp/dT and $d\varphi/dT$ are, hence, already defined. (This is, of course, analogous to the situation where a gas is in equilibrium with liquid—there is one constraint on dp and dT.)

We can think of Eqs. (99) and (100) as two linear non-homogeneous equations in the two unknowns dp/dT and $d\varphi/dT$. Solving for these derivatives and using Eqs. (8) and (60), one finds easily

$$\frac{d\varphi}{dT}=\frac{\Gamma_1\Gamma_2[(v_2-v_G)(H_1-H_G)-(v_1-v_G)(H_2-H_G)]}{T[\Gamma_2(v_2-v_G)-\Gamma_1(v_1-v_G)]}, \tag{101}$$

$$\frac{dp}{dT}=\frac{\Gamma_2(H_2-H_G)-\Gamma_1(H_1-H_G)}{T[\Gamma_2(v_2-v_G)-\Gamma_1(v_1-v_G)]}. \tag{102}$$

If the gas is perfect (this assumption is not involved in going from Eq. (101) to Eq. (103)) and if we assume $v_G\gg v_1$ and $v_G\gg v_2$, then

$$d\varphi/dT=[H_2-H_1]/T[(1/\Gamma_2)-(1/\Gamma_1)], \tag{103}$$

$$\frac{d\ln p}{dT}=\frac{\Gamma_2(H_2-H_G)-\Gamma_1(H_1-H_G)}{kT^2(\Gamma_1-\Gamma_2)}. \tag{104}$$

Now consider the important special case in which phase 1 is a condensed phase in two dimensions and phase 2 is an expanded phase, so that $\Gamma_1\gg\Gamma_2$. Then

$$d\varphi/dT=[H_2-H_1]/[T/\Gamma_2], \tag{105}$$

$$d\ln p/dT=[H_G-H_1]/kT^2. \tag{106}$$

Finally, if the expanded phase 2 happens to have the two-dimensional equation of state, $\varphi/\Gamma_2=kT$, Eq. (105) becomes

$$d\ln\varphi/dT=[H_2-H_1]/kT^2. \tag{107}$$

The above equations can be used to calculate from suitable experimental data the heat and entropy relations between two adsorbate phases in equilibrium with each other and with gas.

Hysteresis

We wish now to make a few remarks about reversible hysteresis as frequently observed, for example, with porous adsorbents. Presumably, metastable equilibrium states are involved.[18]

We consider an hysteresis loop with an adsorption branch a, a desorption branch d, and an equilibrium path e, which, for generality, we take as *not coinciding with either* d or a. Experimentally it is found that the desorption isotherm always lies above the adsorption isotherm, and there is reason

[17a] Paper II of this series, J. Chem. Phys. **14**, 441 (1946). See also reference 9.

[18] Paper III of this series, J. Chem. Phys. **15**, 767 (1947).

to expect this on theoretical grounds.[18] The equilibrium isotherm falls between d and a. Let $p=p_1$ at the point where the hysteresis loop begins, and $p=p_2$ at the point where it ends.

We now assume that φ is calculated (without numerical errors of the type discussed in Section IV) from Eq. (82) along d, e, and a, for $p=p'$ where $p'>p_2$, giving Φ_d, φ and Φ_a, respectively. Let

$$\Phi_d=\varphi+a_d(T),\qquad \Phi_a=\varphi+a_a(T). \tag{108}$$

Now $\Phi_d-\Phi_a=a_d-a_a>0$, if an hysteresis loop exists. If the loop is plotted in the form Γ/p *versus* p, the area of the loop so plotted is $(a_d-a_a)/kT$. φ is the true and unique stable equilibrium value of the spreading pressure while Φ_a and Φ_d are associated with metastable equilibrium states. It is clear that in general (i) incorrect values of H_G-H_s and E_G-E_s will be obtained for $p>p_2$ using either Φ_a or Φ_d (φ is not available in practice) and (ii) that values of these functions obtained from Φ_a will not agree with those obtained from Φ_d. For example, it is easy to see that $(H_G-H_s)_a=(H_G-H_s)_d$ only if $d(a_d-a_a)/dT=0$, that $(H_G-H_s)_a$ is correct only if $da_a/dT=0$, etc. The conclusion is that, in general, the Gibbs equation cannot be applied to either branch of a hysteresis loop in order to calculate thermodynamic functions for $p>p_2$. q_{st} can, of course, be calculated correctly in the usual way for $p>p_2$.

We now consider the range $p_1<p<p_2$ (for $p<p_1$ there is, of course, no problem here), discussing first a simple condensation as in the isotherm of Fig. 4. Hysteresis in a porous adsorbent is associated with capillary condensation in pores of different sizes.[18] Many different curves analogous to Fig. 4 are compounded to give the experimental isotherm. Figure 5 gives, *schematically*, φ/kT as calculated from Fig. 4. In Fig. 5, the curve FBK is φ/kT (from $FBBK$, Fig. 4), FAG is Φ_d/kT (from $FAEK$, Fig. 4), FCH is Φ_a/kT (from $FCDK$, Fig. 4), and $FCEK$ is the "complete" φ/kT, including metastable and unstable regions (from $FCEK$, Fig. 4). Also in Fig. 5, AG and EK are identical except for vertical displacement. The same is true of CH and DK.

All the thermodynamic functions exist and are unique for metastable as well as stable states. Thus the correct φ_d is (Fig. 5) $FAEK$, while the correct φ_a is $FCDK$. Therefore, in the range $p_1<p<p_2$, $\Phi_d\neq\varphi_d$ but $\Phi_a=\varphi_a$ (and $d\Phi_d=d\varphi_d$). Hence, for a *simple* phase change as in Fig. 4, the Gibbs equation will give correctly the thermodynamic functions in $p_1<p<p_2$ on the adsorption branch, but *not* on the desorption branch. For a *compound* phase change such as occurs in ordinary porous adsorbents which exhibit hysteresis, one cannot use the Gibbs equation in $p_1<p<p_2$ on either a or d. For desorption, the reason is given above. For adsorption, as p increases above $p=p_1$, Φ_a will be correct only until point C is reached for those pores which condense (CD) first (say at $p=p''$). p'' is, of course, unknown and could presumably be only slightly greater than p_1.

In summary, for a compound phase change the reason Φ_d and Φ_a are incorrect in $p_1<p<p_2$ is that the discontinuities AE and DC in φ are not taken into account by the Gibbs equation, and discontinuities of this type probably occur all along the hysteresis loop in most cases of interest.

For definiteness, we have assumed implicitly above (and in other papers of this series) that, when a jump in Γ is made from a metastable state ($C\rightarrow D$, for example, in Fig. 4), p stays constant (i.e., μ stays constant). Hence there is a jump in φ($C\rightarrow D$, for example, in Fig. 5). The jump could, however, conceivably take place[19] at constant φ with a jump in p($C\rightarrow J$ in Figs. 4 and 5). From the usual experimental conditions and the shape of observed hysteresis loops, constant p appears to be the case of most interest.[20]

We have seen above that we cannot use φ values obtained from the Gibbs equation to calculate thermodynamic functions on an hysteresis loop ($p_1<p<p_2$) or above the loop ($p>p_2$). Many other relations derived in Section IV are also not valid here. For example, if E_G-E_s is calculated for $p'>p_2$ along a and d from Eq. (91), in general we expect $(E_G-E_s)_a\neq(E_G-E_s)_d$. This means that the usual relation $q_{st}=q_d+kT$ is not valid in the hysteresis loop. An implication of these remarks is that calorimetric measurements should be especially helpful in studying systems which exhibit hysteresis.

Although in a hysteresis loop we cannot find H_G-H_s and S_G-S_s by the methods of Section IV, one can still say something about the relation between these quantities. We consider an hysteresis loop in which Γ is plotted against p at constant T.

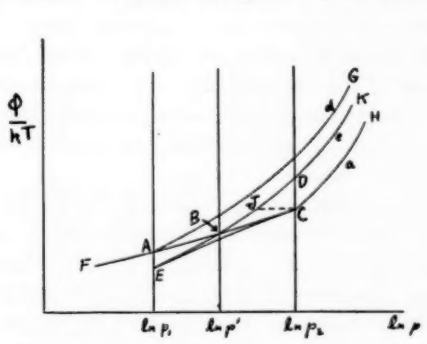

FIG. 5.

[19] In general, neither φ nor p need stay constant (but always $\Delta p\leq 0$). In any case the hysteresis loop will give the wrong φ.

[20] An example of a *simple* phase change, on what is presumably a non-porous solid (glass spheres), in which p does not stay constant was found by J. L. Shereshefsky and C. E. Weir, J. Am. Chem. Soc. **58**, 2022 (1936).

The desorption branch d lies to the left (lower pressures) of the adsorption branch a. Let Γ_0 and T_0 be fixed values of Γ and T. Then $p_a(\Gamma_0,T_0) > p_d(\Gamma_0,T_0)$ where $p_d > p_1$ and $p_a < p_2$. Now, for a perfect gas,

$$\mu_a(\Gamma_0,T_0)=\mu_G(p_a,T_0)=\mu^0(T_0)+kT_0\ln p_a,$$
$$\mu_d(\Gamma_0,T_0)=\mu_G(p_d,T_0)=\mu^0(T_0)+kT_0\ln p_d. \quad (109)$$

Therefore (simplifying notation for convenience),

$$\mu_a-\mu_d=(H_a-T_0S_a)-(H_d-T_0S_d)$$
$$=kT_0\ln(p_a/p_d)>0. \quad (110)$$

The heat (H_G-H_s) of desorption less the heat of adsorption is

$$[H_G(T_0)-H_d]-[H_G(T_0)-H_a]=H_a-H_d. \quad (111)$$

The heat of desorption will exceed the heat of adsorption (at the same Γ and T) if $H_a-H_d>0$. Equation (110) states that $F_a-F_d>0$ always, but it is possible for the entropy change to be such that $H_a-H_d<0$. To be precise, $H_a-H_d>0$, provided that $kT_0\ln(p_a/p_d)>T_0(S_d-S_a)$. So one cannot state with certainty that the heat of desorption will always be greater than the heat of adsorption.

VI. RELATION OF THE WORK OF ROWLEY AND INNES TO THE PRESENT PAPER

This paper was submitted for publication in its original form[21] and presented at an A.A.A.S. Gordon Research Conference before some related work of H. H. Rowley and W. B. Innes,[22] of which the writer was unaware, was called to our attention. We wish to discuss briefly in this section the work of Rowley and Innes and the relation it bears to the present paper.

Rowley and Innes have obtained certain results (see below) found here in a paper[22] which is, however, restricted to unimolecular adsorption (strictly two-dimensional systems). The present paper is more general in the sense that it contains unimolecular adsorption as a special case; multimolecular adsorption is explicitly included here and, in fact, by introducing the term $-pdV_s$ in Eq. (1), the transition $(\Gamma\to\infty)$ to ordinary bulk phase (e.g., liquid) thermodynamics is allowed for in a single discussion.

Some of the equations[22] derived by Rowley and Innes for unimolecular (two-dimensional) adsorption are actually also applicable to multimolecular adsorption (as derived above). These authors were apparently unaware of this and, in fact, give what the present author believes to be an incorrect thermodynamic discussion[23] of multilayer adsorption in which they treat each layer separately and as having its own spreading pressure. This is a *molecular* picture and, as such, it is foreign to the nature of thermodynamics. Thermodynamics is not concerned with such questions as the number of layers or even the existence of "layers." The adsorbed phase should be treated as a single nonhomogeneous phase. Brunauer[1] (p. 440) has offered a similar criticism. Since the treatment of Rowley and Innes was specified as being restricted to unimolecular adsorption, the practical application of some of their equations to experimental adsorption data in general was, of course, not pointed out by them.

In other papers[24], Innes and Rowley extend their treatment of unimolecular adsorption to a consideration of fugacity, the heat of free expansion, and two-component systems.

Equations (12b) and (12c) of Rowley and Innes (reference 22, p. 537) are the unimolecular equivalents of Eqs. (65) and (84) above. Equation (12d) (reference 22, p. 537) (the algebraic sign is apparently wrong) becomes, in our notation (from Eq. (83)),

$$(\partial\varphi/\partial T)_p=\Gamma(H_s-H_G)/T. \quad (112)$$

This equation provides an additional check on the calculation of H_s-H_G or S_s-S_G from experimental data. Equations (118), (117), and (119) in Appendix I are statistical mechanical special cases of the thermodynamic equations (19), (22), and (32) of Rowley and Innes (reference 22, p. 537) for Langmuir adsorption. The integral and differential heats discussed by these authors on pp. 544–546 are not the customary quantities treated above. Their integral heat is $-Q-N_skT$ and their differential heat is $-q_{st}$ in our notation (see our Eq. (91) in this connection).

Finally, the last step in the cycle associated with Fig. 2 (reference 22, p. 537) has been made use of above (Eqs. (41)–(45)) for a slightly different purpose.

ACKNOWLEDGMENTS

I am very much indebted to Dr. P. H. Emmett for his constant encouragement and numerous helpful suggestions. Also, I enjoyed valuable discussions with Doctors R. A. Beebe, J. A. Morrison, and G. B. Kistiakowsky.

APPENDIX I

We summarize here the main results for two statistical models mentioned in Section IV. For simplicity, (a) the atoms are taken as having unexcited electronic degrees of freedom with a nondegenerate ground state and (b) the vibrational

[21] May 17, 1948.
[22] H. H. Rowley and W. B. Innes, J. Phys. Chem. **46**, 537, 548, 694 (1942); **49**, 411 (1945).
[23] See reference 22, p. 694.
[24] See reference 22, p. 548 and H. H. Rowley and W. B. Innes, J. Phys. Chem. **49**, 411 (1945).

degrees of freedom are taken as classical and, in the Langmuir case, isotropic. The partition functions are then

Langmuir:

$$Q_s=\frac{B!}{N_s!(B-N_s)!}\left(\frac{kT}{h\nu}\right)^{3N_s}\exp(N_s\epsilon_1/kT). \quad (113)$$

Van der Waals:

$$Q_s=\frac{1}{N_s!}\left[\frac{2\pi mkT}{h^2}(\mathfrak{A}-N_sb')\frac{kT}{h\nu}\exp(\epsilon_1/kT)\right]^{N_s}. \quad (114)$$

The connection with all the thermodynamic functions (Section II) is established via $A_s=-kT\ln Q_s$. For the gas, $E_G=(3/2)kT$ and $H_G=(5/2)kT$. One finds:

Langmuir:

$$\varphi=\alpha kT\ln[\alpha/(\alpha-\Gamma)],\quad B(T)=\alpha(T)\mathfrak{A}; \quad (115)$$

$$p=\frac{(2\pi mkT)^{\frac{1}{2}}kT}{h^3}\left(\frac{h\nu}{kT}\right)^3[\exp(-\epsilon_1/kT)]\frac{\Gamma}{\alpha-\Gamma}; \quad (116)$$

$$E_G-E_s=\epsilon_1-\tfrac{3}{2}kT-\frac{kT^2}{\Gamma}\frac{d\alpha}{dT}\ln\frac{\alpha}{\alpha-\Gamma}; \quad (117)$$

$$H_G-H_s=\epsilon_1-\tfrac{1}{2}kT-\frac{kT}{\Gamma}\left(T\frac{d\alpha}{dT}+\alpha\right)\ln\frac{\alpha}{\alpha-\Gamma}; \quad (118)$$

$$q_{st}=q_d+kT=\epsilon_1-\tfrac{1}{2}kT-\frac{kT^2}{\alpha-\Gamma}\frac{d\alpha}{dT}; \quad (119)$$

$$kT^2\left(\frac{\partial\ln p}{\partial T}\right)_{\Gamma'}=\epsilon_1-\tfrac{1}{2}kT. \quad (120)$$

Van der Waals:

$$\varphi=\Gamma kT/(1-\Gamma b'); \quad (121)$$

$$p=(2\pi mkT)^{\frac{1}{2}}\nu[\exp(-\epsilon_1/kT)]\times(\Gamma/1-\Gamma b')\exp(\Gamma b'/1-\Gamma b'); \quad (122)$$

$$E_G-E_s=\epsilon_1-\tfrac{1}{2}kT+[\Gamma kT^2/(1-\Gamma b')][db'/dT]; \quad (123)$$

$$H_G-H_s=\epsilon_1+\tfrac{1}{2}kT+[kT/(1-\Gamma b')][\Gamma T(db'/dT)-1]; \quad (124)$$

$$q_{st}=q_d+kT=\epsilon+\tfrac{1}{2}kT+[(2-\Gamma b')\Gamma kT^2/(1-\Gamma b')^2][db'/dT]; \quad (125)$$

$$kT^2(\partial\ln p/\partial T)_{\Gamma'}=\epsilon_1+\tfrac{1}{2}kT-(kT^2/b')(db'/dT). \quad (126)$$

It may be noted that when $d\alpha/dT$ and db'/dT are not zero, all of the energy expressions become infinite as the monolayer approaches completion except Eqs. (120) and (126).

APPENDIX II

Merely to illustrate adsorbent perturbation in a simple case, we consider Langmuir adsorption as in Appendix I and assume further that the adsorbent is an atomic Einstein crystal of N_0 atoms with a classical vibrational partition function (frequency ν_0). Each adsorbate atom perturbs only one (surface) adsorbent atom, the only perturbation being to alter ν_0 to ν for the three vibrational degrees of freedom of the adsorbent atom.

One general technique in taking adsorbent perturbation into account is to write the total Helmholtz free energy A of the system (gas, adsorbate, *and adsorbent*) as a function of N_s, and then minimize A with respect to N_s (at constant V, $\mathfrak{A}$, T, N) to find the equilibrium state.

For our present special case we can separate A and write (making the assignment mentioned in footnote 5—whether this energy ϵ_1 is formally assigned to A_s or A_c is, however, quite immaterial and arbitrary here)

$$A=A_G+A_s+A_{\text{crystal}}, \quad (127)$$

where $A_G=-kT\ln Q_G$, etc. Therefore, we need to maximize $\ln Q_G+\ln Q_s+\ln Q_c$. We have

$$Q_G=\frac{1}{N_G!}\left[\left(\frac{2\pi mkT}{h^2}\right)^{\frac{3}{2}}V_G\right]^{N_G}, \quad (128)$$

$$Q_s=\frac{B!}{N_s!(B-N_s)!}\left(\frac{kT}{h\nu_s}\right)^{3N_s}\exp(N_s\epsilon_1/kT), \quad (129)$$

$$Q_c=\left(\frac{kT}{h\nu_0}\right)^{3(N_0-N_s)}\left(\frac{kT}{h\nu}\right)^{3N_s}j_c^{N_0}, \quad (130)$$

where $N_G=N-N_s$, ν_s is the adsorbate vibrational frequency, and $j_c^{N_0}$ is the non-vibrational part of the crystal partition function (assumed above to be independent of N_s). One finds easily for the (equilibrium) adsorption isotherm

$$p=\frac{(2\pi mkT)^{\frac{1}{2}}kT}{h^3}\left(\frac{h\nu_s}{kT}\right)^3[\exp(-\epsilon_1/kT)]\times\frac{\Gamma}{\alpha-\Gamma}\left(\frac{\nu}{\nu_0}\right)^3. \quad (131)$$

Equation (131) differs from Eq. (116) by the extra factor $(\nu/\nu_0)^3$.

Erratum: Reference 2 of "Thermodynamic Transition from Adsorption to Solution," by Terrell L. Hill, J. Chem. Phys. 17, 507 (1949) should read J. Chem. Phys. 17, 520 (1949).

On the Mechanism of Viscosity of Liquids

M. S. TELANG
Laxminarayan Institute of Technology, Nagpur University, Nagpur, India
(Received July 13, 1948)

A new viscosity-temperature relationship for liquids has been derived, and its application has been studied. The derivation is based upon the theory of viscosity by Eyring *et al.*, rectifying the "activation energy" term. The "activation energy" term has been shown to be equivalent to the free energy of formation of a surface and the error committed by previous workers regarding the evaluation of "activation energy" has been discussed. The proposed equation is free from any arbitrary or empirical terms, and since, in particular, it does not involve any quantities derived from viscosity measurements, it makes a direct calculation of viscosity possible.

INTRODUCTION

REFERENCES to the literature on the viscosity of liquids have been cited in my earlier papers.[1,2] Some preliminary aspects of this subject have been considered in my recent publications.[3–5] The present paper is an attempt to deal with the mechanism of the viscosity of liquids as a whole. This paper incorporates generally the broad outlines of one of the two theories of viscosity of liquids proposed by Eyring *et al.* However, it has been found necessary to rectify the term "activation energy" employed by Eyring *et al.*, and this step is justified by the validity tests. Since the "activation energy" term has been altered, it has been possible to attribute a more precise meaning to the term "frequency factor." It will be observed that the "activation energy" term has been assumed to be equivalent to the free energy involved in the formation of a surface. Consequently, a discussion of the relation between surface tension and molecular volume, as outlined in the next section, has been rendered necessary.

RELATION BETWEEN SURFACE TENSION AND MOLECULAR VOLUME

Recent theories of the liquid state attribute to liquids a so-called "quasi-crystalline" or "pseudo-crystalline" structure.[6,7] It is supposed that the average distribution of molecules about a particular molecule is the same at any instant; however, the structure is supposed to differ from that of a crystal because of thermal agitations in the liquid. As Bernal puts it, "around every molecule of the liquid, the arrangements of other molecules are statistically equivalent; or, put in another way, the probability of finding a molecule at a given distance from another molecule is independent of the position of either of them in the liquid." If a number of instantaneous photographs could be taken, the molecular distribution about any molecule in the liquid state would appear to be random and homogeneous, but if the pictures were all put together, the satistical average would indicate a definite structure analogous to that of a solid. A molecule in a liquid is probably acted on all the time by about as many other molecules as it would be if in the solid state. The forces from these neighboring molecules imprison it in a cell from which it only rarely escapes. The main difference between a solid and a liquid is not that between captivity and freedom; it is only that the particle of a solid is held in fetters *all* the time, while that of a liquid is held in fetters *nearly all* the time, living a life of comparative freedom only in the very brief intervals between one term of imprisonment and the next.[8] In the absence of any precise information, it would be reasonable to assume a uniform packing of molecules in liquids. We may now examine the consequences of such a uniform and close packing.

Consider a portion of a flat interface between liquid and vapor—the liquid being supposed to be made up of a number of molecules, the average distance between the centers of the closest neighbors being r. This assumption is justifiable over periods of time long compared with molecular vibrations. Further, the liquid will appear to consist of a number of layers of molecules parallel to the surface layer and lying in the bulk of the liquid phase below the surface layer. It follows from geometrical considerations that the distance of separation between two such consecutive layers will be $(\sqrt{2}/\sqrt{3})\cdot r$. Each such layer will appear to be composed of a number of horizontal rows of molecules, the distance at right angles to and between two consecutive rows of molecules being obviously $(\sqrt{3}/2)\cdot r$. In a length of *one cm* in the row, the number of molecules will be $1/r$. In a distance of *one cm* at right angles to the row, the number of such parallel rows of molecules in the surface is

[1] M. S. Telang, J. Phys. Chem. **49**, 579 (1945).
[2] M. S. Telang, J. Phys. Chem. **50**, 373 (1946).
[3] M. S. Telang, J. Chem. Phys. **15**, 525 (1947).
[4] M. S. Telang, J. Chem. Phys. **15**, 844 (1947).
[5] M. S. Telang, J. Chem. Phys. **15**, 885 (1947).
[6] J. A. Prins, Trans. Faraday Soc. **33**, 110 (1937).
[7] J. D. Bernal, Trans. Faraday Soc. **33**, 27 (1937).
[8] J. Jeans, *Kinetic Theory of Gases* (Cambridge University Press, London, 1940), p. 7.

given by $(2/r\sqrt{3})$. Therefore, the number of molecules in *one sq. cm* of the interface will be $(2/r^2\sqrt{3})$. If we imagine the molecular volume V to be equivalent to the volume of a cube of a side $V^{\frac{1}{3}}$ taken in the bulk of the liquid phase, and if the top of the cube is made to coincide with the surface of the liquid, the surface area of the top will be $V^{\frac{1}{3}}$. Since $(2/r^2\sqrt{3})$ represents the number of molecules per sq. cm, the number of molecules in $V^{\frac{1}{3}}$ would be $(2V^{\frac{1}{3}}/r^2\sqrt{3})$. Since the distance of separation between two consecutive layers is $(\sqrt{2}/\sqrt{3})\cdot r$, the number of layers in a length $V^{\frac{1}{3}}$ at right angles to the interface will be $(\sqrt{3}\cdot V^{\frac{1}{3}}/\sqrt{2}\cdot r)$. Therefore, the total number of molecules in all the layers in the cubical volume V will be given by

$$(2V^{\frac{1}{3}}/\sqrt{3}\cdot r^2)\times(\sqrt{3}\cdot V^{\frac{1}{3}}/\sqrt{2}\cdot r)=(\sqrt{2}\cdot V/r^3)=N\cdots, \quad (1)$$

where N = Avogadro number.

$$\therefore \quad r=(\sqrt{2}/N)^{\frac{1}{3}}\cdot(M/D)^{\frac{1}{3}}\cdots, \quad (2)$$

where M = molecular weight and D = density of the liquid. Hence, the number of molecules per sq. cm in the surface will be

$$(2/\sqrt{3}\cdot r^2)=((2N)^{\frac{1}{3}}/\sqrt{3})\cdot(D/M)^{\frac{1}{3}}\cdots. \quad (3)$$

Surface tension γ is defined as the work done to bring $(2/\sqrt{3}\cdot r^2)$ molecules from the bulk of the liquid phase to the surface to form a fresh surface of *one sq. cm.* The free energy involved in the formation of one sq. cm of surface will be given by

$$\gamma=(2/r^2\cdot\sqrt{3})\times(\Delta\epsilon_s)\cdots, \quad (4)$$

where $\Delta\epsilon_s$ = the free energy involved in the formation of a surface inhabited by an individual molecule. Combination of (3) and (4) gives

$$\Delta\epsilon_s=\gamma(M/D)^{\frac{1}{3}}\times(\sqrt{3}/(2N)^{\frac{1}{3}})\cdots. \quad (5)$$

Multiplying (5) by N, we have

$$N\Delta\epsilon_s=1.091\cdot N^{\frac{1}{3}}\times\gamma(M/D)^{\frac{1}{3}}\cdots. \quad (6)$$

DERIVATION OF THE VISCOSITY-TEMPERATURE RELATIONSHIP FOR LIQUIDS

Eyring *et al.*[9] have given an equation for fluidity, the reciprocal of which is

$$\eta=(\lambda_1/\lambda\lambda_2\lambda_3)\cdot(v_h/v-v_s)\cdot(2\pi mkT)^{\frac{1}{2}}\cdot e^{\Delta\epsilon_f/kT}\cdots, \quad (7)$$

retaining the original symbols, *viz.*, η = the viscosity, λ_1 = the distance between two layers of molecules in a liquid sliding past each other under the influence of an applied force, λ = the distance between two equilibrium positions in the direction of motion, λ_3 = the distance between neighboring molecules in the same direction, λ_2 = the mean distance between two adjacent molecules in the moving layer in the direction at right angles to the direction of motion, v_h = the volume of a single hole, or the increase in volume per equilibrium position, v = the volume inhabited by a single molecule, v_s = the contribution of a single molecule to the volume of the unexpanded solid, m = the mass of an individual molecule, k = the Boltzmann constant, T = the absolute temperature, and $\Delta\epsilon_f$ = the activation energy required for a single molecule to flow into a hole that is available, *in the absence of a shearing force.* The ratio of the partition functions, $F_\ddagger$ and F, for unit volume, of the molecule in the activated and initial states, respectively, is written as[10] (where v_f = the free volume per molecule and h = Planck's constant)

$$(F/F_\ddagger)=((2\pi mkT)^{\frac{1}{2}}/h)\cdot v_f^{\frac{1}{3}}\cdots. \quad (8)$$

So,

$$(2\pi mkT)^{\frac{1}{2}}=(F/F_\ddagger)\cdot(h/v_f^{\frac{1}{3}})\cdots. \quad (9)$$

Substituting (9) in (7), there results

$$\eta=(\lambda_1/\lambda\lambda_2\lambda_3)\cdot(v_h/v-v_s)\cdot(h/v_f^{\frac{1}{3}})\cdot(F/F_\ddagger)\cdot e^{\Delta\epsilon_f/kT}\cdots. \quad (10)$$

The identity[11]

$$(F/F_\ddagger)\exp(\epsilon_0/kT)=\exp(\Delta F^\ddagger/RT)\cdots, \quad (11)$$

in which ϵ_0 = the energy of activation at 0°K, i.e., the height of the energy barrier, when no force is acting on the liquid, $\Delta F^\ddagger$ = the standard free energy of activation per mole and R = the gas constant per mole, may now be utilized. If we assume ϵ_0 to be synonymous with $\Delta\epsilon_f$, substituting (11) in (10), we get

$$\eta=(\lambda_1/\lambda\lambda_2\lambda_3)\cdot(v_h/v-v_s)\cdot(h/v_f^{\frac{1}{3}})\cdot\exp(\Delta F^\ddagger/RT)\cdots. \quad (12)$$

Further, $\lambda_1\approx\lambda$, and $\lambda_2\lambda_3=(V/N)^{\frac{1}{3}}$, where V = the molar volume and N = the Avogadro number. Using a new symbol $b=Nv_s=V_s$, we have $v-v_s=(V-b/N)=v_f$. Assuming that[5] $v_h=(V_s/N)=(b/N)$, and making appropriate substitutions in (12), we obtain

$$\eta=(hN/V^{\frac{1}{3}})\cdot(b/(V-b)^{4/3})\cdot\exp(\Delta F^\ddagger/RT)\cdots. \quad (13)$$

For reasons to be explained a little later in this paper, we may put $N\Delta\epsilon_s=\Delta F^\ddagger=E_{\text{vis.}}$ per mole $=1.091N^{\frac{1}{3}}\cdot\gamma(M/D)^{\frac{1}{3}}$ according to (6). It is obvious, therefore, that (13) can be written as

$$\eta=(hN/V^{\frac{1}{3}})\cdot(b/(V-b)^{4/3})\cdot\exp(1.091N^{\frac{1}{3}}\gamma(M/D)^{\frac{1}{3}}/RT)\cdots. \quad (14)$$

We may express (14) in the form

$$\eta=Z\cdot\exp(E_{\text{vis.}}/RT)\cdots, \quad (15)$$

where $Z=(hN/V^{\frac{1}{3}})\cdot(b/(V-b)^{4/3})$ = the "frequency factor" and $E_{\text{vis.}}$ = the "activation energy" per mole for viscous flow.

[9] S. Glasstone, K. J. Laidler, and H. Eyring, *The Theory of Rate Processes* (McGraw-Hill Book Company, Inc., New York, 1941), p. 488.

[10] See reference 9, p. 485.

[11] See reference 9, p. 484.

TABLE I.

Substance	Temperature	b	b/V_c
Acetone	20°C	63.9	0.295
Carbon tetrachloride	20	89.3	0.324
Chloroform	10	76.5	0.331
Cyclohexane	20	106.6	0.342
n-hexane	20	117.5	0.319
Ethyl ether	20	91.8	0.325
Benzene	0	77.4	0.301
Benzene	70	88.73	0.345

INTERPRETATION OF THE TERM "ACTIVATION ENERGY"

In the foregoing derivation there are two points which need some clarification. The first one refers to the assumed equality of ϵ_0 and $\Delta\epsilon_f$, both of which imply quantities in the absence of a shearing force. Some confusion has arisen because of the interpretation of Eyring *et al.*[9] that the total activation energy for viscous flow is to be regarded as consisting of two parts: (a) the energy required to form the hole, and (b) that required for the molecule to move into the hole. This conclusion of these authors was based on an erroneous assumption that $(\Delta E_{\text{vap.}}/\Delta F_{\text{vis.}}^{\ddagger}) = 2.45$, as will be demonstrated in the following pages. Since there is no *a priori* reason for splitting the total activation energy into two parts in the manner of Eyring *et al.*, we may assume that the process of forming a site or a hole, and of moving a molecule into the prepared site, should be considered as the performance of one process on the whole. We may consequently put down ϵ_0 to be synonymous with $\Delta\epsilon_f$.

The relation $\Delta F_{\text{vis.}}^{\ddagger} = 1.091 N^{\frac{1}{3}}\gamma(M/D)^{\frac{2}{3}}$ is the next point to be considered. Following Eyring *et al.*, in the treatment of viscous flow of liquids as a rate process, the jump of a moving molecule from one equilibrium position to the next is to be regarded as equivalent to the passage of the system over a potential energy barrier. By definition, surface energy per molecule corresponds to the work done in overcoming the difference in the potential energy of a molecule in the surface and that in the body of the liquid phase in order to bring an interior molecule to the surface to form a fresh surface inhabited by a single molecule. For this process, in order to accommodate the molecule to be brought up to the surface, a suitable site or hole will have to be made in the surface. Subsequently, one of the nearest neighbors from the bulk of the liquid phase will have to be moved into the prepared site. Therefore, the mechanisms of viscosity and surface tension, involving a transfer of molecules from one equilibrium position to another surmounting an energy barrier, appear to be identical so far as this part of the process is concerned. Consequently, it appears reasonable to assume that the activation energy for viscous flow and the free energy of formation of a surface per molecule are equivalent. However, it is to be pointed out that we have no means of ascertaining this statement. The only justification for the assumption is to be sought for in its satisfactory application, as will be seen in the section on the application of the equation.

APPLICATION OF THE PROPOSED EQUATION

The validity of Eq. (14) can be studied in five ways, as shown below: (a) The Eötvös law[12] gives

$$\gamma(M/D)^{\frac{2}{3}} = k'(T_c - T)\cdots, \tag{16}$$

where k' = the Eötvös constant and T_c the absolute critical temperature. Combination of (14)–(16) gives

$$\eta = Z\cdot\exp(1.091 N^{\frac{1}{3}}\cdot k'\times(T_c - T)/RT)\cdots. \tag{17}$$

On taking logarithms and adding $\ln V^{\frac{1}{3}}$ to both sides of (17), we get

$$\ln\eta\cdot V^{\frac{1}{3}} = (\ln Z\cdot V^{\frac{1}{3}} - (1.091 N^{\frac{1}{3}}\cdot k'/R)) + (1.091 N^{\frac{1}{3}}\cdot k'/R)\cdot(T_c/T)\cdots. \tag{18}$$

Recently, Thomas[13] has proposed and tested the following equation:

$$\ln\eta\cdot V^{\frac{1}{3}} = (c - k) + k(T_c/T)\cdots. \tag{19}$$

The close resemblance between (18) and (19) can be readily seen, and a comparison of the two gives

$$c = \ln Z\cdot V^{\frac{1}{3}} \quad \text{and} \quad k = (1.091 N^{\frac{1}{3}}\cdot k'/R).$$

Expressing (18) in logarithms to the base 10,

$$\log_{10}\eta\cdot V^{\frac{1}{3}} = (\log_{10} Z\cdot V^{\frac{1}{3}} - (0.4343\times 1.091 N^{\frac{1}{3}}\cdot k'/R)) + (0.4343\times 1.091 N^{\frac{1}{3}} k'/R)\times(T_c/T)\cdots. \tag{20}$$

Taking the average value of the Eötvös constant $k' = 2$, we obtain

$$0.4343k = (0.4343\times 1.091 N^{\frac{1}{3}}\cdot k'/R) = 0.96,$$

expressing R in ergs, since γ is in ergs/cm^2. This value of $0.4343k = 0.96$ deduced from Eq. (20) is a fair intermediate between the two extreme values of 0.6 and 1.1 given by Thomas[13] in his Table II.

(b) We are further led to a very significant conclusion that the usual method of determining the activation energy according to the relation $E_{\text{vis.}} = R(d\ln\eta/d(1/T))$ from the linear plot of $\ln\eta$ *vs.* $1/T$ is not justifiable. According to (18) (dropping the term $\ln V^{\frac{1}{3}}$), such a plot gives the slope as

$$(1.091 N^{\frac{1}{3}}\cdot k'/R)\times T_c = 2.2 T_c,$$

whereas the true slope ought to be in accordance with (17),

$$(1.091 N^{\frac{1}{3}}\cdot k'/R)\times(T_c - T) = 2.2(T_c - T),$$

taking R in ergs. The activation energy is obtained by multiplying by R, and, for convenience, taking it in calories, we have the "true activation energy"

[12] R. Eötvös, Ann. d. Physik **27**, 448 (1886).
[13] L. H. Thomas, J. Chem. Soc., 573 (1946).

as $4.4(T_c-T)$ calories. The "usual activation energy" is given by $4.4T_c$ calories. From the Guldberg-Guye law,[14] $T_c=1.5T_b$. At the absolute boiling point, T_b, the "true activation energy" will be $4.4(1.5T_b-T_b)=2.2T_b$ calories, whereas the "usual activation energy" will be $4.4\times1.5T_b=6.6T_b$ calories. So, the "usual activation energy" is *three* times greater than the "true activation energy."

Furthermore, Eyring *et al.*[15] have obtained the ratio ($\Delta E_{\text{vap.}}$/usual $E_{\text{vis.}}$) ≈ 2.5 to 3 for a number of substances. Hence, at the boiling point, ($\Delta E_{\text{vap.}}$/true $E_{\text{vis.}}$) $\approx 3\times(2.5$ to $3)\approx 7.5$ to 9. This ratio can be alternatively obtained from Trouton's rule[16]

$$(\Delta H_{\text{vap.}}/T_b)=21, \text{ or, } (\Delta E_{\text{vap.}}/T_b)=(\Delta H_{\text{vap.}}-RT_b)/T_b$$

$=19$. Since, $2.2T_b$ calories is the "true activation energy" at the boiling point, ($\Delta E_{\text{vap.}}$/true $E_{\text{vis.}}$) $=(19T_b/2.2T_b)=8.64$.

(c) Eyring *et al.*[9] have shown that from Eq. (7) in the present paper, at *constant volume*, at the temperatures T_1 and T_2, it is possible to obtain the relation

$$-\Delta E_f((1/T_1)-(1/T_2))=R\ln(1/\eta_1/1/\eta_2)+\tfrac{1}{2}\ln(T_1/T_2)\cdots. \quad (21)$$

The values of ΔE_f derived from viscosity data at constant volume at two temperatures for a number of substances are of the order of 500 calories. It has been shown in (b) that the "true activation energy" is $2.2T_b$ calories. Carbon disulfide, for example, has a boiling point $T_b=319°$K and so its $\Delta E_f=E_{\text{vis.}}=2.2\times319=702$ calories. In view of the various approximations incorporated in obtaining $E_{\text{vis.}}$, the two values of ΔE_f for carbon disulfide may be said to be in good agreement. It is difficult to secure sufficient data to extend this method of testing the equation for a variety of substances. Even from the limited data available, one thing is clear—that the "true activation energy" discussed here is of the right order.

(d) Taking the values of η, γ, and D at two temperatures very close to each other, we can obtain from (14) the following relation:

$$M=2.995\{\log_{10}\eta_1/\eta_2/(\gamma_1/D_1^{\frac{2}{3}}\cdot T_1)-(\gamma_2/D_2^{\frac{2}{3}}\cdot T_2))\}^3\cdots, \quad (22)$$

assuming that the change in V over a small temperature interval is negligible in comparison with the corresponding effect of temperature on η and γ. The values of M calculated from (22) are nearly equal to the theoretical molecular weights.[4] This agreement establishes that the "activation energy" term deduced in the present paper is of the right form. Incidentally, it may be pointed out that the numerical factor 2.995 is slightly different from the original value 3.176 previously used by me.[4] This correction follows from the revision made in the activation energy term in Eq. (14).

(e) So far, our attention has been focused upon establishing that the activation energy term in Eq. (14) was of the right order. It is now necessary to show that the frequency factor in (14) is also of a correct form. Its absolute value independent of viscosity measurements can be calculated and compared with that derived from Eq. (14) by using experimental values of η, γ, and D at one temperature. Alternatively, Eq. (14) may be solved for b by substituting the experimental values of η, γ, etc., at any temperature. The ratio b/V_c, where V_c = the molar critical volume and b = the value obtained by solving (14), indicates that the term b in (14) corresponds to the b of van der Waals, justifying the significance attached to it in deriving (14) (see Table I). However, b is somewhat dependent on temperature, although its temperature coefficient is small, being approximately of the order of that of cubical expansion of the liquid. For example, the average temperature coefficient of b over the temperature interval given in Table I is 2.091×10^{-3} for benzene. Attempts have been made to show that the b of van der Waals is a function of pressure.[17] It is not improbable that it might be a function of temperature also. As all the values in (14), excepting b, are available, if the value of b could be properly chosen, a direct calculation of η from (14) could be done with accuracy, which would be a great achievement of the theory of absolute reaction rates. The substances examined so far are normal unassociated organic liquids. Further work in connection with the behavior of associated or dissociated substances is in progress. It may be of interest to note that (14) can be reduced to the approximate form

$$\eta\approx(hN/V-b)\cdot\exp(1.091N^{\frac{1}{3}}\cdot\gamma(M/D)^{\frac{1}{3}}/RT)\cdots. \quad (23)$$

This equation is a slight modification of an equation given by me in an earlier paper.[5] The term b is somewhat less than V, and $V^{\frac{1}{3}}\times(V-b)^{\frac{1}{3}}$ has the dimensions of a volume being not very different from b. Therefore, $(b/V^{\frac{1}{3}}(V-b))^{\frac{1}{3}}\approx1$. Thus, (14) reduces to (23). Equation (23) is useful in obtaining the approximate value of b for solving Eq. (14) involving fractional exponents.

In conclusion, it may be stated that since Eq. (14) is amenable to a quantitative mathematical treatment, without using any arbitrary or empirical terms and particularly being not derived from viscosity measurements, a satisfactory interpretation of the mechanism of the viscosity of liquids appears to be within reach.

[14] C. M. Guldberg, Zeits. f. physik. Chemie **5**, 374 (1890); P. A. Guye, Bull. Soc. Chim. **4**, 262 (1890).
[15] See reference 9, p. 492.
[16] F. Trouton, Phil. Mag. [5] **18**, 54 (1884).
[17] D. B. Macleod, Trans. Faraday Soc. **41**, 771 (1945).

The Absorption Spectra of Transuranic Salts in Crystals

SIMON FREED AND FRED J. LEITZ, JR.
Oak Ridge National Laboratory, Oak Ridge, Tennessee
(October 6, 1948)

Absorption spectra, mainly in the visible and near ultraviolet regions, were taken of the following anhydrous salts at room temperature and at that of liquid nitrogen: uranium tetrachloride, neptunium tetrachloride, plutonium trichloride, americium trichloride (and americium tribromide).

The spectra of these salts have the features characteristic of rare earth spectra, sharp lines clustered in groups. It follows that the heavy elements have their least stable electrons within the inner 5*f* shell when their ions are in activated as well as in their basic electronic states.

The spectra of the salts of americium are among the sharpest known from crystals—even at room temperature. In this respect they are matched, as far as we know, only by the salts of trivalent europium ion. The spectra confirm the resemblance drawn between these ions on other grounds and make it very likely that trivalent americium has six electrons in the 5*f* shell with $^7F_0$ for its basic electronic state.

The experimental method requires at most several micrograms of the salt for obtaining spectra of considerable dispersion.

IN 1940 and 1941, there were strong indications that the transuranic ions constituted a second rare earth series, that their least stable electrons went into the inner 5*f* shell and that this shell was surrounded and shielded by the completely filled 6*s* and 6*p* shells. It is scarcely necessary to mention[1] how fruitful has been the acceptance of the parallel between the transuranics and the rare earths in their isolation and in characterizing their chemical properties and their crystal structures.

The unique sharpness of the spectra of the rare earths is due to transitions between basic and activated states, both of which result from configurations of electrons within the shielded 4*f* shell. The lines in the spectra fall into groups. The lines within a group are to be identified as components into which a virtual line in the spectrum of the "gaseous" ion is split by the electric fields of the ionic environment in the crystal. A comparable sharpness and grouping of lines in the spectra of the transuranic ions in crystals would be considered as fairly good proof that the transitions are also taking place within a shielded shell—the 5*f* shell—in this case. And the proof would be practically conclusive if these properties continued to hold in a succession of ions just as in the series of rare earths.

As to technique, a microscope magnified a single crystal or a conglomerate within a fine capillary tube such as is employed in x-ray analysis and threw an image magnified about one hundred times onto the slit of a spectrograph or a grating. The transuranic material has weighed from about ten to fifty micrograms. The spectrograph was a single prism instrument from Bausch and Lomb Company with a dispersion in the orange about 60A/mm and in the blue about 30A/mm, and the grating from Jarrel-Ash Company was in Wadsworth mounting, having a dispersion of 5A/mm in the first order.

The absorption spectra of the following anhydrous salts were taken: uranium tetrachloride (Fig. 1), neptunium tetrachloride (Fig. 2), plutonium trichloride (Fig. 3), americium trichloride (Fig. 4), and americium tribromide. Neodymium trichloride (Fig. 5) is given for comparison.

We see from the reproductions that the spectra have the sharpness characteristic of the rare earths. Just as from rare earths, the lines cluster in groups which are fairly well separated.

Examples of extreme sharpness in the spectra are given by americium chloride and also by americium

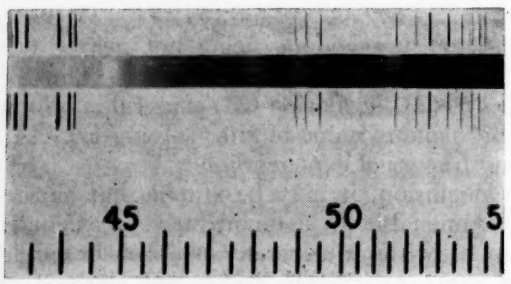

FIG. 1. UCl_4 at 77°K.

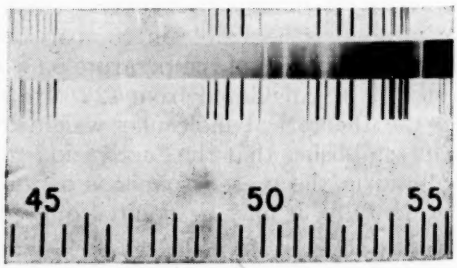

FIG. 2. $NpCl_4$ at 77°K.

[1] Symposium on Transuranic Elements, American Chemical Society Meeting, Chicago, April, 1948.

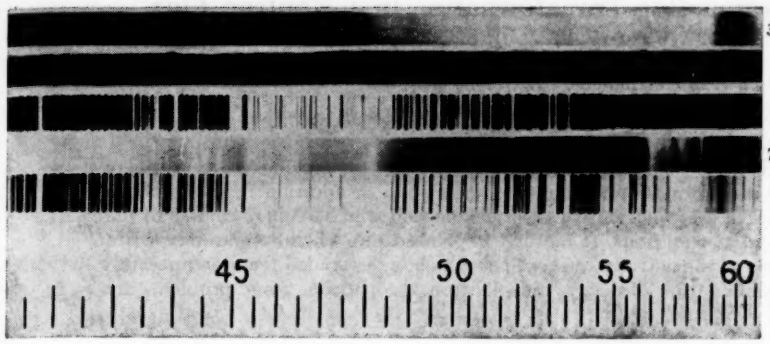

FIG. 3. $PuCl_3$ at 300°K and 77°K.

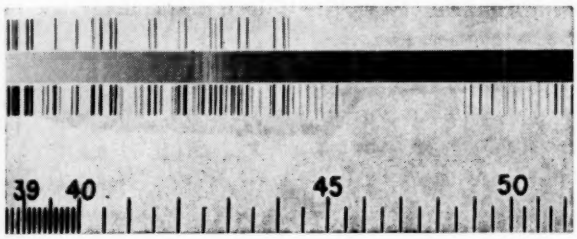

FIG. 4. $AmCl_3$ at 77°K.

bromide. These are among the finest known from crystals; even at room temperature their widths range from 1A to 5A. As far as we know, only trivalent europium ion, the rare earth to which americium has been thought to correspond, possesses so sharp a spectrum. The absorption spectrum of trivalent europium ion originates from six $4f$ electrons forming a $^7F_0$ level, and it seems very likely that $^7F_0$ is the basic electronic state of the americium ion also.

The following are some of the more prominent lines in the absorption spectra of the anhydrous salts at 77°K.

Neodymium Trichloride

3254A	3427A	3596A	4685A	5120A	5300A
3258	3511	4210	4725	5149	5795
3305	3527	4310	4731	5172	5814
3324	3543	4619	4749	5180	5840
3332	3549	4642	4765	5255	5860
3346	3575	4648	4771	5270	5885
3416	3580	4677	5088	5280	5910
					5955

Uranium Tetrachloride

4480A	4905A	5145A	5615A	
4795	4935	5175	6710	

Neptunium Tetrachloride

4413A	5019A	5340A	6367A	7499A	8256A
4455	5073	5503	6552	7585	8410
4737	5115–5175	5722	6740	7746	8570
4768	5190	3 bands	6825	7759	8625
4785	5230	6280–6340	7448	7781	8769

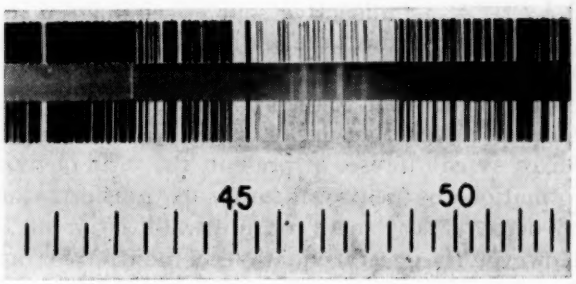

FIG. 5. $NdCl_3$ at 77°K.

Plutonium Trichloride

3450A	3918A	4143A	4359A	4620A	5725A
3508	3928	4154	4370	4630	5780
3643	3970	4235	4432	4642	5820
3729	3981	4291	4450	4805–4820	6090
3798	3992	4309	4480	5175	6115
3810	4003	4317	4539	5450	6275
3830–3860	4058	4328	4548	5465	6745
3902	4073	4345	4579	5645	

Americium Trichloride

3351A	3664A	3784A	4312A
3384	3739	3802	4440
3421	3760	4048	4570
3637	3773	4220–4280	4631
			5075–5105

We wish to express here our gratitude to Dr. Sherman Fried of the Argonne National Laboratory. This work would scarcely have been possible but for his generosity and his rare ability in dry chemical transformations on the microgram scale. We also wish to thank Dr. Glenn Seaborg and Dr. B. Cunningham of Berkeley for generously coming forward and providing our work with transuranic material.

This document is based on work performed under contract No. W-7405 eng. 26 for the Atomic Energy Project at Oak Ridge National Laboratory.

The Equations of Radioactive Transformation in a Neutron Flux

WILLIAM RUBINSON
Brookhaven National Laboratory, Upton, New York
(Received September 20, 1948)

The standard equations of radioactive transformation are generalized to include the case where radioactive nuclei are subject to transformation by neutron absorption in addition to spontaneous decay. Opportunity is taken to derive the equations by a simple method which avoids recourse to the formal methods of solving differential equations. A method is pointed out whereby one may write simply by inspection the equation for the activity of a species which is descended from an ancestral species through a chain of any combination of decays and neutron absorptions. Some problems are solved as illustration.

WHEN a radioactive source is immersed in a neutron flux, the radioactive nuclei in the source are subject to transformation by neutron capture in addition to their transformation by spontaneous radioactive decay. Even with the largest fluxes we can foresee at present, the ratio of transformations by neutron capture to transformations by decay is very small for most radioactive nuclei. However, the general equations of radioactive transformation in a neutron flux will be useful for nuclei of long half-life and large cross-section, and especially for particular problems such as that illustrated by Katcoff's experiment discussed in Section IV below.

For convenience, the discussion is limited to the case of a neutron flux; the equations and methods are, of course, applicable to a flux of any kind of particle.

I. THE ACTIVITIES OF THE DIFFERENT MEMBERS OF A DECAY CHAIN DESCENDED FROM A PRIMAL ANCESTRAL ACTIVITY A_1^0

We consider a series of genetically related activities:

$$A_1 \xrightarrow{\lambda_1} A_2 \xrightarrow{\lambda_2} \cdots \xrightarrow{\lambda_{n-1}} A_n \xrightarrow{\lambda_n}.$$

Nuclei of the ith species transform spontaneously at rate

$$A_i(t)=\lambda_i N_i(t), \tag{I.1}$$

where $A_i(t)$ and $N_i(t)$ are, respectively, the activity (disintegrations per second) and number of nuclei of the ith species at time t, and λ_i is the corresponding decay constant.

Consideration of the fact that $A_i(t)$ is also the rate of creation of nuclei of the $(i+1)$th species leads, in the case of zero flux, to the well-known set of simultaneous linear differential equations with constant coefficients that governs the time dependence of the number of nuclei of the different species:

$$\begin{cases} dN_1/dt=-\lambda_1 N_1, \\ dN_2/dt=\lambda_1 N_1-\lambda_2 N_2, \\ \quad\cdot \\ \quad\cdot \\ \quad\cdot \\ dN_n/dt=\lambda_{n-1}N_{n-1}-\lambda_n N_n. \end{cases} \tag{I.2}$$

If the nuclei are immersed in a constant neutron flux of magnitude ϕ neutrons cm^{-2} $sec.^{-1}$, and the ith species has cross-section σ_i cm^2 for all neutron reactions that permanently alter the nuclei,[1] then the nuclei will transform by two processes: (1) spontaneous radioactive decay at rate $\lambda_i N_i$ and (2) neutron reaction at rate $\phi\sigma_i N_i$. Therefore, the total transformation rate of the ith species at time t is $(\lambda_i+\phi\sigma_i)\mathbf{N}_i(t)$, where bold face type is used to distinguish a symbol pertaining to the case of non-zero flux from the corresponding symbol in the case of zero flux. We denote

$$\Lambda_i \equiv \lambda_i+\phi\sigma_i. \tag{I.3}$$

Now, independently of the flux, nuclei of the $(i+1)$th species arise only by radioactive decay of nuclei of the ith species, so that their rate of creation is $\lambda_i\mathbf{N}_i$. Consequently, for a non-zero neutron flux we have, in place of Eq. (I.2),

$$\begin{cases} d\mathbf{N}_1/dt=-\Lambda_1\mathbf{N}_1, \\ d\mathbf{N}_2/dt=\lambda_1\mathbf{N}_1-\Lambda_2\mathbf{N}_2, \\ \quad\cdot \\ \quad\cdot \\ \quad\cdot \\ d\mathbf{N}_n/dt=\lambda_{n-1}\mathbf{N}_{n-1}-\Lambda_n\mathbf{N}_n. \end{cases} \tag{I.4}$$

The solution of these equations can be written directly by appropriate substitution of Λ's for λ's in the solution of Eqs. (I.2).

The solutions of the latter in a symmetrical form have been known for a long time. They may be ob-

[1] σ_i is the sum of the (n,γ), (n,p), $(n,2n)$, etc. cross sections, but does not include the (n,n) cross section unless the latter reaction results in an excited state whose lifetime for return to the lowest state is not insignificant compared to the lifetime of the nucleus for decay.

tained in a straightforward manner by methods treated in all the texts on differential equations, or by the method of Bateman.[2] However, it is possible to obtain the solutions of these equations without appeal to the formal methods used in differential equations, by a very simple method which emphasizes the physical content of the situation and is at least as compact as the other methods.

We note first that a single nuclear species of decay constant λ and cross-section σ in a constant neutron flux ϕ transforms at a rate given by the first of Eqs. (I.4), so that

$$\mathbf{A}(t)=\lambda\mathbf{N}(t)=A^0e^{-\Lambda t}, \tag{I.5}$$

where $A^0\equiv\mathbf{A}(0)=\lambda N^0$.

Now, suppose that nuclei of this species are created at rate $R(t')$ during time interval $0\leqslant t'\leqslant t$. Of the $R(t')dt'$ nuclei created during time interval dt' at time t', the number still untransformed at time t (which is an amount of time $t-t'$ later), is, by Eq. (I.5),

$$d\mathbf{N}(t', t)=R(t')\exp[-\Lambda(t-t')]dt'.$$

Then the activity at time t is, assuming zero activity at $t'=0$,

$$\mathbf{A}(t)=\lambda\mathbf{N}(t)=\lambda e^{-\Lambda t}\int_0^t R(t')e^{\Lambda t'}dt'. \tag{I.6}$$

We can now derive any of the transformation equations by appropriate specialization of $R(t')$.[3]

We shall assume in the following that $\mathbf{A}_1(0)=A_1{}^0$, and $A_2{}^0=\cdots=A_n{}^0=0$.

The rate of creation $R_2(t')$ of daughter nuclei is equal to the rate of radioactive decay of parent nuclei:

$$R_2(t')=\mathbf{A}_1(t')=A_1{}^0e^{-\Lambda_1 t'}.$$

Putting this into Eq. (I.6) and integrating, we get a result that can be put into the symmetrical form,

$$\mathbf{A}_2(t)=\lambda_2\mathbf{N}_2(t)=\lambda_2\lambda_1N_1{}^0\left(\frac{e^{-\Lambda_1 t}}{\Lambda_2-\Lambda_1}+\frac{e^{-\Lambda_2 t}}{\Lambda_1-\Lambda_2}\right). \tag{I.7}$$

Similarly, the rate of creation $R_3(t')$ of granddaughter nuclei is equal to the rate $\mathbf{A}_2(t')$ of radioactive decay of daughter nuclei. Using Eq. (I.6) again, we find, after a little algebraic manipulation to get the symmetrical form,

$$\mathbf{A}_3(t)=\lambda_3\mathbf{N}_3(t)=\lambda_3\lambda_2\lambda_1N_1{}^0\left[\frac{e^{-\Lambda_1 t}}{(\Lambda_2-\Lambda_1)(\Lambda_3-\Lambda_1)}+\frac{e^{-\Lambda_2 t}}{(\Lambda_1-\Lambda_2)(\Lambda_3-\Lambda_2)}+\frac{e^{-\Lambda_3 t}}{(\Lambda_1-\Lambda_3)(\Lambda_2-\Lambda_3)}\right]. \tag{I.8}$$

The symmetrical form of Eqs. (I.7) and (I.8) permits us to write directly the expression for the activity of the nth generation species:

$$\mathbf{A}_n(t)=\lambda_n\mathbf{N}_n(t)=\left(\prod_{i=1}^{n}\lambda_i\right)N_1{}^0\sum_{i=1}^{n}\mathbf{a}_ie^{-\Lambda_i t}\quad(n>1), \tag{I.9}$$

where

$$\mathbf{a}_i=\prod_{j\neq i}(\Lambda_j-\Lambda_i)^{-1}\quad(j=1, 2, \cdots, n).$$

This equation can be verified formally by mathematical induction.

If $\phi=0$, Eq. (I.9) becomes the solution of the last of Eqs. (I.2):

$$A_n(t)=\lambda_nN_n(t)=\left(\prod_{i=1}^{n}\lambda_i\right)N_1{}^0\sum_{i=1}^{n}a_ie^{-\lambda_i t}\quad(i>1), \tag{I.10}$$

where

$$a_i=\prod_{j\neq i}(\lambda_j-\lambda_i)^{-1}\quad(j=1, 2, \cdots, n).$$

Note that Eq. (I.9) breaks down if any two Λ's are equal. The equation for this case is most easily obtained by setting the Λ's equal before integration. For instance, if $\Lambda_2=\Lambda_1$, the integrand of the integral leading to Eq. (I.7) becomes equal to 1, and

$$\mathbf{A}_2(t)=\lambda_2A_1{}^0te^{-\Lambda_2 t}.$$

It remains to notice that if $A_2{}^0, A_3{}^0\cdots A_n{}^0$ are not all zero, then $\mathbf{A}_n(t)$ is obtained by summing the contributions made to it by the different initial activities,

$$\mathbf{A}_n(t)=\lambda_n\mathbf{N}_n(t)=\sum_{i=1}^{n}\left(\prod_{k=i}^{n}\lambda_k\right)N_i{}^0\sum_{k=i}^{n}\mathbf{a}_ke^{-\Lambda_k t}, \tag{I.11}$$

where $\mathbf{a}_k=1$ when $i=n$, and when $i<n$,

$$\mathbf{a}_k=\prod_{p\neq k}(\Lambda_p-\Lambda_k)^{-1}\quad(p=i, i+1, \cdots, n).$$

If the flux is suddenly shut off at time t, the different activities which are present at that time in amounts given by Eq. (I.5) and the general Eq. (I.9), transform subsequently by radioactive decay alone according to the zero flux equations. With the elapse of T time units after flux shut-off, the activity $\mathbf{A}_1(t, T)$ of the primal ancestor becomes

$$\mathbf{A}_1(t, T)=\mathbf{A}_1(t)e^{-\lambda_1 T}=A_1{}^0\exp[-(\Lambda_1 t+\lambda_1 T)];$$

---

[2] H. Bateman, Proc. Camb. Phil. Soc. **15**, 423 (1910).

[3] This fact is noted by Meyer and Schweidler, *Radioaktivität* (B. G. Teubner, Leipzig, 1927), p. 57. They write (translating to the notation of this paper)

$$N(t)=e^{-\lambda t}\left(N^0+\int_0^t R(t')e^{\lambda t'}dt'\right)$$

as the solution of the differential equation $dN(t')/dt'=R(t')-\lambda N(t')$.

the activity of the daughter will be

$$\mathbf{A}_2(t, T)=\lambda_2\mathbf{A}_1(t)\left(\frac{e^{-\lambda_1 T}}{\lambda_2-\lambda_1}+\frac{e^{-\lambda_2 T}}{\lambda_1-\lambda_2}\right)+\mathbf{A}_2(t)e^{-\lambda_2 T}$$

with $\mathbf{A}_1(t)$ given by Eq. (I.5), and $\mathbf{A}_2(t)$ by Eq. (I.7); and in general

$$\mathbf{A}_n(t, T)=\left(\prod_{i=1}^{n}\lambda_i\right)N_1^0 \times\sum_{i=1}^{n}\left[\sum_{j=1}^{i}\mathbf{a}_j e^{-\Lambda_j t}\sum_{k=i}^{n}a_k e^{-\lambda_k T}\right], \quad \text{(I.12)}$$

where

$\mathbf{a}_j=1$ when $i=1$, and when $i>1$,

$$\mathbf{a}_j=\prod_{m\neq j}(\Lambda_m-\Lambda_j)^{-1} \quad (m=1, 2, \cdots, i),$$

$a_k=1$ when $i=n$, and when $i<n$,

$$a_k=\prod_{p\neq k}(\lambda_p-\lambda_k)^{-1} \quad (p=i, i+1, \cdots, n).$$

II. THE ACTIVITIES OF THE DIFFERENT MEMBERS OF A DECAY CHAIN DESCENDED FROM A PRIMAL ANCESTOR WHICH IS CREATED AT A CONSTANT RATE

The problem we treat in this section will be discussed in terms of a fission product chain of which the primal ancestor is created at constant rate r by fission in a constant neutron flux ϕ.

If the flux is so small that $\phi\sigma_i \ll \lambda_i$ for all i, then the variation in number of nuclei of the different chain members is governed by the differential equations

$$\begin{cases}\dfrac{dN_1}{dt}=r-\lambda_1 N_1,\\ \cdot\\ \cdot\\ \cdot\\ \dfrac{dN_n}{dt}=\lambda_{n-1}N_{n-1}-\lambda_n N_n.\end{cases} \quad \text{(II.1)}$$

The corresponding set of equations for the high flux case is (in the notation of the preceding section)

$$\begin{cases}\dfrac{d\mathbf{N}_1}{dt}=r-\Lambda_1\mathbf{N}_1,\\ \cdot\\ \cdot\\ \cdot\\ \dfrac{d\mathbf{N}_n}{dt}=\lambda_{n-1}\mathbf{N}_{n-1}-\Lambda_n\mathbf{N}_n.\end{cases} \quad \text{(II.2)}$$

The solutions of these equations, like those of the preceding section, may be obtained without recourse to the formal methods used in solving differential equations.

We consider first the case of a high flux. Nuclei of the primal ancestor are produced by fission at constant rate r during a time interval $0\leqslant t'\leqslant\tau$. The activity $\mathbf{A}_1(\tau)$ of the primal ancestor at time τ is easily obtained from Eq. (I.6) with $R(t')=r$.

$$\mathbf{A}_1(\tau)=\lambda_1\mathbf{N}_1(\tau)=r\frac{\lambda_1}{\Lambda_1}(1-e^{-\Lambda_1\tau}). \quad \text{(II.3)}$$

The corresponding expression for $\mathbf{A}_n(\tau)$ can be most simply obtained by modifying the method of Eq. (I.6) in the following way.[4] The $R(t')dt'$ primal ancestor nuclei created during the time interval dt' at time t' $(0\leqslant t'\leqslant\tau)$ will give rise to a certain amount $d\mathbf{A}_n(t', \tau)$ of nth generation activity at time τ, i.e., at an amount of time $\tau-t'$ after the creation of the ancestral nuclei. If $R(t')=r=$ constant, we have, in view of Eq. (I.9),

$$d\mathbf{A}_n(t', \tau)=\left(\prod_{i=1}^{n}\lambda_i\right)r dt'\sum_{i=1}^{n}\mathbf{a}_i\exp[-\Lambda_i(\tau-t')].$$

Integrating between $t'=0$ and $t'=\tau$, and multiplying and dividing through by

$$\prod_{i=1}^{n}\Lambda_i,$$

we get

$$\mathbf{A}_n(\tau)=\lambda_n\mathbf{N}_n(\tau)=\left(\prod_{i=1}^{n}\frac{\lambda_i}{\Lambda_i}\right)r \times\sum_{i=1}^{n}\mathbf{b}_i(1-e^{-\Lambda_i\tau}) \quad (n>1), \quad \text{(II.4)}$$

where

$$\mathbf{b}_i=\prod_{j\neq i}\frac{\Lambda_j}{\Lambda_j-\Lambda_i} \quad (j=1, 2, \cdots, n).$$

If the flux is shut off at time τ, fission stops, and the different activities $\mathbf{A}_i(\tau)$, present at that time in amounts given by Eq. (II.3) and the general Eq. (II.4), change subsequently by radioactive decay alone. With the lapse of t time units after flux shut off, the activity of the primal ancestor becomes

$$\mathbf{A}_1(\tau, t)=\mathbf{A}_1(\tau)e^{-\lambda_1 t}=r\frac{\lambda_1}{\Lambda_1}(1-e^{-\Lambda_1\tau})e^{-\lambda_1 t}; \quad \text{(II.5)}$$

the activity of the daughter becomes

$$\mathbf{A}_2(\tau, t)=\lambda_2\mathbf{A}_1(\tau)\left(\frac{e^{-\lambda_1 t}}{\lambda_2-\lambda_1}+\frac{e^{-\lambda_2 t}}{\lambda_1-\lambda_2}\right)+\mathbf{A}_2(\tau)e^{-\lambda_2 t},$$

where $\mathbf{A}_1(\tau)$ and $\mathbf{A}_2(\tau)$ are given by Eqs. (II.3) and (II.4), respectively, and in general, the activity of

[4] This is essentially the method used in Rutherford, Chadwick, and Ellis, *Radiations from Radioactive Substances* (Cambridge University Press, Teddington, 1930), p. 15.

the nth generation species becomes

$$\mathbf{A}_n(\tau, t) = r(\prod_{i=1}^{n} \lambda_i) \sum_{i=1}^{n} [(\prod_{j=1}^{i} \Lambda_j^{-1}) \times \sum_{j=1}^{i} \mathbf{b}_j(1-e^{-\Lambda_j \tau}) \sum_{k=i}^{n} a_k e^{-\lambda_k t}], \quad \text{(II.6)}$$

where

$\mathbf{b}_j = 1$ when $i=1$, and when $i>1$,

$$\mathbf{b}_j = \prod_{m \neq j} \frac{\Lambda_m}{\Lambda_m - \Lambda_j} \quad (m = 1, 2, \cdots, i),$$

$a_k = 1$ when $i=n$, and when $i<n$,

$$a_k = \prod_{p \neq k} (\lambda_p - \lambda_k)^{-1} \quad (k = i, i+1, \cdots, n).$$

The corresponding expression for the low flux case ($\phi\sigma_i \ll \lambda_i$) can be obtained in a much simpler form. The rdt' primal ancestor nuclei created during time interval dt' at time $t'(0 \leqslant t' \leqslant \tau)$ will, at a time $\tau+t-t'$ later, have an activity

$$rdt' \exp[-\lambda_1(\tau+t-t')],$$

and the activity of the nth generation descendant at that later time will be, by Eq. (I.10),

$$(\prod_{i=1}^{n} \lambda_i) rdt' \sum_{i=1}^{n} a_i \exp[-\lambda_i(\tau+t-t')].$$

Integrating these expressions between $t'=0$ and $t'=\tau$, we get

$$A_1(\tau, t) = \lambda_1 N_1(\tau, t) = r(1-e^{-\lambda_1 \tau})e^{-\lambda_1 t}, \quad \text{(II.7)}$$

$$A_n(\tau, t) = \lambda_n N_n(\tau, t) = r \sum_{i=1}^{n} b_i(1-e^{-\lambda_i \tau})e^{-\lambda_i t}, \quad \text{(II.8)}$$

where

$$b_i = \prod_{j \neq i} \frac{\lambda_j}{\lambda_j - \lambda_i} \quad (j = 1, 2, \cdots, n).$$

III. THE ACTIVITY OF A RADIOACTIVE SPECIES WHICH IS CREATED AS A RESULT OF NEUTRON ABSORPTION BY ANOTHER RADIOACTIVE SPECIES

Suppose that nuclei of species u can absorb neutrons to generate nuclei of species v. Then, if nuclei of species u are created at constant rate r in a neutron flux of magnitude ϕ,

$$\frac{d\mathbf{N}_u}{dt} = r - \Lambda_u \mathbf{N}_u, \quad \text{(III.1)}$$

$$\frac{d\mathbf{N}_v}{dt} = \phi\sigma_u \mathbf{N}_u - \Lambda_v \mathbf{N}_v, \quad \text{(III.2)}$$

where σ_u is the cross section of species u for the creation of species v.[5]

[5] This is not necessarily the same as the σ_u in $\Lambda_u \equiv \lambda_u + \phi\sigma_u$ which may be the sum of several different cross sections in addition to the one in question.

These equations are identical in form with Eqs. (II.2) for $n=2$. The "parent" has a "decay constant" $\phi\sigma_u$ for the formation of the "daughter," and therefore we can write the expression for the activity of species v at time τ directly, by reference to Eq. (2.4) with $n=2$:

$$\mathbf{A}_v(\tau) = \lambda_v \mathbf{N}_v(\tau) = r_u \frac{\lambda_v(\phi\sigma_u)}{\Lambda_v \Lambda_u} \times \left[\frac{\Lambda_v}{\Lambda_v - \Lambda_u}(1-e^{-\Lambda_u \tau}) + \frac{\Lambda_u}{\Lambda_u - \Lambda_v}(1-e^{-\Lambda_v \tau})\right]. \quad \text{(III.3)}$$

The modes of reproduction differ, but the laws of population growth are the same.

This observation is of general validity. It permits us to write directly the equation for the activity of a species whose line of descent consists of any combination of decays and neutron absorptions. We have only to make an appropriate substitution of $\phi\sigma$'s for λ's in the appropiate equation derived in the preceding sections.

A few examples illustrating this procedure are given in the next section.

IV. SOME ILLUSTRATIVE PROBLEMS

As the first illustration, we will solve a fairly complicated case. Consider two two-membered fission product chains:

$$A_{11} \xrightarrow{\lambda_{11}} A_{12} \xrightarrow{\lambda_{12}}$$

$$A_{21} \xrightarrow{\lambda_{21}} A_{22} \xrightarrow{\lambda_{22}}$$

such that the members of the 1 chain can absorb neutrons to become corresponding members of the 2 chain. We suppose that each of the species has its own cross-section σ_{ij} and its own rate of direct formation in fission r_{ij}, and ask after the activity $\mathbf{A}_{22}(\tau)$ of the second member of the second chain at time τ (assuming $A_{ij}^0 = 0$).

Nuclei of species 22 are formed in all of the following ways:

(i) The A_{11} formed directly in fission (at rate r_{11}) decays to A_{12} which absorbs a neutron to give A_{22}:

$$A_{11} \xrightarrow{\lambda_{11}} A \xrightarrow{\lambda_{12}}_{12}$$

$$\downarrow\phi\sigma_{11} \quad \downarrow\phi\sigma_{12}$$

$$A_{22} \xrightarrow{\lambda_{22}}$$

$$\downarrow\phi\sigma_{22}.$$

Here we use the granddaughter equation with

daughter "decay constant" $\phi\sigma_{12}$:

$$\mathbf{A}_{22}{}^{(i)}(\tau)=\frac{\lambda_{22}(\phi\sigma_{12})\lambda_{11}}{\Lambda_{22}\Lambda_{12}\Lambda_{11}}r_{11}f_3(\tau),$$

where $f_3(\tau)$ is the expression under the summation sign in Eq. (II.4) with $n=3$.

(ii) The A_{11} formed directly in fission (at rate r_{11}) absorbs a neutron to give A_{21} which decays to A_{22}:

$$\begin{array}{l} A_{11}\xrightarrow{\lambda_{11}} \\ \downarrow\phi\sigma_{11} \\ A_{21}\xrightarrow{\lambda_{21}}A_{22}\xrightarrow{\lambda_{22}} \\ \downarrow\phi\sigma_{21}\ \downarrow\phi\sigma_{22}. \end{array}$$

Here we again use the granddaughter equation, this time with parent "decay constant" $\phi\sigma_{11}$:

$$\mathbf{A}_{22}{}^{(ii)}=\frac{\lambda_{22}\lambda_{21}(\phi\sigma_{11})}{\Lambda_{22}\Lambda_{21}\Lambda_{11}}r_{11}f_3(\tau).$$

(iii) The A_{12} formed directly in fission (at rate r_{12}) absorbs a neutron to give A_{22}:

$$\begin{array}{l} A_{12}\xrightarrow{\lambda_{12}} \\ \downarrow\phi\sigma_{12} \\ A_{22}\xrightarrow{\lambda_{22}} \\ \downarrow\phi\sigma_{22}. \end{array}$$

Here we use the daughter equation with "parent decay constant" $\phi\sigma_{12}$:

$$\mathbf{A}_{22}{}^{(iii)}=\frac{\lambda_{22}(\phi\sigma_{12})}{\Lambda_{22}\Lambda_{12}}r_{12}f_2(\tau),$$

where $f_2(\tau)$ is the expression under the summation sign in Eq. (II.4) with $n=2$.

(iv) The A_{21} formed directly in fission (at rate r_{21}) decays to A_{22}:

$$\begin{array}{l} A_{21}\xrightarrow{\lambda_{21}}A_{22}\xrightarrow{\lambda_{22}} \\ \downarrow\phi\sigma_{21}\ \downarrow\phi\sigma_{22}. \end{array}$$

Here we use the regular daughter Eq. ((II.4), with $n=2$):

$$\mathbf{A}_{22}{}^{(iv)}=\frac{\lambda_{22}\lambda_{21}}{\Lambda_{22}\Lambda_{21}}r_{21}f_2(\tau).$$

(v) A_{22} is formed directly in fission at rate r_{22}:

$$\begin{array}{l} A_{22}\xrightarrow{\lambda_{22}} \\ \downarrow\phi\sigma_{22}. \end{array}$$

Here we use Eq. (II.3),

$$\mathbf{A}_{22}{}^{(v)}(\tau)=r_{22}\frac{\lambda_{22}}{\Lambda_{22}}f_1(\tau).$$

The answer sought is the sum of the equations for the five paths of formation.

As a second illustration, we ask after the activity $A_\nu(\tau)$ of a radioactive species that results from ν successive neutron absorptions by a species created at constant rate r. The required equation is obtained directly from Eq. (II.4) on substitution of $\phi\sigma$'s for all the progenitor λ's:

$$\mathbf{A}_\nu(\tau)=\lambda_\nu\mathbf{N}_\nu(\tau)=r\frac{\lambda_\nu}{\Lambda_\nu}\left(\prod_{k=1}^{\nu-1}\frac{\phi\sigma_k}{\Lambda_k}\right)\sum_{i=1}^{\nu}\mathbf{b}_i(1-e^{-\Lambda_i\tau}),$$

$$\mathbf{b}_i=\prod_{j\neq i}\frac{\Lambda_j}{\Lambda_j-\Lambda_i}\quad(j=1,2,\cdots,\nu).$$

If all the members of the chain of neutron absorptions are stable against radioactive decay, we have

$$\mathbf{N}_\nu(\tau)=\frac{r}{\phi\sigma_\nu}\sum_{i=1}^{\nu}\mathbf{B}_i(1-e^{-\phi\sigma_i\tau}),$$

where

$$\mathbf{B}_i=\prod_{j\neq i}\frac{\sigma_j}{\sigma_j-\sigma_i}\quad(j=1,2,\cdots,\nu).$$

If, in addition, $\phi\sigma_i\tau\ll 1$ for all i, the corresponding expression for $N_\nu(\tau)$ can be obtained (laboriously) by expanding the exponentials in the above equation to the νth order. It is easier to solve the problem directly. Assume all $N_i{}^0=0$. Then, for $r\gg\phi\sigma_1N_1$, and $\sigma_iN_i(t)\gg\sigma_{i+1}N_{i+1}(t)$,

$$\frac{dN_1}{dt}=r;\quad N_1(\tau)=r\tau$$

$$\frac{dN_2}{dt}=\phi\sigma_1N_1;\quad N_2(\tau)=r\phi\sigma_1\frac{\tau^2}{2!}$$

$$\vdots$$

$$\frac{dN_\nu}{dt}=\phi\sigma_{\nu-1}N_{\nu-1};\quad N_\nu(\tau)=r\phi^{\nu-1}\sigma_1\sigma_2\cdots\sigma_{\nu-1}\frac{\tau^\nu}{\nu!}.$$

As a final illustration, we shall solve a practical problem that has risen in the measurement of the neutron cross section of radioactive isotopes. Katcoff mentions parenthetically in a paper[6] that he has measured the (n,γ) cross-section of 85-m Ba^{139} by neutron bombardment of Ba^{138} in the pile. Let us

[6] S. Katcoff, Phys. Rev. **72**, 1160 (1947). The work was completely reported in Manhattan Project Report CC-2908 (April 7, 1945).

derive the necessary equation by our procedure. The sequence of transformations was

$$\text{stable Ba}^{138}$$
$$\downarrow\phi\sigma_s$$
$$\text{85-m Ba}^{139}\xrightarrow{\lambda_1}$$
$$\downarrow\phi\sigma_1$$
$$\text{12.5-d Ba}^{140}\xrightarrow{\lambda_2}$$

where the notation is self-explanatory.

The activity of Ba^{140} after bombardment of Ba^{138} in a flux ϕ for a time τ can be calculated as follows. Let M be the number of Ba^{138} nuclei bombarded. Then the rate of formation of Ba^{139} is

$$r=\phi\sigma_s M.$$

Using Eq. (II.4) with $n=2$, and a "parent decay constant" $\phi\sigma_1$, we have for the Ba^{140} activity $\mathbf{A}_2(\tau)$,

$$\mathbf{A}_2(\tau)=\phi\sigma_s M\frac{\lambda_2(\phi\sigma_1)}{\Lambda_2\Lambda_1(\Lambda_2-\Lambda_1)}\times[\Lambda_2(1-e^{-\Lambda_1\tau})-\Lambda_1(1-e^{-\Lambda_2\tau})].$$

Now, $\Lambda_1\gg\Lambda_2$, and the circumstances of the experiment were such that τ was large, and $\lambda_2\gg\phi\sigma_2$, $\lambda_1\gg\phi\sigma_1$. Under these circumstances, the above equation becomes

$$\mathbf{A}_2(\tau)=\frac{\phi^2\sigma_s\sigma_1 M}{\lambda_1}(1-e^{-\lambda_2\tau}).$$

THE JOURNAL OF CHEMICAL PHYSICS VOLUME 17, NUMBER 6 JUNE, 1949

Calculation of the Energy of Vaporization of Perfluorocyclopentane from Intermolecular Forces

GILSON H. ROHRBACK
Department of Chemistry and Chemical Engineering, University of Washington, Seattle, Washington
(Received November 30, 1948)

By assuming a probable representative orientation of perfluorocyclopentane molecules in the liquid state, the energy of vaporization has been calculated, using both the London-Margenau equation of dispersion forces and the Slater-Kirkwood formula. Using only the data from density and dispersion measurements, fair agreement was found to the value experimentally determined. It is seen on the basis of this calculation that the contribution of the dipole-quadrupole interaction to the London formula is important.

THE extremely low dispersion of the perfluoropentanes as described in a previous paper[1] is one of the types of evidence indicating very small intermolecular forces in fluorocarbons. Of these compounds, perfluorocyclopentane, because of its symmetrical structure, lends itself more easily to theoretical treatment than either the linear or branched chain molecules. On this account this substance has been chosen as a material whose experimental energy of vaporization could be compared with that calculated using existing theories of intermolecular attraction and the physical constants determined in these laboratories.

The molar energy of vaporization U of a liquid represents the energy required to separate all the molecules of a gram mole of that liquid. If we let ΣV_i be the total attractive energy between a given molecule and all of its neighbors, then the molar energy of vaporization would be given by the relation

$$U=-\tfrac{1}{2}N\sum_{i=1}^{N}V_i, \qquad (1)$$

where N is Avogadro's number and $\frac{1}{2}$ is included to avoid counting each bond twice. Equation (1) assumes, of course, that the force acting on every molecule is the same, which cannot be the case for the surface molecules. However, for any large number of molecules being considered, this factor may be neglected. This equation further neglects the small configurational energy of the vapor and also assumes that there is no difference between the kinetic energies in the liquid and vapor phases.

Attraction between the non-polar molecules of perfluorocyclopentane must be due entirely to van der Waals forces of the dispersion type. As a first approximation these forces are known to be proportional to the inverse 6th power of the distance R, such a relation for the attraction between two spherical atoms being first derived by London.[2] It is generally recognized at present that there is attractive contribution from still higher inverse terms, and a better representation for the attractive potential is given by[3]

$$V=-C_1/R^6-C_2/R^8-C_3/R^{10}, \qquad (2)$$

[1] G. H. Rohrback and G. H. Cady, J. Am. Chem. Soc., to be published.

[2] F. London, Zeits. f. physik. Chemie **B11**, 222 (1930).

[3] H. Margenau, Rev. Mod. Phys. 11, 1 (1939). This paper is an excellent review of the theories of intermolecular forces

TABLE I.

Distance between molecular centers	No. of pairs of centers	$\Sigma 1/R^6$ (cm^{-6})	$\Sigma 1/R^8$ (cm^{-8})
7.07A	300	4.25×10^{45}	1.41×10^{60}
10.0A	150	0.207×10^{45}	0.01×10^{60}
12.24A	100*	0.102×10^{45}	0.01×10^{60}
Total	550	4.56×10^{45}	1.43×10^{60}

* Only the terms with $R < 11$A were considered. In all there are 600 pairs for this distance between centers, but the larger R values made negligible contribution.

where the constants C_1, C_2 and C_3 are all temperature independent. Just what contribution is made by each term cannot be stated simply. Certainly the first, London's dipole-dipole interaction, is dominant, although at small distances the others may become important. For example, by deriving an expression to account for the dipole-quadrupole interaction ($-C_2/R^8$), Margenau[4] has shown that the calculated potential attraction for hydrogen and helium is increased 25–50 percent. Again Sponer and Bruch-Willstatter[5] in the calculation of the sublimation energy of solid CO_2 found that the second term amounted to 52–56 percent of the first.

In addition to the attractive forces there exist at small distances repulsive forces which are very nearly represented by a term proportional to the inverse 12th power. These repulsive forces would tend to cancel in part some of the contribution of the higher terms of attraction.

For the purpose of the calculations for perfluorocyclopentane two different formulae will be used. The first is Margenau's[4] second approximation to London's dispersion formula, which includes the dipole-quadrupole energy contribution:

$$V = -\tfrac{3}{4} h\nu_0 \alpha^2 [\Sigma_i 1/R_i^6 + (9\alpha h\nu_0/2e^2)\Sigma_i 1/R_i^8]. \quad (3)$$

In this equation the factor e is the elementary electron charge, h is Planck's constant, α is the polarizability, and ν_0 is London's zero-point frequency. The attractive term of still higher power and the repulsive term are considered to have canceling contribution and are neglected.

Slater and Kirkwood[6] have derived another formula by a different method in which the molar binding energy of non-polar atoms is given by

$$U = 1.63 \times 10^{-10} n^{\frac{1}{2}} \alpha^{\frac{1}{2}} \Sigma_i 1/R_i^6 \text{ (kcal./mole)}, \quad (4)$$

where n is the number of electrons in the valence shell of the atoms. If it is to be applied to the case where more than one atom constitutes the attracting center, n is taken as equal to the total number of valence electrons. Again the factor α is the polarizability of the attracting center.

Although this latter relation does not include a term for dipole-quadrupole interaction (which still should be added), it is probable that this is not as important as with the London formula. This is apparent since the results from the Slater-Kirkwood formula are consistently higher than those from the simple London equation. Indeed, as Sponer and Bruch-Willstatter point out, if recent calculations of Page[7] on helium are capable of generalization, the result of the Slater-Kirkwood formula would be the same as that of London's equation with Margenau's second approximation included. In the calculation of the sublimation energy of solid benzene, deBoer[8] obtained satisfactory results using the single term of the Slater-Kirkwood approximation.

The factor α in the two dispersion formulas represents the polarizability of the attracting center, and it is obtainable from the well known relation:

$$4/3\pi N\alpha = [(n_\infty^2 - 1)/(n_\infty^2 + 2)](M/\rho) = P_E + P_A. \quad (5)$$

Here n_∞ is the refractive index at infinite wave-length, N is Avogadro's number, while M and ρ represent the molecular weight and density, respectively. To obtain directly the desired value of α it is necessary to measure the refractive index in the infra-red, since extrapolation from the visible region only gives the contribution of the electron polarization (P_E). However, for most substances the additional atomic polarization term (P_A) is small, about 3 cc, and as a fair approximation the extrapolated value may be increased by this amount. In the case of perfluorocyclopentane the extrapolation to infinite wave-length gives $P_E = 24.3$ cc; then if we include 3 cc for the polarization contribution due to nuclear displacement, we obtain

$$\alpha = 1.08 \times 10^{-23} \text{ cc.}$$

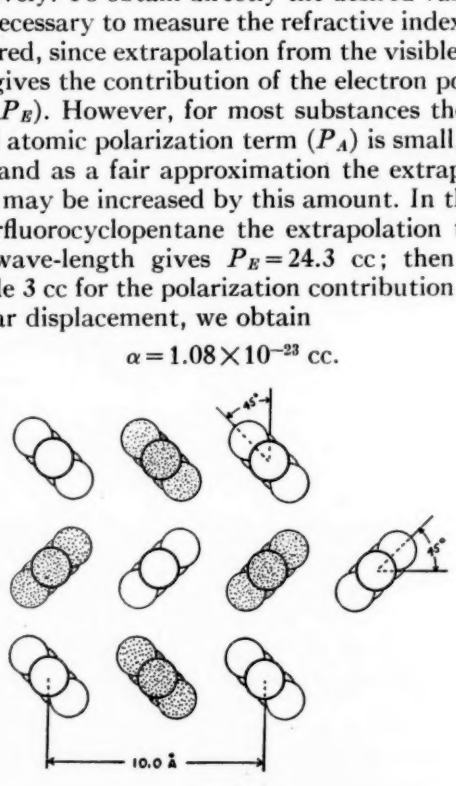

FIG. 1.

with a discussion of the importance of the various terms. The first term ($-C_1/R^6$) is the "dipole-dipole" interaction of London, the second ($-C_2/R^8$) is the "dipole-quadrupole" contribution, while the third ($-C_3/R^{10}$) is due to the "quadrupole-quadrupole" interaction.

[4] H. Margenau, Phys. Rev. **38**, 747 (1931).

[5] H. Sponer and M. Bruch-Willstatter, J. Chem. Phys. **5**, 745 (1937).

[6] J. C. Slater and J. G. Kirkwood, Phys. Rev. **37**, 682 (1931).

[7] C. H. Page, Phys. Rev. **51**, 1002 (1937).

[8] J. H. deBoer, Trans. Faraday Soc. **32**, 10 (1936).

The refractive index of a medium varies with the wave-length of the light according to the form

$$n=1+\sum_i (a_i/(\nu_{0_i}{}^2-\nu^2)), \qquad (6)$$

as has been derived in the classical electromagnetic theory and confirmed by quantum theory. In Eq. (6) n is the refractive index measured with light of frequency ν, a is a constant in each term of the series, and ν_0 is the same characteristic frequency as found in the London dispersion equation. Using the simple form of only one term of the summation, from the dispersion data* of perfluorocyclopentane we have for the characteristic frequency:

$$\nu_0=4.87\times10^{15}\ \text{sec.}^{-1}.$$

The first calculation of the energy of vaporization is made considering the intermolecular forces to originate from the centers of the molecules. From density measurements at 15°C ($\rho=1.6610$),[9] assuming a close-packed cubic face centered orientation (which is probably very nearly the case with molecules of this shape), the distances to the two nearest sets of surrounding molecules are calculated (12 molecules at $R=7.07$A; 6 molecules at $R=10.0$A). Neglecting any anisotropy of the polarizability, application of the two formulas gives:

London (R^{-6} term only):	$U=2.1$ kcal./mole,
Slater and Kirkwood:	$U=2.8$ kcal./mole.

These are considerably lower than the value measured by Barber,[10] who gives the energy of vaporization at constant volume for 15°C as equal to 5.80 kcal./mole. Inclusion of the inverse 8th term in the London formula increases the energy value to very nearly 3 kcal./mole.

The second calculation is made by considering each CF_2 group as an attracting center for the similar groups in the other molecules. This procedure should provide a more reasonable basis for calculation than does the assumption of a single attracting center for each molecule, since the peripheral atoms approach each other much more closely than do the molecular centers. Again, a close-packed cubic arrangement for the centers of the molecules is assumed, but in this case it is necessary to assume some instantaneous orientation pattern as well. Actually, the molecules of perfluorocyclopentane are rotating, but in order to calculate the attractive energies between CF_2 groups we assume an instantaneous orientation having substantially the same total attractive potential as with random orientation. The arrangement chosen is as pictured in Fig. 1, with the shaded molecules having their centers in a plane either 5.00A** above or below the plane of the drawing.

The polarizability for the CF_2 group is now taken as equal to one-fifth the molecular polarizability,

$$\alpha_{CF_2}=2.16\times10^{-24}\ \text{cc},$$

while the characteristic frequency of the five identical subparts is assumed to be that of the entire molecule; thus

$$\nu_{0CF_2}=4.87\times10^{15}\ \text{sec.}^{-1}.$$

The anisotropy of the polarizability is again neglected, but, by reason of the assumed relative positions of the molecules, it is felt that this neglect is not serious. It is recognized, of course, that the polarizability of the CF_2 centers is not spherical but that it probably does not have an anisotropy very much greater than 2:1. Because the value used is an average one between the three component directions and because the pairing occurs between a large number of separate groups with varying orientations, the anisotropic effects should tend to balance out.

Using the bond distance C–C = 1.45A[11] and C–F = 1.35A[12] with a tetrahedral angle between the two fluorine atoms on each carbon, the positions of the five centers can be calculated. They are located not at the centers of the carbon atoms, but at a distance 0.51A farther out corresponding to the center of electron density. Each center is located by finding the center of gravity of three negative charges 3, 7, 7 assumed to exist at the centers of the carbon and two fluorine atoms, respectively.

Rather than calculate all the possible distances, metal pentagons were carefully machined to scale (1A = I inch) and set up in the various positions according to the orientation model. Distances were then measured by calipers and read to the nearest 0.01 inch. The summation of the reciprocal 6th and 8th powers of the distances are given in Table I. Using the values from the 3rd and 4th columns of the above table, application of the formulas gives

London (R^{-6} term only):	3.7 kcal./mole,
London and Margenau:	5.3 kcal./mole,
Slater and Kirkwood:	5.1 kcal./mole,

this time in much better agreement with the measured value of 5.80 kcal./mole.

ACKNOWLEDGMENT

This work was performed under contract with the Office of Naval Research, U. S. Navy Department. The author wishes to thank Dr. George H. Cady for his willing aid and many valuable suggestions.

* The determined values of refractive index at 15°C are:

$H_\alpha\cdots(6563\text{A})$; $n=1.2576$;
$H_\beta\cdots(4861\text{A})$; $n=1.2595$.

[9] L. L. Burger, Thesis, University of Washington (1948).
[10] E. J. Barber, Thesis, University of Washington (in preparation).

** Using density value $\rho=1.6610$.

[11] E. L. Pace, J. Chem. Phys. **16**, 74 (1948). (C–C distance in C_2F_6.)
[12] L. O. Brockway, J. Phys. Chem. **41**, 185 (1937).

Transport Properties of Multicomponent Gas Mixtures*

CHARLES F. CURTISS AND JOSEPH O. HIRSCHFELDER
University of Wisconsin, Naval Research Laboratory, Madison, Wisconsin
(Received November 1, 1948)

Equations are derived for the viscosity, ordinary (pressure) diffusion, and thermal diffusion of multicomponent mixtures of gases. The ordinary diffusion velocities are expressed in terms of the usual diffusion coefficients for binary mixtures. The analysis is an extension of the work of Chapman and Cowling. It is shown that the Chapman-Cowling and Enskog procedure can be justified on the basis of a variational principle. This variational principle should be generally applicable to a large class of problems.

EQUATIONS are derived for the viscosity, ordinary (pressure) diffusion, and thermal diffusion of a multicomponent gaseous mixture. Only in the case of ordinary diffusion was it possible to express the results in terms of the corresponding property for the binary components.[1] The analysis is an extension of the work of Chapman and Cowling.[2] Previously, Hellund[3] derived a system of equations for both ordinary and thermal diffusion of multicomponent systems. His equations are somewhat more complicated than ours, since he has taken quantum corrections into account. Hellund used a variational procedure to obtain approximate solutions to the integral equations which describe the first-order perturbations of the Boltzmann equations. Chapman and Cowling proceed through a system of expansions of functions in terms of Sonine polynomials. In the appendix of the present paper, it is shown that the two methods are equivalent.

A gaseous mixture can be described completely by a set of distribution functions,

$$f_i = f_i(\mathbf{r}, \mathbf{c}_i, t),$$

which give the probability of finding a molecule of "i" at the position $\mathbf{r}$ with velocity $\mathbf{c}_i$ at time t. These distribution functions f_i must satisfy a set of "equations of change," which are the integro-differential Boltzmann equations,

$$(\partial f_i/\partial t)+\mathbf{c}_i\cdot\nabla_{\mathbf{r}} f_i+\mathbf{F}_i\cdot\nabla_{\mathbf{c}_i} f_i = -\sum_j \int\int\int (f_i f_j - f_i' f_j')\, g b db d\epsilon d\mathbf{c}_j. \quad (1)$$

In these equations, $\nabla_{\mathbf{r}}$ and $\nabla_{\mathbf{c}_i}$ indicate gradients in coordinate space and in velocity space; and the distribution function, f_i', for the states formed on impact is functionally the same as the initial distribution function, f_i, except that its argument is the velocity after the collision:

$$f_i' = f_i(\mathbf{c}_i').$$

Here $\mathbf{c}_i'$ is the value of $\mathbf{c}_i$ after a collision characterized by three parameters: The first of the collision parameters, g, is the magnitude of the relative velocity of the molecules before they begin to interact; b is the "impact parameter," i.e., the distance between the initial line of motion of one molecule and the center of the other molecule; and ϵ is the azimuthal angle. Since no drastic changes in temperature or pressure or average velocity occur within one mean free path, we assume that all of the distribution functions deviate only slightly from the equilibrium or local Maxwellian distribution $f_i^{(0)}$. The arguments of the Maxwellian distribution functions $f_i^{(0)}$ are

(a) the velocities relative to the local mass average velocity of the gas mixture, $\mathbf{C}_i$,
(b) the local temperature, T,
(c) the number density, n_i, of molecules of the ith kind.

The number average velocity of molecules of "i" at a particular point in space is

$$\bar{\mathbf{c}}_i = \frac{1}{n_i}\int \mathbf{c}_i f_i d\mathbf{c}_i. \quad (2)$$

Then the mass average velocity of all molecules, $\mathbf{c}_0$, is

$$\mathbf{c}_0 = \frac{1}{\rho}\sum_i n_i m_i \bar{\mathbf{c}}_i, \quad (3)$$

where m_i is the molecular weight of "i" and ρ the over-all density of the gas, is

$$\rho = \sum_i n_i m_i. \quad (4)$$

The "peculiar" velocity is defined as the velocity of a molecule relative to the local average velocity:

$$\mathbf{C}_i = \mathbf{c}_i - \mathbf{c}_0. \quad (5)$$

For many purposes, it is convenient to use a reduced

* This work was carried out under Contract NOrd 9938 with the Navy Bureau of Ordnance.

[1] Equations have been derived for thermal conductivity of a gaseous mixture, but they have been omitted from this paper because they are incomplete insofar as they neglect the internal degrees of freedom of the molecule.

[2] S. Chapman and T. G. Cowling, *The Mathematical Theory of Non-Uniform Gases* (Cambridge University Press, London, 1939).

[3] E. J. Hellund, Phys. Rev. **57**, 319 (1940).

velocity, $\mathfrak{C}_i$, defined in terms of $\mathbf{C}_i$ by the equation:

$$\mathfrak{C}_i = (m_i/2kT)^{\frac{1}{2}}\mathbf{C}_i. \quad (6)$$

The local Maxwellian distribution is then:

$$f_i^{(0)} = n_i(m_i/2\pi kT)^{\frac{3}{2}} \exp(-\mathfrak{C}_i^2). \quad (7)$$

The true distribution function is obtained by a perturbation method similar to Enskog's.[2] For the first approximation we write

$$f_i = f_i^{(0)}(1+\phi_i), \quad (8)$$

where ϕ_i is a small correction function. Substituting f_i into the Boltzmann equations, it appears that to the first approximation ϕ_i does not occur in the left-hand side of the equation, and on the right-hand side it occurs in a linear fashion. Thus,

$$f_i^{(0)}[\mathbf{b}_i : \nabla_r \mathbf{c}_0 + (n/n_i)\mathbf{C}_i \cdot \mathbf{d}_i - ((5/2)-\mathfrak{C}_i^2)\mathbf{C}_i \cdot \nabla_r \ln T] = -\sum_j \iiint [\phi_i + \phi_j - \phi_i' - \phi_j'] \times f_i^{(0)} f_j^{(0)} g b db d\epsilon d\mathbf{c}_j. \quad (9)$$

Here $\mathbf{b}_i$ (not to be confused with impact parameter) is defined by

$$\mathbf{b}_i = 2\mathfrak{C}_i\mathfrak{C}_i - \tfrac{2}{3}\mathfrak{C}_i^2\mathbf{I}, \quad (10)$$

where $\mathbf{I}$ is the unit tensor; the vector $\mathbf{d}_i$ is given by

$$\mathbf{d}_i = \nabla_r(n_i/n) + ((n_i/n) - (n_i m_i/\rho))\nabla_r \ln p - (n_i m_i/\rho p)(\rho \mathbf{F}_i - \sum_j n_j m_j \mathbf{F}_j)$$

and p is the ordinary gas pressure

$$p = nkT; \quad n = \sum_i n_i. \quad (12)$$

Now the local temperature, mass average velocity, and the individual number densities can be varied arbitrarily at each point by varying either the initial conditions or the boundary conditions. In order that ϕ_i satisfy Eq. (9), regardless of the variations in these parameters, it must have the functional form

$$\phi_i = -\mathbf{A}_i \cdot \nabla_r \ln T - \mathbf{B}_i : \nabla_r \mathbf{c}_0 + (n^2/\rho kT) \sum_{j \neq i} (m_i m_j/n_i)\mathbf{D}_{ij} \cdot \mathbf{d}_j, \quad (13)$$

where $\mathbf{A}_i$, $\mathbf{B}_i$, and $\mathbf{D}_{ij}$ are of the form

$$\mathbf{A}_i = \mathbf{C}_i A_i(C_i^2), \quad (14)$$

$$\mathbf{B}_i = (\mathbf{C}_i\mathbf{C}_i - \tfrac{1}{3}C_i^2\mathbf{I})B_i(C_i^2), \quad (15)$$

and

$$\mathbf{D}_{ij} = \mathbf{C}_i D_{ij}(C_i^2). \quad (16)$$

The arguments for this functional form of ϕ_i are similar to those given by Chapman and Cowling[2] in the case of a binary mixture. Because T, $\mathbf{c}_0$, and the n_i are regarded as arbitrary parameters to be varied at will, it follows that when the above expression for ϕ_i is substituted into Eq. (9), this equation can be split up into a number of separate conditions which serve to completely determine the functions A_i, B_i, and D_{ij}. All of the transport properties can be described in terms of these functions.

Any arbitrary function of $\mathfrak{C}_i^2 = x_i$ can be expanded in a series of Sonine (or generalized Laguerre) polynomials, $S_m^{(p)}(x)$. In our problem, this type of expansion is convenient because of the orthogonality condition

$$\int_0^\infty x^m e^{-x} S_m^{(i)}(x) S_m^{(j)}(x) dx = \delta_{ij}\Gamma(m+i+1)/i! \quad (17)$$

A finite series made up of the first n terms of such a series serves as an approximation to the required function. The coefficients of such a finite series are obtained by requiring that the resulting function be the best approximation to the true function. The criterian of best approximation is set by the variational principle discussed in the appendix.

Various approximations to the values of the transport coefficients are then obtained by considering successively a larger number of terms in the required series. This is essentially the method of solution used by Chapman and Cowling. In the cases of gases containing one or two components, the first approximation in which the transport phenomena appears is quite good, i.e., higher approximations (obtained by considering a larger number of terms in the series) do not differ from the first value by more than 2 percent. Thus, in the following treatment we will consider only the lowest approximation for each transport property.

I. ORDINARY DIFFUSION

The diffusion velocity of a component "i" is the average velocity of molecules of "i" compared to the velocity of the stream, $\mathbf{c}_0$, i.e.,

$$\overline{\mathbf{C}}_i = \bar{\mathbf{c}}_i - \mathbf{c}_0. \quad (18)$$

This velocity is made up of two terms:

$$\overline{\mathbf{C}}_i = \mathbf{V}_i^{(p)} + \mathbf{V}_i^{(t)}. \quad (19)$$

The first term,

$$\mathbf{V}_i^{(p)} = (n^2/3\rho kT)(m_i/n_i^2) \sum_{j \neq i} \mathbf{d}_j m_j \times \int D_{ij}(C_i^2) C_i^2 f_i^{(0)} d\mathbf{C}_i \quad (20)$$

is the contribution of ordinary or pressure diffusion, while the second term,

$$\mathbf{V}_i^{(t)} = -(1/3n_i)(\nabla_r \ln T) \int A_i(C_i^2) f_i^{(0)} d\mathbf{C}_i, \quad (21)$$

is the thermal diffusion term.

In considering the ordinary diffusion, it is necessary to use only the constant term $D_{ij}^{(0)}$ in the series expansion. In terms of this quantity the ordinary diffusion velocity becomes

$$\mathbf{V}_i^{(p)} = (n^2/n_i\rho) \sum_{j\neq i} m_j D_{ij}^{(0)} \mathbf{d}_j. \tag{22}$$

The constants $D_{ij}^{(0)}$ are related to the binary diffusion coefficients $\mathfrak{D}_{ij}$ by the set of equations:

$$\sum_j (1/\mathfrak{D}_{ij})[n_j m_k D_{ij}^{(0)} + n_i m_i D_{ji}^{(0)} - n_i m_k D_{jk}^{(0)}] = \rho(1-\delta_{ik}). \tag{23}$$

By definition,

$$D_{ii}^{(0)} = 0. \tag{24}$$

The diagonal equations, $i=k$, of this set are identically satisfied. Thus, if there are s components in the gas mixture, the set is a set of $s(s-1)$ equations for the $s(s-1)$ coefficients $D_{ij}^{(0)}$ for which $i\neq j$.

The set of Eqs. (22) and (23) suffices to determine the diffusion velocities. However, a considerably simpler set of equations may be obtained by a rearrangement of these sets of equations. One obtains

$$\sum_j (n_i n_j/\mathfrak{D}_{ij})(\mathbf{V}_i^{(p)} - \mathbf{V}_j^{(p)}) = -n^2 \mathbf{d}_i. \tag{25}$$

This is a set of $(s-1)$ independent equations. They can be used to obtain the $(s-1)$ values of the diffusion velocities relative to any particular one, e.g., $\mathbf{V}_i^{(p)} - \mathbf{V}_1^{(p)}$. Making use of the relation

$$\sum_i n_i m_i \mathbf{V}_i^{(p)} = 0, \tag{26}$$

one can then obtain all of the diffusion velocities. Equations (25) are similar to a set of diffusion equations which have been obtained through a study of experimental data.[4] Carrying out the solution of Eq. (25) and writing the result in the form of Eq. (22), we obtain

$$D_{12}^{(0)} = -(\rho n_1/m_2) \frac{\begin{vmatrix} 0 & F_{23} & F_{24} & \cdots & F_{2s} \\ F_{32} & 0 & F_{34} & \cdots & F_{3s} \\ F_{42} & F_{43} & 0 & \cdots & F_{4s} \\ \cdot & \cdot & \cdot & & \cdot \\ \cdot & \cdot & \cdot & & \cdot \\ \cdot & \cdot & \cdot & & \cdot \\ F_{s2} & F_{s3} & F_{s4} & \cdots & 0 \end{vmatrix} + \begin{vmatrix} F_{12} & F_{13} & F_{14} & \cdots & F_{1s} \\ F_{32} & 0 & F_{34} & \cdots & F_{3s} \\ F_{42} & F_{43} & 0 & \cdots & F_{4s} \\ \cdot & \cdot & \cdot & & \cdot \\ \cdot & \cdot & \cdot & & \cdot \\ \cdot & \cdot & \cdot & & \cdot \\ F_{s2} & F_{s3} & F_{s4} & \cdots & 0 \end{vmatrix}}{\begin{vmatrix} 0 & F_{12} & F_{13} & \cdots & F_{1s} \\ F_{21} & 0 & F_{23} & \cdots & F_{2s} \\ F_{31} & F_{32} & 0 & \cdots & F_{3s} \\ \cdot & \cdot & \cdot & & \cdot \\ \cdot & \cdot & \cdot & & \cdot \\ \cdot & \cdot & \cdot & & \cdot \\ F_{s1} & F_{s2} & F_{s3} & \cdots & 0 \end{vmatrix}}, \tag{27}$$

where the elements F_{ij} are

$$F_{ij} = (n_i n_j/\mathfrak{D}_{ij}) + (n_j m_j/m_i) \sum_{k\neq i} (n_k/\mathfrak{D}_{ik}), \quad (i\neq j). \tag{28}$$

The entire set of $D_{ij}^{(0)}$ is obtained by permuting the indices, in the final expression for D_{12} or by suitable modifications of the determinants in the numerator of the expression in Eq. (27).

In considering problems of reaction kinetics in flow systems, it becomes necessary to discuss the diffusion of active particles, such as atoms and free radicals. Such components are always present to a very small extent. It is possible to show from Eqs. (22) and (23) that for any component which is present as a trace the mass rate of diffusion is given by

$$n_i m_i \mathbf{V}_i^{(p)} = -[(n^2 m_i(1-(n_i m_i/\rho))/\sum_{j\neq i} (n_j/\mathfrak{D}_{ij})]\mathbf{d}_i. \tag{29}$$

This equation indicates roughly that the reciprocal of the average diffusion coefficient for a multicomponent mixture should be taken as the molal average of the reciprocals of the binary coefficients.

II. THERMAL DIFFUSION

In order to obtain an expression for thermal diffusion, one must consider two terms in the series expansion of the function $A_i(C_i^2)$, the coefficients of which are $m_i A_i^{(1)}$ and $m_i A_i^{(2)}$, although only $A_i^{(1)}$ appears in the expression for the thermal diffusion velocity:

$$\mathbf{V}_i^{(t)} = -A_i^{(1)} kT \nabla_r \ln T. \tag{30}$$

The coefficients are given as solutions of the $2s$ linearly independent equations:

$$\sum_j \{\alpha_{ij}^{(1)} A_j^{(1)} + \alpha_{ij}^{(2)} A_j^{(2)}\} = 0, \tag{31}$$

$$\sum_j \{\beta_{ij}^{(1)} A_j^{(1)} + \beta_{ij}^{(2)} A_j^{(2)}\} = 1. \tag{32}$$

[4] O. Hougen and K. Watson, *Kinetics and Catalysis* (John Wiley and Sons, Inc., New York, 1947); T. K. Sherwood, *Absorbtion and Extraction* (McGraw-Hill Book Company, Inc., New York, 1937), Chapter I.

Here

$$\alpha_{ij}^{(1)} = \sum_{k\neq i} (n_k m_k m_j/(m_i+m_k))\Omega_{ik}^{(1)}(1) \times[(m_i/m_j)(\delta_{ij}-\delta_{jk})-(n_j/n_i)],$$

$$\alpha_{ij}^{(2)} = -(m_i^2/m_j)\sum_k (n_k m_k^2/(m_i+m_k)^2) \times[\Omega_{ik}^{(1)}(2)-(5/2)\Omega_{ik}^{(1)}(1)](\delta_{ij}-\delta_{kj}),$$

$$\beta_{ij}^{(1)} = (32m_i/15)\sum_k (n_k m_k^2/(m_i+m_k)^2) \times[\Omega_{ik}^{(1)}(2)-(5/2)\Omega_{ik}^{(1)}(1)](\delta_{ij}-\delta_{kj}),$$

$$\beta_{ij}^{(2)} = -(32m_i^2/15m_j)\sum_k (n_k m_k/(m_i+m_k)^3) \times\begin{bmatrix}(5/4)(6m_j^2+5m_k^2)\Omega_{ik}^{(1)}(1)(\delta_{ij}-\delta_{kj}) \\ -[5m_k^2\Omega_{ik}^{(1)}(2)-m_k^2\Omega_{ik}^{(1)}(3)](\delta_{ij}-\delta_{kj}) \\ +2m_j m_k\Omega_{ik}^{(2)}(2)(\delta_{ij}+\delta_{kj})\end{bmatrix}.$$

The Ω's are collision integrals defined by

$$\Omega_{ij}^{(l)}(s) = \pi^{\frac{1}{2}}[m_i m_j/2kT(m_i+m_j)]^{(2s+3)/2} \times\int_0^\infty\int_0^\infty \{\exp-(m_i m_j g^2/2kT(m_i+m_j))\} \times(1-\cos^l\chi)g^{2s+3}b\,dg\,db, \quad (37)$$

where

$$\chi = \chi(g, b) \quad (38)$$

is the angle through which the path of a molecule is deflected when it is involved in a collision characterized by the relative velocity g and the impact parameter, b. It is in this relation that the law of force between the interacting molecules appears. If one considers the case of rigid sphere molecules we have

$$\Omega_{ij}^{(1)}(s) = \tfrac{1}{4}\sigma_{ij}^2\left(\frac{2\pi kT(m_i+m_j)}{m_i m_j}\right)^{\frac{1}{2}}(1+s)! \quad (39)$$

and

$$\Omega_{ij}^{(2)}(2) = \sigma_{ij}^2\left(\frac{2\pi kT(m_i+m_j)}{m_i m_j}\right)^{\frac{1}{2}}, \quad (40)$$

where σ_{ij} is the average diameter of the two molecules, "i" and "j." However, it is well known that the approximation of rigid sphere molecules is of no value at all in treating problems of thermal diffusion. In a recent paper, Hirschfelder, Bird, and Spotz[5] have published tables of values of integrals closely related to the Ω-integrals, in which the values were obtained using a Lennard-Jones type of interaction potential.

The equations for thermal diffusion involve four types of collision integrals:

$\Omega_{ik}^{(1)}(1)$ which determines normal diffusion,
$\Omega_{ik}^{(2)}(2)$ which determines viscosity, and
$\Omega_{ik}^{(1)}(2)$, $\Omega_{ik}^{(1)}(3)$ which do not occur elsewhere.

The simultaneous solution of Eqs. (31) and (32) determines the coefficients of thermal diffusion $A_i^{(1)}$. In the general case, the velocity of thermal diffusion may be expressed as the ratio of two determinants.

$$\mathbf{V}_i^{(l)} = \frac{\begin{vmatrix} \alpha_{11}^{(1)} & \alpha_{12}^{(1)} & \cdots & \alpha_{1s}^{(1)} & \alpha_{11}^{(2)} & \alpha_{12}^{(2)} & \cdots & \alpha_{1s}^{(2)} & 0 \\ \alpha_{21}^{(1)} & \alpha_{22}^{(1)} & \cdots & \alpha_{2s}^{(1)} & \alpha_{21}^{(2)} & \alpha_{22}^{(2)} & \cdots & \alpha_{2s}^{(2)} & 0 \\ \cdot & \cdot & & \cdot & \cdot & \cdot & & \cdot & \cdot \\ \cdot & \cdot & & \cdot & \cdot & \cdot & & \cdot & \cdot \\ \cdot & \cdot & & \cdot & \cdot & \cdot & & \cdot & \cdot \\ \alpha_{s1}^{(1)} & \alpha_{s2}^{(1)} & \cdots & \alpha_{ss}^{(1)} & \alpha_{s1}^{(2)} & \alpha_{s2}^{(2)} & \cdots & \alpha_{ss}^{(2)} & 0 \\ \beta_{11}^{(1)} & \beta_{12}^{(1)} & \cdots & \beta_{1s}^{(1)} & \beta_{11}^{(2)} & \beta_{12}^{(2)} & \cdots & \beta_{1s}^{(2)} & 1 \\ \beta_{21}^{(1)} & \beta_{22}^{(1)} & \cdots & \beta_{2s}^{(1)} & \beta_{21}^{(2)} & \beta_{22}^{(2)} & \cdots & \beta_{2s}^{(2)} & 1 \\ \cdot & \cdot & & \cdot & \cdot & \cdot & & \cdot & \cdot \\ \cdot & \cdot & & \cdot & \cdot & \cdot & & \cdot & \cdot \\ \cdot & \cdot & & \cdot & \cdot & \cdot & & \cdot & \cdot \\ \beta_{s1}^{(1)} & \beta_{s2}^{(1)} & \cdots & \beta_{ss}^{(1)} & \beta_{s1}^{(2)} & \beta_{s2}^{(2)} & \cdots & \beta_{ss}^{(2)} & 1 \\ \delta_{i1} & \delta_{i2} & \cdots & \delta_{is} & 0 & 0 & \cdots & 0 & 0 \end{vmatrix}}{\begin{vmatrix} \alpha_{11}^{(1)} & \alpha_{12}^{(1)} & \cdots & \alpha_{1s}^{(1)} & \alpha_{11}^{(2)} & \alpha_{12}^{(2)} & \cdots & \alpha_{1s}^{(2)} \\ \alpha_{21}^{(1)} & \alpha_{22}^{(1)} & \cdots & \alpha_{2s}^{(1)} & \alpha_{21}^{(2)} & \alpha_{22}^{(2)} & \cdots & \alpha_{2s}^{(2)} \\ \cdot & \cdot & & \cdot & \cdot & \cdot & & \cdot \\ \cdot & \cdot & & \cdot & \cdot & \cdot & & \cdot \\ \cdot & \cdot & & \cdot & \cdot & \cdot & & \cdot \\ \alpha_{s1}^{(1)} & \alpha_{s2}^{(1)} & \cdots & \alpha_{ss}^{(1)} & \alpha_{s1}^{(2)} & \alpha_{s2}^{(2)} & \cdots & \alpha_{ss}^{(2)} \\ \beta_{11}^{(1)} & \beta_{12}^{(1)} & \cdots & \beta_{1s}^{(1)} & \beta_{11}^{(1)} & \beta_{12}^{(1)} & \cdots & \beta_{1s}^{(2)} \\ \beta_{21}^{(1)} & \beta_{22}^{(1)} & \cdots & \beta_{2s}^{(1)} & \beta_{21}^{(2)} & \beta_{22}^{(2)} & \cdots & \beta_{2s}^{(2)} \\ \cdot & \cdot & & \cdot & \cdot & \cdot & & \cdot \\ \cdot & \cdot & & \cdot & \cdot & \cdot & & \cdot \\ \cdot & \cdot & & \cdot & \cdot & \cdot & & \cdot \\ \beta_{s1}^{(1)} & \beta_{s2}^{(1)} & \cdots & \beta_{ss}^{(1)} & \beta_{s1}^{(2)} & \beta_{s2}^{(2)} & \cdots & \beta_{ss}^{(2)} \end{vmatrix}} \nabla_r(kT). \quad (41)$$

[5] J. O. Hirschfelder, R. B. Bird, and E. Spotz; J. Chem. Phys. 16, 968 (1948).

III. VISCOSITY

The coefficient of viscosity is given in terms of the function $B_i(C_i^2)$. In this case, as in the case of ordinary diffusion, it is necessary to consider only the first term in the expansion of $B_i(C_i^2)$. In terms of these coefficients, $B_i^{(0)}$, we obtain the coefficient of viscosity:

$$\mu = k^2T^2 \sum_i (n_i/m_i)B_i^{(0)}. \tag{42}$$

The values of the $B_i^{(0)}$ are given as the solutions of the set of equations

$$k^2T^2 \sum_j (n_j/m_j)G_{ij}B_j^{(0)} = -1, \tag{43}$$

where

$$G_{ij} = (-32m_i/15n_jkTm_j) \sum_k (n_km_k/(m_i+m_k)^2)$$
$$\times[5m_j\Omega_{ik}^{(1)}(1)(\delta_{ij}-\delta_{kj}) + \tfrac{3}{2}m_k\Omega_{ik}^{(2)}(2)(\delta_{ij}+\delta_{kj})].$$

Using formal methods of solutions, we can write

$$\mu = \frac{\begin{vmatrix} G_{11} & G_{12} & G_{13} & \cdots & G_{1s} & 1 \\ G_{21} & G_{22} & G_{23} & \cdots & G_{2s} & 1 \\ G_{31} & G_{32} & G_{33} & \cdots & G_{3s} & 1 \\ \cdot & \cdot & \cdot & & \cdot & \cdot \\ \cdot & \cdot & \cdot & & \cdot & \cdot \\ \cdot & \cdot & \cdot & & \cdot & \cdot \\ G_{s1} & G_{s2} & G_{s3} & \cdots & G_{ss} & 1 \\ 1 & 1 & 1 & \cdots & 1 & 0 \end{vmatrix}}{|G_{ij}|}. \tag{45}$$

APPENDIX

The functions, A_i, B_i, and D_{ij}, which determine the transport properties, are all obtained through the solution of sets of integral equations of the type:

$$F_i(\mathbf{C}_i) = -\sum_j \int\int\int [A_i + A_j - A_i' - A_j']$$
$$\times f_i^{(0)} f_j^{(0)} gbdbd\epsilon d\mathbf{c}_j \tag{46}$$

one for each component in the mixture. The solution of the integral Eqs. (46) is not unique. However, the functions, A_i, B_i, and D_{ij}, must satisfy in addition a set of three auxiliary condition, which, in effect, require that the values of n_i, $\mathbf{c}_0$, and T are unaffected by the perturbation. The auxiliary conditions serve to specify exactly one of the solutions of Eq. (46), i.e., they serve to remove an indeterminacy obtained later. In this section we will prove a variational principle[6] related to this problem and show how one may make use of this principle to obtain approximate solutions to the integral equation.

[6] The statement of the variational principle was first made by E. J. Hellund and E. A. Uehling, Phys. Rev. **56**, 818 (1939).

Let A_i^* be a set of functions which satisfy the equation

$$\int F_i(\mathbf{C}_i)A_i^* d\mathbf{c}_i = -\sum_j n_in_j[A_i^*, A_i^* + A_j^*]_{ij}. \tag{47}$$

The bracket notation indicates the integral

$$[G, H]_{ij} = (1/n_in_j)\int\int\int G[H - H']$$
$$\times f_i^{(0)} f_j^{(0)} gbdbd\epsilon d\mathbf{c}_j d\mathbf{c}_i. \tag{48}$$

It is easily shown that this is identical with

$$[G, H]_{ij} = (1/2n_in_j)\int\int\int [G - G']$$
$$\times [H - H'] f_i^{(0)} f_j^{(0)} gbdbd\epsilon d\mathbf{c}_j d\mathbf{c}_i, \tag{49}$$

so that

$$[G, H]_{ij} = [G, H]_{ji} = [H, G]_{ij}. \tag{50}$$

From Eqs. (46) and (47) we find

$$\sum_j n_in_j[A_i^*, A_i + A_j]_{ij}$$
$$= \sum_{ij} n_in_j[A_i^*, A_i^* + A_j^*]_{ij}. \tag{51}$$

Now we sum this equation over i and make use of the symmetry properties, Eq. (50). The result is

$$\{A^*, A\} = \{A^*, A^*\}, \tag{52}$$

where the curly bracket indicates

$$\{G, H\} = \sum_{ij} n_in_j[G_i + G_j, H_i + H_j]_{ij}. \tag{53}$$

It is clear that $\{\ \}$ also possess the symmetry property

$$\{G, H\} = \{H, G\}. \tag{54}$$

Since $\{G, G\}$ is the sum of integrals, the integrands of which are essentially positive,

$$\{G, G\} \geqslant 0. \tag{55}$$

If G satisfies the auxiliary conditions, then the equality sign can apply only if G is identically zero.

Let us consider a particular curly bracket

$$\{A - A^*, A - A^*\} \geqslant 0. \tag{56}$$

From the above, the equality sign can apply only if A^* is identically equal to A. The $\{\ \}$ is a linear operator. Hence, from Eq. (56) we have

$$\{A, A\} - 2\{A^*, A\} + \{A^*, A^*\} \geqslant 0 \tag{57}$$

or from Eq. (52)

$$\{A^*, A^*\} \leqslant \{A, A\}. \tag{58}$$

Since the equality sign applies only if A^* is A, the best approximation to A that can be obtained with a particular functional form for A^* is that obtained by maximizing $\{A^*, A^*\}$ with respect to all of the available parameters.

In order to implement the variational principle, we will consider in detail the case that the trial function is a linear combination of known functions, e.g.,

$$A_i^* = \sum_k a_{ik} S_k(\mathbf{C}_i), \tag{59}$$

where the a_{ik} are the coefficients to be fixed by the variational principle, and the S_k are known functions. It is this form of a trial function which is used in this paper. If we sum Eq. (47) over all i, then symmetrize as above, we find

$$\{A^*, A^*\} = -2 \sum_i \int F_i(\mathbf{C}_i) A_i^* d\mathbf{c}_i. \tag{60}$$

Thus, the problem of finding a maximum of $\{A^*, A^*\}$ is that of finding a minimum of

$$g = \sum_i \int F_i(\mathbf{C}_i) A_i^* d\mathbf{c}_i. \tag{61}$$

Now we introduce the explicit form of A_i^*, Eq. (59), and let

$$F_{ik} = \int F_i(\mathbf{C}_i) S_k(\mathbf{C}_i) d\mathbf{c}_i \tag{62}$$

and

$$\omega_i = \sum_k a_{ik} F_{ik} + \sum_{jkk'} n_i n_j a_{ik} \times \begin{bmatrix} a_{ik'}[S_k(C_i),\ S_{k'}(C_i)]_{ij} \\ + a_{jk'}[S_k(C_i),\ S_{k'}(C_j)]_{ij} \end{bmatrix}. \tag{63}$$

Then g becomes

$$g = \sum_{ik} a_{ik} F_{ik} \tag{64}$$

and the condition, Eq. (47), becomes

$$\omega_i = 0. \tag{65}$$

The problem now is that of finding an extremum of g, Eq. (64), subject to the condition that the set of Eqs. (65) be satisfied. Let us use the method of Lagrangian multipliers. Letting λ_i be the multipliers, the set of equations which specify the sets λ_i and a_{ik} are

$$(\partial g/\partial a_{ik}) + \sum_j \lambda_j (\partial \omega_j / \partial a_{ik}) = 0, \tag{66}$$

$$\omega_j = 0. \tag{67}$$

Carrying out the operations, we have

$$(1+\lambda_i) F_{ik} + \sum_{jk'} n_i n_j \times \begin{bmatrix} 2\lambda_i a_{ik'}[S_k(C_i),\ S_{k'}(C_i)]_{ij} \\ + (\lambda_i + \lambda_j) a_{jk'}[S_k(C_i),\ S_{k'}(C_j)]_{ij} \end{bmatrix} = 0,$$

$$\sum_k a_{ik} F_{ik} + \sum_{jkk'} n_i n_j a_{ik} \times \begin{bmatrix} a_{ik'}[S_k(C_i),\ S_{k'}(C_i)]_{ij} \\ + a_{jk'}[S_k(C_i),\ S_{k'}(C_j)]_{ij} \end{bmatrix} = 0.$$

A solution of this set of equations is

$$\lambda_i = 1 \tag{70}$$

for all i and a_{ik} determined so that

$$F_{ik} + \sum_{jk'} n_i n_j [a_{ik'}[S_k(C_i),\ S_{k'}(C_i)]_{ij} + a_{jk'}[S_k(C_i),\ S_{k'}(C_j)]_{ij}] = 0. \tag{71}$$

The set of Eqs. (71) are not linear independent. However, a unique solution is obtained by requiring that in addition to satisfying Eqs. (71), the a_{ik} must be such that the A_i^* satisfy the auxiliary conditions. This method of obtaining the constants in a finite series approximation to the functions A_i, B_i, and D_{ij} is equivalent to the procedure used by Chapman and Cowling[2] and is the method used in this paper.

Vibration Spectra of *Cis* and *Trans* $C_2H_2Cl_2$ and $C_2D_2Cl_2$

H. J. BERNSTEIN AND D. A. RAMSAY
National Research Council, Ottawa, Canada

(Received November 12, 1948)

The infra-red spectra of gaseous and liquid *cis* and *trans* $C_2H_2Cl_2$ and $C_2D_2Cl_2$ have been obtained in the region 3500 to 400 cm^{-1}.

The fine structure of a $\perp$ band in *trans* $C_2H_2Cl_2$ was also resolved and the least moment of inertia obtained.

An assignment of all the fundamentals for the four molecules has been made.

Calculations of potential functions and of the equilibrium constants for the reaction *cis*$\rightleftharpoons$*trans* support the assignment.

INTRODUCTION

ALTHOUGH *cis* and *trans* dichloroethylene are relatively simple planar molecules with symmetries C_{2v} and C_{2h}, respectively, considerable disagreement exists between the assignments by various authors[1–4] of the twelve fundamental frequencies for each of these molecules. This disagreement is largely caused by the lack of reliable infra-red data, particularly on the contours of the infra-red bands in the vapor. We have therefore re-investigated the infra-red spectra of these molecules and their deuterium analogues. Using these data and the existing Raman data, we have been able to make satisfactory assignments of the twelve frequencies in the *cis* molecule and ten frequencies in the *trans* molecule. The two remaining frequencies in the *trans* molecule are active in the infra-red, but lie beyond the range of a KBr prism. These frequencies have been obtained from combination tones.

Our values for the low frequencies are in agreement with the data of Wood and Stevenson[5] for the equilibrium constants of the *cis*$\rightleftharpoons$*trans* reaction at different temperatures. These authors deduced from their results that the sum of the two low frequencies must lie between 420 and 450 cm^{-1}.

We have found it necessary, however, to revise the potential function calculation of Pitzer and Freeman[4] for the out-of-plane vibrations of *cis*- and *trans*-dichloroethylene, since these authors used an erroneous value for the *trans* wagging frequency and assumed that the 620 cm^{-1} band reported by Wu[2] for the *cis* molecule was a combination of the Raman frequency at 350 cm^{-1} with the torsion frequency at 270 cm^{-1}. We have shown, however, that the 620 cm^{-1} band was caused by an impurity.

MATERIALS

A mixture of *cis* and *trans* $C_2H_2Cl_2$ was prepared from Eastman Kodak sym $C_2H_4Cl_2$ by reaction with Zn, and the isomers separated by fractional distillation.

$$\textit{trans}\ \text{b.p.} = 48.1 \pm 0.1°\text{C.}$$
$$\textit{cis}\ \text{b.p.} = 60.1 \pm 0.1°\text{C.}$$

The two samples were judged from their spectra to be about 99 percent pure.

A mixture of *cis* and *trans* $C_2D_2Cl_2$ was prepared in the following manner:

1. $CaC_2 + D_2O = CaO + C_2D_2$,
2. $C_2D_2 + 2Cl_2 = C_2D_2Cl_4$,
3. $C_2D_2Cl_4 + Zn = C_2D_2Cl_2 + ZnCl_2$,

and the isomers were separated by fractional distillation.

The spectra indicated that these samples were about 99 percent deuterated. Owing to the small quantity of material available, it was not possible to obtain as complete a separation as for the "light" isomers. The *cis* $C_2D_2Cl_2$ contained about 2 percent of *trans* $C_2D_2Cl_2$ as impurity and the *trans* $C_2D_2Cl_2$ contained about 10 percent of *cis* $C_2D_2Cl_2$ as impurity.

EXPERIMENTAL

The infra-red spectra of these four molecules were investigated using a Perkin Elmer Model 12*B* infra-red spectrometer with a G-M amplifier and a Brown Pen Recorder. NaCl and KBr prisms were used for the regions 3500–700 cm^{-1} and 700–400 cm^{-1}, respectively. Vapor spectra were investigated using a 10-cm absorption cell, various pressures being used to resolve all the bands observed; liquid spectra were obtained using 0.1-mm and 0.025-mm absorption cells, the more intense bands being resolved using dilute solutions in CS_2 and CCl_4.

The infra-red spectra are reproduced in Figs. 1–4 and the infra-red and Raman frequencies given in Tables I–IV.

[1] G. Herzberg, *Infrared and Raman Spectra of Polyatomic Molecules* (D. Van Nostrand Company, Inc., New York, 1945), p. 330.
[2] Ta-You Wu, J. Chem. Phys. **5**, 392 (1937); Phys. Rev. **46**, 465 (1934).
[3] B. Trumpy, Zeits. f. Physik. **98**, 672 (1935).
[4] K. S. Pitzer and N. K. Freeman, J. Chem. Phys. **14**, 586 (1946).
[5] R. E. Wood and D. P. Stevenson, J. Am. Chem. Soc. **63**, 1650 (1941).

ASSIGNMENT OF FREQUENCIES[6]

(a) *Cis* $C_2H_2Cl_2$

The five strong polarized lines in the Raman spectrum may be assigned to the totally symmetric A_1 vibrations. These frequencies are also active in the infra-red though the 1183-cm^{-1} band is extremely weak.[7] The two depolarized lines at 406 cm^{-1} and 876 cm^{-1} which do not have corresponding infra-red absorptions may be assigned to the two A_2 vibrations since these vibrations are active only in the Raman spectrum. The five remaining vibrations give strong absorptions in the infra-red.

The contours of the infra-red bands may be predicted qualitatively from the curves of Badger and Zumwalt.[8] For vibrations with change of electric moment parallel to the greatest axis of inertia (type B_2) the bands should exhibit a P, Q, R structure with a strong central Q branch. The 697-cm^{-1} band may be assigned therefore to the lone vibration of this type, ν_{12}. For changes of electric moment parallel to the middle axis of inertia (type A_1) a doublet structure is expected. This is in agreement with the above assignment of frequencies to this type, though for the 714-cm^{-1} band the doublet structure is overlapped by the rotational contour of the 697-cm^{-1} band. Finally for changes of electric moment parallel to the least axis of inertia (type B_1), the bands should exhibit P, Q, and R branches of similar intensity. Such contours are observed for the 571, 857, and 1303 cm^{-1} bands. The fourth frequency of this type, the C—H stretching frequency, corresponds to the strong 3072-cm^{-1} absorption. Further confirmation of the assignment is afforded by the fact that all the remaining weak bands have been interpreted as simple combination tones.

(b) *Trans* $C_2H_2Cl_2$

The five strong polarized Raman lines again correspond to the totally symmetric A_g vibrations. The Raman line of medium intensity at 758 cm^{-1} is probably the B_g wagging frequency, though this line should be depolarized.[9] This assignment, however, is supported by the appearance of a corresponding line at 658 cm^{-1} in the spectrum of *trans* $C_2D_2Cl_2$ as expected from the Teller-Redlich[10] product rule.

The strong infra-red bands at 817, 895, 1200, and 3080 cm^{-1} are presumably infra-red active fundamentals. The 895-cm^{-1} band which shows a clearly resolved rotational fine structure in the vapor spectrum, may be assigned to type A_u and the 817- and 1200-cm^{-1} bands which exhibit doublet structures in the vapor spectrum may be assigned to type B_u. The 3080 cm^{-1} band is obviously the type B_u C—H stretching frequency. This leaves two low frequencies

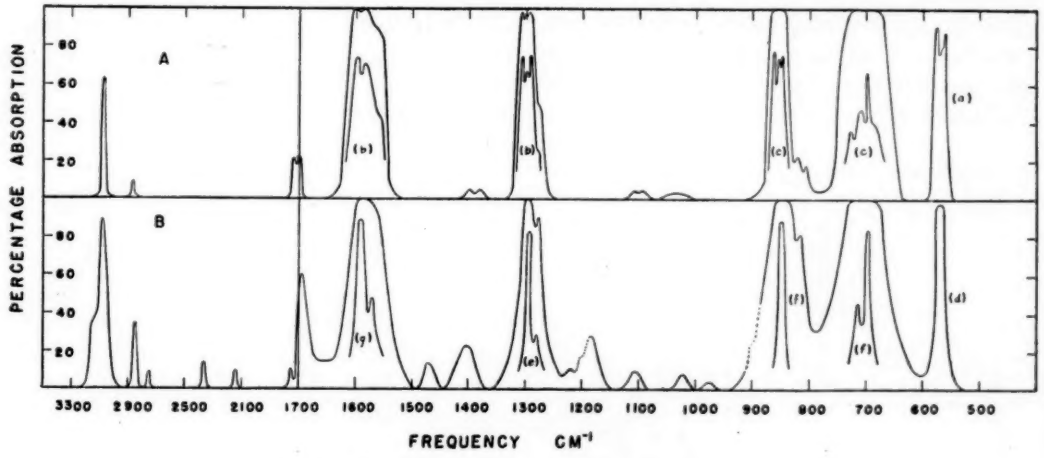

FIG. 1. Infra-red spectra of *cis*-dichloroethylene.

A. Vapor	Cell length 10 cm Pressure (a) 120-mm Hg	Temperature 20°C (b) 30-mm Hg (c) 10-mm Hg
B. Liquid	(d) Pure liquid 0.1-mm cell (f) 10 percent solution in CS_2 0.025-mm cell	(e) 10 percent solution in CS_2 0.1-mm cell (g) 10 percent solution in CCl_4 0.1-mm cell
------	*trans* impurity	

[6] The normal modes of vibration of *cis*- and *trans*-dichloroethylene, their symmetry classes and selection rules, have been given by G. Herzberg (see reference 1) and are not reproduced here. The same system of numbering has been used.

[7] It is interesting to note that the first overtone of this band at 2367 cm^{-1} has approximately the same intensity as the fundamental. A similar phenomenon is found in the *cis* $C_2D_2Cl_2$ molecule.

[8] R. M. Badger and L. R. Zumwalt, J. Chem. Phys. **6**, 711 (1938). Using the electron diffraction values for the molecular dimensions (see section on product rule) the parameters ρ and S, used by Badger and Zumwalt to express the asymmetry of the molecule, take the values $\rho = 3.89$, $S = -0.91$.

[9] The polarization of this line has been discussed by Herzberg (see reference 1).

[10] E. Teller, quoted in J. Chem. Soc. p. 966 (1936). O. Redlich, Zeits. f. Physik chemie **B28**, 371 (1935).

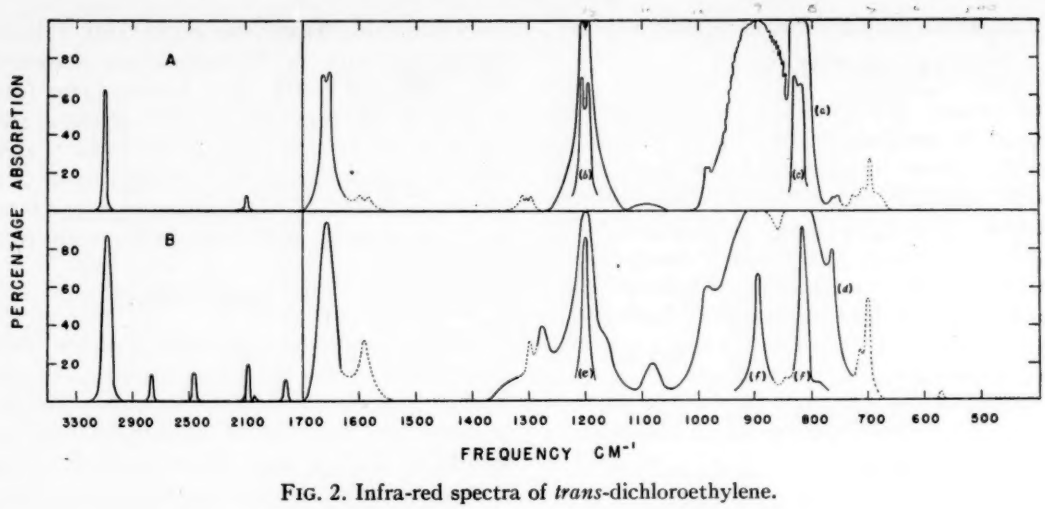

FIG. 2. Infra-red spectra of *trans*-dichloroethylene.

A. Vapor — Cell length 10 cm; Temperature 20°C; Pressure (a) 120-mm Hg (b) 30-mm Hg (c) 5-mm Hg

B. Liquid (d) Pure liquid 0.1-mm cell; (e) 10 percent solution in CS_2 0.1-mm cell; (f) 10 percent solution in CS_2 0.025-mm cell

------ *cis* impurity

unassigned, one of type A_u and the other of type B_u. All the remaining weak bands may be interpreted as simple combination tones with the exception of the bands at 763, 983, 1080, 1276, and 1816 cm^{-1}.

The two low frequencies must lie below 400 cm^{-1} since they were not observed using a KBr prism. Moreover, the results of Wood and Stevenson[5] indicated that the sum of these frequencies should lie between 420 and 450 cm^{-1}. Pitzer and Freeman[4] assigned a value of 270 cm^{-1} to the A_u torsion frequency by assuming that the 620-cm^{-1} band reported by Wu[2] was a combination tone, 350+270 cm^{-1}. The 620-cm^{-1} band, however, must have been caused by an impurity, since we have not observed it using even longer absorption paths than Wu.

The in-plane bending frequency of type B_u may be computed from the rotational product rule[11] for *cis-trans* isomers, a value of approximately 280 cm^{-1} being obtained. The torsion frequency of type A_u however, cannot be obtained by this means, as the rule is not applicable to out-of-plane vibrations.

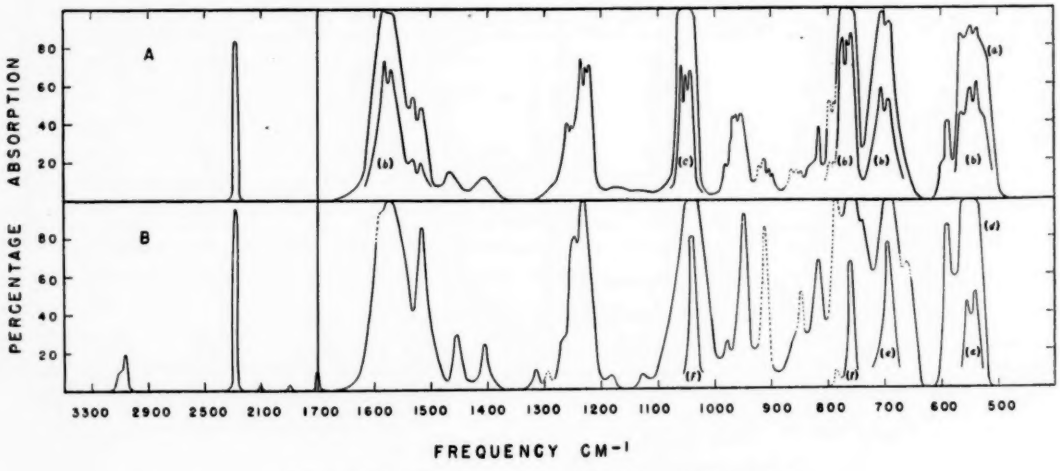

FIG. 3. Infra-red spectra of *cis*-dichloroethylene-d_2.

A. Vapor — Cell length 10 cm; Temperature 20°C; Pressure (a) 120-mm Hg (b) 30-mm Hg (c) 10-mm Hg

B. Liquid (d) Pure liquid 0.1-mm cell; (e) 10 percent solution in CS_2 0.1-mm cell; (f) 10 percent solution in CS_2 0.025-mm cell

------ *trans*-d_2 and *cis* impurities

[11] H. J. Bernstein, J. Chem. Phys. **17**, 256 (1949).

TABLE I. Infra-red and Raman frequencies for *cis* $C_2H_2Cl_2$.

Infra-red (cm^{-1}) Vapor	Liquid	Raman (cm^{-1}) liquid[a]	Assignment
		173 (*s*) pol.	$\nu_8(A_1)$
		406 (*s*) depol.	$\nu_7(A_2)$
P 564 *Q* 571 *R* 578	571 (*s*)	563 (*m*) depol.	$\nu_{11}(B_1)$
P 688 *Q* 697 *R* ?	697 (*vs*)		$\nu_{12}(B_2)$
? 727	714 (*s*)	711 (*s*) pol.	$\nu_4(A_1)$
808 823	815 (*w*)	807 (*vw*)	$406+406=812\ (A_1)$
P 851 *Q* 857 *R* 864	848 (*vs*)		$\nu_{10}(B_1)$
		876 (*w*) depol.	$\nu_6(A_2)$
	975 (*vw*)		$406+571=977\ (B_2)$
	1022 (*vw*)		$173+848=1021\ (B_1)$
	1105 (*w*)		$406+697=1103\ (B_1)$
	1183 (*w*)	1179 (*s*) pol.	$\nu_3(A_1)$
	1218 (*w*)		$2\times697-173=1221\ (A_1)$
	1254 (*w*)		$406+848=1254\ (B_2)$
	1279 (*m*)		$571+714=1285\ (B_1)$
P 1296 *Q* 1303 *R* 1310	1294 (*s*)		$\nu_9(B_1)$
	1404 (*w*)		$697+714=1411\ (B_2)$
	1470 (*w*)		$173+1294=1467\ (B_1)$
	1571 (*w*)		$697+876=1573\ (B_1)$ $714+848=1562\ (B_1)$
1583 1598	1590 (*s*)	1587 (*s*) pol.	$\nu_2(A_1)$
	1695 (*w*)	1689 (*w*) depol. ?	$848+848=1696\ (A_1)$ $406+1294=1700\ (B_2)$
	1753 (*vw*)		$876+876=1752\ (A_1)$ $571+1183=1754\ (B_1)$ $173+1590=1763\ (A_1)$
	2137 (*w*)		$848+1294=2142\ (A_1)$
	2367 (*w*)		$1183+1183=2366\ (A_1)$
	2753 (*w*)		$1183+1590=2773\ (A_1)$
2860	2855 (*w*)		$1294+1590=2884\ (B_1)$
3072	3072 (*s*)		$\nu_5(B_1)$
		3077 (*vs*) pol.	$\nu_1(A_1)$
	3150 (*w*)	3160 (*w*) depol. ?	$1590+1590=3180\ (A_1)$

[a] See reference 1.

Since the sum of the two low frequencies must lie between 420 and 450 cm^{-1} the torsion frequency may be expected to lie in the region 150 ± 50 cm^{-1}.

Better estimates of these frequencies may be obtained from combination tones. The only simple combinations of the low frequencies which are active in the infra-red are combinations of the Raman frequency at 349 cm^{-1} with the two low infra-red frequencies. These combination bands should appear in the region 450 to 650 cm^{-1}. The absorption of 1 mm of liquid in this region was investigated using a KBr prism and two weak bands were observed at 541 and 614 cm^{-1} (see Fig. 5) in addition to the *cis* impurity band at 571 cm^{-1}. If these bands are interpreted in the above manner values of 192 cm^{-1} and 265 cm^{-1} are obtained for the two low infra-red frequencies. Using these values, simple interpretations are obtained for the five remaining weak bands hitherto unexplained.

(c) *Cis* $C_2D_2Cl_2$

The five strongest lines in the Raman spectrum, *viz.* 171, 689, 850, 1570, 2325 cm^{-1}, correspond to the five totally symmetric lines for the non-deuterated molecule. Similarly, the 368-cm^{-1} Raman line corresponds to the A_2 vibration at 406 cm^{-1} in the light molecule. The other frequency of this species has not been observed but may be estimated from the Teller-Redlich product rule to be in the region of 710 cm^{-1} (see below).

The lone frequency of type B_2 must correspond to one of the strong infra-red bands at 540 and 558 cm^{-1}. The contours of these bands overlap in the vapor spectrum and are not readily separated, but the isotopic product rule indicates that the band at 558 cm^{-1} is the B_2 frequency. The band at 540 cm^{-1} must be assigned then to type B_1 together with the strong infra-red bands at 761, 1040, and 2280 cm^{-1}. The 761 and 1040 cm^{-1} bands show well defined *PQR* structures in the vapor spectrum.

Most of the remaining bands may be interpreted as simple combination tones corresponding to those found for the non-deuterated molecule. A few weak bands, *viz.* 818, 976, 1179, 1314, however, cannot be explained as simple combination tones and probably represent combinations perturbed by Fermi resonance. This is to be expected since many combinations of the same symmetry have approximately the same frequency in the region 800–1400 cm^{-1}. Tentative assignments have been given in these cases.

TABLE II. Infra-red and Raman frequencies for *trans* $C_2H_2Cl_2$.

Infra-red (cm^{-1}) Vapor	Liquid	Raman (cm^{-1}) liquid[a]	Assignment
		349 (*s*) pol.	$\nu_8(A_g)$
	541 (*vw*)		$349+192=541\ (A_u)$
	614 (*vw*)		$349+265=614\ (B_u)$
		758 (*m*) pol.	$\nu_5(B_g)$
754 763	763 (*w*)		$844+265-349=760\ (B_u)$
823 832	817 (*vs*)		$\nu_{11}(B_u)$
		844 (*s*) pol.	$\nu_4(A_g)$
898	895 (*vs*)		$\nu_6(A_u)$
	985 (*w*)		*$2\times349+265=963\ (B_u)$ $265+895-192=968\ (B_u)$
	1080 (*w*)		$1270-192=1078\ (A_u)$
	1166 (*w*)		$349+817=1166\ (B_u)$
1195 1205	1200 (*s*)		$\nu_{10}(B_u)$
		1270 (*s*) pol.	$\nu_3(A_g)$
	1276 (*w*)		$192+265+817=1274\ (A_u)$
		1576 (*s*) pol.	$\nu_2(A_g)$
		1626 (*vw*) pol.	$817+817=1634\ (A_g)$
1654 1663	1658 (*m*)		$758+895=1653\ (B_u)$ $817+844=1661\ (B_u)$
		1692 (*w*) pol.	$844+844=1688\ (A_g)$
	1816 (*w*)		$2\times817+192=1826\ (A_u)$
	2047 (*w*)		$844+1200=2044\ (B_u)$
2092	2082 (*w*)		$817+1270=2087\ (B_u)$
	2460 (*w*)		$1200+1270=2470\ (B_u)$ $895+1576=2471\ (A_u)$
	2760 (*w*)		$1200+1576=2776\ (B_u)$
		3071 (*s*) pol.	$\nu_1(A_g)$
3090	3080 (*s*)		$\nu_9(B_u)$
		3142 (*w*) depol. ?	$1576+1576=3152\ (A_g)$

[a] See reference 1.

* Fermi resonance gives 985 cm^{-1} and 945 cm^{-1} the latter being obscured by the intense 895 cm^{-1} band.

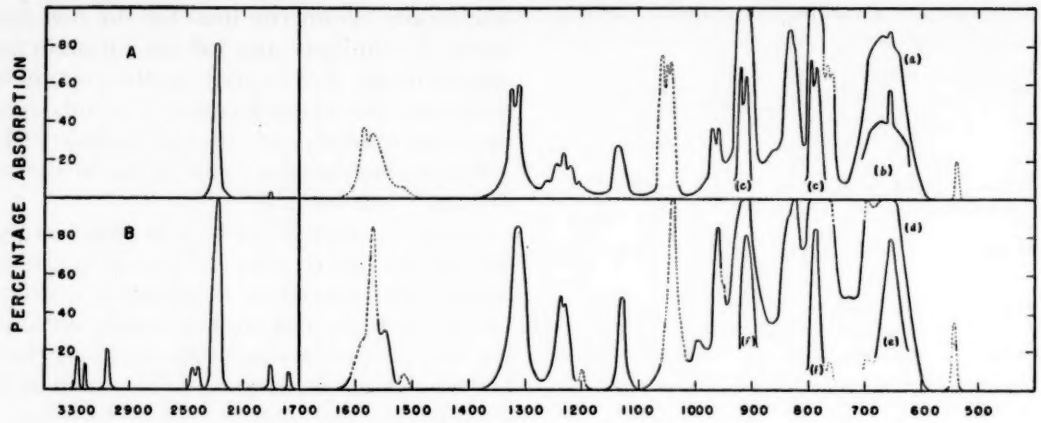

FIG. 4. Infra-red spectra of *trans*-dichloroethylene-d_2.

A. Vapor — Cell length 10 cm; Temperature 20°C; Pressure (a) 120-mm Hg (b) 30-mm Hg (c) 10-mm Hg

B. Liquid — (d) Pure liquid 0.1-mm cell; (e) 10 percent solution in CS_2 0.1-mm cell; (f) 10 percent solution in CS_2 0.025-mm cell

------ *cis*-d_2 impurity

(d) *Trans* $C_2D_2Cl_2$

By comparison with the assignment for *trans* $C_2H_2Cl_2$, the Raman frequencies at 346, 765, 992, 1570, and 2325 cm^{-1} may be assigned unambiguously to type A_g and the 657-cm^{-1} Raman line to type B_g. The infra-red band at 658 cm^{-1} which exhibits a *P*, *Q*, *R* structure in the vapor spectrum corresponds to the 895 cm^{-1} band for the light molecule though the resolving power proved insufficient to resolve the rotational fine structure for the heavy molecule. The strong infra-red bands at 784, 912, and 2285 cm^{-1} may be assigned to type B_u, the doublet structures for the 784- and 912-cm^{-1} bands being resolved in the vapor spectrum. If it is assumed that the two low frequencies in the light molecule, *viz.* 192 and 265 cm^{-1} are not appreciably affected by substitution of deuterium, a complete assignment is obtained and all the remaining weak bands may be satisfactorily interpreted as simple combination tones.

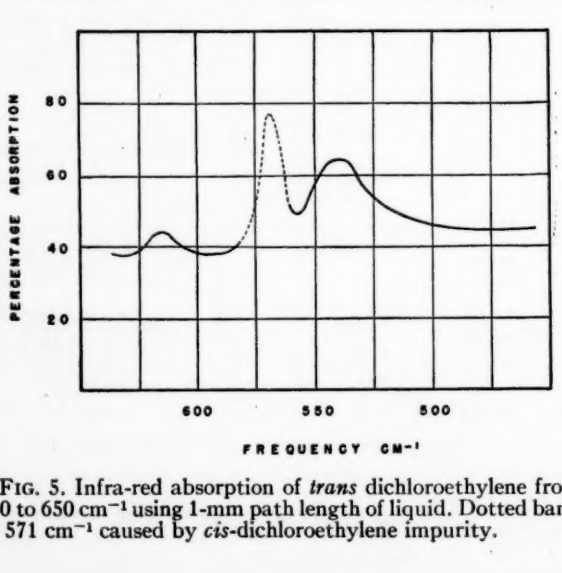

FIG. 5. Infra-red absorption of *trans* dichloroethylene from 450 to 650 cm^{-1} using 1-mm path length of liquid. Dotted band at 571 cm^{-1} caused by *cis*-dichloroethylene impurity.

PRODUCT RULE RATIOS FOR *CIS* AND *TRANS* $C_2H_2Cl_2$ AND $C_2D_2Cl_2$

Using the dimensions for the *cis* and *trans* molecules obtained by the electron diffraction method[12] *viz.*

	cis	*trans*
$r_{C=C}$	1.38A (assumed)	1.38A (assumed)
r_{C-Cl}	1.67±0.03A	1.69±0.02A
Cl−C=C	123.5 ±1°	122.5 ±1°

and further assuming $r_{C-H}=1.07$A, H−C=C $=120°$ as in ethylene[13] the principal moments of inertia for the light and heavy molecules are evaluated as follows:

	cis $C_2H_2Cl_2$	*cis* $C_2D_2Cl_2$	*trans* $C_2H_2Cl_2$	*trans* $C_2D_2Cl_2$
I_A	70.3	82.4	15.8	23.2
I_B	329.8	334.8	548.2	548.6
I_C	400.1	417.2	564.0	571.8

units of 10^{-40} g cm²

The theoretical product rule ratios for the various symmetry types of the *cis* and *trans* molecules may now be calculated and compared with the observed ratios (Tables V and VI). The agreement, in general, is good though the observed ratio for the *cis* B_1

[12] L. O. Brockway, J. Y. Beach, and L. Pauling, J. Am. Chem. Soc. **57**, 2693 (1935).

[13] W. S. Gallaway and E. F. Barker, J. Chem. Phys. **10**, 88 (1942).

vibration is slightly high. Liquid frequencies have been used throughout.

ANALYSIS OF THE FINE STRUCTURE OF THE 898-CM^{-1} BAND OF *TRANS* $C_2H_2Cl_2$

The frequencies of the individual rotation lines were obtained from the ammonia data given by Oetjen, Kao and Randall[14] (see Fig. 6) and are listed in Table VII. The frequencies have been corrected to vacuum and are probably accurate to ± 0.1 cm^{-1}. The *trans* $C_2H_2Cl_2$ molecule approximates very closely to a symmetric top whose figure axis passes approximately through the two chlorine atoms. Since the 898-cm^{-1} band corresponds to an out-of-plane wagging motion of the CHCl groups, the change in electric moment is perpendicular to this axis, hence we should expect a perpendicular type band. Moreover since $I_A \ll I_B$ or I_C the band will consist mainly of a series of Q branches of the various sub-bands present, the PR separations in the individual sub-bands being considerably smaller than the separations between the various Q branches.

The fact that a strong "Q branch" is found in the region of the band origin gives the band the appearance of a $\parallel$ band. This is altogether out of the question however due to the magnitude of the spacing. The appearance of this Q branch is probably due to the slight deviation of the molecule from a perfect symmetric top, c.f., the type C band at 949 cm^{-1} for ethylene.[15] The spacing of the Q branches is given by the equation[16]

$$\nu = \nu_0 + (A' - B') \pm 2(A' - B')K + [(A' - B') - (A'' - B'')]K^2, \quad (1)$$

where A', B', are the rotational constants for the upper state, A'', B'', are the rotational constants for the lower state, the positive sign applies to the ^RQ

TABLE III. Infra-red and Raman frequencies for *cis* $C_2D_2Cl_2$.

Infra-red (cm^{-1}) Vapor	Liquid	Raman (cm^{-1}) liquid[a]	Assignment
		171 (*s*)	$\nu_8(A_1)$
		368 (*m*)	$\nu_7(A_2)$
		515 (*w*)	689 − 171 = 518 (A_1)
	540 (*s*)		$\nu_{11}(B_1)$
	558 (*s*)		$\nu_{12}(B_2)$
	590 (*m*)		761 − 171 = 590 (B_1)
693 / 706	695 (*s*)	689 (*s*)	$\nu_4(A_1)$
	741 (*w*)		368 + 368 = 736 (A_1)*
P 759 / *Q* 766 / *R* 773	761 (*vs*)		$\nu_{10}(B_1)$
818	818 (*w*)		†
		850 (*m*)	$\nu_3(A_1)$
P 899 / *Q* 905 / *R* 912	912 (*m*)#		368 + 558 = 926 (B_1)* Fermi Resonance
P 955 / *Q* 962 / *R* 967	949 (*m*)		171 + 761 = 932 (B_1)*
	976 (*w*)		†
P 1045 / *Q* 1051 / *R* 1058	1040 (*vs*)		$\nu_9(B_1)$
	1129 (*w*)		368 + 761 = 1129 (B_2)*
	1179 (*w*)		††
P 1222 / *Q* 1228 / *R* 1235	1228 (*m*)		540 + 695 = 1235 (B_1)*
	1247 (*w*)		558 + 695 = 1253 (B_2)*
	1263 (*w*)		558 + 710 = 1268 (B_1)*
	1314 (*w*)		††
	1405 (*w*)		368 + 1040 = 1408 (B_2)*
	1455 (*w*)		695 + 761 = 1456 (B_1)*
1518 / 1532	1515 (*m*)	1507 (*w*)	761 + 761 = 1522 (A_1)*
1569 / 1582	1572 (*s*)	1570 (*s*)	$\nu_2(A_1)$
	1702 (*w*)		850 + 850 = 1700 (A_1)*
	1885 (*vw*)		850 + 1040 = 1890 (B_1)
	2107 (*vw*)		540 + 1572 = 2112 (B_1)
2280	2280 (*s*)		$\nu_5(B_1)$
		2325 (*s*)	$\nu_1(A_1)$
	3060 (*w*)		2325 + 761 = 3086 (B_1)
	3110 (*w*)		2280 + 850 = 3130 (B_1)
		3150 ? (*vw*)	1572 + 1572 = 3144 (A_1)*

[a] See reference 3.
* The corresponding combination tone was observed for *cis* $C_2H_2Cl_2$.
# *Trans* $C_2D_2Cl_2$ impurity contributes partly to the intensity of this band.
† Fermi resonance between 2 × 171 + 558 = 900 (B_2); 368 + 540 = 908 (B_2).
†† Fermi resonance between two of the following; 171 + 368 + 710 = 1249 (A_1); 2 × 710 − 171 = 1249 (A_1); 2 × 540 + 171 = 1251 (A_1).

TABLE IV. Infra-red and Raman frequencies for *trans* $C_2D_2Cl_2$.

Infra-red (cm^{-1}) Vapor	Liquid	Raman (cm^{-1}) liquid[a]	Assignment
		346 (*s*)	$\nu_8(A_g)$
		657 (*m*)	$\nu_3(B_g)$
P ? / *Q* 660 / *R* ?	658 (*s*)		$\nu_6(A_u)$
	729 (*vw*)		265 + 658 − 192 = 731 (B_u)*
		765 (*m*)	$\nu_4(A_g)$
786 / 796	784 (*vs*)		$\nu_{11}(B_u)$
	826 (*m*)#		†
	836 (*w*)		657 + 192 = 849 (B_u)
911 / 921	912 (*vs*)		$\nu_{10}(B_u)$
960 / 969	960 (*m*)		265 + 2 × 346 = 957 (B_u)*
		992 (*s*)	$\nu_2(A_g)$
	995 (*w*)		992 cm^{-1} Raman line
	1130 (*w*)		346 + 784 = 1130 (B_u)*
	1230 (*w*)		765 + 657 − 192 = 1230 (B_u)
	1238 (*w*)		192 + 265 + 784 = 1241 (A_u)
1314 / 1324	1314 (*m*)		657 + 658 = 1315 (B_u)*
		1312 (*w*) ?	658 + 658 = 1316 (A_g)
		1545 (*m*)	765 + 765 = 1530 (A_g)*
	1549 (*w*)		765 + 784 = 1549 (B_u)*
		1570 (*s*)	$\nu_3(A_g)$
	1780 (*w*)		784 + 992 = 1776 (B_u)*
	1900 (*w*)		912 + 992 = 1904 (B_u)*
2290	2285 (*s*)		$\nu_9(B_u)$
		2325 (*s*)	$\nu_1(A_g)$
	2417 (*w*)		2 × 765 + 912 = 2442 (B_u)
	2462 (*w*)		912 + 1570 = 2482 (B_u)
	3054 (*w*)		765 + 2285 = 3050 (B_u)
		3154 (*w*)	1570 + 1570 = 3140 (A_g)*
	3226 (*w*)		912 + 2325 = 3237 (B_u)
	3265 (*w*)		992 + 2285 = 3277 (B_u)

[a] See reference 3.
* The corresponding combination tone was observed for *trans* $C_2H_2Cl_2$.
# Part of the intensity of this band is contributed by *trans* $C_2H_2Cl_2$ impurity.
† Probably Fermi resonance between; 346 + 657 − 192 = 811 (B_u); 3 × 265 = 795 (B_u); to give 826 cm^{-1} and a component which is masked by the intense 784 cm^{-1} band.

[14] R. A. Oetjen, C. L. Kao, and H. M. Randall, Rev. Sci. Inst. **13**, 515 (1942).

[15] See reference 1, p. 483.
[16] See reference 1, p. 424.

TABLE V. Frequency assignments and product rule ratios for *cis* $C_2H_2Cl_2$ and *cis* $C_2D_2Cl_2$.

Type	*Cis* $C_2H_2Cl_2$	*Cis* $C_2D_2Cl_2$	Theor. ratio	Obs. ratio
A_1	ν_1 3077 R	2325 R		
	ν_2 1587 R	1570 R		
	ν_3 1179 R	850 R	1.98	1.94
	ν_4 711 R	689 R		
	ν_5 173 R	171 R		
A_2	ν_6 876 R	710*	1.40	(1.36)
	ν_7 406 R	368 R		
B_1	ν_8 3072 I.R.	2280 I.R.		
	ν_9 1294 I.R.	1040 I.R.	1.94	1.97
	ν_{10} 848 I.R.	761 I.R.		
	ν_{11} 571 I.R.	540 I.R.		
B_2	ν_{12} 697 I.R.	558 I.R.	1.29	1.25

* Calculated from the theoretical ratio after correction for anharmonicity.

TABLE VI. Frequency assignments and product rule ratios for *trans* $C_2H_2Cl_2$ and *trans* $C_2D_2Cl_2$.

Type	*Trans* $C_2H_2Cl_2$	*Trans* $C_2D_2Cl_2$	Theor. ratio	Obs. ratio
A_g	ν_1 3071 R	2325 R		
	ν_2 1576 R	1570 R		
	ν_3 1270 R	992 R	1.98	1.89
	ν_4 844 R	765 R		
	ν_5 349 R	346 R		
A_u	ν_6 895 I.R.	658 I.R.	1.40	1.36
	ν_7 192 I.R.*	192 I.R.*		
B_g	ν_8 758 R	657 R	1.17	1.15
B_u	ν_9 3080 I.R.	2285 I.R.		
	ν_{10} 1200 I.R.	912 I.R.	1.96	1.85
	ν_{11} 817 I.R.	784 I.R.		
	ν_{12} 265 I.R.*	265 I.R.*		

* From combination tones.

branch ($K=0, 1, 2, \cdots$) the negative sign applies to the ^PQ branch ($K=1, 2, \cdots$).

The band center may be determined from the relation

$$^RQ_K+{}^PQ_{K+1}=2\nu_0 +[(A'-B')-(A''-B'')][K^2+(K+1)^2]$$

by plotting $^RQ_K+{}^PQ_{K+1}$ against $K^2+(K+1)^2$ and extrapolating to zero (see Fig. 7). From this graph it is found that $\nu_0=898.1$ cm^{-1} and $(A'-B')-(A''-B'')=-0.0084$ cm^{-1}.

Individual values for $(A'-B')$ and $(A''-B'')$ may be obtained from the combination relations

$$^RQ_K-{}^PQ_K=4(A'-B')K,$$
$$^RQ_{K-1}-{}^PQ_{K+1}=4(A''-B'')K.$$

Since the band positions were determined with an accuracy of ±0.1 cm^{-1}, the probable errors in the values of $(A'-B')$ and $(A''-B'')$ will depend on the K value but will be of the order of $\pm(0.2/4\times15)\sim0.004$ cm^{-1}. Hence from Table VII we see that

$$A'-B'=1.674\pm0.004 \text{ cm}^{-1},$$
$$A''-B''=1.682\pm0.004 \text{ cm}^{-1},$$

these values being consistent with the difference found above. Substituting into Eq. (1) the frequencies of the rotation lines were calculated and found to agree with the observed values in most cases to ±0.1 cm^{-1}, though occasional differences of ±0.2 cm^{-1} were found.

If we take $I_{B'}=I_{B''}=$ mean of I_B and I_C (obtained from electron diffraction data),

$$B'=B''=0.050\pm0.001 \text{ cm}^{-1}.$$

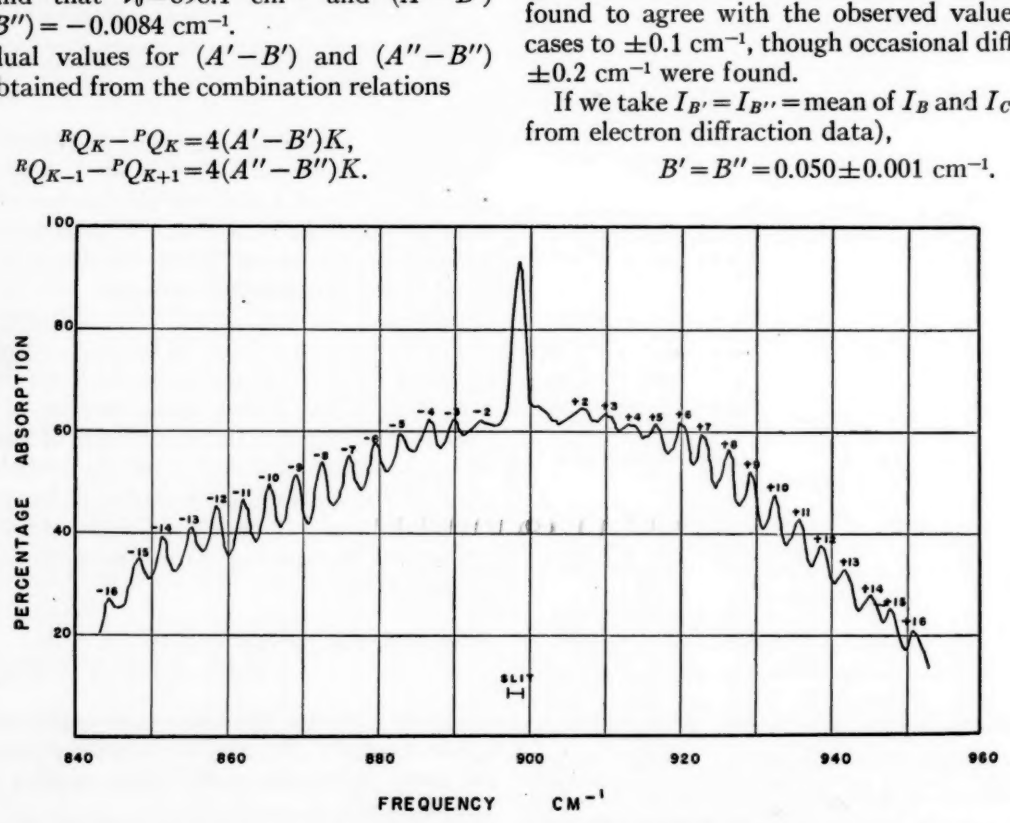

FIG. 6. Rotational fine structure of the 898.1-cm^{-1} band of *trans*-dichloroethylene. Absorption path 10-cm, pressure 30-mm Hg, Temperature 20°C.

Hence,

$A'=1.724\pm0.005$ cm^{-1}; $A''=1.733\pm0.005$ cm^{-1},

and

$$I_{A'}=16.23\pm0.05\times10^{-40}\text{ g cm}^2;$$
$$I_{A''}=16.15\pm0.05\times10^{-40}\text{ g cm}^2.$$

These values are considerably more accurate than the value obtained from the electron diffraction results *viz.* 15.8×10^{-40} g cm^2.

A slight refinement of the molecular dimensions for the *trans* molecule may be made in the following manner. For small changes in the C−Cl and C=C bond lengths and the Cl−C=C bond angle, the contribution from the hydrogen atoms to the least moment of inertia is approximately constant. Hence by taking the C−H bond length to be 1.07A and the H−C=C bond angle to be 120°, the hydrogen contribution may be evaluated and subtracted from the moment of inertia. The remaining contributions from the carbon and chlorine atoms depend on three variables, the C−Cl and C=C bond lengths and the Cl−C=C bond angle. By using the electron diffraction result for the distance between the two chlorine atoms *viz.* 4.27±0.02A, the number of independent variables is reduced to two. Moments of inertia are then calculated for reasonable ranges of values of the C=C and C−Cl bond lengths and the values compared with the spectroscopic figure. The ranges used were $r_{C=C}=1.34$ to 1.40A and $r_{C-Cl}=1.65$ to 1.75A and it was found that the moments of inertia were consistent with the spectroscopic data only when

$$r_{C=C}+r_{C-Cl}=3.08\pm0.01\text{A}.$$

TABLE VII. Rotational fine structure for 898 cm^{-1} *trans* $C_2H_2Cl_2$ band.

K	ν obs.	ν calc.	Diff.	K	$^RQ_K-{}^PQ_K$	$4K(A'-B')$	$(A'-B')$
−16	844.3	844.1	0.2	2	906.7 −893.1	13.6	(1.700)
−15	847.8	847.7	0.1	3	909.7 −889.6	20.1	1.675
−14	851.4	851.3	0.1	4	913.0 −886.3	26.7	1.669
−13	854.9	854.8	0.1	5	916.4 −882.8	33.6	1.680
−12	858.3	858.4	−0.1	6	919.7 −879.3	40.4	1.683
−11	861.9	861.9	0.0	7	922.9 −875.9	47.0	1.679
−10	865.4	865.5	−0.1	8	926.0 −872.4	53.6	1.675
−9	868.9	869.0	−0.1	9	929.2 −868.9	60.3	1.675
−8	872.4	872.5	−0.1	10	932.4 −865.4	67.0	1.675
−7	875.9	875.9	0.0	11	935.6 −861.9	73.7	1.675
−6	879.3	879.4	−0.1	12	938.7 −858.3	80.4	1.675
−5	882.8	882.8	0.0	13	941.7 −854.9	86.8	1.669
−4	886.3	886.3	0.0	14	945.0 −851.4	93.6	1.671
−3	889.6	889.7	−0.1	15	947.9 −847.8	100.1	1.668
−2	893.1	893.1	0.0	16	951.0 −844.3	106.7	1.667
−1		896.4					
0		899.8				Mean	=1.674
1		903.1					
2	906.7	906.5	0.2	K	$^RQ_{K-1}-{}^PQ_{K+1}$	$4K(A''-B'')$	$(A''-B'')$
3	909.7	909.8	−0.1	3	906.7 −886.3	20.4	(1.700)
4	913.0	913.0	0.0	4	909.7 −882.8	26.9	1.681
5	916.4	916.3	0.1	5	913.0 −879.4	33.6	1.680
6	919.7	919.6	0.1	6	916.4 −875.9	40.5	1.687
7	922.9	922.8	0.1	7	919.7 −872.5	47.2	1.686
8	926.0	926.0	0.0	8	922.9 −869.0	53.9	1.684
9	929.2	929.2	0.0	9	926.0 −865.5	60.5	1.681
10	932.4	932.4	0.0	10	929.2 −861.9	67.3	1.683
11	935.6	935.6	0.0	11	932.4 −858.4	74.0	1.682
12	938.7	938.8	−0.1	12	935.6 −854.8	80.8	1.683
13	941.7	941.9	−0.2	13	938.7 −851.3	87.4	1.681
14	945.0	945.0	0.0	14	941.7 −847.7	94.0	1.679
15	947.9	948.1	−0.2	15	945.0 −844.1	100.9	1.682
16	951.0	951.2	−0.2				
						Mean	=1.682

POTENTIAL FUNCTION FOR OUT-OF-PLANE FREQUENCIES

Type A_2 (*Cis*)

A general quadratic potential function was used (Fig. 8) *viz.*

$$V=k_\theta\theta^2+k_\phi\phi^2+k'\theta\phi,$$

where θ = angle of wag between the CHCl group and the extended C=C axis, ϕ = angle of twist about the extended C=C referred to the equilibrium plane, k_θ, k_ϕ, k' are the appropriate force constants.

The equations for the frequencies were derived by

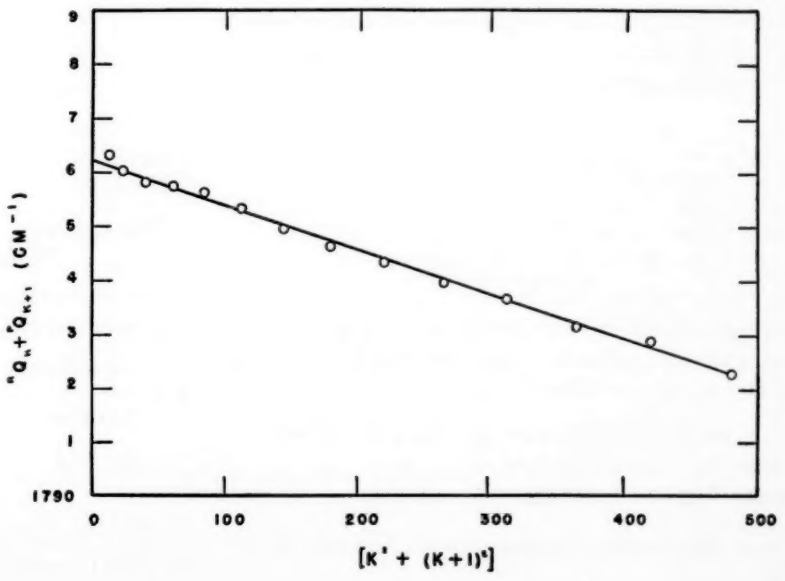

FIG. 7. Determination of the band center for the 898-cm^{-1} band of *trans* dichloroethylene.

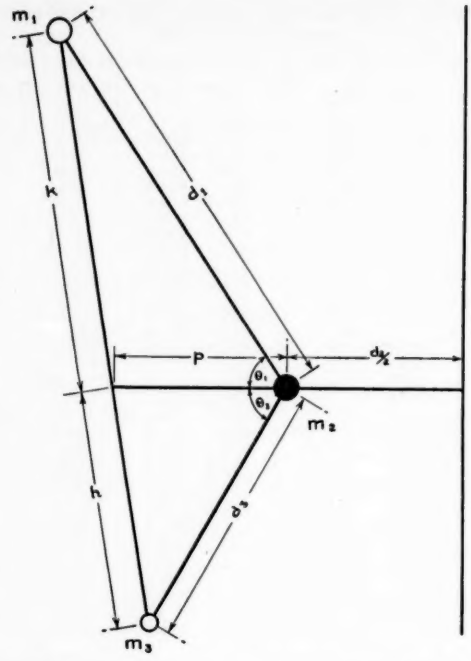

FIG. 8. ●=C, ○=Cl, o=H. Structural parameters for one half of the dichloroethylene molecule.

the method of Eliashevich[17] and may be expressed as follows:

$$\lambda_1^2+\lambda_2^2=2(ak_\theta+ck_\phi-bk'),$$
$$\lambda_1^2\lambda_2^2=(4k_\theta k_\phi-k'^2)(ac-b^2),$$

where

$$\lambda=2\pi c\nu,$$

$$a=\left(\frac{h'^2}{m_1}+\frac{f^2}{m_2}+\frac{k'^2}{m_3}\right),$$

$$b=\left(-\frac{h'}{m_1d_1\sin\theta_1}+\frac{fg}{m_2}+\frac{k'}{m_3d_3\sin\theta_3}\right),$$

$$c=\left(\frac{1}{m_1d_1^2\sin^2\theta_1}+\frac{g^2}{m_2}+\frac{1}{m_3d_3^2\sin^2\theta_3}\right);$$

$$h'=\frac{h}{p(h+k)},\quad k'=\frac{k}{p(h+k)},\quad f=\frac{1}{p}+\frac{2}{d_2},$$

$$g=-\frac{1}{d_1\sin\theta_1}+\frac{1}{d_3\sin\theta_3}.$$

The equations for the other out-of-plane vibrations for the *cis* and *trans* molecules may be obtained from the above as follows:

type B_2 (*cis*): let $d_2=\infty$, $k_\phi=0$, $k'=0$,
type A_u (*trans*): let $d_2=\infty$,
type B_g (*trans*): let $k_\phi=0$, $k'=0$.

[17] M. A. Eliashevich, Comptes. Rendus. U.R.S.S. **28**, 604 (1940).

The condition that $d_2=\infty$ eliminates the contribution to the potential energy from the relative motion of the carbon atoms.

Force constants may be evaluated as follows. Using $\nu_8(B_g)=758$ cm^{-1} for the *trans* molecule,

$$k_\theta=1.12\times10^{-12}\text{ dyne cm/radian.}$$

Assuming that this force constant may be taken over for type A_2 (*cis*) as has been done by Pitzer and Freeman[4] and using $\nu_6=876$ cm^{-1}, $\nu_7=406$ cm^{-1} in the above equations,

$$k_\phi=1.46\times10^{-12}\text{ dyne cm/radian,}$$
$$k'=0.62\times10^{-12}\text{ dyne cm/radian.}$$

Using these force constants to calculate the two frequencies for *cis* $C_2D_2Cl_2$ we obtain

$$\nu_6=678\text{ cm}^{-1},\quad \nu_7=374\text{ cm}^{-1}.$$

The low frequency agrees well with the Raman frequency observed at 368 cm^{-1} while the other frequency is in tolerable agreement with the value deduced from the product rule *viz.* 710 cm^{-1}.

In a similar manner the wagging force constant for type B_2 (*cis*) may be used in type A_u (*trans*). Using $\nu_{12}(B_2)=697$ cm^{-1} for the *cis* molecule, we obtain

$$k_\theta=1.51\times10^{-12}\text{ dyne cm/radian.}$$

Only one of the A_u frequencies for the *trans* molecule, however, has been observed, *viz.* at 895 cm^{-1} for $C_2H_2Cl_2$ and 658 cm^{-1} for $C_2D_2Cl_2$. Since the unobserved frequency is expected to be low, it will change very little from $C_2H_2Cl_2$ to $C_2D_2Cl_2$ and may be assumed to be unchanged to a very good approximation. The three unknowns for type A_u, *viz.* k_ϕ, k', and ν_7 may then be evaluated from the three equations, for the sums of the frequencies in $C_2H_2Cl_2$ and $C_2D_2Cl_2$ and the product of the frequencies in either $C_2H_2Cl_2$ or $C_2D_2Cl_2$. Solution of these equations gives

$$k_\phi=1.00\times10^{-12}\text{ dyne cm/radian,}$$
$$k'=0.20\times10^{-12}\text{ dyne cm/radian,}$$
$$\nu_7=196\text{ cm}^{-1}.$$

This value for the low frequency is in good agreement with the value 192 cm^{-1} deduced from combination tones.

THE ENERGY DIFFERENCE BETWEEN *CIS* AND *TRANS* DICHLOROETHYLENE

For an equilibrium of the type *cis*⇌*trans* the equilibrium constant[18]

$$K=\frac{\text{Number of } cis \text{ molecules}}{\text{Number of } trans \text{ molecules}}$$
$$=\frac{f_{cis}}{f_{trans}}\cdot\exp(-\Delta E_0^0/RT),\quad (2)$$

[18] R. H. Fowler and E. A. Guggenheim, *Statistical Thermodynamics* (The Macmillan Company, New York, 1939), p. 157.

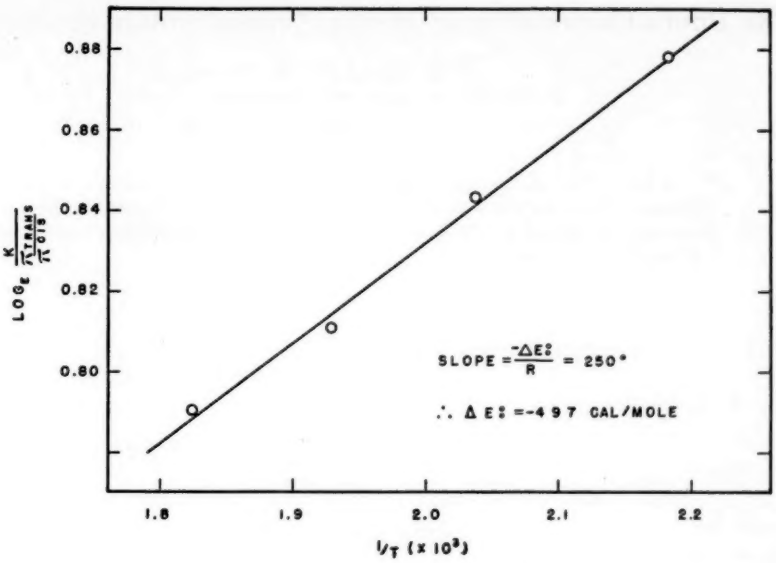

FIG. 9. Plot of $\log_e K/(\Pi\ trans/\Pi\ cis)$ against $1/T$.

where f_{cis}, f_{trans} are the partition functions of *cis*- and *trans*-dichloroethylene, respectively, R is the gas constant, and ΔE_0^0 is the energy difference between the two forms at 0°K.

Assuming the rigid rotator and harmonic oscillator approximations[19]

$$\frac{f_{cis}}{f_{trans}}=\left[\frac{(I_AI_BI_C)_{cis}}{(I_AI_BI_C)_{trans}}\right]^{\frac{1}{2}}\frac{\prod_{i=1}^{12}(1-e^{-h\nu_i/kT})_{trans}}{\prod_{i=1}^{12}(1-e^{-h\nu_i/kT})_{cis}}. \quad (3)$$

Substituting in Eq. (2) and taking logarithms, we get

$$\log_e\frac{K}{\Pi_{trans}/\Pi_{cis}}=\tfrac{1}{2}\log_e\left[\frac{(I_AI_BI_C)_{cis}}{(I_AI_BI_C)_{trans}}\right]-\Delta E_0^0/RT. \quad (4)$$

Hence by plotting $\log_e K/(\Pi_{trans}/\Pi_{cis})$ against $1/T$ a straight line is obtained whose slope is $-\Delta E_0^0/R$ and intercept $\frac{1}{2}\log_e(I_AI_BI_C)_{cis}/(I_AI_BI_C)_{trans}$. In this way the value of ΔE_0^0 is not dependent on experimental errors in the determination of the principal moments of inertia of the two molecules.

[19] See reference 1, p. 503, *et. seq.*

Wood and Stevenson[5] have obtained equilibrium data for the isomerization of *cis* and *trans* dichloroethylene at 185°C, 215°C, 245°C, and 275°C. Using their values of K and our values of Π_{trans}/Π_{cis} and plotting $\log_e K/(\Pi_{trans}/\Pi_{cis})$ against $1/T$ (see Fig. 9) the best straight line obtained by the method of least squares gives

$$\Delta E_0^0=-497 \text{ cal./mole.}$$

The principal source of inaccuracy in this determination lies in the assignment to the *trans* molecule of the two low frequencies obtained from combination tones. If we assume that these frequencies *viz.* 192 and 265 cm^{-1}, are accurate to ± 5 cm^{-1}, the error introduced into ΔE_0^0 is ± 30 cal./mole. Hence for dichloroethylene the *cis* isomer is more stable than the *trans* isomer by 500 ± 30 cal./mole.

The moment of inertia ratio $[(I_AI_BI_C)_{cis}/(I_AI_BI_C)_{trans}]^{\frac{1}{2}}$ may also be evaluated from Eq. (4) a range of values of 1.39 ± 0.04 being obtained. This is consistent with the value calculated from electron diffraction results *viz.* 1.38.

ACKNOWLEDGMENT

The authors wish to express their thanks to Dr. R. N. Jones who kindly placed the infra-red spectrometer at their disposal, to Mr. L. C. Leitch for the preparation of the deuterated compounds, and to Mr. D. J. Keir and Miss E. Miller for technical assistance.

The Photo-Chlorination of Methyl Chloroformate in Carbon Tetrachloride Solution*

T. L. BATKE, L. M. DORFMAN,** AND D. J. LEROY
Department of Chemistry, University of Toronto, Toronto, Ontario, Canada

(Received November 16, 1948)

A study has been made of the kinetics and photo-chemistry of the chlorination of methyl chloroformate to monochloromethyl chloroformate in carbon tetrachloride solution at 25°C. The reaction is strongly inhibited by oxygen. The following mechanism has been proposed for the reaction in the absence of oxygen:

$$Cl_2+h\nu=2Cl$$

$$Cl+CH_3-O-\overset{\overset{O}{\|}}{C}-Cl=CH_2-O-\overset{\overset{O}{\|}}{C}-Cl+HCl$$

$$CH_2-O-\overset{\overset{O}{\|}}{C}-Cl+Cl_2=CH_2Cl-O-\overset{\overset{O}{\|}}{C}-Cl+Cl$$

$$Cl+CH_2Cl-O-\overset{\overset{O}{\|}}{C}-Cl=CH_2-O-\overset{\overset{O}{\|}}{C}-Cl+Cl_2$$

$$Cl+CH_2-O-\overset{\overset{O}{\|}}{C}-Cl=CH_2Cl-O-\overset{\overset{O}{\|}}{C}-Cl$$

$$Cl=\tfrac{1}{2}Cl_2.$$

THE chlorination of methyl chloroformate under the influence of light was first studied by Hentschel.[1] Extensive chlorination gave the compound, trichloromethyl chloroformate, boiling at 127.5° to 128°C; milder treatment gave a liquid containing 60.7 percent chlorine and boiling in the range 108° to 109°C. Hentschel believed the latter substance to be a compound with the formula $C_4H_3Cl_3O_4$, but later work by Kling *et al.*[2] showed conclusively that it was a mixture of monochloromethyl chloroformate and dichloromethyl chloroformate.

During the war of 1914–1918 the Germans used the chlorinated derivatives of methyl chloroformate as chemical warfare agents; in the early stages they employed a liquid containing from 58 to 59 percent chlorine, and later one containing up to 71 percent chlorine, corresponding approximately to trichloromethyl chloroformate or diphosgene.[2] The military importance of this material led to the study of its production by several investigators. Kling *et al.*[2] used both methyl formate and methyl chloroformate as the starting material. A parallel investigation was made by Grignard *et al.*[3] Delépine[4] found that some dichloromethyl formate was produced on chlorinating methyl formate. While the early stages of the chlorination of methyl chloroformate can be conducted at room temperature, the trichlorinated derivative can only be prepared in quantity at temperatures of the order of 100°C.[2,3,5]

The present investigation was undertaken from the point of view of a study of the kinetics and photo-chemistry of the reaction. The previous work was all preparative in nature; nothing was reported about such factors as rate constants, quantum yields or the elementary reactions involved in the successive stages of the chlorination. We have made an extensive investigation of the photo-chlorination of methyl chloroformate in carbon tetrachloride solution at 25°C under conditions where the reaction is confined almost exclusively to the first stage, the formation of monochloromethyl chloroformate.

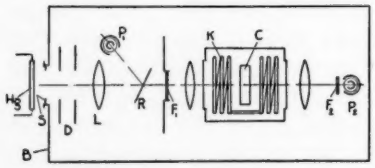

FIG. 1. Optical arrangement.

EXPERIMENTAL

Light Source and Optical Arrangement

A direct current medium pressure quartz mercury arc was used. To reduce fluctuations in the light in-

* This paper was presented, in part, at the Annual Convention of the Chemical Institute of Canada, Montreal, June, 1948.

** Present address: Department of Chemistry, University of Rochester, Rochester, New York.

[1] W. Hentschel, J. prakt. Chem. (2) **36**, 99 (1887).

[2] A. Kling, D. Florentin, A. Lassieur, and R. Schmutz, Comptes Rendus **169**, 1046 (1919).

[3] V. Grignard, G. Rivat, and E. Urbain, Comptes Rendus **169**, 1074 (1919).

[4] M. Delépine, Bull. Soc. Chim. (4°) **27**, 39 (1920).

[5] H. P. Hood and R. Murdock, J. Phys. Chem. **23**, 509 (1919).

tensity the arc was shielded from draughts and the voltage was stabilized to ±0.02 volt by a specially designed voltage regulator.[6] Corning filters were used to give light of the required wave-lengths. The optical arrangement is shown in Fig. 1. Light from the arc Hg entered the black wooden box B through the iris diaphragm and shutter S. The beam was collimated by the diaphragms D and the two lenses before entering the cell C. The cell was placed inside a small copper tank containing distilled water. Its temperature was controlled by circulating water from an auxiliary thermostat through the concentric copper spirals K; by insulating the small tank with a wooden box and lid its temperature was maintained at 25±0.1°C. After passing through the cell the light was focused on a vacuum type GL 441 photo-tube P_2. In order to obtain accurate measurements of the percentage of light absorbed in the cell, part of the beam was reflected onto the reference photo-tube P_1 by the polished quartz plate R. The filters are shown at F_1 and F_2, but other arrangements were used as well. Corning filters, rather than screens, were used to reduce the light intensity when required.

Three different wave-length ranges were used in this work. Source I was obtained by placing a standard Corning filter No. 5874 at F_1. This transmitted chiefly 3650A, with a small amount of 3126A and 3341A and a trace of 4047A. No filter was placed at F_2 during the photolysis. Source II consisted mostly of 4047A and 4358A and was obtained with a No. 3060 filter; traces of 4916A and 5461A were also present. Source III was essentially monochromatic 4358A. A No. 3389 filter placed at F_1 transmitted this and the longer wave-lengths. However, the intensities of 4916A and 5461A were much less than that of 4358A, and their absorption by chlorine solutions, particularly 5461A, is considerably less. Maddock[7] found that for a lamp similar to the one used here the ratio of the intensities of 4358A to 4916A was 100:2.7; using less precise methods we found the ratio to be 100:3.2. In general, taking into account the weaker absorption of the longer wave-lengths, about 99 percent of the light from Source III which was absorbed by the solutions was 4358A. However, since the photo-tube was sensitive to the longer wave-lengths a No. 5113 filter was placed at F_2 so that it gave a true measure of the absorption of 4358A. Placing this filter at F_2 rather than at F_1 permitted higher light intensities to be used.

Curves of percent light absorption *vs.* chlorine concentration were obtained for Sources I and II. In the case of the latter, the measurements were made with a No. 5113 filter at F_2. All measurements of chlorine concentration were made with Source III.

[6] J. M. McCrea and D. J. LeRoy, Rev. Sci. Inst. **19**, 692 (1948).

[7] A. J. Maddock, Proc. Phys. Soc. **47**, 424 (1935).

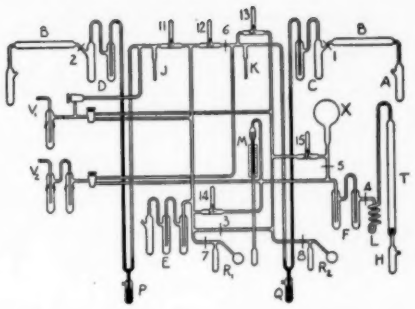

FIG. 2. Apparatus used to prepare solutions free from air.

Light intensities were measured by passing the current from the phototube through a one-megohm resistor which formed one of the grid resistors of a 6SC7 double triode. The voltage drop in this resistor was balanced out by applying an opposite voltage to the same grid from a Leeds and Northrup double range thermocouple potentiometer. A galvanometer with a sensitivity of 0.09 microamp. per division indicated the balance of the two plate currents. Since the amplifier acted simply as a null detector, the voltage readings on the potentiometer were directly proportional to the phototube current. To insure stability, two 45-volt batteries were used to supply the 90 volts for the plates of the 6SC7 and the photo-tube; a storage battery supplied the filament current. The photo-tubes were surrounded by metal containers having apertures just large enough to admit the light beams. These containers, the shielding on the microphone cables connecting the phototubes to the amplifier, the chassis of the amplifier and the metal envelope of the 6SC7 were all grounded. Either photo-tube could be connected to the amplifier by throwing a switch. Corrections were applied for dark current.

The reaction cells were supplied by the American Instrument Company, style F, 41-mm O.D., and either 5-mm or 10-mm internal length. The lengths were given to the nearest 0.001 mm and the Pyrex or Corex windows were alleged to be flat to within 6 wave-lengths and parallel to ±10 min. Matched pairs were used in making transmission measurements. For the experiments done in the presence of air the cells were supplied with ground stoppers lubricated with syrupy phosphoric acid. In the later work each cell was sealed to a glass tube having a volume slightly greater than that of the cell, as shown at R_1 and R_2 in Fig. 2. The reagents were condensed into this tube with liquid air and the cell and its associated tube removed from the filling apparatus after sealing off at 7 or 8. The liquid air was then removed and the cell filled by tilting it.

Actinometry

Absolute light intensities were measured by the photolysis of oxalic acid-uranyl oxalate solutions;

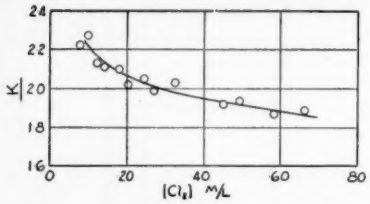

FIG. 3. Extinction coefficient of chlorine in carbon tetrachloride, defined by the expression $I_{trans}=I_0\times 10^{-K[Cl_2]d}$.

the concentrations used were 0.005 and 0.001 moles per liter, respectively. Leighton and Forbes' values[8] for the quantum yield were employed. Transmission measurements were made with matched cells, one containing the oxalate solution, the other containing water; these were identical with the cells used in the photochlorination.

Reagents and Procedure

The methyl chloroformate was obtained from Eastman. In the preliminary experiments this was used without further treatment. In the later experiments, including all those in which oxygen-free reagents were used, it was purified by bulb-to-bulb distillation taking middle fractions or by distillation through a Stedman column; no differences in rate could be attributed to the two methods. The most likely impurity, dimethyl carbonate, has a considerably higher boiling point than methyl chloroformate.

For the experiments done in the presence of air, chlorine was simply bubbled into carbon tetrachloride to give a saturated solution; this was subsequently diluted with more solvent to give the desired concentration. In the later experiments the chlorine was treated as described below.

C.P. carbon tetrachloride was purified by shaking it with concentrated sulphuric acid, washing with strong alkali, followed by water, and drying over calcium chloride. It was then distilled from phosphorus pentoxide; the first and last fractions were discarded.

It was necessary to perform a number of experiments in which monochloromethyl chloroformate was present initially. This material was prepared in quantity in a separate apparatus. The cell used for this purpose was about 50 cc in capacity, annular in shape and was completely surrounded by an outer annular vessel through which cold water was circulated. The light source was a 6 watt, 360BL fluorescent lamp having a maximum output in a band at 3600A; this was placed in the center of the cell. The product obtained contained approximately 85 percent monochloromethyl chloroformate, the rest being dichloromethyl chloroformate. Attempts to separate pure monochloromethyl chloroformate by distillation were not successful.

The apparatus used to prepare solutions free from air is shown in Fig. 2. Two cells could be filled in a single series of operations, thereby eliminating slight variations in possible traces of oxygen or other impurities. This was particularly advantageous when a comparison was to be made between the rates with and without added monochloromethyl chloroformate. A spark coil was used to assist in the removal of adsorbed gases from the walls of the apparatus and as an indicator of the presence or absence of non-condensible gases.

Purified carbon tetrachloride was placed in one of the tubes, E, and the dissolved gases removed by freezing, pumping, melting and distillation over a period of five hours. A slight excess over the desired amount was distilled into the calibrated tubes at R_1 and R_2 and frozen with liquid air. The connecting tube was sealed off at 3 and the carbon tetrachloride in R_1 and R_2 was pumped down to the correct volume by a mercury diffusion pump and Hyvac pump connected to V_1. From this time on the calibrated tubes were kept in liquid air until they were removed from the apparatus.

Chlorine from a commercial cylinder was condensed into H. After closing the connection to the cylinder the gas was passed from H through the tower, T, containing concentrated sulphuric acid and glass beads, and through the spiral, L, immersed in a mixture of dry ice and acetone. The middle third was condensed into one of the traps, F, with liquid air, and isolated from the residue by sealing off at 4. Non-condensible gases were removed by freezing, pumping, melting, and distillation between the two traps over a period of about $2\frac{1}{2}$ hours. A second diffusion pump and Hyvac pump connected at V_2 were used in this operation. The gas was allowed to evaporate and was pumped down to the desired pressure as indicated by the glass bellows manometer M; it was then frozen back into F.

The methyl chloroformate was added to A and distilled back and forth from A to C through drierite in B. The drying tube was then sealed off at 1 and the non-condensible gases were removed from

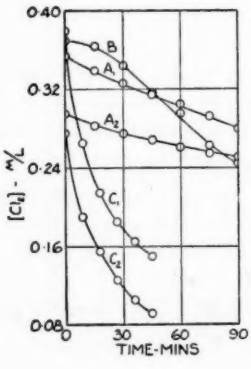

FIG. 4. Effect of oxygen on the reaction. A_1, A_2: oxygen present; B: nitrogen; C_1, C_2: high vacuum technique.

[8] W. G. Leighton and G. S. Forbes, J. Am. Chem. Soc. 52, 3139 (1930).

the liquid by the method already described. Treatment with drierite was later found to be unnecessary. The amount of methyl chloroformate used was small enough that sufficient could be stored in C for a large number of experiments. It was isolated from the rest of the system by the mercury cut-off Q. In filling a cell the cut-off was lowered and a slight excess distilled into the calibrated tube K; the cut-off was raised and the liquid in K pumped down to the correct volume through V_2. The break-off valve 12 was opened and the contents of K condensed into R_1; a seal was then made at 6. A second sample of methyl chloroformate could be measured out in K in the same way and introduced into R_2 through the break-off valve 13.

Monochloromethyl chloroformate was treated in the same way as the methyl chloroformate, in B and D. It was sealed off at 2, measured in J and introduced into R_1 through the break-off valve 11.

The chlorine in F was quickly evaporated and a seal made at the constriction 5. The volume of the bulb X, the traps F, and the manifold to which they were connected were known to a fair approximation and hence the amount of chlorine in each section could be computed; the actual chlorine concentrations were subsequently determined by light absorption in the cells. The chlorine remaining in F was admitted to R_1 through the break-off valve 14; a seal was made at 7 and the cell and its associated tube removed to the darkened room where the photolysis took place. Here the contents of the tube were melted and poured into the cell. The chlorine in X was added to R_2 in the same way, through the break-off valve 15.

The cell containing the reaction mixture was normally kept in the dark for approximately sixteen hours before starting the photo-chlorination. The mercury arc was allowed to warm up for two hours, the amplifier for three quarters of an hour. The duration of each experiment was such that, in general, less than fifty percent of either the chlorine or the methyl chloroformate was consumed. No noticeable dark reaction was observed in solutions left for a period of two weeks.

Extinction Coefficient of Chlorine in Carbon Tetrachloride

The chlorine concentration was followed during an experiment by measuring its light absorption at 4358A. Dickenson and Jefferies[9] reported a value of 2.26 for K in the expression $I_{trans}=I_0\times10^{-K[Cl_2]d}$, where $[Cl_2]$ is the concentration of chlorine in moles per liter and d is the length of the light path in cm.*** Their value was obtained for a single chlorine concentration of 0.214 mole per liter. They used a single sheet of glass of the same type as the window of their cell to obtain the correction for reflected light. In attempting to obtain a possibly more reliable value of K we used two matched cells, one containing the solution, the other containing the solvent. Aliquots of a stock solution were added first to an iodine flask, then to the cell, and finally to a second iodine flask. The average of the analyses of the first and third samples was taken to be the concentration of chlorine in the cell. Analyses and transmission measurements were made for a range of chlorine concentrations extending from 0.07 to 0.7 mole per liter. Light Source III was used in this work.

TABLE I.[a]

Expt.	$[Cl_2]_0$ moles/L	$[RH]_0$ moles/L	$[RCl]_0$ moles/L	I_0[b] mv	$(-d[Cl_2]/dt)_0$ moles/L/hr (corrected)	k' (L/mole/hr)$^{\frac{1}{2}}$ $\times10^{-3}$
1	0.182	0.597	—	56.6	0.510	6.68
2	0.201	0.592	—	55.7	0.431	4.45
3	0.134	0.603	—	55.4	0.312	4.27
4	0.297	0.575	—	60.3	0.644	4.65
5	0.274	0.586	—	56.0	0.413	3.27
6	0.087	0.597	—	56.6	0.196	4.38
7	0.220	0.592	—	54.7	0.402	3.72
8	0.219	0.574	—	17.5	0.148	3.34
9	0.158	0.597	—	52.6	0.465	6.56
10	0.158	0.590	—	18.2	0.204	5.95
11	0.572	0.573	—	49.0	0.762	4.50
12	0.550	0.573	—	53.6	1.01	5.38
13	0.496	0.573	—	52.1	0.856	3.90
14	0.651	0.573	—	60.0	0.935	4.60
15	0.555	1.120	—	54.5	1.30	3.85
16	0.568	0.270	—	55.0	0.493	3.90
17	0.500	1.100	—	50.5	1.40	4.12
18	0.769	0.573	—	33.8	0.940	4.05
19	0.838	0.551	—	50.8	1.07	4.83
20	0.904	0.562	—	39.0	1.01	3.79
21	0.832	0.562	—	39.5	1.19	5.57
22	0.677	0.583	0.420	45.0	0.308	3.90
23	0.852	0.585	—	45.0	0.920	3.53
24	0.164	0.672	0.420	53.5	0.104	3.68
25	0.180	0.673	—	53.5	0.354	4.20
26	0.182	0.660	—	57.0	0.398	4.65
27	0.193	—	0.420	57.0	0.06	—
28	0.164	0.673	0.200	54.0	0.148	4.05
29	0.179	0.673	—	54.0	0.362	4.27
30	0.455	0.650	—	59.4	0.605	3.53
31[c]	0.438	0.650	—	12.8–56.5	0.155–0.386	4.08
32[c]	0.436	0.650	—	13.2–58.3	0.134–0.303	3.80
33[d]	0.420	0.660	—	13.4–58.0	0.143–0.355	3.68
34	0.607	1.07	—	59.0	1.42	4.27
35	0.558	2.16	—	57.0	2.04	4.45
					mean	4.34 ±0.59

[a] Experiments 1 to 10 were done with the 10-mm cell, the remainder with the 5-mm cell.
[b] One millivolt $=2.9_1\times10^{-9}$ einstein/cm^2/hr.
[c] Light intensity changed at the end of 40 min.
[d] Light intensity changed at the end of 20 min.

Chemical Analysis of Products

The assumption that monochloromethyl chloroformate was the only product of importance was checked by chemical analysis. The procedure was based on the formation of formaldehyde in the alkaline hydrolysis of monochloromethyl chloroformate.[4] At the end of an experiment residual chlorine was removed by shaking the contents of the cell with about 2 cc of mercury; although the yellow color disappeared almost immediately, the solution was left for at least half an hour before filtering it into a small stoppered bottle. An aliquot of ap-

[9] R. G. Dickinson and C. E. P. Jeffries, J. Am. Chem. Soc. 52, 4288 (1930).

*** The calculations in this paper are based on the relation $I_{trans}=I_0\exp(-\alpha[Cl_2]d)$; $\alpha=2.303K$.

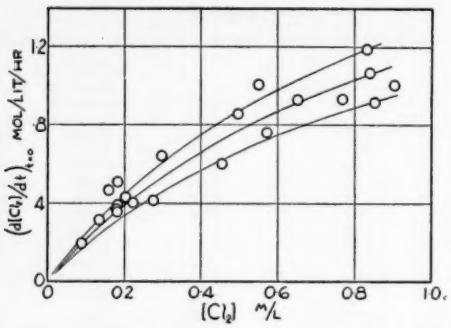

FIG. 5. Initial rate *vs.* $[Cl_2]$ for $I_0=54.0$ mv, $d=0.500$ cm, $[RH]=0.580$ mole per liter.

proximately one cc was weighed in a small weighing bottle and introduced into about 15 cc of $3N$ sodium hydroxide contained in an iodine flask. To ensure complete hydrolysis the solution was left for one hour; twenty minutes was found to be insufficient time. The formaldehyde was oxidised to formate with 10 cc of $N/10$ iodine. After twenty minutes the solution was acidified with $3N$ hydrochloric acid and back-titrated with $N/10$ sodium thiosulphate, using starch. Blank determinations, using one cc of carbon tetrachloride in place of the cell solution, required not more than 0.05 to 0.07 cc of iodine.

RESULTS

The values obtained for the extinction coefficient, K, are shown in Fig. 3. Beer's Law is not obeyed, although for small changes in concentration the change in K is not large. Values taken from the smooth curve were used in all calculations.

Experiments in the Presence of Oxygen

No extensive data pertaining to the experiments done in the presence of oxygen will be reported at this time. The effect of oxygen is shown clearly in Fig. 4. Curves A_1 and A_2 were obtained when oxygen was bubbled both into the chlorine solution and into the methyl chloroformate before adding it to the chlorine solution. Curve B was obtained when nitrogen was bubbled through the liquids before placing them in the cell in an atmosphere of nitrogen; it shows an induction period which was probably due to the incomplete removal of oxygen. Curves C_1 and C_2 were obtained when the high vacuum technique was used. The initial concentration of methyl chloroformate for A_1, A_2, B and C_2 was 0.51 mole per liter; for C_1 it was 0.50. The initial chlorine concentrations (determined by light absorption) may be read from the figure. The incident light intensity (Source III) was the same in each case.

Sources I and II were used for most of the experiments. In both cases the rates were approximately linear in chlorine concentration and in the square root of the absorbed light intensity. The effect of methyl chloroformate concentration was not investigated; a uniform concentration of 1.68 moles per liter was used throughout. With Source I absorption was almost complete for all concentrations of chlorine, varying from 87 percent at 0.030 to 100 percent at 1.09 moles per liter. For a maximum light absorption of 4.7×10^{-7} einstein per cc per hour the quantum yields, over the same range of chlorine concentration, varied from 7 to 160 moles of chlorine per einstein. With Source II a quantum yield of 550 was obtained at 0.92 mole of chlorine per liter and 1.5×10^{-7} einstein per cc per hour

Experiments in the Absence of Oxygen

For fixed temperature and wave-length the factors affecting the rate of disappearance of chlorine are the concentration of chlorine, $[Cl_2]$, the concentration of methyl chloroformate, [RH], the incident light intensity, I_0, the length of the cell, d, and, as was shown later, the concentration of monochloromethyl chloroformate, [RCl].

In attempting to obtain the mechanism of the reaction two more or less distinct methods of approach were used. The first was to study the effect on the *initial* rate of changing the variables one at a time. Initial rates were obtained by tabular differentiation of the data on chlorine concentration *vs.* time. In addition to the errors inherent in this procedure, small corrections had to be applied because of the fact that it was impossible to duplicate exactly the conditions which were to be held constant. A further complication was that not inconsiderable differences in initial rates were found even when all the conditions were fairly accurately duplicated. This effect was attributed to small traces of oxygen. The second method of approach was to consider the whole course of each experiment, and to attempt to obtain a mechanism in agreement with this as well as with the initial rates. Instead of trying to correlate an entirely empirical mathematical expression with a theoretical rate law, a large number of possible combinations of elementary reactions were considered and their corresponding rate laws compared with the experimental data. The data on initial rates, although not very precise, served to reject many of these mechanisms. Of the remainder, all but one were rejected because they did not agree

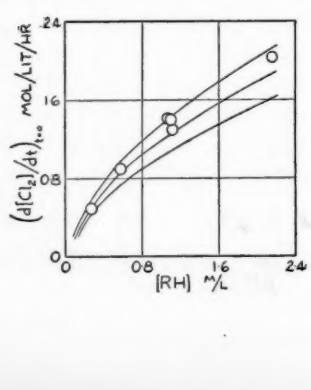

FIG. 6. Initial rate *vs.* [RH] for $I_0=54.0$ mv, $d=0.500$ cm, $[Cl_2]=0.580$ mole per liter.

with the observed chlorine *vs.* time curves. Unfortunately, space limitations make it impossible to present all of these curves.

The initial rates obtained under various conditions are given in Table I. The initial concentrations of Cl_2, RH and RCl are given in columns two, three and four. The values of I_0, the light intensity incident on the front face of the solution, are given in terms of the voltages developed by the phototube P_1 (Fig. 1); from the actinometer measurements one millivolt was equal to $2.9_1\times10^{-9}$ einstein/cm²/hour. From experiments 7 and 8, and 9 and 10 it was evident that the rate was nearly proportional to the square root of the light intensity, although the exact dependence was difficult to obtain because of having insufficient points on the $[Cl_2]$ *vs.* time curves for these experiments. Using a square root law, it was possible to correct the observed initial rates to an arbitrary constant incident light intensity of 54.0 mv. It was also possible to correct the observed initial rates obtained with the 10-mm cell to the rates which would obtain in the 5-mm cell. The conversion factor is given by the expression

$$\text{rate}_{\text{5-mm cell}}=\text{rate}_{\text{10-mm cell}}\times2\times\frac{1-\exp(-\alpha[Cl_2]5/2)}{1-\exp(-\alpha[Cl_2]10/2)}. \quad \text{(i)}$$

It was found later that the power of the light intensity involved was slightly greater than 0.5 but the resulting error in the above corrections was less than one percent. From experiments 15, 16, and 17 it was found that the initial rates were approximately proportional to the square root of the concentration of RH. The initial rates for the other experiments were, accordingly, corrected to an arbitrary value of [RH] of 0.580 mole per liter. The initial rates given in column six (with the exception of those for experiments 8, 10, 15, 16, 17, 22, 24, 27, 28, 31, 32, 33, 34 and 35) thus apply to the case where $I_0=54.0$ mv, $d=0.500$ cm and $[RH]=0.580$ mole per liter. These values are plotted as a function of $[Cl_2]$ in Fig. 5. The last column of Table I will be refered to later.

The effect of [RH] on the initial rate is shown in Fig. 6. The data were obtained from experiments 13, 15, 16, 17, 34 and 35. These rates were corrected to $I_0=54.0$ mv by the procedure outlined above; they were corrected to $[Cl_2]=0.580$ mole per liter after drawing the "best" curve through the points of Fig. 5.

While it is clear that the mechanism for the reaction must not be in disagreement with the data of Figs. 5 and 6, it is apparent that the random fluctuations in initial rates make it difficult to arrive at accurate functional relationships. Furthermore, initial rates can give no indication of possible inhibition by the products of the reaction. An attempt was therefore made to obtain a mechanism in agreement, not only with the initial rates, but also with the whole course of each experiment. Reactions (1), (2), and (3) were common to all of the mechanisms considered.

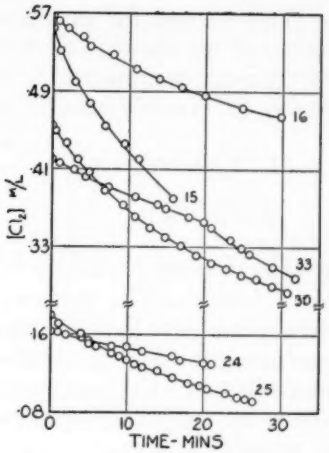

FIG. 7. Typical $[Cl_2]$ *vs.* time curves. The numbers refer to Table I.

$$Cl_2+h\nu=2Cl \quad (1)$$

$$Cl+RH=HCl+R \quad (2)$$

$$R+Cl_2=RCl+Cl. \quad (3)$$

Reaction (1) is an obvious choice since RH does not absorb 4358A. Reaction (2) is exothermic, whereas the alternative,

$$Cl+RH=RCl+H, \quad (2a)$$

is endothermic. The large quantum yields obtained would indicate that (2) and (3) are the chain-carrying steps.

Evidence that an inhibition reaction occured was found on comparing the $[Cl_2]$ *vs.* time curves for experiments in which different chlorine concentrations were used. For example, at the time when an initially high chlorine concentration had decreased to, say, 60 percent of its original value the rate of disappearance of chlorine would be considerably less than the *initial* rate for an experiment in which the original chlorine concentration was 60 percent of the high value. Such differences could not be accounted for by the RH concentrations and were therefore attributed to inhibition by one of the products. Typical chemical analyses gave $[RCl]=0.097$ for $-\Delta[Cl_2]=0.101$, and $[RCl]=0.300$ for $-\Delta[Cl_2]=0.300$. Since no appreciable quantity of dichloromethyl chloroformate was formed it was clear that the inhibitor was either hydrogen chloride or monochloromethyl chloroformate. It was found, by deliberately adding it to the reagents, that the latter did cause inhibition. This is shown by the data for experiments 22, 23; 24, 25 and 28, 29 in

Table I. The rates quoted for experiments 22, 24 and 28 are corrected for the rate of chlorination of RCl using the data of experiment 27. The possible reactions whereby RCl could cause inhibition are

$$Cl+RCl=Cl_2+R \quad (4)$$

and

$$R+RCl=R_2+Cl. \quad (4a)$$

Reaction (4a) was considered unlikely in view of the close agreement between the amount of monochloromethyl chloroformate formed and the amount of chlorine consumed; it was finally rejected when it was found impossible to fit the experimental $[Cl_2]$ *vs.* time curves to any mechanism for which it was the inhibiting step.

The following reactions were considered for chain termination

$$R+Cl=RCl \quad (5)$$

$$R+R=R_2 \quad (5a)$$

$$Cl+Cl=Cl_2. \quad (5b)$$

Reaction (5a) can be immediately rejected since it would result in the initial rate being independent of [RH]. The choice between (5) and (5b) could not be based on initial rates alone. For the former the initial rate would be proportional to $[RH]^{\frac{1}{2}}I_0^{\frac{1}{2}}(1-\exp(-\alpha[Cl_2]d/2))$; for the latter, to $[RH]I_0^{\frac{1}{2}}[Cl_2]^{-\frac{1}{2}}(1-\exp(-\alpha[Cl_2]d/2))$. Although (5) appeared to fit the initial rate data better than (5b) the evidence was not conclusive. However (5b), in conjunction with (1), (2), (3), and (4), leads to a rate equation in which [RCl] does not appear. The data of Table I show clearly that the reaction is inhibited by RCl, and the chemical analyses indicate that (4) is the inhibiting step. The only possible conclusion would seem to be that (5b), if it occurs at all, must play a very minor role, and that (5) is the main chain-stopping step.

The *local* rate equation corresponding to reactions (1)–(5) is

$$(-d[Cl_2]/dt)_{loc.} = k'\frac{I_a[RH]}{\{I_a([RH]/[Cl_2])(1+k''[RCl]/[RH])\}^{\frac{1}{2}}} \quad (ii)$$

where $k'=(k_2k_3/k_5)^{\frac{1}{2}}$, $k''=k_4/k_2$, and I_a is the light absorption per unit volume. The corresponding *observed* rate equation is obtained by integrating this expression over the length of the cell:

$$(-d[Cl_2]/dt)_{obs.} = (1/d)\int_{d=0}^{d=d}(-d[Cl_2]/dt)_{loc.}\cdot dd. \quad (iii)$$

The resulting expression is

$$(-d[Cl_2]/dt)_{obs.} = k'\frac{2(I_0[RH])^{\frac{1}{2}}(1-\exp(-\alpha[Cl_2]d/2))}{d\alpha^{\frac{1}{2}}(1+k''[RCl]/[RH])^{\frac{1}{2}}}. \quad (iv)$$

Equation (iv) may be written in the form

$$\psi d[Cl_2]=k'dt, \quad (v)$$

where ψ is a function of $[Cl_2]$ only, since $[RH]=[RH]_0+\Delta[Cl_2]$, $[RCl]=[RCl]_0-\Delta[Cl_2]$ and α is a known function of $[Cl_2]$. A plot of $\int\psi d[Cl_2]$ *vs.* t should then give a straight line through the origin with slope k'. With suitable values of k'' the experimental data did give straight lines when plotted in this way, but the values of k'' varied from experiment to experiment. Furthermore, when the light intensity was changed considerably part way through an experiment, as in 31, 32, and 33, no single choice of k'' was sufficient to make the two parts colinear.

In each of these three experiments the chlorine concentrations were measured at frequent intervals, so that it was possible to obtain accurate values of the two tangents to the $[Cl_2]$ *vs.* time curve at the time when the light intensity was changed. The values of these tangents, given in column six of Table I, permit a more accurate estimate of the effect of light intensity than could be obtained from separate experiments; by this method the concentrations of the reactants are exactly duplicated and any effect due to traces of impurities is eliminated. A comparison of the data in columns five and six shows that for the three experiments the power of the light intensity involved is 0.6_1, 0.5_5 and 0.6_2 respectively.

The absence of colinearity in the integral curves, together with the fact that the exponent of I_0 is greater than 0.5, indicated that in addition to (5) there must be some *first order* chain-stopping step.

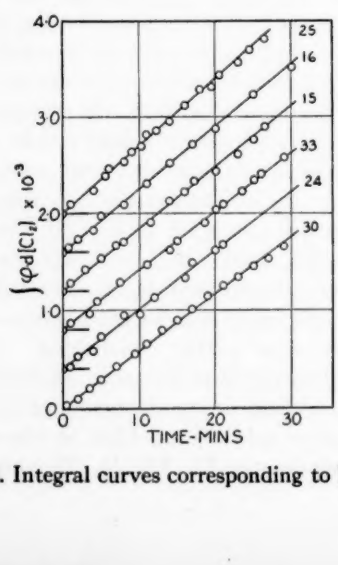

FIG. 8. Integral curves corresponding to Fig. 7.

Without giving a detailed picture, possible processes are

$$Cl(+M)=\tfrac{1}{2}Cl_2(+M) \qquad (6)$$

and

$$R(+M)=\tfrac{1}{2}R_2(+M). \qquad (6a)$$

Because the effect is small it was not possible to distinguish between the two reactions. However, the arbitrary choice was made that (6) was the reaction involved. The modified *local* rate equation is identical with (ii) with the exception that a term $A(=(k_6/2)(k_3/k_2k_5)^{\frac{1}{2}})$ is added to the denominator. The corresponding *observed* rate equation is

$$(-d[Cl_2]/dt)_{obs.}$$

$$=k'\frac{2(I_0[RH])^{\frac{1}{2}}(1-\exp(-\alpha[Cl_2]d/2)-D)}{d\alpha^{\frac{1}{2}}(1+k''[RCl]/[RH])^{\frac{1}{2}}}. \qquad (vi)$$

D is given by the expression

$$D=B\ln\frac{1+B}{\exp(-\alpha[Cl_2]d/2)+B} \qquad (vii)$$

where

$$B=\frac{A}{\{\alpha I_0[RH](1+k''[RCl]/[RH])\}^{\frac{1}{2}}}.$$

A mutually consistent set of values of A and k'' was obtained by equating the ratio of the tangents to the $[Cl_2]$ *vs.* time curve for one of experiments 31, 32, 33, to the theoretical ratio predicted by Eq. (vi). A second set of mutually consistent values was obtained from a comparison of the rates of pairs of experiments such as 22, 23; 24, 25; or 28, 29, for which the reagents were prepared in duplicate as previously described, one set of reagents including RCl, the other not. When curves of A *vs.* k'' were plotted using the two types of data they intersected at the values, $A=1.8\times10^{-4}$ and $k''=15$. The units of A are (moles·liters^{-1}·hours^{-1})$^{\frac{1}{2}}$; k'' is, of course, dimensionless.

It is clear that Eq. (vi) may be written in the form

$$\varphi d[Cl_2]=k'dt, \qquad (viii)$$

where φ is a function of $[Cl_2]$, and hence a plot of $\int\varphi d[Cl_2]$ *vs.* time should give a straight line through the origin with slope k'. Using the values of A and k'' given above, it was found that all of the data for the various experiments satisfied this criterion, and furthermore the two parts of the integral curves for experiments 31, 32, and 33 were then colinear.

Some typical $[Cl_2]$ *vs.* time curves are given in Fig. 7; the corresponding integral curves are given in Fig. 8. The values of k', derived from the slopes

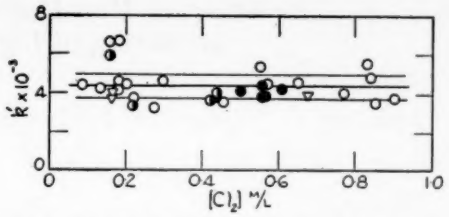

FIG. 9. Values of k'. ○ I_0 approx. 54 mv, [RH] approx. 0.6; ◑ I_0 variation; ● [RH] variation; ▽ RCl added initially.

of the integral curves, are tabulated in the last column of Table I. Although these show considerable fluctuation, it is clear from Fig. 9 that even for large changes in conditions k' shows no appreciable trend; its average value was 4.34×10^3 with a mean deviation of 0.59×10^3; its units are (liters·moles^{-1}·hours^{-1})$^{\frac{1}{2}}$. Using Eq. (vi), three curves of initial rate *vs.* $[Cl_2]$ were drawn for the conditions, $I_0=54.0$ mv, $d=0.500$ cm, $[RH]=0.580$ mole per liter, $k''=15$, $A=1.8\times10^{-4}$, and $k'=4.34\times10^3$, $(4.34+0.59)\times10^3$ and $(4.34-0.59)\times10^3$. These curves are shown in Fig. 5. The theoretical effect of [RH] on the initial rates is shown by a similar set of curves in Fig. 6.

DISCUSSION

Because of the complexity of Eq. (vi), no simple expression can be given for the quantum yield, although its value can be computed for any particular set of conditions. For example, with $I_0=54.0$ mv (1.57×10^{-7} einstein/cm^2/hr.), $[Cl_2]=0.580$ mole per liter, $[RH]=0.580$ mole per liter and $d=0.5$ cm, the initial rate, derived from (vi), is 0.849 mole/liter/hr. For a cell volume of V cc the rate of consumption of chlorine is $0.849V/1000$ mole/hr. The light transmission is given by $I_T=I_0\exp(-\alpha[Cl_2]d)$ einstein/cm^2/hr.; the light absorption is therefore $I_0(1-\exp(-\alpha[Cl_2]d))V/d$ $=1.12\times10^{-7}V/d$ einstein per hour. The initial quantum yield is equal to $0.849d/1.12\times10^{-4}=3.78\times10^3$ moles per einstein.

The mechanism which has been derived is applicable, of course, only to the formation of monochloromethyl chloroformate. If the reaction were carried to completion some di-, and possibly trichloromethyl chloroformate, would undoubtedly be formed, even at 25°C. At the present time no information is available regarding these subsequent steps other than the fact that they are slow.

The authors would like to express their appreciation for the financial assistance received from the National Research Council and the Defence Research Board of Canada. One of the authors (L.M.D.) held a Bursary and a Studentship from the National Research Council, another (T.L.B.) is holding a Canadian Industries Limited Fellowship.

The Effect of Non-Homogeneity of Molecular Weight on the Scattering of Light by High Polymer Solutions

H. C. BRINKMAN
Laboratorium N. V. Bataafsche Petroleum Maatschappij, Amsterdam (Royal Dutch Shell Group), Nederland

AND

J. J. HERMANS
Laboratory for inorgan. and phys. Chemistry, University of Groningen, Bloemsingel, Nederland

(Received December 6, 1948)

The general theory of the turbidity of a mixture of many components is applied to a solution of homologous polymers.

It is found that the concentration dependence of the turbidity is intimately related to that of the osmotic pressure. The molecular weight distribution does not have any influence on the concentration dependence of the turbidity.

SEVERAL authors[1] have considered the scattering of light by a solution of a polymer homologous mixture. According to these authors the light scattering of the polymer mixture is obtained as a sum over all the homologues of the solute, each term being of the same form as that found for a single polymer species in solution. It can be shown that on this assumption the concentration dependence of the turbidity would give information about the distribution of the polymer homologues over the molecular weights.

We want to show that this opinion is incorrect; the density fluctuations of the various polymer species which determine the turbidity are not independent.

The theoretical treatment of the turbidity has been given by Zernike[2] in his dissertation, which seems to have been overlooked by later authors. It contains an exhaustive treatment of the general problem. According to Zernike the turbidity τ of a solution of N components in a solvent (indicated by the index 0) is determined by the ratio of two determinants, as follows,

$$\tau = -A\,VD/\Delta \tag{1}$$

where V is the volume of the solution,

$$A = 32\pi^3 kT\nu^2/3\lambda^4, \tag{2}$$

ν is the index of refraction of the solution, λ is the wave-length in vacuum,

$$D = \begin{vmatrix} 0 & \nu_0 & \nu_1 & \nu_2 & \cdots & \nu_N \\ \nu_0 & F_{00} & F_{01} & F_{02} & \cdots & F_{0N} \\ \nu_1 & F_{10} & F_{11} & & \cdots & F_{1N} \\ \nu_2 & F_{20} & & & \cdots & F_{2N} \\ \cdot & \cdot & \cdot & \cdot & \cdot & \cdot \\ \nu_N & F_{N0} & & & \cdots & F_{NN} \end{vmatrix};$$

$$\Delta = \begin{vmatrix} F_{00} & F_{01} & \cdots & F_{0N} \\ F_{10} & F_{11} & \cdots & F_{1N} \\ \cdot & \cdot & \cdot & \cdot \\ F_{N0} & F_{N1} & \cdots & F_{NN} \end{vmatrix}.$$

In the following these and similar determinants will be written as

$$D = \begin{Vmatrix} 0 & \nu_j \\ \nu_i & F_{ij} \end{Vmatrix}; \quad \Delta = \|F_{ij}\|; \quad i, j = 0, 1, \cdots N.$$

The following symbols were introduced,

$$\nu_i = (\partial\nu/\partial n_i)_V, \quad F_{ij} = (\partial^2 F/\partial n_i \partial n_j)_V,$$

n_i is the number of moles of component i; F is the Helmholtz free energy. This result was obtained by Zernike by averaging

$$(\nu - \nu_{Av})^2 = (\Sigma_i \nu_i \Delta n_i)^2$$

over a grand ensemble as introduced by Gibbs.[3] The same average may be derived by calculating

$$\int_{-\infty}^{\infty} \cdots \int (\Sigma_i \nu_i \Delta n_i)^2 \exp(-\Delta F/kT) \Pi_i d(\Delta n_i) \Big/ \int_{-\infty}^{\infty} \cdots \int \exp(-\Delta F/kT) \Pi_i d(\Delta n_i)$$

where

$$\Delta F = \Sigma_i \Sigma_j F_{ij} \Delta n_i \Delta n_j.$$

We convert the derivatives of the Helmholtz free energy, F, into those of the Gibbs free energy, G, by the relations

$$F_{ij} = G_{ij} + v_i v_j/\kappa V$$

where

$$G_{ij} = (\partial^2 G/\partial n_i \partial n_j)_p, \tag{3}$$

$$\kappa = -(\partial V/V\partial p)_{n_i}, \tag{4}$$

$$v_i = (\partial V/\partial n_i)_p \tag{5}$$

[1] P. Debye, Report Cornell University 1945; B. H. Zimm and P. M. Doty, J. Chem. Phys. **12**, 203 (1944); P. M. Doty, B. H. Zimm, and H. Mark, J. Chem. Phys. **13**, 159 (1945); J. Waser, R. M. Badger, and V. Schomaker, J. Chem. Phys. **14**, 43 (1946).

[2] F. Zernike, L'Opalescence critique, Dissertation, Amsterdam 1915; Archives Neerland. (3A) **4**, 74 (1918).

[3] J. W. Gibbs, *Statistical Mechanics* (Yale University Press 1948) p. 201.

and eliminate the G_{0i} by means of the Gibbs-Duhem relation. This gives

$$\frac{\tau}{A}=\nu_V{}^2\kappa V-\frac{V}{\|G_{ij}\|}\begin{Vmatrix}0 & \bar{\nu}_j\\ \bar{\nu}_i & G_{ij}\end{Vmatrix},\quad i,j=1,2,\cdots N, \tag{6}$$

where

$$\nu_V=(\partial\nu/\partial V)_{n_i}, \tag{7}$$

$$\bar{\nu}_i=(\partial\nu/\partial n_i)_p. \tag{8}$$

Now this general result may be simplified by the introduction of some assumptions regarding the polymer solution. Assuming that the index of refraction, ν, depends only on the total concentration by weight, c, of the polymer and on the volume V, we get

$$\frac{\tau}{A}=\nu_V{}^2\kappa V^2-\frac{\nu_c{}^2}{V\|G_{ij}\|}\times\begin{Vmatrix}0 & m_j-cv_j\\ m_i-cv_i & G_{ij}\end{Vmatrix},\quad i,j=1,2,\cdots N. \tag{9}$$

$$\nu_c=(\partial\nu/\partial c)_p;\quad c=\sum_{i=1}^{N}n_im_i/V \tag{10}$$

m_i being the molecular mass of species i. We conclude that it is possible to split the general formula into two terms, one of which contains the influence of the compressibility. It is not possible, however, to split up the second term into a sum of terms containing the influence of each component separately.

For a further discussion of this result we introduce expressions for G_{ij}, putting[4]

$$G/RT=\sum_{i=0}^{N}n_i\ln\varphi_i+\mu V\varphi\varphi_0/v_0 \tag{11}$$

where φ_i is the volume fraction of component i.

$$\varphi_i=n_iv_i/V;\quad \varphi=\sum_{i=1}^{N}\varphi_i;\quad \varphi_0=1-\varphi, \tag{12}$$

μ is the constant in the van Laar expression for the heat of mixing. This expression for G represents the most obvious extension of the Flory-Huggins[5] theory to a solution of a polymer homologous mixture. Assuming

$$\alpha=m_i/v_i \tag{13}$$

to have the same value for all the homologues, and introducing further the density,

$$\rho=\sum_{i=0}^{N}n_im_i/V,$$

of the solution,

$$\frac{\tau}{A}=\kappa\rho^2\nu\rho^2-c\nu_c{}^2\frac{M_w}{RT}\left[1+\frac{v_w}{v_0}\frac{\varphi}{\varphi_0}(1-2\mu\varphi_0)\right]^{-1} \tag{14}$$

where M_w and v_w are the weight average molecular weight and the weight average molecular volume. The first term is due to fluctuations in the pressure. The second, which we denote by τ_c/A, results from fluctuations in the composition. If, in accordance with Eq. (2), we introduce the constant

$$H=A\nu_c{}^2/RT=32\pi^3\nu^2\nu_c{}^2/3\lambda^4N_{Av} \tag{15}$$

and expand in powers of φ, we find

$$H\frac{c}{\tau_c}=\frac{1}{M_w}+\frac{(1-2\mu)\varphi+\varphi^2+\varphi^3+\varphi^4\cdots}{\alpha v_0}. \tag{16}$$

We conclude, that the molecular weight distribution does not influence the concentration dependence of the turbidity. We see, further, that a plot of c/τ_c against $c=\alpha\varphi$ has zero initial slope if $\mu=0.5$, a result which was already known to apply to the solution of a single polymer species. Comparing the result, Eq. (16), with the osmotic pressure, $P=-\partial G/v_0\partial n_0$, and abbreviating $K=HRT$, we obtain

$$\frac{\partial P}{\partial c}-K\frac{c}{\tau_c}=RT\left(\frac{1}{M_n}-\frac{1}{M_w}\right), \tag{17}$$

M_n being the number average molecular weight. When differentiating P with respect to c in this equation, the ratios between the concentrations of the various polymer species are kept constant. One might object, that this simple relation has been derived from a special choice of the G-function. It can be shown, however, that Eq. (17) is valid for a polymer homologous mixture whenever

$$G/RT=\Sigma_in_i\ln\varphi_i+n_0f(\varphi), \tag{18}$$

$f(\varphi)$ being an arbitrary function of the volume fraction of total polymer. This is the general form of G to which all existing theories of polymer solutions reduce provided (a) the molecular weights of the polymer species are high and (b) the heat ΔH of mixing the polymer with the solvent is sufficiently small to write G as the sum of ΔH and $-T$ times the entropy of athermal mixing. For example, Guggenheim's expression[6] for the entropy in the absence of a heat term can be shown to reduce to the form of Eq. (18) if the molecular weights are high. Since, further, the heat term will be of the form $n_0h(\varphi)$ if the effect of end groups is negligible, Eq. (18) for G will be valid.

[4] P. J. Flory, J. Chem. Phys. **12**, 425 (1944); R. L. Scott and M. Magat, J. Chem. Phys. **13**, 172 (1945).

[5] M. L. Huggins, J. Phys. Chem. **46**, 151 (1942); J. Am. Chem. Soc. **64**, 1712 (1942); P. J. Flory, J. Chem. Phys. **9**, 660 (1941); **12**, 425 (1944).

[6] E. A. Guggenheim, Proc. Roy. Soc. London **A183**, 203 (1944).

It should not be concluded from Eq. (17), in conjunction with Eq. (18), that Eq. (17) is a general law which applies to any mixture, irrespective of the form of G. For example, in a perfect solution of polymers, where

$$G/RT=\Sigma_i n_i \ln(n_i/\Sigma_i n_i), \qquad (19)$$

one finds the following relation between turbidity and osmotic pressure,

$$\tau_e/Kc-\partial c/\partial P=\varphi_0^2(M_w-M_n)/RT.$$

This shows that it is essential, for Eq. (17) to be applicable, that the molar fractions in Eq. (19) are replaced by volume fractions. Conversely, Eq. (17) may be used to check the statistical theory of polymer solutions.

THE JOURNAL OF CHEMICAL PHYSICS VOLUME 17, NUMBER 6 JUNE, 1949

The Vapor Pressure, Orthobaric Liquid Density, and Critical Constants of Isobutane

JAMES A. BEATTIE, DAVID G. EDWARDS, AND STANLEY MARPLE, JR.
Department of Chemistry, Massachusetts Institute of Technology, Cambridge, Massachusetts
(Received December 16, 1948)

The vapor pressures and orthobaric liquid densities of isobutane (propane-2-methyl) were measured from 30° to 125°C. The equation

$$\log_{10}p \text{ (normal atmos.)}=4.31269-1126.71/T \quad (T=t°\text{C (Int.)}+273.13)$$

gives a fair representation of the vapor pressures.

The critical constants of isobutane are determined by the compressibility method. They are: $t_c=134.98\pm0.05$°C (Int.), $p_c=36.00\pm0.05$ normal atmos., $v_c=0.263$ liters per mole (4.53 ml per g), $d_c=3.80$ moles per liter (0.221 g per ml). The uncertainty in the critical volume and density is 2 percent.

IN recent years the vapor pressure and critical constants of a number of hydrocarbons have been determined.[1] The vapor pressures and orthobaric densities of isobutane have been studied over various temperature ranges by several investigators[2–6] and the critical constants determined[3,7] by the disappearance of the meniscus method. Recently several compilations of the vapor pressure and critical constants have been published.[8,9]

The isobutane used in the present investigation was furnished by the Linde Air Products Company through the courtesy of Dr. L. I. Dana.

The method of procedure for the determination of vapor pressure and compressibility has been described elsewhere.[10] The bomb with the glass liner was used. No attempt at further fractionation of the isobutane was made but it was distilled, frozen, and pumped several times in the process of loading the weighing bomb in order to remove any non-condensible gas.

The mass of the isobutane sample used was about 7 grams. In the determination of vapor pressure the volume of the sample was varied at each tem-

TABLE I. Vapor pressures and orthobaric liquid densities of isobutane.

Temp. °C (Int.)	Largest and smallest vapor volumes ml		Increase in vapor pressure atmos.	Vapor pressure normal atmos.	Orthobaric liquid density g/ml
30	77	41	0.005	3.941	0.549
50	96	4	0.002	6.701	0.518
75	98	2	0.004	11.932	0.480
100	103	0.01	0.004	19.573	0.428
125	46	20	0.008	30.440	0.353

TABLE II. Comparison of calculated with observed vapor pressures of isobutane.
$\log_{10}p$ (calcd.) $=4.31269-1126.71/T$.

Temp. °C (Int.)	Vapor pressure normal atmos.	Obs.-calc. atmos.
30	3.941	−0.001
50	6.701	+0.005
75	11.932	+0.013
100	19.573	−0.064
125	30.440	+0.073

[1] For the last report on this work see J. A. Beattie and D. G. Edwards, J. Am. Chem. Soc. **70**, 3382 (1948).
[2] G. A. Burrell and L. W. Robertson, J. Am. Chem. Soc. **37**, 2482 (1915).
[3] F. M. Sibert and G. A. Burrell, J. Am. Chem. Soc. **37**, 2683 (1915).
[4] Dana, Jenkins, Burdick, and Timm, Refrig. Eng. **12**, 387 (1926).
[5] B. H. Sage and W. N. Lacey, Ind. Eng. Chem. **30**, 673 (1938).
[6] W. M. Morris, B. H. Sage, and W. N. Lacey, Am. Inst. Mining and Met. Eng., Tech. Pub. 1128, Petroleum **2** (Nov. 1939).
[7] J. Harand, Monats. F. Chem. **65**, 153 (1935).
[8] Anon., Oil and Gas J. **44**, No. 23, 115 (Oct. 1945).
[9] K. Hochmuth, G. H. Hanson, and M. L. Smith, Trans. Am. Inst. Chem. Eng. **42**, 975 (1946).
[10] J. A. Beattie, Proc. Am. Acad. **69**, 389 (1934).

TABLE III. Isotherms of isobutane in the critical region
Molecular Weight, 58.077.

Temp. °C density moles/liter	(Int.) volume liters/mole	134.60	134.70	134.80	134.85	134.88	134.90	134.95	134.97	134.98	134.99	135.00	135.05	135.15
		Pressure, normal atmospheres												
3.108	0.3218	35.705	35.769	35.823	35.847	35.861	35.870	35.895	35.907			35.923	35.946	35.997
3.227	0.3099	35.733	35.801	35.852	35.882	35.899	35.908	35.931	35.939			35.961	35.986	36.038
3.291	0.3039	35.753	35.809	35.868										
3.356	0.2980	35.773	35.816	35.874	35.904	35.919	35.928	35.955	35.966	35.970	35.977	35.981	36.010	36.065
3.423	0.2921	35.770	35.823	35.882	35.910	35.926	35.934							
3.495	0.2861	35.771	35.828	35.886	35.915	35.932	35.940	35.973	35.978	35.988	35.993	35.998	36.024	36.084
3.569	0.2802	35.769	35.829	35.889	35.922	35.939	35.946	35.974	35.983	35.993	35.998	36.004		
3.647	0.2742		35.828	35.887	35.922		35.952	35.979	35.990	35.994	36.004	36.007	36.034	36.092
3.686	0.2713							35.982	35.990					
3.727	0.2683	35.773	35.831	35.890	35.921	35.946	35.953	35.983	35.992	36.000	36.005	36.009		
3.768	0.2654							35.983	35.994	35.997				
3.811	0.2624		35.825	35.889	35.922	35.944	35.953	35.983	35.994	35.999	36.008	36.012	36.042	36.100
3.855	0.2594							35.983	35.996					
3.899	0.2565	35.770	35.832	35.892		35.944	35.954	35.984	35.996	36.002	36.008	36.013		
3.992	0.2505	35.769	35.826	35.894	35.925	35.945	35.956	35.988	36.000	36.003	36.011	36.018	36.048	36.110
4.088	0.2446	35.769	35.833	35.893		35.945		35.990	36.002			36.020		
4.189	0.2387	35.770	35.832	35.895	35.927	35.947	35.960	35.995	36.005	36.013	36.019	36.026	36.054	36.117
4.297	0.2327		35.838											
4.409	0.2268	35.776		35.907	35.943	35.965	35.978	36.015	36.024			36.046	36.080	36.144
4.653	0.2149	35.799	35.890	35.967	36.010	36.028	36.045	36.084	36.092			36.119	36.153	36.226

perature from about 90 ml to a value less than the orthobaric liquid volume. The change of vapor pressure with vapor volume gives an indication of the purity of the sample. The orthobaric liquid density was determined at each temperature from the break in the curve of pressure *versus* volume.

The measured vapor pressures are listed in Table I. The small increase in pressure with decrease in vapor volume indicates that the sample was of exceptional purity. The vapor pressures were represented by the equation:

$$\log_{10} p \text{ (normal atmos.)} = 4.31269 - (1126.71/T), \quad (T = t°\text{C (Int.)} + 273.13),$$

and the representation of the measurements by this equation is given in Table II. Our vapor pressures are in fair agreement with those of Dana and co-workers[4] and of Sage and Lacey,[5] and are in even better agreement with the two values published by Morris, Sage, and Lacey.[6]

Our measured orthobaric liquid densities are listed in Table I. The estimated uncertainty is 0.001 g per ml. Our measured densities are on the average 0.002 g per ml lower than those of Sage and Lacey,[5,6] and are higher than the values of Dana and co-workers[4] at 30° by 0.003 g per ml and lower at 50° by 0.001.

The measurements of the compressibility of isobutane in the critical region are given in Table III and plotted in Fig. 1. From the plot we find for the critical point: $t_c = 134.98 \pm 0.05$°C (Int.), $p_c = 36.00 \pm 0.05$ normal atmospheres, $v_c = 0.263$ liter per mole (4.53 ml per g), $d_c = 3.80$ moles per liter (0.221 g per ml). The uncertainty in the critical volume and density is 2 percent. Sibert and Burrell[3] give $t_c = 133.7$°C, $p_c = 36.54$ atmos., and Harand[7] gives $t_c = 133.8$°C.

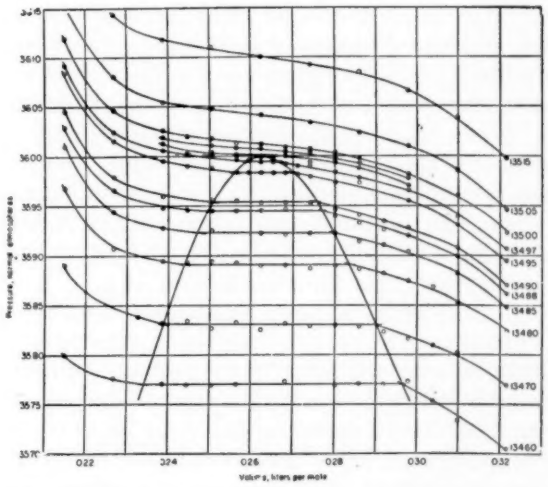

FIG. 1. Isotherms of isobutane in the critical region. The isotherms immediately above 134.97 are 134.98 and 134.99.

Thermodynamic Properties of Diiodoacetylene and Some Symmetrical-Top Acetylenes

JOSEPH S. ZIOMEK* AND FORREST F. CLEVELAND
Departments of Chemistry and Physics, Illinois Institute of Technology, Chicago, Illinois
(Received December 16, 1948)

In this paper tables are presented of the thermodynamic functions—heat content, free energy, entropy, and heat capacity—of diiodoacetylene, methylchloroacetylene, methylbromoacetylene, methyliodoacetylene, methylacetylene, and methyldeuteroacetylene, for several temperatures from their boiling points up to 1000°K, for the ideal gaseous state at one atmosphere pressure. These functions were calculated from the Raman spectral data for all of the substances except methyldeuteroacetylene, for which the frequencies used were those calculated with force constants transferred from methylacetylene.

INTRODUCTION

THERMODYNAMIC properties can be calculated from spectroscopic data—to a rigid rotator, harmonic oscillator approximation—if the vibrational frequencies and their degeneracies are known and if the internuclear distances have been determined from spectroscopic or electron diffraction data. In the present investigation, such calculations have been made for diiodoacetylene, methylchloroacetylene, methylbromoacetylene, methyliodoacetylene, methylacetylene, and methyldeuteroacetylene. The thermodynamic properties calculated were the heat capacity, entropy, heat content, and free energy for several temperatures.

Previous calculations were made by Crawford[1] of the entropy, free energy, and heat capacity for methylacetylene, with results that are only slightly different from those obtained in the present investigation. Calculated values of the heat capacity for methylbromoacetylene and methyliodoacetylene also were reported previously by Cleveland and Murray;[2] each of their values was slightly greater than the corresponding value in the present results.

The values obtained for methyldeuteroacetylene are tentative since they were obtained from the calculated frequencies, with force constants transferred from methylacetylene. This was necessary because no Raman or infra-red data have been reported for this molecule.

TABLE I. Fundamental frequencies for diiodoacetylene.

Designation	Frequency (cm^{-1})	Degeneracy
ν_1	191	1
ν_2	2109	1
ν_3	710	1
ν_4	310	2
ν_5	115	2

The values of the physical constants used in the present calculations were:

$R = 1.98714$ cal. mole^{-1} deg.$^{-1}$,
$c_2 = hc/k = 1.4384$ cm deg.,
$N_0 = 6.0228 \cdot 10^{23}$ mole^{-1},
Atomic weight of hydrogen = 1.0083,
Atomic weight of deuterium = 2.01418,
Atomic weight of carbon = 12.0146,
Atomic weight of chlorine = 35.4570,
Atomic weight of bromine = 79.916, and
Atomic weight of iodine = 126.915.

SPECTROSCOPIC AND MOLECULAR DATA

Diiodoacetylene

Raman spectral data, for solutions in acetone and in absolute alcohol, have been obtained for diiodoacetylene by Glockler and Morrell[3] and by Cleveland and Meister.[4] Infra-red data, for the solid and for a carbon disulfide solution, were obtained by Emschwiller and Lecomte[5] in the region 650 to 1450 cm^{-1}. Since the observed dipole moment for this molecule was nearly zero[6] and since the electron diffraction data[7] indicated a linear structure, Cleveland and Meister[4] assumed that diiodoacetylene is linear and symmetrical and found that a satisfactory assignment of frequencies could be made upon this basis. As an aid in making the assignment, an *FG* matrix calculation of the frequencies was made, with force constants transferred from the similar molecule, methyliodoacetylene. According to this assignment, the fundamental frequencies and their degeneracies are those given in Table I.

The internuclear distances required for the calculation of the moments of inertia were taken from the electron diffraction results;[7] they were 1.18A for the

* Present address, Chemistry Department, De Paul University, Chicago 14, Illinois.

[1] Bryce L. Crawford, Jr., J. Chem. Phys. **8**, 526 (1940).

[2] Forrest F. Cleveland and M. J. Murray, J. Chem. Phys. **11**, 450 (1943); **12**, 320 (1944).

[3] G. Glockler and C. E. Morrell, J. Chem. Phys. **2**, 349 (1934); **4**, 15 (1936).

[4] Forrest F. Cleveland and Arnold G. Meister, paper presented at the international colloquium, Bordeaux, France, April 1948; see also J. Chem. Phys. **17**, 212 (1949).

[5] G. Emschwiller and J. Lecomte, J. de phys. et rad. **8**, 130 (1937).

[6] L. E. Sutton, R. G. A. New, and J. B. Bentley, J. Chem. Soc. 652 (1933).

[7] H. de Laszlo, Trans. Faraday Soc. **30**, 825 (1934); Nature **135**, 474 (1935).

TABLE II. Fundamental frequencies for methylchloroacetylene.

Designation	Frequency (cm^{-1})	Degeneracy
ν_1	2926	1
ν_2	2263	1
ν_3	1380	1
ν_4	1078	1
ν_5	579	1
ν_1	2971	2
ν_2	1449	2
ν_3	1029	2
ν_4	353	2
ν_5	184	2

C≡C bond and 2.03A for the C−I bond. The moments of inertia calculated from these bond distances were

$$I_1 = I_2 = 2.91 \cdot 10^{-37} \text{ g cm}^2,$$

and

$$I_3 = 0.$$

Methylchloroacetylene

Raman spectral data for a solution of methylchloroacetylene were obtained by Cleveland and Murray,[2] but no vibrational assignment could be made by them because of uncertainties introduced by the presence of the solvent lines. To overcome this difficulty, Meister[8] calculated the frequencies for this molecule by the *FG* matrix method, assuming a C_{3v} symmetry and using force constants obtained in a previous investigation.[9] The remaining force constants were determined from some of the observed frequencies and finally all of the frequencies were calculated and compared with the observed values. The agreement between the observed and calculated frequencies was within two percent. In this way, a rather certain assignment of the fundamental frequencies could be made. According to this assignment, the fundamental frequencies and their degeneracies are those given in Table II. The frequency designations are those used by Meister.[8] No infra-red data have been reported for this molecule.

The bond distances and interbond angles used in calculating the moments of inertia were the ones used by Meister;[8] they were: C−Cl, 1.68A; C−H, 1.093A; C≡C, 1.21A; C−C, 1.462A; and for the H−C−C angle, 109° 28′. The resulting values for the moments of inertia were

$$I_1 = I_2 = 386 \cdot 10^{-40} \text{ g cm}^2,$$

and

$$I_3 = 5.33 \cdot 10^{-40} \text{ g cm}^2.$$

TABLE III. Fundamental frequencies for methylbromoacetylene.

Designation	Frequency (cm^{-1})	Degeneracy
ν_1	2921	1
ν_2	2230	1
ν_3	1375	1
ν_4	1034	1
ν_5	464	1
ν_1	2968	2
ν_2	1443	2
ν_3	1026	2
ν_4	343	2
ν_5	171	2

[8] Arnold G. Meister, J. Chem. Phys. 16, 950 (1948).
[9] Arnold G. Meister and Forrest F. Cleveland, J. Chem. Phys. 15, 349 (1947).

TABLE IV. Fundamental frequencies for methyliodoacetylene.

Designation	Frequency (cm^{-1})	Degeneracy
ν_1	2913	1
ν_2	2197	1
ν_3	1375	1
ν_4	1008	1
ν_5	405	1
ν_1	2958	2
ν_2	1438	2
ν_3	1021	2
ν_4	343	2
ν_5	163	2

Methylbromoacetylene

No infra-red data have been obtained for methylbromoacetylene, but Raman spectral data for the liquid state and an assignment of frequencies on the basis of a C_{3v} symmetry have been reported by Cleveland and Murray.[2] Later, Meister[8] carried out an *FG* matrix treatment for this molecule and made some revisions in the previous assignment; his assignment of the fundamental frequencies and their degeneracies are given in Table III.

The bond distances and interbond angles used in calculating the moments of inertia for this molecule again were those used by Meister;[8] they were: C−Br, 1.80A; C≡C, 1.204A; C−C, 1.462A; C−H, 1.093A; and for the H−C−C angle, 109° 28′. The

TABLE V. Fundamental frequencies for methylacetylene.

Designation	Frequency (cm^{-1})	Degeneracy
ν_1	2941	1
ν_2	2146	1
ν_3	1382	1
ν_4	928	1
ν_5	3429	1
ν_1	2982	2
ν_2	1448	2
ν_3	1038	2
ν_4	336	2
ν_5	642	2

TABLE VI. Fundamental frequencies for methyldeuteroacetylene.

Designation	Frequency (cm^{-1})	Degeneracy
ν_1	2941	1
ν_2	2009	1
ν_3	1376	1
ν_4	914	1
ν_5	2674	1
ν_1	3059	2
ν_2	1454	2
ν_3	1037	2
ν_4	309	2
ν_5	518	2

resulting values for the moments of inertia were

$$I_1 = I_2 = 541 \cdot 10^{-40} \text{ g cm}^2,$$

and

$$I_3 = 5.33 \cdot 10^{-40} \text{ g cm}^2.$$

Methyliodoacetylene

No infra-red data have been obtained for methyliodoacetylene, but Raman data for the liquid state and a frequency assignment were given by Cleveland and Murray[2] on the basis of a C_{3v} symmetry. Later, Meister[8] carried out an *FG* matrix treatment for this molecule also and made some revisions in the previous assignment; his assignment of the fundamental frequencies and their degeneracies is given in Table IV.

The bond distances and interbond angles used in calculating the moments of inertia for this molecule were those used by Meister;[8] they were: C−I, 2.03A; C≡C, 1.18A; C−C, 1.462A; C−H, 1.093A; and the H−C−C angle, 109° 28′. The resulting values for the moments of inertia were

$$I_1 = I_2 = 673 \cdot 10^{-40} \text{ g cm}^2,$$

and

$$I_3 = 5.33 \cdot 10^{-40} \text{ g cm}^2.$$

Methylacetylene

Raman spectral data have been reported by Glockler and Davis[10] and both Raman and infra-red data by Crawford.[1,11] An assignment of the frequencies was made by Crawford[1] upon the basis of a C_{3v} symmetry, which was also the structure which was found to be consistent with the electron diffraction data.[12] The fundamental frequencies have been calculated by Crawford[1] and by Meister.[8] The values of the fundamental frequencies[1,5] and their degeneracies used in the present work are given in Table V. The frequency designations are those of Meister.

The bond distances and interbond angles[13,12] used in calculating the moments of inertia were: C−H (methyl), 1.093A; C−H (terminal), 1.057A; C−C, 1.462A; C≡C, 1.204A; and the H−C−C angle, 109° 28′. These values yield the following moments of inertia:

$$I_1 = I_2 = 97.87 \cdot 10^{-40} \text{ g cm}^2,$$

and

$$I_3 = 5.333 \cdot 10^{-40} \text{ g cm}^2.$$

Methyldeuteroacetylene

As yet no Raman or infra-red spectral data have been reported for methyldeuteroacetylene. How-

TABLE VII. Heat content, free energy, entropy, and heat capacity of diiodoacetylene for the ideal gaseous state at one atmosphere pressure.*

T	$(H^0-H_0^0)/T$	$-(F^0-H_0^0)/T$	S^0	C_p^0
373.16	13.90	64.75	78.65	17.44
400	14.14	65.72	79.86	17.61
600	15.47	71.73	87.20	18.55
800	16.32	76.32	92.63	19.17
1000	16.94	80.02	96.96	19.60

* In this and subsequent tables, T is in °K and the other four quantities are in cal. deg.$^{-1}$ mole^{-1}.

TABLE VIII. Heat content, free energy, entropy, and heat capacity of methylchloroacetylene for the ideal gaseous state at one atmosphere pressure.

T	$(H^0-H_0^0)/T$	$-(F^0-H_0^0)/T$	S^0	C_p^0
400	14.04	59.27	73.31	19.72
600	16.66	65.47	82.13	23.87
800	18.87	70.57	89.44	26.98
1000	20.74	74.99	95.73	29.32

TABLE IX. Heat content, free energy, entropy, and heat capacity of methylbromoacetylene for the ideal gaseous state at one atmosphere pressure.

T	$(H^0-H_0^0)/T$	$-(F^0-H_0^0)/T$	S^0	C_p^0
400	14.36	61.80	76.16	20.02
600	16.96	68.13	85.08	24.08
800	19.13	73.31	92.44	27.13
1000	20.98	77.79	98.76	29.43

TABLE X. Heat content, free energy, entropy, and heat capacity of methyliodoacetylene for the ideal gaseous state at one atmosphere pressure.

T	$(H^0-H_0^0)/T$	$-(F^0-H_0^0)/T$	S^0	C_p^0
400	14.54	63.44	77.97	20.18
600	17.12	69.85	86.96	24.19
800	19.28	75.08	94.36	27.22
1000	21.11	79.59	100.60	29.51

[10] G. Glockler and H. M. Davis, J. Chem. Phys. **2**, 881 (1934).
[11] Bryce L. Crawford, Jr., J. Chem. Phys. **7**, 140 (1939).
[12] L. Pauling, H. D. Springall, and K. J. Palmer, J. Am. Chem. Soc. **61**, 927 (1939).
[13] G. Herzberg, F. Patat, and H. Verleger, J. Phys. Chem. **41**, 123 (1937).

TABLE XI. Heat content, free energy, entropy, and heat capacity of methylacetylene for the ideal gaseous state at one atmosphere pressure.

T	$(H^0-H_0^0)/T$	$-(F^0-H_0^0)/T$	S^0	C_p^0
250	9.75	47.06	56.81	13.05
298.16	10.40	48.84	59.23	14.55
400	11.81	52.09	63.89	17.32
600	14.43	57.38	71.81	21.79
800	16.70	61.85	78.55	25.12
1000	18.66	65.79	84.45	27.69

TABLE XII. Tentative values of the heat content, free energy, entropy, and heat capacity of methyldeuteroacetylene for the ideal gaseous state at one atmosphere pressure.

T	$(H^0-H_0^0)/T$	$-(F^0-H_0^0)/T$	S^0	C_p^0
250	10.15	47.52	57.67	13.78
298.16	10.85	49.36	60.22	15.16
400	12.29	52.76	65.04	17.84
600	14.90	58.24	73.14	22.20
800	17.16	62.85	80.00	25.55
1000	19.11	66.90	86.01	28.13

ever, Meister[8] has calculated frequencies for this molecule with force constants transferred from methylacetylene; from the nature of the potential function used, one would expect these frequencies to be reliable to within two percent. Consequently, it seemed worth while to include this molecule in the present series in order that tentative results for its thermodynamic properties might be available. The values of the fundamental frequencies and their degeneracies are given in Table VI.[8]

The bond distances and interbond angles were assumed to be the same as for methylacetylene. The calculated values for the moments of inertia were

$$I_1 = I_2 = 107.4 \cdot 10^{-40} \text{ g cm}^2,$$

and

$$I_3 = 5.333 \cdot 10^{-40} \text{ g cm}^2.$$

THERMODYNAMIC FUNCTIONS

The frequencies, degeneracies, and moments of inertia listed in the above sections were used to calculate the heat capacity, free energy, heat content, and entropy for the diiodoacetylene, methylchloroacetylene, methylbromoacetylene, methyliodoacetylene, methylacetylene, and methyldeuteroacetylene molecules. The calculations were made to the rigid rotator, harmonic oscillator approximation and nuclear spins and the effect of isotopic mixing were neglected. The calculated values are for the ideal gaseous state at one atmosphere pressure. The symmetry number σ for diiodoacetylene is 2 and for the methylacetylenes it is 3. The molecular weights for diiodoacetylene, methylchloroacetylene, methylbromoacetylene, methyliodoacetylene, methylacetylene, and methyldeuteroacetylene were respectively 277.86, 74.526, 118.98, 165.98, 40.077, and 41.083.

The results obtained for diiodoacetylene are given in Table VII. The first column gives the temperatures in °K for which calculations were made and the next four columns give in succession the heat content, free energy, entropy, and heat capacity in calories per degree per mole.

The results for methylchloroacetylene are given in Table VIII.

The results for methylbromoacetylene and methyliodoacetylene are given in Tables IX and X, respectively. The present results for the heat capacity should replace those obtained in earlier calculations;[2] the present values are, on the average, 1.5 percent smaller than the previous values.

The results for methylacetylene are given in Table XI. The present values are in excellent agreement with the values calculated by Crawford[1] for the entropy, free energy, and heat capacity at constant volume. (Since the present heat capacities were calculated for constant pressure, rather than constant volume, it is necessary to add 1.99 to each of Crawford's heat capacities in order to obtain values comparable with the present heat capacities.) Rossini *et al.* also list some values[14] for the thermodynamic properties of methylacetylene.

The results for methyldeuteroacetylene are given in Table XII. These results must be regarded as tentative since they were determined with calculated frequencies in the absence of observed values; it seems probable, however, that they should be reliable to within about two percent.

ACKNOWLEDGMENT

The authors wish to express their appreciation to Dr. Arnold G. Meister for giving them the assignments of the fundamental frequencies for the methylacetylenes prior to publication.

[14] F. D. Rossini, K. S. Pitzer, W. J. Taylor, J. P. Ebert, J. E. Kilpatrick, C. W. Beckett, M. G. Williams, and H. G. Werner, A. P. I. Research Project 44, Circular of the National Bureau of Standards *C*461, "Selected Values of Properties of Hydrocarbons," (U. S. Government Printing Office, Washington, D. C., 1947), pp. 184, 202, 220, 226, and 291.

Letters to the Editor

THIS section will accept reports of new work, provided these are terse and contain few figures, and especially few halftone cuts. The Editorial Board will not hold itself responsible for opinions expressed by the correspondents. Contributions to this section should not exceed 600 words in length and must reach the office of the Managing Editor not later than the 15th of the month preceding that of the issue in which the letter is to appear. No proof will be sent to the authors. The usual publication charge ($4.00 per page) will not be made and no reprints will be furnished free.

Diffusion of Oxygen in Potassium Chloride

W. S. Koski
Department of Chemistry, The Johns Hopkins University, Baltimore, Maryland
April 13, 1949

THE diffusion of halogens in alkali halide[1] crystals has been studied by saturating the crystal with thallium vapor. This treatment imparts a brown coloration to the crystal, and as the halogen gas diffuses inward the brown coloration disappears due to the formation of colorless thallium halide. The rate of diffusion can be determined from the observed motion of the color boundary.

With the present day availability of high neutron fluxes, a modification of the above thallium indicator technique might shed some new light on the mechanism of diffusion of gases in solids. As an example of how this technique could be applied, we can consider the case of diffusion of oxygen in potassium chloride. When potassium chloride is irradiated with slow neutrons S^{35} is formed through the reaction Cl^{35} (n.p.)S^{35}. If appropriate care is taken to exclude oxidizing agents the bulk of the S^{35} is in the form of elementary sulfur or more probably as sulfide ion. We now have a unique system in which radiosulfide ions are distributed randomly through the KCl crystal. If oxygen is permitted to diffuse into such a crystal the sulfide ions will be oxidized to SO_3. The progress of the oxidation boundary could be utilized to measure the rate of diffusion. The position of the oxidation boundary in any one crystal can be determined by permitting the crystal to dissolve slowly in an appropriate solvent and analyzing the resulting solution for sulfate and sulfide activity from time to time. As the oxidation boundary is reached there is an abrupt drop in sulfate activity and from the knowledge of the amount of the crystal that has dissolved one can determine the depth of penetration of the oxygen.

A preliminary qualitative check has been made of this technique. Some KCl crystals which had been carefully outgassed by heating and pumping were irradiated in the Oak Ridge pile. After the irradiation a few selected crystals which measured about 0.5 mm in length were heated to 600°C and exposed to oxygen at a pressure of one atmosphere for five hours. Analysis showed that all of the sulfur had been oxidized to the hexavalent state, indicating that the oxygen had permeated all parts of the crystal. Results of this type may indicate that diffusion is taking place in the crystal not only through the flaws but also homogeneously through the body of the crystal. However, such conclusions can only be drawn with some reservation since the recoiling sulfide ions in the Cl^{35} (n.p.)S^{35} reaction have a range of a few angstroms in KCl and as a result flaws and imperfections are produced in the crystal which remain associated with the sulfide tracer throughout the experiment.

Some experiments have been performed to test the feasibility of determining the position of the oxidation boundary. Figure 1 gives a typical result when a single irradiated crystal which had been exposed to oxygen was put into ethyl alcohol. The solvent was tested for activity from time to time, and the percent activity appearing as sulfate ion was plotted against time. As the crystal layers in which the sulfur was oxidized by the oxygen are dissolved the solution indicates 100 percent of the activity as sulfate but as the oxidation boundary is reached there is an abrupt fall in sulfate activity. This region can be

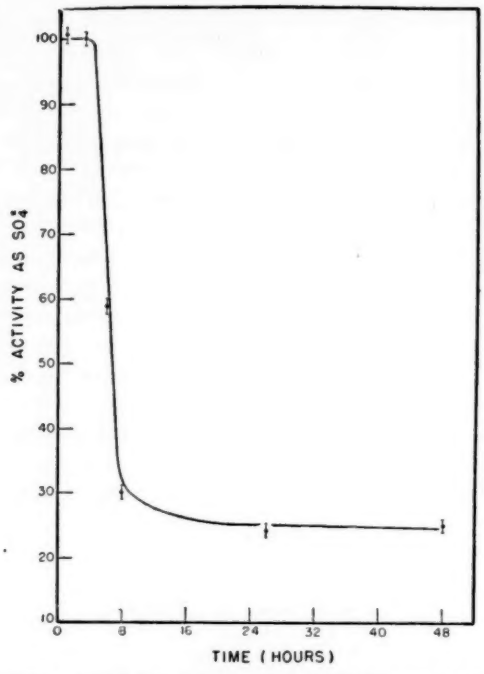

FIG. 1. Variation of sulfate activity with time when an irradiated potassium chloride crystal which had been exposed to oxygen is dissolved in ethyl alcohol.

considered as the depth to which the oxygen had diffused in the KCl. The sulfate activity does not fall to zero presumably because all of the oxidizing material had not been removed during the outgassing process.

[1] R. M. Barrer, *Diffusion in and through Solids* (Cambridge University Press, London, England, 1941), p. 110.

Viscosity of Liquid Hydrocarbon Mixtures

D. J. Trevoy and H. G. Drickamer
Department of Chemistry, University of Illinois, Urbana, Illinois
April 1, 1949

IN the course of a study of diffusion and thermal diffusion in hydrocarbon mixtures, including normal paraffins, benzene, and 2, 4 dimethyl pentane (i-C_7), it was necessary to obtain viscosities on these binary mixtures in 50 mole percent concentration. The viscometer, the method of operation, and of purifying the compounds was the same as that used by Giller and Drickamer.[1] The results are shown in Table I.

The viscosity of a mixture does not appear to bear any simple relation to the viscosities of the pure liquid components. Adding fluidities on a mole fraction basis to obtain the fluidity of the mixture has been suggested for ideal solutions, but errors in the calculated viscosity up to 58 percent occur for binary mixtures of n-paraffin hydrocarbons. Adding the logarithm of the viscosity on a mole fraction basis to obtain the logarithm of the viscosity of the mixture has also been suggested. By this method of calculation errors up to 26 percent occur in the viscosity of the mixture.

TABLE I.* The viscosity of 50 mole percent liquid mixtures obtained using a Cannon-Fenske-Ostwald viscometer.

Mixtures	T°K	t sec.	$\frac{10^4\eta}{\rho t}$	$\frac{10^2\eta}{\rho}$	ρ	$10^2\eta$
Ph−*n*-C_7	298.0	203.2	0.2724	0.5534	0.753	0.4167
	318.0	170.7	0.2719	0.4642	0.734	0.3407
	335.8	146.4	0.2715	0.3975	0.717	0.2850
Ph−*n*-C_{10}	298.0	318.3	0.2724	0.8672	0.774	0.6712
	318.0	255.6	0.2719	0.6951	0.757	0.5262
	335.8	212.1	0.2715	0.5758	0.742	0.4272
Ph−*n*-C_{12}	298.0	374.5	0.3099	1.1607	0.780	0.9053
	318.0	293.0	0.3088	0.9049	0.763	0.6904
	335.8	237.8	0.3089	0.7345	0.748	0.5494
Ph−*n*-C_{14}	298.0	506.3	0.3099	1.5689	0.790	1.2394
	318.0	385.1	0.3088	1.1893	0.775	0.9217
	335.8	305.6	0.3089	0.9439	0.760	0.7175
Ph−*n*-C_{16}	298.0	762.6	0.2724	2.0783	0.794	1.6502
	318.0	562.0	0.2729	1.5281	0.780	1.1919
	335.8	437.2	0.2715	1.1870	0.765	0.9081
	298.0	671.2	0.3099	2.0799	0.794	1.6515
	318.0	495.2	0.3088	1.5292	0.780	1.1928
	335.8	385.1	0.3089	1.1897	0.765	0.9100
Ph−*n*-C_{18}	298.0	975.3	0.2724	2.6416	0.799	2.1226
	318.0	702.4	0.2719	1.9099	0.786	1.5012
	335.8	538.4	0.2715	1.4617	0.772	1.1284
n-C_7−*n*-C_{12}	298.0	402.0	0.2724	1.0950	0.719	0.7873
	318.0	317.4	0.2719	0.8630	0.702	0.6058
	335.8	260.1	0.2715	0.7062	0.688	0.4859
	298.0	353.1	0.3099	1.0943	0.719	0.7868
	318.0	279.3	0.3088	0.8624	0.702	0.6054
	335.8	228.1	0.3089	0.7047	0.688	0.4849
n-C_7−*n*-C_{14}	298.0	517.3	0.2724	1.4091	0.732	1.0314
	318.0	398.3	0.2719	1.0830	0.716	0.7754
	335.8	322.6	0.2715	0.8759	0.702	0.6149
n-C_7−*n*-C_{16}	298.0	600.3	0.3099	1.8603	0.740	1.3766
	318.0	448.7	0.3088	1.3856	0.725	1.0046
	335.8	353.1	0.3089	1.0906	0.712	0.7765
n-C_7−*n*-C_{18}	298.0	746.3	0.3099	2.3128	0.748	1.7300
	318.0	546.9	0.3088	1.6888	0.735	1.2412
	335.8	422.2	0.3089	1.3042	0.722	0.9416
i-C_7−*n*-C_{12}	298.0	338.0	0.3099	1.0474	0.715	0.7489
	318.0	269.1	0.3088	0.8310	0.699	0.5809
	335.8	221.6	0.3089	0.6845	0.684	0.4682
i-C_7−*n*-C_{16}	298.0	574.7	0.3099	1.7810	0.738	1.3144
	318.0	432.0	0.3088	1.3340	0.722	0.9631
	335.8	342.9	0.3089	1.0592	0.709	0.7510
Ph−*i*-C_7	298.0	188.0	0.2724	0.5121	0.747	0.3825
	318.0	158.4	0.2719	0.4307	0.729	0.3140
	335.8	136.6	0.2715	0.3709	0.712	0.2641
i-C_7	298.0	185.5	0.2724	0.5054	0.671	0.3391
	318.0	158.1	0.2719	0.4298	0.654	0.2811
	335.8	137.0	0.2715	0.3720	0.639	0.2377

* *Note*: T = temperature °K; ρ = density g/cc; t = time, sec.; η = viscosity poises.

An empirical equation, the form of which was suggested by Roegiers and Roegiers,[2] best correlates the present viscosity data.

$$\eta = \eta_2\left(\frac{\eta_1}{\eta_2}\right)^{c_1\epsilon/(c_1\epsilon+c_2)}. \quad (1)$$

For a value of the parameter $\epsilon = 1.45$ and for 50 mole percent mixtures, (1) takes the form

$$\eta = \eta_2\left(\frac{\eta_1}{\eta_2}\right)^{0.592}. \quad (2)$$

Use of (2) to calculate the viscosity of mixtures in the *n*-C_7 −*n*-C_X and *Ph*−*n*-C_X series at 25°, 45°, and 63°C yielded values subject to an average error of about 5 percent and a maximum error of 14 percent.

Figure 1 shows typical results for the two series at a temperature of 25°C. As well as calculated and experimental values of the viscosity for 50 mole percent mixtures the viscosity of the pure compounds is also indicated.

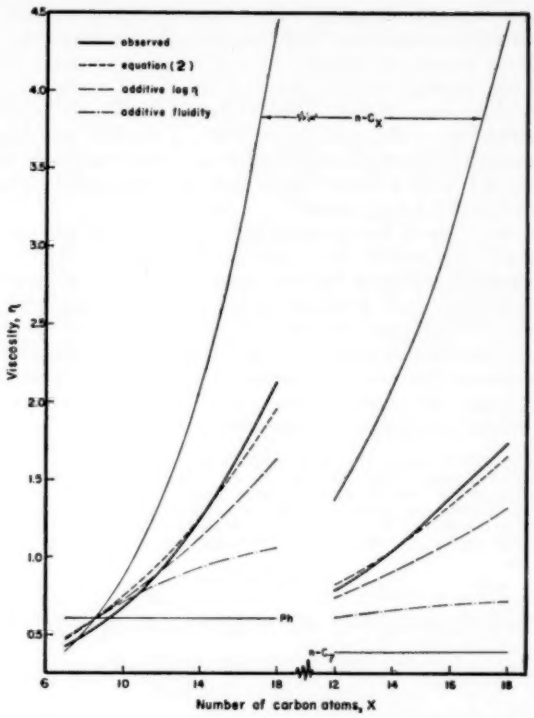

FIG. 1. A comparison of experimental and calculated values for the viscosity of liquid mixtures in the series: *Ph*−*n*-C_X and *n*-C_7−*n*-C_X at 25°C.

Viscosities were also calculated using the equation suggested by Eyring, *et al.*[3] for liquid mixtures. The results are not shown on the graph, but coincide quite closely with the results predicted from additive fluidities.

[1] Giller and Drickamer, Ind. Eng. Chem. (to be published).
[2] M. Roegiers, and L. Roegiers, *The Viscosities of "Normal" Fluids* (Société des Huiles de Cavel et Roegiers (Electron Oil Works) Coupure 197, Ghent, 1945).
[3] Glasstone, Laidler, and Eyring, *Theory of Rate Processes* (McGraw-Hill Book Company, Inc., New York, 1941), p. 516.

Crystals of Luminescent ZnF_2:Mn*

PETER D. JOHNSON AND FERD E. WILLIAMS
Chemistry Department, University of North Carolina, Chapel Hill, North Carolina

April 18, 1949

IN the course of a fundamental study of ZnF_2:Mn[1] it has been found possible to prepare clear transparent crystals of this phosphor, efficiently excited by cathode rays and 2537A radiation, of dimensions 1×1×2 mm.

Preliminary unsuccessful attempts to grow large crystals of ZnF_2:Mn involved slow cooling both under pressure and in vacuum, evaporating in vacuum, and lifting a platinum rod slowly from a melt. A modification of the simple method of Tamman and Veszi[2] was successful and has yielded the best results to date. The components of the phosphor mixed with a small amount of NH_4F were fused at atmospheric pressure in a platinum crucible, with a tightly fitting cover, over a Bunsen burner. The gas supply to the burner was gradually decreased over a period of one hour. By means of platinum *vs.* platinum-rhodium thermocouples at various points in the melt, it was found that the crystallization occurred over a period of 15 minutes. The clear transparent crystals formed near the upper outside edge of the melt, where the temperature gradient was estimated to be 3°C/mm. The method, in addition, invariably yielded larger opaque fragments with definite parallel and perpendicular cleavage planes.

Effort was made to prepare clear crystals of diverse activator content. 4.0 mole percent MnF_2 was found to be the maximum activator content for which evidence of clear crystal formation was encountered. A lower limit of 0.5 mole percent MnF_2 also was evident. Apparently, the activator inhibits the reduction of Zn^{++} on fusing ZnF_2. Chemical analysis of the transparent crystals obtained from a melt originally containing 2.2 mole percent MnF_2 indicated an activator concentration of 1.4 mole percent.

Examination of the crystals under a polarizing microscope revealed considerable strain and some twinning. Laue x-ray photographs indicated that the crystals consist of a number of crystallites oriented to within a few degrees of each other.** Conchoidal fracture of the crystals was common.

Fundamental measurements of the significant luminescent properties of the clear transparent crystals of ZnF_2:Mn are in progress, and effort is being made to prepare even larger transparent crystals of the phosphor.

* Supported by the ONR under Contract N7onr-284, T.O. 1.
[1] F. E. Williams, J. Opt. Soc. Am. **37**, 302 (1947).
[2] Tamman and Veszi, Z. Anorg. Allgem. Chem. **150**, 355 (1925).
** The authors are indebted to Mr. E. Fullam and Mr. E. Asp of the Research Laboratory of the General Electric Company for making, respectively, the microscopic and x-ray examinations.

Mass Spectrum of Hydrogen Deuteride (HD)

R. A. FRIEDEL AND A. G. SHARKEY, JR.
Bureau of Mines, Synthetic Liquid Fuels, Research and Development Branch, Bruceton, Pennsylvania
April 1, 1949

THE direct chemical preparation of hydrogen deuteride, 99± percent pure, has been reported by Wender, Friedel, and Orchin.[1] The fragmentation pattern under electron impact of this compound is of theoretical importance for comparison with the fragmentation patterns of H_2 and D_2, and is of analytical importance for determination of hydrogen-deuterium mixtures, as in the calculation of equilibrium constants for the reaction $H_2+D_2 \rightleftharpoons 2HD$. The unknown production of D+, mass 2, from fragmentation of HD interferes with the analysis of H_2. This interference has been supposed slight, as is the unknown interference of D+ from D_2[2], but if neglected, these can produce errors of several percent in calculation of equilibrium constants.

The relative abundance of D+ from HD cannot be determined directly because of the interference of unknown H_2 impurity. This difficulty was circumvented by measurements of rates of diffusion through the leak system of the mass spectrometer (Consolidated Model 21–102). Relative rates for H_2, measured at mass 2, and for HD, measured at mass 3, were found to be 12.72 and 10.46 percent per minute, respectively. These two values were plotted *versus* H_2 and HD percentages, and a straight line was drawn between them (Fig. 1). Then, measurements were made at mass 2 for two samples of HD with unknown H_2 impurity; thus, the rates of diffusion were due to mixtures of HD and H_2.* The rate values were applied to the straight-line plot and the percentages of D+ and H_2+ which comprised the mass 2-ion peak were read from the abscissa. From these values the percentages of H_2 impurity and the relative abundance of D+, 1.13±0.05, were determined. Composition of the HD sample of higher purity was found to be 98.8 percent HD, 0.4 percent H_2, plus 0.8 percent D_2 determined by direct analysis. Linearity of the relationship, rate of diffusion *versus* concentration, was checked by measuring the rates for six synthetic blends of HD plus small amounts of H_2. The resulting points fit the straight line within experimental error of the measurements (Fig. 1).

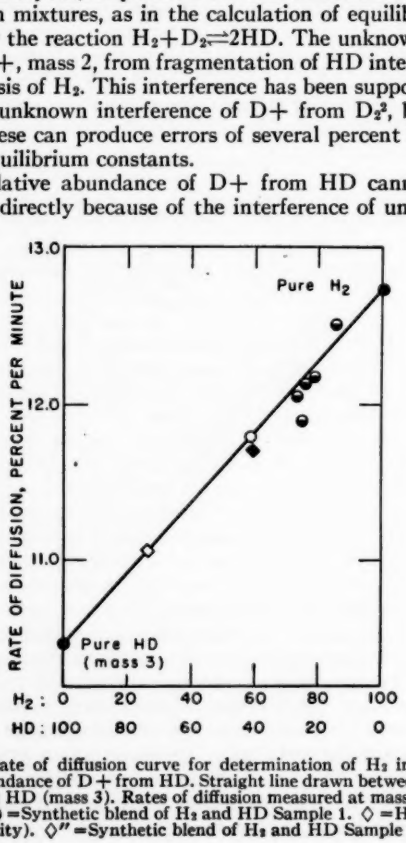

FIG. 1. Rate of diffusion curve for determination of H_2 impurity and relative abundance of D+ from HD. Straight line drawn between values for pure H_2 and HD (mass 3). Rates of diffusion measured at mass 2: ⊙ =HD Sample 1; ◒ =Synthetic blend of H_2 and HD Sample 1. ◇ =HD Sample 2 (highest purity). ◇″ =Synthetic blend of H_2 and HD Sample 2.

TABLE I. Mass spectra of H_2, HD, and D_2; 70-electron volts.

Mass	Ions	H_2	HD	D_2
1	H+	2.01[a]	0.82	
2	H_2+ or D+	100.0	1.13	1.06[b]
3	HD+		100.0	
4	D_2+			100.0
Sensitivity coefficients (ionization per unit pressure)		25.4	25.5	25.6
H+ from H_2/D+ from D_2		1.9[c]		

[abc] Corresponding values from Bauer and Beach, J. Chem. Phys. **15**, 150 (1947), are: (*a*) 2.52, (*b*) 1.32, and (*c*) 1.9.

The relative abundances of all ions from HD, H_2 (100 percent), and D_2 (99.2 percent D_2, 0.8 percent HD) are given in Table I. Data were obtained with 70-volt electrons and magnetic scanning. It will be noted that the total monatomic ions from H_2 and HD are practically equal and are twice the amount of monatomic ions obtained from D_2. The values for H+ and D+ from H_2 and D_2, obtained by Bauer and Beach[2] with 70-volt electrons, are included in the table. Absolute values of the two sets of data are not expected to compare; but the ratios, H+ from H_2/D+ from D_2, compare exactly with each other and quite well with Stevenson's[3] calculated value. The relative sensitivity coefficients (ionization of the parent molecule per unit pressure) from four sets of data for H_2, HD, and D_2 are essentially equal, as expected.[4]

Equilibrium constants at 500°C for $H_2+D_2 \rightleftharpoons 2HD$ have been calculated, using the calibration data in Table I, for three samples[5] equilibrated over an iron catalyst. The corrected average $K_{500°C}$ in Table II is 3.87±0.02, as compared to the theoretical value of 3.83.[6] If mass 2 values are not corrected for D+ ions from HD, in these samples of low H_2 content, the average $K_{500°C}$ is low, 3.70±0.02. This correction was not

TABLE II. Calculation of equilibrium constants at 500°C for $H_2+D_2 \rightleftharpoons 2HD$ from mass spectrometer analyses.

Sample	Mass 2 corrected for D+ from HD: D_2	HD	H_2	$K_{500°C}$	No HD correction $K_{500°C}$	Theory $K_{500°C}$
		Percent				
A	39.1	46.5	14.4	3.84	3.71	
A	38.8	46.6	14.6	3.84	3.71	
B	41.6	45.5	12.9	3.86	3.71	
B	41.6	45.5	12.9	3.86	3.72	
C	55.1	38.1	6.8	3.90	3.68	
C	55.2	38.1	6.7	3.90	3.68	
				Average 3.87±0.02	3.70±0.02	3.83

Rittenberg, Bleakney, and Urey, $K_{468°C}=3.75\pm0.07$
Theoretical, $K_{468°C}=3.82$

used by Rittenberg, Bleakney and Urey[7] in determining equilibrium at 468°C; however, with 35± percent H_2 the correction is less important. Their results produce an average $K_{468°C}$ of 3.75±0.07, as compared to the theoretical value of 3.82.

* Rate measurements were made in eight minutes or less to minimize possible diffusion separation; linearity of the semilog plots of diffusion rates indicated that separation, if any, was negligible.

[1] Wender, Friedel, and Orchin, J. Am. Chem. Soc. (in press).
[2] N. Bauer, and J. Y. Beach, J. Chem. Phys. 15, 150 (1947).
[3] D. P. Stevenson, J. Chem. Phys. 15, 409 (1947).
[4] R. Honig, J. Chem. Phys. 16, 837 (1948).
[5] Kindly supplied by Dr. J. Kummer, Mellon Institute.
[6] Wooley, Scott, and Brickwedde, J. Res. N. Bur. Stand. 41, 379 (1948).
[7] Rittenberg, Bleakney, and Urey, J. Chem. Phys. 2, 48 (1934).

On the Exchange of Cyanide with Nitriles

L. S. Tsai* and M. D. Kamen
Department of Chemistry, Washington University, St. Louis, Missouri

April 7, 1949

THE existence of exchange equilibriums between free cyanide ion and the −CN group of nitriles has been reported in the case of beta-hydroxy propionitrile which is claimed to exchange its nitrile carbon with cyanide to the extent of a few percent of equilibrium exchange when maintained under alkaline conditions at 100°C for one hour in the presence of approximately equimolar amounts of cyanide labeled with the 21-min. carbon isotope C^{11}.[1] Aside from its theoretical interest, this observation implies that a variety of carboxylic acids labeled in the carboxyl group could be synthesized merely by exchanging the appropriate nitrile with labeled cyanide, separating the nitrile, and hydrolyzing to the corresponding acid. We have re-investigated the exchange properties of beta-hydroxypropionitrile under a variety of conditions and in addition have extended our observations to methyl, phenyl, and succinyl cyanides. The following is a preliminary report of the procedures followed and results obtained.

A stock solution of labeled sodium cyanide** in distilled water was prepared which upon precipitation as AgCn exhibited an activity of 8400±100 ct/min. assayed in thick sample geometry with a RCL nucleometer. The assay technique was reproducible to within ±3 percent on many duplicate standard samples. In all experiments, nitrile in a large molar excess was added to a convenient amount of the labeled cyanide solution and brought to the desired acidity or alkalinity with HNO_3. Under these conditions, any appreciable exchange occurring would be indicated by a marked decrease in the specific activity of the cyanide. The corresponding specific activity of the nitrile following exchange could be calculated and compared with that observed. In addition, the recovery of total activity was checked. In calculating the activity to be expected, account was taken of the difference in carbon content of the various silver salts compared to silver cyanide. All samples were corrected to a standard thickness whenever the amounts collected were insufficient to give a true "infinite" thickness. The area of precipitate (2.26 sq. cm) was constant in all cases cited in this report.

In Table I, the results of the experiments with the one aromatic and two aliphatic unsubstituted nitriles are shown. It is seen that under the conditions noted there was no exchange between the organonitrile group and the free cyanide.

The experiments with beta-hydroxy propionitrile were carried out in acid, slightly alkaline and alkaline media, again with a large excess of the nitrile to enhance any change in specific activity of the cyanide consequent upon exchange. The procedure employed in the early experiments[1] involved alkaline distillation of the nitrile. This procedure did not appear adequate to prevent traces of cyanide from contaminating the nitrile. The procedure finally adopted involved precipitation of the cyanide in dilute acid, followed by extraction under alkaline conditions of the residual nitrile with chloroform. Control experiments in which unlabeled cyanide was mixed with a large excess of nitrile showed quantitative recovery of the cyanide to be possible by this procedure.

TABLE I. Exchange experiments with unsubstituted nitriles.

Experimental conditions†	Separation procedure	Percent random exchange
3.5 ml 0.5 M NaC* *N* 0.5 ml CH_3CN 5 ml *N* NaOH in 10 cc H_2O. Heated for two hours at 75°C	Cooled, cyanide ppt with Ag+ in dil. HNO_3 Filtrate acidified with conc. H_3PO_4 (1 vol. H_3PO_4:1 vol. filtrate). Refluxed 4 hrs., resultant acetic acid distilled and collected as $AgC_2H_3O_2$	<0.5 percent
0.5 M NaC* *N* 1 ml C_6H_5CN 1 ml 5*N* NaOH dil. 1:1 with alcohol, brought to final vol. 50 cc with dist. H_2O. Heated one hour at 75°C	Cyanide precipitated with Ag+ in dilute HNO_3 Filtrate hydrolyzed with conc. NaOH, solution acidified, benzoic acid separated by crystallization	<0.08 percent
1 ml 0.5 M NaC* *N* 1 ml *N* NaOH 200 mgm $(CH_2)_2(CN)_2$ brought to final vol. 10 cc with dist. H_2O. Heated in boiling water 1 hr.	Nitrile extracted with chloroform, after precipitation of cyanide in dil. acid solution	<0.3 percent

† The asterisk (*) denotes labeled carbon.

Incubation of the cyanide with 20-fold molar excess nitrile under acid conditions followed by separation of cyanide and nitrile revealed no change in the specific activity (<0.5 percent) random exchange. Under alkaline conditions (*p*H 9–14), the specific activity of the cyanide was observed to drop from 8400 to an average value of 7700 (see Table II). From this figure alone one could calculate 9.2 percent randomization of the cyanide with nitrile. However, the recovery of activity in the separated nitrile was 10-fold too high for the amount of specific activity loss observed for the cyanide. Furthermore it proved impossible to precipitate the cyanide completely (Table II) once it had been allowed to interact with the nitrile at 75°C or 100°C for one or two hours. The basis for this behavior is not known. Presumably complex formation or reaction of the reagents, or hydrolysis products thereof, could account for the observed incompleteness of cyanide recovery, as well as for the disproportionation in specific activity of nitrile and cyanide. The possibility that labeled formate formed by hydrolysis was reacting with the nitrile or its hydrolysis products has been excluded in control experiments with unlabeled formate. This matter is being investigated further.

TABLE II. Change in specific activity of cyanide in experiments with beta-hydroxy propionitrile.

Experimental conditions	Wt. of Ag CN ppt. (mgm)	Specific activity†	Standard specific activity
A. 1 ml 0.5*N* NaCN, 0.6 ml beta-hydroxy propionitrile (dist.), HNO_3 to final vol. 10 cc (0.1*N* HNO_3). Heated at 100°C for 1 hr.	57.2	8250	8400
B. as in *A* but no acid or alkali added	32.3	8300	8400
C. as in *A*, but 0.1*N* in NaOH	19.1 18.2	7710 7700	8400
D. as in *A*, but 0.5*N* in NaOH	34.6 35.6	7950 7740	8400
E. as in *A*, but 1.0*N* in NaOH	46.3 45.4	7800 7550	8400

† Activity of "infinitely" thick sample, corrected to standard thickness.

The existence of these phenomena call into question interpretation of the data on loss of cyanide activity as indicating a true exchange. It does not appear from the results of the present researches that exchange between any nitrile and free cyanide ion has been established.

* Present address: Department of Chemistry, Yenching University, Peking, China.
** The labeled sample in the form of $NaC^{14}N$ (0.5 millicurie C^{14}) was purchased from Tracerlab, Inc., Boston, Massachusetts.
[1] P. Nahinsky, Ph.D. Dissertation, University of California, 1942.

Erratum: An Asymptotic Expression for the Energy Levels of the Asymmetric Rotor. II. Centrifugal Distortion Correction

[J. Chem. Phys. 16, 250 (1948)]

S. GOLDEN
Hydrocarbon Research, Inc., New York, New York

IT has been kindly pointed out by Dr. J. K. Bragg that the quantities: $\Delta\theta_0$ and $\Delta\theta_0'$, defined immediately following Eq. (3), have an incorrect sign and should be replaced by $-\Delta\theta_0$ and $-\Delta\theta_0'$, respectively.

A Further Interpretation of Interaction Terms in the Potential Function of Polyatomic Molecules

JULES DUCHESNE AND ANDRÉ MONFILS
Department of Chemical Physics, Institute of Astrophysics, University of Liège, Liège, Belgium

April 22, 1949

IN recent papers[1] Duchesne and Coulson, Duchesne and Manneback have interpreted in general terms the physical meaning of the sign of the length-length and length-angle cross-terms appearing in the vibrational potential function of linear and angular triatomic molecules. In particular, they have discussed qualitatively the contribution of the interactions between non-bonded atoms on these cross-terms. Among other types of potential functions to represent those interactions, they have considered a Lennard-Jones function which they have written in the form

$$g(r_{12})=A[m(a/r)^n-n(a/r)^m]. \quad (1)$$

In this function, A is a constant which has been supposed to be positive; a is a distance, it is in fact the distance at which the net force changes sign, m and n are 6 and 12, whereas r_{12} is the distance between the non-bonded atoms.

Using this form of potential function, it has been shown that the length-length cross-term has the expression

$$f_{12}=A\sin^2\frac{\theta}{2}\left\{\frac{n^2ma^n}{r_{12}^{n+2}}-\frac{m^2na^m}{r_{12}^{m+2}}\right\}. \quad (2)$$

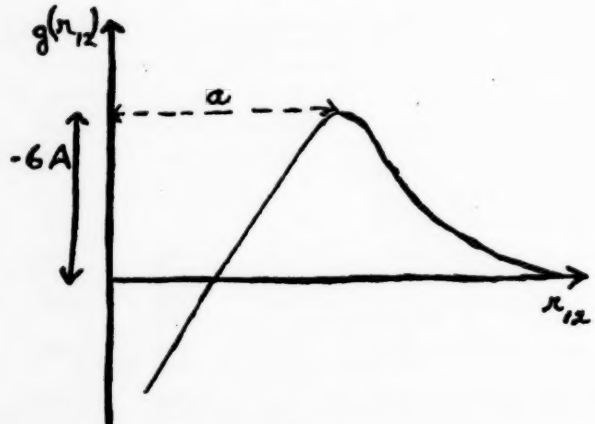

FIG. 1.

The conditions to obtain either a positive or a negative sign for f_{12} have been analysed on this basis with the result that for repulsion, f_{12} is always positive, whereas for attaction, f_{12} is generally attractive except in a small region in the neighborhood of the equilibrium position. In particular, the negative sign of f_{12} observed for HCN had been explained by an electrostatic attraction between H and N which are differently charged. It is to be remarked that the formula (2) applies to linear molecules if we put $\theta=180°$.

Until now one had not succeeded in calculating even the relative values of these cross-terms, in order to check the validity of the potential used and to try to develop a clearer basic understanding of the origin of the interactions and of the relative importance of their contributions. It is this problem that we have undertaken to deal with in this paper, using the most precise experimental data we had at our disposal for the frequencies. We will mainly confine our discussion to the symmetrical and asymmetrical linear triatomic molecules, and will reserve its extension to other kinds of molecules for a future paper.

By assuming that all the vibrations are genuinely harmonic, and applying the most general form of potential energy describing the parallel movements,

$$2V=f_1\langle\Delta r_1\rangle_{Av}^2+f_2\langle\Delta r_2\rangle_{Av}^2+2f_{12}\Delta r_1\Delta r_2,$$

we have calculated from the two parallel frequencies the cross, term f_{12} in cases of related molecules such as: CO_2, CS_2, COS-COSe, and HCN, ClCN, BrCN, ICN. However, the two parallel frequencies were not sufficient to fix the exact values for the three force constants appearing for asymmetrical molecules (for the symmetrical ones $f_1\equiv f_2$). In order to overcome this difficulty, we have assumed that the CO force constant deduced from CO_2, remains the same in COS and in COSe, and that the CN force constant determined from HCN and DCN remains the same in ClCN, BrCN, and ICN. This assumption seems very obvious since accurate values have been obtained for the interatomic distances[2] in those molecules from microwave measurements. It is shown indeed that the CO and the CN distances are independent of the adjacent atom within a range of at most 0.006A.

We summarize our results in the following Table I. We give

TABLE I.

	I				II			
	CO_2	COS	COSe	CS_2	HCN	ClCN	BrCN	ICN
f_{12}	1.32	0.90	0.76	0.59	−0.30	1.014	0.956	1.07

only the value of f_{12}, which is of interest to us. It is to be noticed that the values for CO_2, CS_2, COS had already been calculated in recent papers[1] and that the fundamental frequencies for COSe have been kindly communicated to us by Professor Lord, to whom we are very indebted. For the series of XCN molecules we have adopted for the CN force constant the value 18.065. The values of the force constants are deduced from the fundamental frequencies and expressed in 10^5 dynes/cm units. Let us now see what happens when we suppose that the whole contribution to f_{12} arises from the interactions between the non-bonded atoms, and is represented in terms of a Lennard-Jones potential.

In the upper expression[2] of f_{12}, we have two unknowns A and a. Our simplifying assumption is that A is a constant which has the same numerical value for each member of a group of molecules and that a is proportional to the square root of r_{12} ($a=k\sqrt{r_{12}}$). Therefore, if we calculate A and k from f_{12} in two molecules, say from CO_2 and COS in the first group, we may predict the value of f_{12} in the others, COSe and CS_2.

The results are summarized in Table II. It is to be noticed that A is expressed in ev.

TABLE II.

	A(ev)	a(A)	r_{12}(A)	f_{12} obs.	f_{12} calc.
CO_2	−0.85	1.88	2.30	1.32	—
COS	--	2.034	2.69	0.90	—
COSe	—	2.093	2.85	0.76	0.79
CS_2	—	2.176	3.08	0.59	0.59

The agreement between observed and computed values of f_{12} is very striking.

If we introduce the values found for the constants A and a, in the function $g(r_{12})$, we obtain the Fig. 1.

We see that instead of obtaining a conventional curve representing the change of potential in diatomic molecules, we obtain a reversed curve which is due to the fact that A is negative, contrary to the assumption which had been made before.[1] As r_{12} is always sufficiently greater than a, i.e., beyond a small region where the concavity is turned downwards, f_{12} has to be positive. It is worth while to note that A determines the height of the potential barrier as it is shown on the figure. We have extended these calculations to the second group of molecules which contain a molecule with a negative sign of f_{12} and therefore is particularly suited to check the validity of the potential function used. We have calculated A and a from HCN and ClCN and have obtained the results shown in Table III. Again the agreement is very good except for ICN.

TABLE III.

	A(ev)	a	r_{12}	f_{12} obs.	f_{12} calc.
HCN	−0.91	1.990	2.22	−0.30	—
ClCN	—	2.231	2.789	1.013	—
BrCN	—	2.294	2.95	0.95	0.90
ICN	—	2.373	3.155	1.07	0.735

In that particular case, however, the experimental value of f_{12} has itself a surprisingly high value. This seems to indicate that either there is another factor playing an important part or the experimental data are not precise. It is quite interesting to note that this new kind of representation interprets so nicely the negative cross-term in HCN. Even in that case r_{12} is greater than a, which means that there is repulsion as in the other cases and not attraction as in the first interpretation which had been given. The negative sign is due to the fact that the point on the potential curve appears on the right-hand side as for the other molecules, but between the maximum and the inflexion point. We see, therefore, that the repulsion is not at all offset by the electrostatic attraction, as had been supposed. The large decrease of the repulsion is obvious for such a small atom as hydrogen. On this basis, we might expect, therefore, to obtain a negative sign in other hydrogenated molecules. In fact, in H_2O, f_{12} is negative.[1] This again does not mean an attraction but a repulsion, and is much more in agreement with all the expectations. Thus, our recent interpretation of the negative sign of f_{12} in H_2O in terms of interactions between charges on the separate atoms no longer seems appropriate. This point of view is reinforced by the fact that other types of hydrogenated molecules in which the electric dipole moment is very small (ASH_3 etc.) also have a negative length-length cross-term, according to new and unpublished results obtained by Duchesne and Ottelet. This leads to the fundamental idea that at least in those molecules we cannot represent the interactions which arise between non-paired electrons in terms of forces between the bonds, i.e., in terms of changes of hybridization giving a positive sign, nor in terms of forces between charges on the separate atoms. The agreement obtained between experimental and calculated values of f_{12} may be to some extent fortuitous as it sometimes neglects the presence of net charges on the atoms which would give a further term of type e_1e_2/r. It is nonetheless true that the sign itself can only be predicted by taking into account our assumed interaction between the non-bonded atoms. This does not seem to exclude, however, that the hybridization factor would play a certain part which would be offset by the other factor. As a consequence of general interest it seems already possible to assert that the f_{12} cross-term is always negative when the bonds to which it refers are adjacent and contain at least one hydrogen atom.

An extended development of this note will appear elsewhere. Our best thanks are due to Professor C. A. Coulson for a helpful correspondence.

[1] J. Duchesne, Mémoires Soc. Roy. Sci., Liège (1943), p. 429; V. Henri, Mem. Vol. Desoer, Liège (1948), p. 47; *ibid.*, p. 33; Coulson, Duchesne, and Manneback, Nature **160**, 793 (1947).
[2] Smith, Ring, Smith, and Gordy, Phys. Rev. **74**, 370 (1948); Strandberg, Wentink, and Hill, Phys. Rev. **75**, 827 (1949).

Near Ultraviolet Absorption Spectra of the Isomeric Picolines*

H. SPONER AND J. H. RUSH
Department of Physics, Duke University, Durham, North Carolina
April 19, 1949

ABSORPTION studies of the isomeric picolines in the liquid and gaseous phase were undertaken for two reasons: (1) to see whether pyridine derivative spectra show a similar relation to the spectrum of pyridine as benzene derivative spectra do to that of benzene, (2) to possibly obtain information on some uncertain assignments in the pyridine spectrum.

The results obtained are interesting. All three compounds show in the gaseous phase a few broad diffuse bands in the region 2700–2450A, and narrow relatively sharp bands at 3000–2700A. The limits vary a little in the three compounds. The γ-compound exhibits only a few of these narrower bands, but the α- and β-picolines have quite a number of them in a pattern that resembles the pyridine spectrum, whereas the broad diffuse bands resemble the diffuse absorption system of some substituted benzenes. Thus, frequency differences of about 544 and 530 cm^{-1} occur in the pyridine-like "sharp" regions of the α- and β-picoline spectra, respectively, and differences of about 1000 cm^{-1} in the "benzene-like," "diffuse" part of the spectra. In the γ-compound a prominent frequency of 745 cm^{-1} is found in the region of the narrow bands. In α-picoline the diffuse spectrum appears at definitely lower pressures (below 0.1 mm) than the sharp spectrum, while in the other two isomers both spectra begin to appear at comparable pressures. The absorption of γ-picoline is definitely weaker than that of the other picolines.

Our measurements of the narrow α-picoline bands agree well with those of P. Angenot,[1] and so does the location of the 0,0 band at 34753 cm^{-1}. This means a shift of 16 cm^{-1} towards longer wave-lengths as compared to pyridine. There is a further small shift in the β-picoline spectrum whereas the shift in the γ-spectrum is towards shorter wave-lengths.

The solution spectra which were taken by Harold P. Stephenson in this laboratory do not show the two absorption regions separated as in the gas phase. This is understandable from the fairly even distribution of fine bands in the long wave region close to the diffuse bands.

The experimental results—vapor spectra exhibiting two absorption regions of different appearance, general shape of the curves obtained in solution in comparison to the vapor spectra—suggest the existence of two close-lying electronic levels. This seems surprising since the spectroscopic data hitherto published[2] on pyridine do not give evidence of two neighboring levels although their existence is possible, particularly in view of the diffuseness of the intense short wave part of the spectrum which makes measurements extremely difficult. Indeed, a reexamination of our pyridine plates[2] confirms this possibility and a rough estimate would place the

beginning of the second transition around 38350 cm^{-1}, while the 0,0 band of the diffuse bands in α-picoline is taken tentatively as 37640 cm^{-1} and in β-picoline as 37380 cm^{-1}. Again, in γ-picoline the shift goes toward larger wave numbers.

If one assumes that the excitation in pyridine is caused by the π-electrons of the ring as in benzene, then the first two excited electronic levels in pyridine and the picolines are of symmetry types B_1 and A_1 (assuming approximately C_{2v} symmetry for all four compounds). Dr. Gertrud P. Nordheim undertook to calculate roughly the position of the levels on that basis using the MO method. The calculations show that the two levels may be located relatively close in pyridine and that they move closer together in the picolines when a perturbation (of the type described by Wheland and Pauling[3] caused by the substitution of the methyl group is introduced. A close agreement between these theoretical results and the experiments can, of course, not be expected.

Detailed reports on the picoline spectra and their interpretation will be published later.

* This research was supported by the ONR Contract N6ori-107, T.O. I.
[1] P. Angenot, Ph.D. Dissertation, Liège, Belgium, 1936. One of us (H. S.) received knowledge of these measurements through the courtesy of Drs. J. Duchesne and L. d'Or of Liège for which grateful acknowledgment is made.
[2] V. Henri and P. Angenot, J. de Chim. Phys. **33**, 641 (1936). H. Sponer and H. Stücklen, J. Chem. Phys. **14**, 101 (1946).
[3] G. W. Wheland and L. Pauling, J. Am. Chem. Soc. **57**, 2086 (1935).

Solubility of Heterogeneous Polymers

W. H. Stockmayer
Department of Chemistry, Massachusetts Institute of Technology, Cambridge, Massachusetts
April 15, 1949

SEVERAL years ago, Scott[1] deduced that the critical or consolute point for a solution of a heterogeneous polymer conforming to the Flory[2]–Huggins[3] theory should be determined by the *number-average* molecular weight of the polymer. In view of the very dependence of polymer solubility on molecular weight, this conclusion is highly unexpected; moreover, as pointed out by Spurlin[4] in a recent review, it is not well supported by experiment. In this note the question is reconsidered, and the critical point is found to depend on both *weight-* and *z-average* molecular weights.

For brevity, we start from the equations of Flory[2] (1944) expressing the conditions of equilibrium between a solution (unprimed) and a precipitate (primed):

$$\ln(v_x'/v_x)=\alpha x, \tag{1}$$

$$[2-(\gamma+1)v_2]\ln[(1-v_2)/(1-\gamma v_2)] = 2(\gamma-1)v_2+\alpha(\gamma+1)v_2-2\delta v_2, \tag{2}$$

$$\gamma=\frac{v_2'}{v_2}=\frac{\Sigma v_x'}{\Sigma v_x}=\frac{\Sigma[Q_x^0 e^{\alpha x}/(1+re^{\alpha x})]}{\Sigma[Q_x^0/(1+re^{\alpha x})]}, \tag{3}$$

$$\delta=\frac{\Sigma[Q_x^0(e^{\alpha x}-1)/x(1+re^{\alpha x})]}{\Sigma[Q_x^0/(1+re^{\alpha x})]}, \tag{4}$$

$$\mu=\frac{\alpha+(\gamma-1)v_2-\delta v_2}{(\gamma-1)v_2[2-(\gamma+1)v_2]}. \tag{5}$$

The notation is that of Flory, in which v_x denotes volume-fraction of x-mer, Q_x^0 the total volume or mass of x-mer (i.e., the molecular weight distribution of the whole polymer), r the ratio of volume of precipitate to volume of solution, and μ the familiar interaction-constant. The physical significance of v_2, α, and γ is clear from Eqs. (1) and (3), while δ is a convenient parameter.

Now, since the two phases must become identical at the critical point, α is zero and γ is unity there. Thus, for states near the critical, the functions of Eqs. (2) to (5) can be expanded as power series in α or $(\gamma-1)$. Accordingly, we first expand the left-hand member of Eq. (2) in powers of $(\gamma-1)$, and develop series in powers of α for the quantities γ and δ of Eqs. (3) and (4). With these latter expressions, γ and δ are then eliminated from the expanded form of Eq. (2). In the resulting power series in α, the coefficients of α and α^2 vanish identically, while the coefficient of α^3 does not contain the volume-ratio r. Upon letting α approach zero, all higher terms vanish and the critical concentration is found to be

$$(v_2)_c=1/(1+x_w x_z^{-\frac{1}{2}}), \tag{6}$$

where

$$x_w=\Sigma x Q_x^0/\Sigma Q_x^0,$$

and

$$x_z=\Sigma x^2 Q_x^0/\Sigma x Q_x^0.$$

It is then a simple matter to evaluate the critical value of μ from Eq. (5), the result being

$$2\mu_c=(1+x_w^{-\frac{1}{2}})^2+(x_z^{\frac{1}{2}}-x_w^{\frac{1}{2}})^2/x_w x_z^{\frac{1}{2}}. \tag{7}$$

It is seen that Eqs. (6) and (7) reduce to the previously known results[2] for homogeneous polymers. It should also be noted that the last term of Eq. (7) is negligible for most heterogeneous polymers of interest, so that μ_c (and hence critical temperature or solvent-precipitant ratio) is virtually determined by the weight-average molecular weight.

The method employed above is not a general one for determining a critical state of a multi-component system,[5] but is well suited to the form in which the special relations among the polymeric components (i.e., the molecular weight distribution) are given in the present case. Scott's procedure[1] consisted in equating to zero the first and second derivatives of a_1 (solvent activity) with respect to v_2, and hence failed to take necessary account of the fractionation of the polymer between the two phases; for, while this fractionation vanishes at the critical point, its influence on the derivatives persists. Qualitatively, of course, the solubilizing effect of the smaller polymer molecules on the larger ones, emphasized by Scott, is still seen in the present results, though to a lesser degree.

Applied to equilibria in the two-phase region, the expansions described above soon become unwieldy, except for the case of incipient precipitation ($r=0$). Even here, the equations are scarcely simple for arbitrary molecular weight distributions, and we confine ourselves to the remark that, for $\alpha>0$, *all* positive moments of the weight distribution are included. Nowhere does the number-average molecular weight play a role.

There seem to be few published data affording a direct demonstration of these conclusions. An apparent confirmation is found in an experiment of Morey and Tamblyn,[6] who observed that the concentration of non-solvent required to produce incipient precipitation of a mixture of two cellulose acetate-butyrate fractions was equal to that for a single fraction whose molecular weight lies slightly above the z-average of the mixture. However, in this experiment the rate of addition of non-solvent was too rapid to ensure equilibrium. Indeed, in other systems the point of incipient precipitation has been found in this laboratory[7] to depend more nearly on number-average molecular weight, probably because at the high rates of addition of non-solvent employed the precipitation process was diffusion-controlled.

[1] Robert L. Scott, J. Chem. Phys. **13**, 178 (1945).
[2] Paul S. Flory, J. Chem. Phys. **10**, 51 (1942); **12**, 425 (1944).
[3] Huggins, Ann. N. Y. Acad. Sci. **43**, 1 (1942).
[4] Spurlin, J. Polymer Sci. **3**, 714 (1948).
[5] See J. W. Gibbs, *Collected Works* (Longmans, Green and Company, New York, 1928), Vol. I, pp. 129–134.
[6] D. R. Morey and J. W. Tamblyn, J. App. Phys. **16**, 419 (1945), Fig. 1.
[7] H. G. Lauterbach, unpublished measurements.

The Mechanism of the Initiation of the Oxidation of Acetaldehyde in the Gas Phase

C. A. McDowell and J. H. Thomas
Department of Inorganic and Physical Chemistry, University of Liverpool, Liverpool, England
April 29, 1949

WE recently discovered that small quantities of nitrogen peroxide inhibit the oxidation of acetaldehyde in the gas phase at temperatures between 90 and 140°C. This in-

hibition turns out to be exactly analogous to the inhibition of the polymerization of styrene by quinones,[1-4] and it is similarly found that the length of the induction period is directly proportional to the concentration of the inhibitor. It would thus seem reasonable to assume that this oxidation is also a chain reaction. Under these conditions it is easy to show that the rate of removal of inhibitor, $-dI/dt$, is given by the equation

$$-dI/dt=r_i, \tag{1}$$

where r_i is the rate of the initiation reaction.

This gives us an experimental criterion for deciding the nature of the initiation step, and we have applied it to investigate the feasibility of our suggested[5] initiation reaction,

$$CH_3CHO+O_2=CH_3CO+HO_2 \tag{2}$$

If we assume that most of the inhibitor is consumed during the induction period, τ, then with initiation reaction (2), Eq. (1) becomes

$$I_0/\tau=k_1[CH_3CHO][O_2], \tag{3}$$

where I_0 is the initial concentration of nitrogen peroxide. Thus a plot of I_0/τ against $[CH_3CHO][O_2]$ should yield a straight line. We have determined I_0/τ for quite a range of concentrations of acetaldehyde and oxygen, and find that Eq. (3) is rigorously obeyed, thus, showing that the initiation is, in fact, a bimolecular reaction between acetaldehyde and oxygen in contrast with the views of earlier work.[6] This does not of course, justify us in completing Eq. (1) in the manner indicated, but a study of the temperature dependence of k_1 leads us to the view that this is the initiation reaction in the temperature range indicated.

A complete account of this work will be published shortly.

[1] Foord, J. Chem. Soc., 1940, 48.
[2] Breitenbach and Breitenbach, Zeits. f. Physik. Chemie **190A**, 361 (1941).
[3] Goldfinger, Skeist, and Mark, J. Phys. Chem. **47**, 578 (1943).
[4] Melville and Watson, Trans. Faraday Soc. **44**, 886 (1948).
[5] McDowell and Thomas, Nature **162**, 367 (1948); also work in course of publication.
[6] Bodenstein, Sitz. Preuss. Akad. Wiss., **III**, 1 (1931); Zeits. f. Physik. Chemie **B12**, 151 (1931); Recuil de Travaux Chem. de Pay-Bas **59**, 48 (1940).

The Isotope Effect in the Decomposition of Oxalic Acid

J. G. Lindsay, D. E. McElcheran, and H. G. Thode
Department of Chemistry, McMaster University, Hamilton, Ontario.

April 1, 1949

A CONSIDERABLE isotope effect in the dissociation of propane $1-C^{13}$ by electron impact and also in the thermal cracking of C^{13} labeled propane, has been reported by Stevenson *et al.*[1,2] Their results indicated a 20 percent more frequent rupture of a $C^{12}-C^{12}$ bond than a $C^{12}-C^{13}$ bond in the former case and an 8 percent more frequent rupture in the latter case. Further, Yankwich and Calvin,[3] using C^{14} labeled malonic acid, found an isotope effect in the decarboxylation process, again indicating a preferential splitting of the $C^{12}-C^{12}$ bond over that of the $C^{12}-C^{14}$ bond. We have studied the decomposition of oxalic acid into CO, CO_2, and H_2O in the presence of concentrated sulphuric acid. In this work, variations in the natural C^{13} content of the oxalic acid and products were measured to determine the isotope effect. This procedure eliminates the need for synthesizing labeled material and reduces certain contamination problems.

Normal oxalic acid was decomposed in the presence of concentrated sulphuric acid at a controlled temperature. The products of the reaction CO_2 and CO were collected and the CO_2 separated out in a liquid air trap. The CO was burned to CO_2. A third sample of CO_2 was prepared by the complete oxidation of a sample of the original oxalic acid. These three samples were then analysed with a mass spectrometer with which their C^{13} contents were compared with a precision of better than 0.1 percent.

Table I. C^{13} distribution in oxalic acid decomposition products.

Run	% C^{13}* CO_2	% C^{13}* CO	Details	k_2/k_3	$k_1/(k_2+k_3)$
1	1.090		complete	1.040	
		1.059		1.019	
2	1.087		complete	1.034	
		1.050		1.036	
3	1.053		first CO_2 evolved		1.034
		1.137	last CO_2 evolved		

* Percent C^{13} in oxalic acid—1.069, temperature of runs—100°C.

Two effects have been observed: (1) a preference for the C^{13} to appear in the CO_2 rather than the CO; (2) a higher rate of decomposition of oxalic acid molecules containing only C^{12} carbon atoms over those containing C^{13} atoms. These two effects can be expressed quantitatively in terms of the three specific rate constants defined by the equations:

$$(C^{12}OOH)_2 \xrightarrow{k_1} C^{12}O_2+C^{12}O+H_2O$$

$$\begin{matrix} C^{13}OOH \\ | \\ C^{12}OOH \end{matrix} \xrightarrow{k_2} C^{13}O_2+C^{12}O+H_2O$$

$$\begin{matrix} C^{12}OOH \\ | \\ C^{12}OOH \end{matrix} \xrightarrow{k_3} C^{12}O_2+C^{13}O+H_2O.$$

If these are first-order reactions, then

$$\frac{(C^{12}O_2)}{(C^{13}O_2)}=\frac{(C^{13}O)}{(C^{12}O)}$$

$$=\frac{Ox^{12}(1-e^{-k_1t})+Ox^{13}(1-e^{-(k_2+k_3)t})\dfrac{k_3}{k_2+k_3}}{Ox^{13}(1-e^{-(k_2+k_3)t})\dfrac{k_2}{k_2+k_3}}. \tag{1}$$

If reaction is carried to completion ($t=\infty$), then

$$\frac{(C^{12}O_2)}{(C^{13}O_2)}=\frac{(C^{13}O)}{(C^{12}O)}=\frac{Ox^{12}(k_2+k_3)+k_3Ox^{13}}{k_2Ox^{13}}, \tag{2}$$

where Ox^{12} and Ox^{13} are the number of moles of the two isotopic species of oxalic acid in starting material.

As seen from Eq. (2), the ratio k_2/k_3 can be calculated from either the C^{13} abundance data for the CO_2 or the CO. The results of Table I give $k_2/k_3=1.033$. If there were no isotope effects in (1), k_2/k_3 would equal unity.

If, instead of carrying out the reaction to completion, a very small fraction of the oxalic acid is decomposed, so that the C^{13} content of the oxalic acid can be assumed to remain constant, then Eq. (2) becomes

$$\frac{(C^{12}O_2)}{(C^{13}O_2)}=\frac{(C^{13}O)}{(C^{12}O)}=\frac{k_1Ox^{12}+k_3Ox^{13}}{k_2Ox^{13}}. \tag{3}$$

Thus, from a C^{13} analysis of the first CO_2 or CO to be evolved from a 3-gram sample of oxalic acid, the ratio $k_1/(k_2+k_3)$ can be determined. The difference between this ratio and unity is a measure of the second isotope effect mentioned above. The ratio $k_1/(k_2+k_3)$ turns out to be 1.034.

Again it is seen that the isotope effects in unidirectional processes are appreciable, amounting in this case to 3.5 percent. The fact that C^{13} is favored in the CO_2 seems to indicate a preferential splitting of the $C^{12}-O^{16}$ bond over that of the $C^{13}-O^{16}$ bond, although it seems likely that the C—C bond is also involved because of the second isotope effect. Further experiments are in progress to determine also the distribution of O^{18} between the products of the reaction.

[1] Beeck, Otvos, Stevenson, and Wagner, J. Chem. Phys. **16**, 255 (1948).
[2] Stevenson, Wagner, Beeck, and Otvos, J. Chem. Phys. **16**, 993 (1948).
[3] P. E. Yankwich, and M. Calvin, J. Chem. Phys. **17**, 109 (1949).

Physical Adsorption and the Free Volume Model for Liquids

TERRELL L. HILL
Department of Chemistry, University of Rochester, Rochester, New York
April 19, 1949

SURFACE tension has been treated by Lennard-Jones and Corner,[1] using a free volume model for the liquid state. We extend this method here to a liquid-like adsorbate (of, say, three or more layers) on a free adsorbent surface.

For a "free-volume" liquid,[2]

$$-A_0/kT=N[\ln(2\pi mkT/h^2)^{\frac{3}{2}}j(T)+1+\ln v_f^0+(\chi_0/kT)]. \quad (1)$$

Consider a molecule at x, y, z in a cell with center at x', y', z' (same origin). If we now remove the liquid occupying the regions $z<0$ and $z>h$ and insert the adsorbent in the region $z<0$, we have a slab of adsorbate (assumed as a first approximation to have the liquid density uniformly) between $z=0$ and $z=h$. This alters the potential field in which the molecule is moving from φ_0 to

$$\varphi=\varphi_0-\Phi(z)-\Phi(h-z)+\varphi_a(z), \quad (2)$$

where $\Phi(z)$ is the energy of interaction of a molecule at z with the semi-infinite liquid, $z<0$, and $\varphi_a(z)$ is analogous for the adsorbent, $z<0$. Suppose the minimum in φ is at $z=z_0$. Then for the adsorbate, we replace N, $-\chi_0$, and v_f^0 in Eq. (1) by Ndz'/h,

$$-\chi(z')=\tfrac{1}{2}\varphi_0(z_0-z')-\tfrac{1}{2}\Phi(z_0)-\tfrac{1}{2}\Phi(h-z_0)+\varphi_a(z_0), \quad (3)$$

and

$$v_f(z')=\int\exp[-(\varphi-\varphi(z_0))/kT]dxdydz, \quad (4)$$

and integrate[3] from $z'=0$ to $z'=h$ to give $-A/kT$. Then,

$$\ln p/p_0=\partial[(A-A_0)/kT]/\partial N \quad (5)$$

$$(A-A_0)/kT=N[\ln v_f^0-\langle\ln v_f\rangle_{Av}+(\chi_0-\bar{\chi})/kT], \quad (6)$$

where $\bar{\chi}$ is $\chi(z')$ averaged from $z'=0$ to $z'=h$, etc.

As an initial *rough* approximation, we cancel[1] the free volume terms in Eq. (6) (putting $z_0=z'$) and compute $\chi_0-\bar{\chi}$ from a van der Waals model[4] (neighbor distribution *uniform* outside of $r=r^*$), taking for the interaction between two liquid molecules,

$$u(r)=\infty \quad r\leqslant r^*$$
$$=-\epsilon(r^*/r)^6 \quad r>r^*. \quad (7)$$

An analogous expression (parameters ϵ_1, r_1) is used for the liquid molecule-adsorbent molecule interaction. From[5] Eqs. (5) and (6), without further approximation, we find eventually (details to be published)

$$\ln p/p_0=(\delta/\Gamma^3)-[\delta_1/(\Gamma+r_1\rho)^3] \quad (8)$$

$$\cong(\delta-\delta_1)/\Gamma^3 \quad (9)$$

$$\delta=\pi\rho^4\epsilon r^{*6}/6kT \quad (10)$$

$$\delta_1=\pi\rho_1\rho^3\epsilon_1 r_1^6/6kT, \quad (11)$$

where $\Gamma=N/\mathcal{A}$, ρ is the liquid density (N/V), ρ_1 the adsorbent density, and $\mathcal{A}$ the surface area. The case of physical interest is $\delta-\delta_1<0$. The power three in Eq. (9) follows from Eq. (7) (i.e., $m-3$ with $m=6$). Introduction of a repulsive term should, *in effect* (for h not too large), reduce this power slightly. Near $p/p_0=1$, Γ is proportional to $[1-(p/p_0)]^{-\frac{1}{3}}$. This leads to convergence at $p/p_0=1$ of the Gibbs integral for the surface pressure.

Halsey[6] has obtained essentially Eq. (9) by a rather less explicit argument. He finds excellent agreement with experiment for N_2 on anatase with 2.267 in place of 3 in Eq. (9).

We are using a modified Lennard-Jones and Devonshire liquid model for a detailed application of Eqs. (2)–(6).

In a future note we shall outline the analogous extension of Fowler's[1,7] treatment of surface tension.

[1] Lennard-Jones and J. Corner, Trans. Faraday Soc. **36**, 1156 (1940); J. Corner, *ibid.* **44**, 1036 (1948). Also, see J. G. Kirkwood and F. P. Buff, J. Chem. Phys. **17**, 338 (1949), for a rigorous treatment.
[2] T. L. Hill, J. Phys. and Coll. Chem. **51**, 1219 (1947).
[3] In calculations it will probably prove desirable to treat the top and bottom layers separately, as in reference 1 (top layer). Otherwise, a smeared out (average) distribution of *cell centers* is physically realistic.
[4] T. L. Hill, J. Chem. Ed. **25**, 347 (1948).
[5] Using Eq. (2) of T. L. Hill, J. Chem. Phys. **16**, 181 (1948).
[6] G. Halsey, J. Chem. Phys. **16**, 931 (1948).
[7] R. H. Fowler, Proc. Roy. Soc. **A159**, 229 (1937).